ULTRASTRUCTURAL AND PHYSIOLOGICAL STUDIES ON THE CANNABINOID CB_1 RECEPTOR LOCALIZED IN ASTROGLIA

DOCTORAL THESIS

Svein Achicallende Urcaregui

Leioa, 2021

eman ta zabal zazu
Universidad del País Vasco
Euskal Herriko Unibertsitatea
NEUROZIENTZIAK SAILA
DEPARTAMENTO DE NEUROCIENCIAS
MEDIKUNTZA ETA ERIZAINTZA FAKULTATEA
FACULTAD DE MEDICINA Y ENFERMERÍA

A thesis submitted in fulfillment of the requirements for the degree of PhD in NEUROSCIENCES

University of the Basque Country

The author was the recipient of a PhD contract (PIF 16/251) from the University of the Basque Country/Euskal Herriko Unibertsitatea (UPV/EHU)
This work was funded by: the Basque Government (IT1230-19); MINECO/FEDER, UE (SAF2015-65034-R); Ministry of Science and Innovation (PID2019-107548RBI00)

Supervised by:

Pedro Rolando Grandes Moreno, MD, PhD

María Inmaculada Gerrikagoitia Marina, PhD

Department of Neurosciences
Faculty of Medicine and Nursing
University of the Basque Country (UPV/EHU) Leioa, 2021

INDEX

ABBREVIATIONS

2-AG: 2-arachidonoylglycerol

A1R: adenosine receptor type 1
A2AR: adenosine receptor type 2A
AA: arachidonic acid
ABC: avidin-biotin complex
aCSF: artificial cerebrospinal fluid
AEA: N-arachidonoylethanolamine or anandamide
AED: antiepileptic drug
AMG: amygdala
AMP: adenosine monophosphate
AMPA: D-amino-3-hydroxy-5-methyl-4-isoxazole-propionic acid
ANOVA: analysis of variance
AR: adenosine receptor
ATP: adenosine triphosphate

BNST: bed nucleus of the striata terminals
BSA: bovine serum albumin

CA: Cornu ammonis or Ammon´s horn
CA1: region 1 of Cornu ammonis
Ca^{2+}: calcium
cAMP: cyclic adenosine monophosphate
CB_1 receptor: cannabinoid receptor type-1
CB_2 receptor: cannabinoid receptor type-2
CCK: cholecystokinin
CNS: central nervous system
CPu: caudate putamen
Cre: cyclization recombination enzyme
Ctx: cortex

D1R: dopamine receptor type 1
DAB: 3,3´-diaminobenzidine
DAG: diacylglycerol
DAGL: diacylglycerol lipase
DG: dentate gyrus
DML: dentate molecular layer
DMSO: dimethyl sulfoxide
DRN: dorsal raphe nucleus
DSE: suppression of excitation
DSI: suppression of inhibition

EAAT1: excitatory amino acid transporter 1
EC: entorhinal cortex
eCB-LTD: endocannabinoid-mediated long-term depression
eCB-LTP: endocannabinoid-mediated long-term potentiation
eCB: endocannabinoid

ECS: endocannabinoid system
EGFP: enhanced green fluorescent protein
EM: electron microscopy
EtNH2: ethanolamine

FAAH: fatty acid amide hydrolase
fEPSP: field excitatory postsynaptic potential
FIJI: Fiji is just IMAGE J

GABA: gamma-aminobutyric acid
$GABA_AR$: GABA receptor type A
$GABA_BR$: GABA receptor type B
GC: granule cell
GFAP: glial fibrillary acidic protein
GLAST: glutamate aspartate transporter
GP: globus pallidus
GPCR: G-protein-coupled receptors
GPR55: G-protein-coupled receptor 55

HIF-1: hypoxia-induced factor-1
hrGFP: humanized renilla green fluorescent protein

IP3: inositol (1,4,5)-triphosphate

KO: knock-out mice

LC: locus coeruleus
LFS: low frequency stimulation
LPP: lateral perforant path
LTD: long-term depression
LTP: long-term potentiation

MAGL: monoacylglycerol lipase
MCF: mossy cell fibers
mGluR: metabotropic glutamate receptor
MOR: m-type opioid receptor
MPP: the medial perforant path
mRNA: messenger ribonucleic acid
$mtCB_1$ receptor: mitochondrial CB_1 receptor

NAc: nucleus accumbens
NAPE-PLD: phospholipase D selective N-acylphosphatidylethanolamine
NMDAR: N-methyl-D-aspartate receptor
NNST: bed nucleus of the striatal terminalis
NT: neurotransmitter
NTS: nucleus of the solitary tract

OB: olfactory bulb
OT: olfactory tubercle

P2XR: purinergic receptor type P2X
P2YR: purinergic receptor type 2
PAG: periaqueductal gray
PB: phosphate buffer
PBS: phosphate buffered saline
PFC: prefrontal cortex
PKA: protein kinase A
PKG: cGMP-dependent protein kinase
PLC: phospholipase C
PPAR-α: peroxisome proliferator-activated receptors
PPR: paired-pulse-ratio
PTX: picrotoxin

RS: Racine´s scale
RT: room temperature

SEM: standard error mean
SNr: substantia nigra pars reticulata

TBS: tris-hydrogen chloride buffered saline
TNFα: tumor necrosis factor alpha
TRP: transient receptor potential
TRPA1: transient receptor potential ankyrin 1
TRPV1: transient receptor potential vanilloid 1

VTA: ventral tegmental area

WT: wild-type mice

Δ9-THC: trans-Δ-9-tetrahydrocannabinol

SUMMARY

The cannabinoid CB_1 receptor-mediated functions in astrocytes are highly dependent on the CB_1 receptor distribution in these glial cells relative to neuronal sites, particularly at the nearby synapses under normal or pathological conditions. However, the whole picture of the subcellular CB_1 receptor distribution in astroglial compartments remains uncompleted due to the scattered CB_1 receptor expression, and therefore difficult to detect, in astrocytes. Our laboratory has in previous studies estimated that about 5-6% of the total CB_1 receptors in the hippocampal CA1 stratum radiatum are localized in astrocytes identified by the marker glial fibrillary acidic protein (GFAP). Similar values were obtained in the basolateral amygdala and posterior parietal association cortical layers II/III. However, GFAP is a cytoskeleton protein mostly restricted to the astroglial cell bodies and their main branches. This might be distorting the actual proportion and total amount of CB_1 receptors in astrocytes. Therefore, the search for alternative astroglial markers to decipher the precise mapping of CB_1 receptors in astrocytes is a timely goal in the cannabinoid field.

The glutamate aspartate transporter (GLAST) is used as astroglial marker for several reasons: 1) most of the dendritic spines are contacted by astrocytes; 2) it is estimated that 3,200 transporters are distributed per μm^3 in the hippocampal CA1 stratum radiatum; 3) as the total astroglial cell surface is estimated to be 1.4 m^2/cm^3, the average density of GLAST molecules in astrocytic membranes is ~ 2,300 μm^{-2}; 4) GLAST labeling is localized on astrocytic plasma membranes along the astroglial surface. Therefore, GLAST raises as a good astroglial marker candidate to study in detail the CB_1 receptor distribution in astrocytes.

To prove this hypothesis, I have used a pre-embedding immunogold method for electron microscopy to compare first the astroglial distribution of GLAST versus GFAP. GLAST labeling was along the plasma membrane of astrocytes, including cell bodies and the smallest astrocytic projections in close contact with neurons, capillaries and other glial cells, covering altogether a much broader labeled area than GFAP. Furthermore, the use of a pre-embedding immunoperoxidase method for electron microscopy served me to assess that almost three times more astroglial area is visualized with GLAST than GFAP, and that GLAST detects four times as much astroglial membranes as GFAP. Finally, a double pre-embedding

immunogold/immunoperoxidase method allowed to estimate that about 12% of the total CB_1 receptor particles are localized in GLAST-positive astrocytes, but the value drops to 5-6% in GFAP-positive astrocytes, as published previously by our laboratory.

Once these findings were obtained, I studied in more detail the CB_1 receptor localization in astroglial mitochondria. We discovered the presence of functional CB_1 receptors in mitochondrial membranes of hippocampal neurons and astrocytes. However, doubts raised in the scientific community as whether other brain regions were actually expressing CB_1 receptors in mitochondria, as no studies had been conducted so far to explore this possibility. Accordingly, I used double GLAST-CB_1 immunolabeling to analyze in the electron microscope the density of mitochondrial CB_1 receptors in neurons and astrocytes in four brain regions: CA1 hippocampus, prefrontal cortex, piriform cortex and nucleus accumbens. The results showed that the CB_1 receptor density in astrocytic mitochondria of CA1 hippocampus (3.24 ± 0.94 particles/μm^2), prefrontal cortex (2.45 ± 0.49 particles/μm^2), nucleus accumbens (1.16 ± 0.44 particles/μm^2) and piriform cortex (1.35 ± 0.57 particles/μm^2), is higher than in neuronal mitochondria of CA1 (0.76 ± 0.09 particles/μm^2), prefrontal cortex (1.04 ± 0.13 particles/μm^2), nucleus accumbens (0.42 ± 0.12 particles/μm^2) and piriform cortex (0.82 ± 0.12 particles/μm^2). Altogether, despite the lower absolute levels of CB_1 receptors in astrocytes than in neurons, the density of mitochondrial CB_1 receptors in astrocytes is higher than in neurons in the four brain regions studied. Namely, CB_1 receptors are more expressed in astroglial than neuronal mitochondria. Activation of mitochondrial CB_1 receptors alters energy production in neurons and can cause memory impairment. Likewise, activation of mitochondrial CB_1 receptors in astrocytes interferes with glucose metabolism and lactate production, disrupting neuronal functions and social behavior.

In conclusion, the findings that astrocytes of the four brain regions studied contain more CB_1 receptors in their mitochondria than the neuronal mitochondria, and that the cannabinoid-induced reduction of oxygen consumption is absent in mitochondria isolated from the forebrain of GFAP-CB_1-KO mice, suggest that mitochondrial CB_1 receptors in astrocytes play a crucial role in the global effects of cannabinoids on brain mitochondrial respiration.

The anatomical findings of my thesis on mitochondrial CB_1 receptors in astrocytes have been published in Nature (Jimenez-Blasco et al., 2020).

INTRODUCTION

2.1. THE ENDOCANNABINOID SYSTEM (ECS)

Cannabis sativa L. is possibly one of the oldest plants cultivated by man but has remained a source of controversy throughout history (Russo, 2007). This annual dioecious plant shares its origins with the inception of first agricultural societies in Asia (Bonini et al., 2018). *C. sativa* has been used as a source of fibers, food, oil, and medicine as well as for recreational and religious purpose over centuries (Piluzza et al., 2013). It contains a number of chemically active compounds, such as cannabinoids, terpenoids, flavonoids, and alkaloids (Andre et al., 2016). The most active compounds are the cannabinoids, a class of terpenophenolic compounds, accumulated mainly in the trichrome cavity of the female flowers (Taura et al., 2007; Bonini et al., 2018). The trans-Δ-9-tetrahydrocannabinol (Δ9-THC) is the most potent out of over 100 cannabinoids identified so far, and mainly responsible for the psychoactive effects of marijuana (Whiting et al., 2015).

The discovery of the endocannabinoid system (ECS) has revealed a complex and multimodal system involved in a wide variety of physiological processes. This system consists of cannabinoid receptors, endogenous lipophilic ligands or endocannabinoids and enzymatic machinery for their production, release and degradation (Piomelli, 2003; Marsicano and Lutz, 2006; Kano et al., 2009; Navarrete and Araque, 2008; Katona and Freund, 2012; Lu and Mackie, 2016; Oliveira Da Cruz et al., 2016).

The ECS is widely distributed throughout the mammalian organism and, even if it is present in many other organs (Piazza et al., 2017), is widely distributed in the central and peripheral nervous system (Katona and Freund et al., 2012; Lu and Mackie et al., 2016). The system regulates different brain functions by acting at specific compartments of neurons and glial cells (Katona and Freund et al., 2012; Lu and Mackie et al., 2016; Gutiérrez-Rodríguez et al., 2017; Busquets-García et al., 2018). Besides, the ECS is involved in many brain processes spanning from food intake to cognition (Marsicano and Kuner, 2008; Bellocchio et al., 2010; Katona and Freund, 2012). The endocannabinoids (eCBs) participate in complex cellular and molecular mechanisms and synaptic plasticity providing important computational properties to brain circuits, such as coincidence detection and input specificity, needed for high brain functions (Castillo

et al., 2012). Thus, the alteration of the ECS is part of the pathogenesis of multiple neurological and neuropsychiatric disorders (Pertwee, 2009).

2.1.1. Cannabinoid receptors

Cannabinoid receptors are known to be present in many vertebrate species from rodents to primates, including both monkeys and humans (Elphick and Egertová, 2005). Two main cannabinoid receptors have been cloned: cannabinoid receptor type-1 (CB_1 receptor) (Matsuda et al., 1990; Matsuda et al., 1993) and cannabinoid receptor type-2 (CB_2 receptor) (Munro et al., 1993). The CB_1 and CB_2 receptors belong to G-protein-coupled receptors (GPCRs) superfamily, the largest family of transmembrane proteins in human genome, and are crucial for many essential physiological processes. GPCRs are characterized by seven hydrophobic transmembrane segments connected by intracellular and extracellular loops, an N-terminal extracellular domain that contains glycosylation sites and a C-terminal intracellular domain coupled to a G protein (Howlett et al., 2002).

2.1.1.1. CB_1 receptor

It is one of the most abundant G protein-coupled receptors in the central nervous system (CNS) and is present in neuronal and non-neuronal cells (Herkenham et al., 1990; Tsou et al., 1998; Moldrich and Wenger, 2000). Its expression is widespread, heterogeneous and has crucial roles in brain function, dysfunction and cognition (Marsicano et al., 2002; Monory et al., 2006; Marsicano and Kuner, 2008; Bellocchio et al., 2010; Puente et al., 2011; Castillo, 2012; Katona and Freund, 2012; Steindel et al., 2013; Ruehle et al., 2013; Soria-Gómez et al., 2014, 2015; Hu and Mackie, 2015; Katona, 2015; Martín-García et al., 2015; Gutiérrez-Rodríguez et al., 2017, 2018; Bonilla-Del Río et al., 2019, 2021). The deleterious effects of cannabinoids on locomotion, perception or memory, and the cannabinoid-positive effects as anti-convulsive or food intake enhancers, fit with the CB_1 receptor distribution in the CNS. Thus, its localization is very abundant in the prefrontal cortex (PFC), cingulate gyrus, hippocampus, basal ganglia, substantia nigra and cerebellum (Mackie, 2005; Hillard, 2014; Gutiérrez-Rodríguez et al.,

2017), but the receptor is poorly expressed in hypothalamus, brainstem and spinal cord (Tsou et al., 1998). This low amount of CB_1 receptors in the brainstem correlates with the low toxicity and lethality of marijuana.

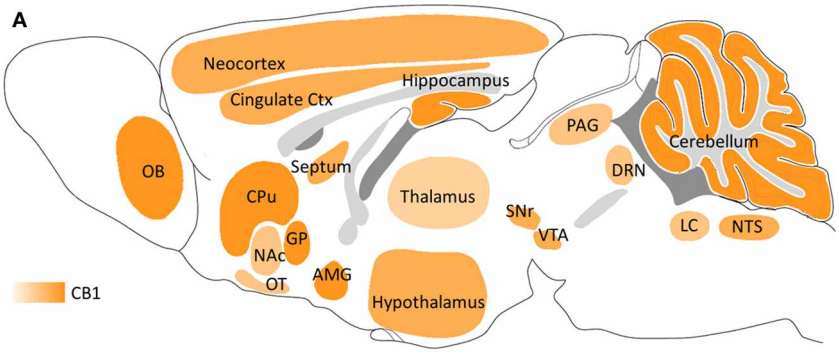

Figure 1. Schematic representation of the main brain areas expressing CB_1 receptor. AMG, amygdala; CPu, caudate putamen; Ctx, cortex; DRN, dorsal raphe nucleus; GP, globus pallidus; LC, locus coeruleus; NAc, nucleus accumbens; NTS, nucleus of the solitary tract; OB, olfactory bulb; OT, olfactory tubercle; PAG, periaqueductal gray; SNr, substantia nigra pars reticulata; VTA, ventral tegmental area. Obtained from Flores et al., 2013.

The localization of the CB_1 receptor is mainly in presynaptic terminals, and its activation triggers suppression of neurotransmitter release (Kano et al., 2009). In the CNS, CB_1 receptors are expressed in GABAergic, glutamatergic, serotonergic, noradrenergic or cholinergic neurons, suggesting that the ECS is involved in the suppression of the release of these neurotransmitters (Hermann et al., 2002; Oropeza et al., 2007; Azad et al., 2008; Kano et al., 2009; Morozov et al., 2009; Lutz et al., 2015; Soria-Gómez et al., 2015; Gutiérrez-Rodríguez et al., 2017), with the predominant effects of the eCB signaling taking place at GABAergic and glutamatergic synapses (Katona and Freund, 2012). Glial cells like astrocytes (Salio et al., 2002; Navarrete and Araque, 2008, 2010; Han et al., 2012; Gutiérrez-Rodríguez et al., 2017; Bonilla-Del Río et al., 2019, 2021) and oligodendrocytes (Moldrich and Wegner, 2000) as well as cells of the cerebral vasculature (Golech et al., 2004), express CB_1 receptors. Furthermore, the CB_1 receptor is also localized in the outer mitochondrial membrane of both presynaptic and postsynaptic terminals and astrocytes (Hebert-Chatelain et al., 2014a, 2014b, 2016; Koch et al., 2015; Lutz et al., 2015; Gutiérrez-Rodríguez et al., 2018; Jimenez-Blasco et al., 2020). The activation of the mitochondrial CB_1 receptors modulates energy metabolism by the inhibition of oxidative phosphorylation and ATP production, that

results in memory impairment (Hebert-Chatelain et al., 2016), altered neuronal functions and impaired social interaction (Jimenez-Blasco et al., 2020). Finally, CB_1 receptors are also expressed in many peripheral organs and tissues: fat, muscle, liver, heart, gastrointestinal tract, pancreas, spleen, tonsils, prostate, testicle, uterus, ovary, skin, eye or peripheral presynaptic sympathetic nerve terminals (Galiègue et al., 1995; Ishac et al., 1996; Pertwee, 2001; Maccarone et al., 2016; Zou and Kumar, 2018). They are also in mitochondria of skeletal muscles and myocardium whose activation by Δ9-THC reduces mitochondria-coupled respiration (Mendizabal-Zubiaga et al., 2016).

The ECS exerts important functions in the brain through the activation of CB_1 receptors. For example, retrograde inhibition of neurotransmitter release (Alger, 2002; Marsicano and Lutz, 2006; Heifets and Castillo, 2009; Kano et al., 2009), control of neuronal excitability (Marsicano et al., 2003), regulation of various forms of short- and long-term synaptic plasticity (Gerdeman and Lovinger, 2003; Marsicano and Lutz, 2006; Heifets and Castillo, 2009; Kano et al., 2009, Puente et al., 2011), neuron-astrocyte communication (Navarre and Araque, 2008, 2010), proliferation of neuronal progenitors and neurogenesis induced by excitotoxic insults (Aguado et al., 2006, 2007), or control of neuronal survival (Galve-Roperh et al., 2009).

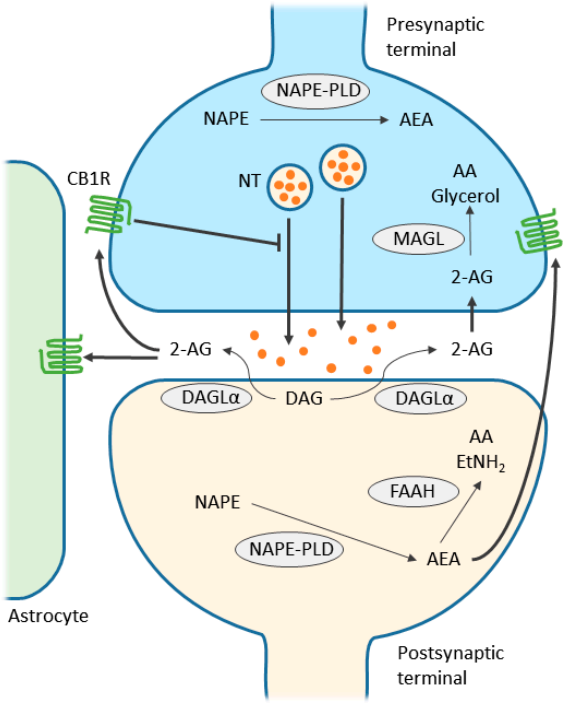

Figure 2. Simplified scheme representing endocannabinoid retrograde signaling mediated synaptic transmission. eCBs are produced from postsynaptic terminals upon neuronal activation. As lipids, eCBs, mainly 2-AG, readily cross

the membrane and travel in a retrograde fashion to activate CB_1 receptors located in presynaptic terminals. Activated CB_1 receptors will then inhibit neurotransmitter (NT) release through the suppression of calcium influx. 2-AG is also able to activate CB_1 receptors located in astrocytes, leading to glutamate release. Extra 2-AG in the synaptic cleft is taken up into the presynaptic terminals, via a yet unclear mechanism, and degraded to arachidonic acid (AA) and glycerol by MAGL. On the other hand, AEA, synthesized in postsynaptic terminals, activates intracellular CB_1 receptor and other non-cannabinoid receptor targets, such as the TRPV1 receptor. Although eCB retrograde signaling is mainly mediated by 2-AG, AEA can activate presynaptic CB_1 receptors as well. FAAH is primarily found in postsynaptic terminals and is responsible for degrading AEA to AA and ethanolamine (EtNH2). Although NAPE-PLD is expressed in presynaptic terminals in several brain regions, it is not clear yet whether AEA is responsible for anterograde signaling in the ECS. Note that alternative routes exist for the metabolism of eCBs, depending on the brain region and physiological conditions. Thin arrows indicate enzymatic process; thick arrows indicate translocation; Blunted arrow indicates inhibition. Obtained from Zou and Kumar, 2018.

2.1.1.2. CB_2 receptor

The CB_2 receptor was first described in spleen (Munro et al., 1993), and apart from this organ, it was believed to be specific of the immune system (tonsils, B and T lymphocytes, natural killer cells, macrophages, and CD8 and CD4 T-lymphocytes) (Galiègue et al., 1995; Ameri, 1999; Cabral et al., 2015). Despite this, CB_2 receptors are also expressed in heart, endothelium, bone, liver, pancreas and testicle (Zou and Kumar, 2018). Due to the lack of specific antibodies, the localization of CB_2 receptors in the CNS is a debatable issue (Atwood and Mackie, 2010; Lu and Mackie, 2016). To avoid this limitation, new genetic strategies based on mutant mice lines expressing enhanced green fluorescent protein (EGFP) under the control of CB_2 promoter have been developed (López et al., 2018).

2.1.1.3. Other cannabinoid receptors

There are also other receptors mediating the effects of eCBs (Pertwee, 2015), such as the transient receptor potential vanilloid 1 (TRPV1) (Maccarrone et al., 2008; De Petrocellis and Di Marzo, 2009b; Tóth et al., 2009; Alhouayek et al., 2014; Rossi et al., 2015). In addition, eCBs are also able to activate the transient receptor potential ankyrin 1 (TRPA1) receptor (De Petrocellis et al., 2008), peroxisome proliferator-activated receptor (PPAR-α) (Sun et al., 2006; Alhouayek et al., 2014) and non-CB_1/CB_2 GPCRs such as G-protein-coupled receptor 55 (GPR55) (Ryberg et al., 2007).

2.1.2. Endocannabinoids

The eCBs are lipid messengers considered as promiscuous molecules because they activate CB_1 and CB_2 receptors but also other receptors (Piomelli, 2003; Kano et al., 2009; Katona and Freund, 2012; Lutz et al., 2015; Lu and Mackie, 2016; Zou and Kumar, 2018). Due to the vast distribution of the numerous components and the features of the system, the physiology and pharmacology of eCBs is complex. They perform their effects in a paracrine and autocrine manner, and as they can diffuse and cross membranes because their lipid nature, probably even in endocrine mode. The eCBs are not accumulated in secretory vesicles like neurotransmitters (though might be stored in adiposomes); conversely, they are synthesized on demand and released to the extracellular space following physiological and pathological stimuli (Piomelli, 2003; Kano et al., 2009; Pertwee et al., 2010; Katona and Freund, 2012; Lutz et al., 2015; Lu and Mackie, 2016; Zou and Kumar, 2018).

eCBs are endogenous lipid compounds synthesized from the cellular membranes. Among them, N-arachidonoylethanolamine (also known as anandamide, AEA) (Devane et al., 1992) and 2-arachidonoylglycerol (also known as 2-AG) (Mechoulam et al., 1995) are the two main eCBs which are better identified and characterized. AEA triggers the "tetrad" effects (catalepsy, antinociception, hypolocomotion and hypothermia) of cannabinoids in rodents, while 2-AG plays a key role in most of the CB_1 receptor-dependent modulation of synaptic transmission and plasticity (Kano et al., 2009).

The eCB with higher brain concentration is 2-AG (200-fold higher than AEA) (Bisogno et al., 1999) and correlates well with the cannabinoid receptor density in the brain (Sugiura et al., 2006). However, AEA accumulates evenly in brain regions with high (hippocampus, cortex, striatum), and low cannabinoid receptor expression (thalamus, brainstem) (Felder and Glass, 1998). 2-AG activates with high efficacy both CB_1 and CB_2 receptors, whereas AEA efficacy is low on CB_1 receptors and very low on CB_2 receptors (Showalter et al., 1996; Gonsiorek et al., 2000; Sugiura et al., 2000; Luk et al., 2004).

A wide variety of biochemical pathways for the synthesis, transport, release and degradation of eCBs have been described to date. Consequently, the biosynthetic

enzymes diacylglycerol lipases (DAGL) α and β for 2-AG, and phospholipase D selective N-acylphosphatidylethanolamine (NAPE-PLD) for AEA, together with the hydrolytic enzymes monoacylglycerol lipase (MAGL) for 2-AG and fatty acid amide hydrolase (FAAH) for AEA, among others, are responsible for the distinct physiological and pathophysiological roles of both eCBs (Kano et al., 2009; Fezza et al., 2014; Piomelli, 2014; Lu and Mackie, 2016; Zou and Kumar, 2018).

Under certain circumstances, AEA inhibits presynaptic GABA and glutamate release, and activates TRPV1 receptor (Zygmunt et al., 1999; Ross, 2003; Chávez et al., 2010; Puente et al., 2011; Lu and Mackie, 2016; Zou and Kumar, 2018). 2-AG signals retrogradely and activates presynaptic CB_1 receptors to reduce neurotransmitter release, but also activates TRPV1 though a higher concentration is required for reaching a similar effect to AEA. Moreover, FAAH and MAGL are localized in different subcellular sites, suggesting the existence of different signaling mechanisms for AEA and 2-AG, respectively (Cravatt et al., 1996; Cristino et al, 2008; Kano et al., 2009).

2.2. ASTROCYTES

Glial cells, the most abundant cell population in the brain, were originally described by Rudolf Virchow in 1846 as non-neuronal cells constituting the “glue” of the brain. Later studies classified CNS glial cells into two groups, microglia and macroglia. Microglia is composed of macrophage like-cells with phagocytic functions, and macroglia is constituted of two cell types: oligodendrocytes, responsible for myelinization in the CNS, and astrocytes. Astrocytes are crucial players in the development and physiology of the CNS involved in key aspects, such as trophic support, neuronal survival and differentiation, neuronal guidance, neurite outgrowth or synaptic efficacy (Perea and Araque, 2002). Moreover, astrocytes contribute to brain homeostasis regulating the local concentrations of ions and neuroactive substances (Perea and Araque, 2002).

Astrocytes interact with neurons at many different levels and have been known for their protective role against CNS injury and as energy supporters for neurons (Magistretti and Pellerin, 1999; Bélanger and Magistretti, 2009; Bélanger et al., 2011; Yi et al., 2011; Oliveira Da Cruz et al., 2015; Bolaños, 2016). However, this view has been challenged because many signaling pathways that modulate neuronal activity also regulate astrocytic-neuronal communication (Araque et al., 1999; Haydon and Carmignoto, 2006; Perea et al., 2009; Gómez-Gonzalo et al., 2015). These findings have led to the concept of “tripartite synapse” made up of the presynaptic and postsynaptic neuronal sites and the surrounding astrocytes (Araque et al., 1999). In this background, different authors have demonstrated the tripartite synapse to play a crucial role in the bidirectional communication between neurons and astrocytes (Navarrete and Araque, 2008, 2010; Navarrete et al., 2013, 2014; Gómez-Gonzalo et al., 2015). Astrocytes are also essential in the regulation of energy metabolism and brain activity by detecting central and peripheral changes that affect brain homeostasis (Bélanger et al., 2011; Barros and Weber, 2018; Magistretti and Allaman, 2018; Jimenez-Blasco et al., 2020). Their morphology is particularly complex and they are distributed in close apposition to the synaptic structures contacting tens of thousands of synapses (Halassa et al., 2007).

The expression of some key ion channels is relatively low in astrocytes making them not electrically excitable cells with membrane potential relatively stable (Perea and Araque, 2002; Araque and Navarrete, 2010). Voltage-gated channels expressed by astrocytes

mainly function for the homeostatic maintenance of extracellular ion levels (Araque and Navarrete, 2010). Also, astrocytes contain functional receptors for many different neurotransmitters that lead to changes and oscillations in intracellular calcium (Ca^{2+}) (Araque et al., 2001). Many of these receptors are GPCRs that stimulate phospholipase C and inositol (1,4,5)-triphosphate (IP3) formation, which increases intracellular Ca^{2+} concentration through the release of Ca^{2+} from internal calcium stores. Astrocytes mainly use Ca^{2+} stored in the endoplasmic reticulum as the source for cytosolic Ca^{2+} acting as a cellular signal (Perea and Araque, 2005a).

Astrocytes show spontaneous intracellular Ca^{2+} variations in response to different neurotransmitters. They serve as intracellular signals reaching different sites of the cell and establish long-range communications between astrocytes with relevant functional consequences in the CNS, as Ca^{2+} elevations originated in one astrocyte propagate to neighboring astrocytes forming a "Ca^{2+} wave" that extend several hundreds of micrometers (Perea and Araque, 2005a, Araque and Navarrete, 2010).

Numerous studies have shown the existence of bidirectional signaling between neurons and astrocytes. The calcium-based cellular excitability displayed by astrocytes can be triggered by neuronal and synaptic activity through activation of neurotransmitter receptors expressed by astrocytes (Perea and Araque, 2005a, Araque and Navarrete, 2010). In turn, calcium elevations in astrocytes stimulate the release of different neuroactive substances named gliotransmitters, such as glutamate, ATP, tumor necrosis factor alpha (TNFα), adenosine, prostaglandins, GABA or D-serine, which regulate neuronal excitability and synaptic transmission (Perea and Araque, 2010; Araque and Navarrete, 2010). Thus, astrocytes are integral part of the synapses, being involved not only in passive homeostatic control of adequate conditions for synaptic function, but also actively involved in synaptic function (Perea et al., 2009).

As a single astrocyte is in contact with thousands of synapses and astrocytes communicate between them, probably the simplest effect of astrocytes on neural networks is their ability to simultaneously activate populations of neurons. Thus, astrocytic calcium waves and subsequent glutamate release lead to the synchronous excitation of clusters of hippocampal pyramidal neurons, indicating that gliotransmission may contribute to neuronal synchronization (Angulo et al., 2004; Fellin,

2009). Besides, a single gliotransmitter may exert multiple effects on the neuronal network, depending on the target neurons and neuronal elements (pre- or postsynaptic) as well as the activated receptor subtypes, which provides a high degree of complexity for astrocytic effects on neuron-glia network activity (Araque and Navarrete, 2010).

Astrocytes influence neurotransmission at different time scales because they transiently control synaptic strength (during seconds or few minutes) but also contribute to long-term changes in synaptic transmission, which are thought to be the mechanism of learning and memory at the cellular level. Different mechanisms underlying the astrocyte effects on long-term potentiation (LTP) have been described (Perea and Araque, 2010). Astrocytes are dynamic elements of synapses that display notable structural as well as functional modifications (Theodosis et al., 2008). Indeed, synaptically evoked astrocytic responses mediated by membrane expression of neurotransmitter receptors and transporters undergo activity-dependent modifications similar to short-term and long-term plasticity (Perea and Araque, 2010). Therefore, it is important to develop new tools to decipher the distribution and exact localization of receptors in the astrocytes.

2.2.1. Astrocytes and ECS

Expression of CB_1 receptors in astrocytes has been a matter of debate in the past. The first reports of the presence of the receptor in these cells was in human and rodent cultures (Bouaboula et al., 1995a; Sánchez et al., 1998; Molina-Holgado et al., 2002b; Sheng et al., 2005). However, discordant results were obtained in mice (Sagan et al., 1999; Walter and Stella, 2003), suggesting that CB_1 receptors in astrocytes could vary among different animal species, strains or different culture conditions. Moreover, due to the low expression of astroglial CB_1 receptors, it was difficult to detect by *in situ* hybridization or immunohistochemistry.

Luckily, immunoelectron microscopy enabled to reveal astrocytic CB_1 receptors (Rodríguez et al., 2001; Han et al., 2012; Bosier et al., 2013). Moreover, enzymes for the synthesis and degradation of the main eCBs co-localize with glial fibrillary acidic protein (GFAP) (Suárez et al., 2010). Importantly, many different works have demonstrated the

presence of astroglial CB_1 receptors and their functional relevance (Navarrete and Araque, 2008, 2010; Stella, 2010; Han et al., 2012; Bosier et al., 2013; Gómez-Gonzalo et al., 2014; Navarrete et al., 2014; Metna-Laurent and Marsicano, 2015; Viader et al., 2015; Oliveira da Cruz et al., 2016; Gutiérrez- Rodríguez et al., 2017; Robin et al., 2018; Bonilla-del Río et al., 2019, 2021). Thus, various authors have proposed different signaling pathways after CB_1 activation in astrocytes. For example, some have suggested that astroglial CB_1 receptors are coupled to $G_{\alpha i/o}$-protein (Guzmán et al., 2001), while others have proposed that the receptor regulates intracellular Ca^{2+} levels through $G_{\alpha q}$-proteins (Navarrete and Araque, 2008; Navarrete et al., 2014). In this regard, diverse intracellular signaling pathways modulated by eCBs provide astrocytes with an unique functional flexibility (Metna-Laurent and Marsicano, 2015). Besides, CB_1 receptors in astrocytes evoke glutamate release at distant synapses (Navarrete and Araque, 2008; 2010), but also locally eliciting long-term depression (LTD) of the excitatory synaptic transmission in the hippocampus responsible for the working memory impairment caused by acute THC (Han et al., 2012). Also, CB_1 receptors in astrocyes are involved in energy supply to the brain through the control of leptin receptor expression in these glial cells (Bosier et al., 2013). Furthermore, astrocytes produce and release lactate, which is one of the major fuel sources for neurons (Bélanger et al., 2011; Suzuki et al., 2011; Barros and Weber, 2018; Magistretti and Allaman, 2018; Jimenez-Blasco et al., 2020). Actually, a large body of studies have shown that astroglial release and neuronal uptake of lactate play fundamental roles in a range of behaviors, such as sleep (Petit and Magistretti, 2016; Haydon, 2017), learning and memory (Suzuki et al., 2011) or social behavior (Jimenez-Blasco et al., 2020). Now is clear that the modulation of astroglial bioenergetics represents a powerful primary signaling contributor to brain activity, plasticity and behavior (Allen and Barres, 2009; Bélanger et al., 2011; Suzuki et al., 2011; Oliveira et al., 2015; Magistretti and Allaman, 2018; Robin et al., 2018; García-Cáceres et al., 2019).

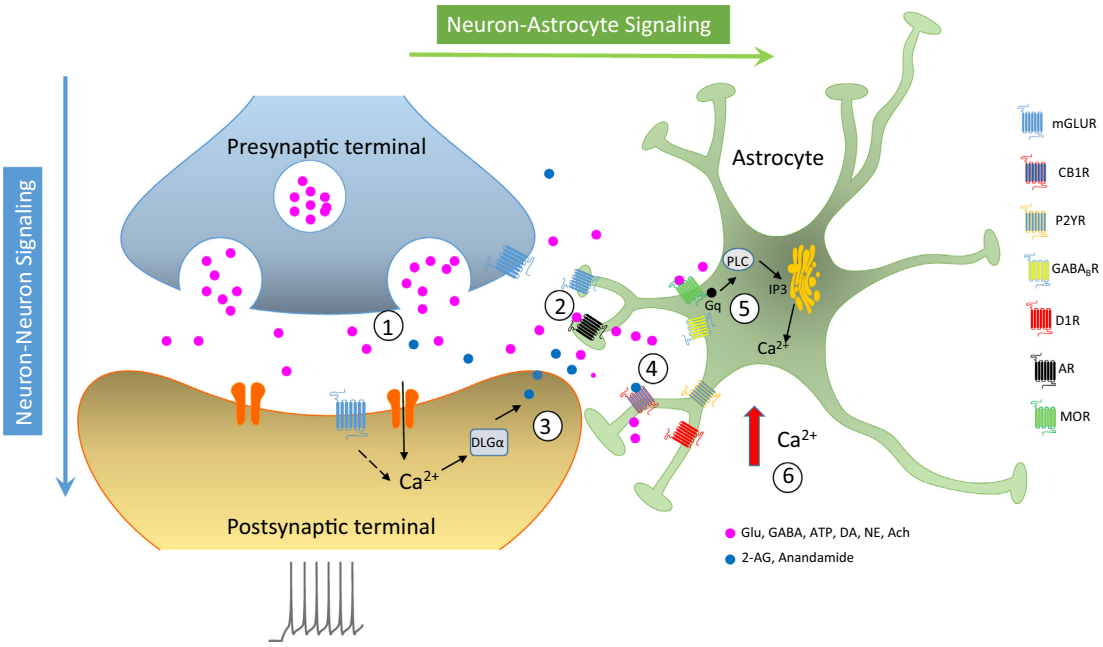

Figure 3. Neuron-astrocyte signaling at the tripartite synapse. Presynaptic neurons release neurotransmitters (1) that bind to GPCR in postsynaptic cells and astrocytes (2). Activation of GPCRs in astrocytes elicits the activation of PLC cascade (5) resulting in elevation of intracellular Ca^{2+} (6). Increases in postsynaptic Ca^{2+} also leads to release of eCBs (3) that activate CB_1 receptors (4). mGluR, metabotropic glutamate receptor; CB_1 receptor, cannabinoid receptor type 1; P2YR, purinergic receptor type 2; GABABR, GABA receptor type B; D1R; dopamine receptor type 1; AR, adenosine receptor; MOR, m-type opioid receptor; DLGα, diacylglycerol lipase type a; PLC, phospholipase C. Obtained from Kofuji and Araque, 2021.

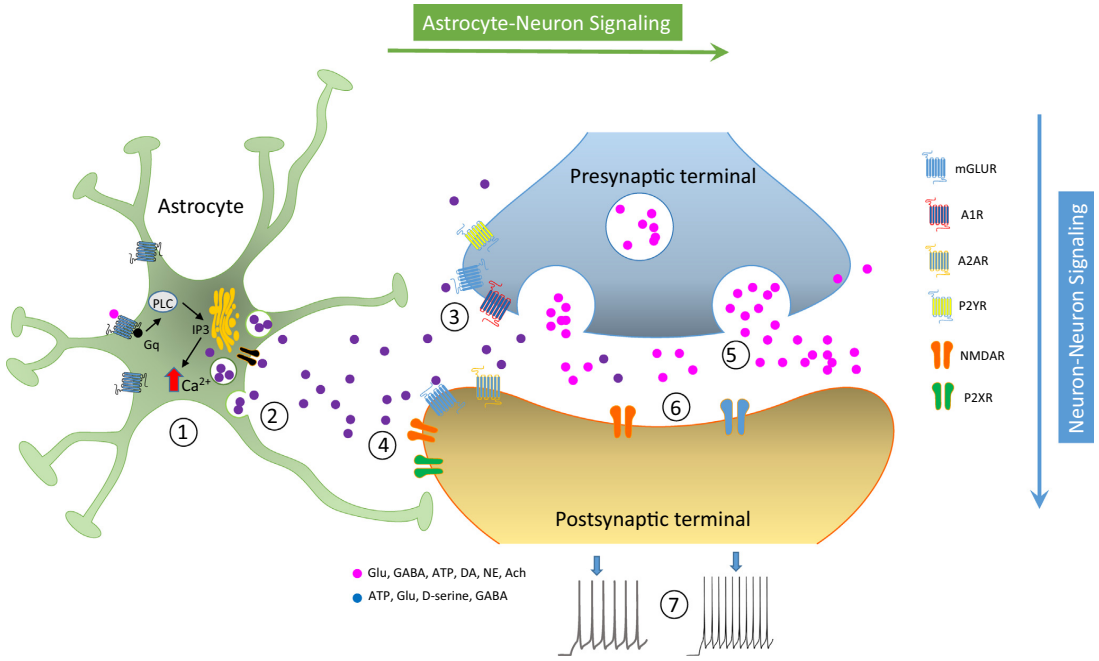

Figure 4. Astrocyte-neuron signaling at the tripartite synapse. Activation of PLC cascade and the resulting intracellular Ca2+ increase (1) promotes release of gliotransmitters (2) that act upon presynaptic (3) or postsynaptic

(4) GPCRs or channels. Presynaptic release (5) or postsynaptic excitability are therefore regulated by gliotransmitters. mGluR, metabotropic glutamate receptor; P2YR, purinergic receptor type 2; A1R, adenosine receptor type 1; A2AR, adenosine receptor type 2A; NMDAR, N-methyl-D-aspartate receptor; P2XR, purinergic receptor type P2X; PLC, phospholipase C. Obtained from Kofuji and Araque, 2021.

Although it is generally assumed that CB_1 receptors in neurons account for most of the cannabinoid-induced brain effects, recent studies have emphasized the crucial role of astroglial CB_1 receptors in regulating astrocyte-neuron communication at both, synaptic and behavioral levels (Araque et al., 2017; Martín-Fernandez et al., 2017; Busquets-Garcia et al., 2018; Robin et al., 2018; Jimenez-Blasco et al., 2020). Actually, low-frequency astrocytic activation without presynaptic activity is enough to induce postsynaptic AMPA receptor removal and LTD expression in the CA1 hippocampus (Gómez-Gonzalo et al., 2015; Navarrete et al., 2019). Therefore, astrocytic CB_1 receptors, in addition to promote astroglial differentiation (Aguado et al., 2006), play a role in synaptic plasticity, memory and behavior (Navarrete and Araque, 2008, 2010; Han et al., 2012; Araque et al., 2014; Navarrete et al., 2014; Gómez-Gonzalo et al., 2015; Metna-Laurent and Marsicano, 2015; Olivera da Cruz et al., 2016; Robin et al., 2018; Durkee and Araque, 2019). However, the potential impact of pathological conditions on the expression and function of astroglial CB_1 is still poorly known.

2.2.2. Mitochondrial CB_1 ($mtCB_1$) receptor and astrocytes

Bioenergetics is crucial in the brain due to the fact that although this organ is only 2% of the body weight, it consumes about 20% of the energy of the body (Attwell and Laughlin, 2001; MacAskill and Kittler, 2010). Mitochondria ensure and regulate the cellular energy supply (Nicholls and Ferguson, 2002; MacAskil and Kittler, 2010). Thus, mitochondrial oxidative phosphorylation transforms most of the energy held in nutrients into ATP. They also modulate several other relevant physiological processes, like calcium homeostasis, apoptosis, oxidative stress and steroidogenesis. Mitochondrial structure and function are continuously adapting to conserve cellular metabolic homeostasis (Hebert-Chatelain et al., 2014). Furthermore, the influence of neuronal bioenergetics in brain pathophysiology has been a topic of exhaustive research (Laughlin

et al., 1998; Mattson et al., 2008; MacAskill and Kittler, 2010), although the molecular mechanisms linking mitochondrial activity to brain functions are still poorly understood.

GPCRs are one of the largest protein family regulating brain activity. Besides, there are also important evidences that mitochondria contain G proteins (Lyssand and Bajjalieh, 2007; Andreeva et al., 2008), and different studies have demonstrated the intra-mitochondrial localization of potential downstream effectors of G protein signaling, like soluble adenylyl cyclase (Zippin et al., 2003), phosphodiesterase (Acin-Pérez et al., 2009, 2011) and protein kinase A (PKA) (Ryu et al., 2005). In accordance, mitochondria produce cAMP (Chen et al., 2004; Helling et al., 2008; Acin-Pérez et al., 2009, 2011). Also, intra-mitochondrial $G_{\alpha i}$-protein activation by $mtCB_1$ receptors leads to the inhibition of soluble adenylyl cyclase and, therefore, to a decrease in intra-mitochondrial PKA activity (Hebert-Chatelain et al., 2016). Thus, the presence of functional $mtCB_1$ receptors in different tissues (Aquila et al., 2010; Koch et al., 2015; Hebert-Chatelain et al., 2016; Mendizabal-Zubiaga et al., 2016; Gutiérrez-Rodríguez et al., 2018), endorses the contribution of the ECS to key bioenergetic processes in the CNS. Actually, $mtCB_1$ receptors modulate the activation of cellular respiration and energy production in mouse hippocampal neurons (Hebert-Chatelain et al., 2016). Mitochondrial dysfunction can cause degenerative diseases, stroke or disorders associated with ageing, so it is important to determine the mitochondrial effects of cannabinoids to open new perspectives in the potential therapeutic use of cannabinoids in CNS disease. Therefore, it is crucial to decipher the distribution of CB_1 receptors in neuronal and astroglial mitochondria in the healthy and diseased brain. In this sense, activation of $mtCB_1$ receptors in astrocytes hampers the metabolism of glucose and the production of lactate in the brain, resulting in altered neuronal functions and impaired social interactions (Jimenez-Blasco et al., 2020). This publication to which we have contributed with the anatomical evidence of astroglial $mtCB_1$ receptors in several brain structures, suggests that $mtCB_1$ receptor signaling can directly regulate astroglial glucose metabolism to fine-tune neuronal activity and behavior in mice (Jimenez-Blasco et al., 2020).

2.3. HIGH RESOLUTION ELECTRON MICROSCOPY

To localize CB_1 receptors in different cell types and/or subcellular compartments is extremely difficult because CB_1 is not uniformly distributed throughout the brain regions expressing it (Busquets-Garcia et al., 2015). In the 1990´s, autoradiography of radioligand binding ([3H] CP55,940) was used to assess qualitatively and quantitatively cannabinoid receptors in the brain (Herkenham et al., 1990). When the CB_1 receptor was cloned, *in situ* hybridization techniques were applied to study the CB_1 mRNA distribution in the CNS (Mailleux and Vanderhaeghen, 1992; Matsuda et al., 1993; Marsicano and Lutz, 1999). Later, the Mackie laboratory raised polyclonal antibodies against a specific N-terminal amino acid sequence of the CB_1 receptor protein (Twitchell et al., 1997) and soon after a new CB_1 receptor antiserum was raised against C-terminal amino acid sequence of the rat CB_1 receptor (Egertova et al., 1998). These immunological tools combined with the proper histochemical techniques for light microscopy permitted to visualize the pattern of CB_1 receptor-like immunoreactivity in the brain (Egertova et al., 1998; Tsou et al., 1998). However, the precise cellular and subcellular distribution of the CB_1 receptor remained unknown at that time. Then, the pre-embedding immunohistochemical technique for electron microscopy emerged as a very valuable tool for the study of the exact CB_1 receptor localization in brain and peripheral organs. This method made it possible to demonstrate that CB_1 receptors are not distributed homogenously throughout brain cell types and subcellular compartments, as the CB_1 receptor concentrates at inhibitory GABAergic synaptic terminals (Katona et al., 1999, 2000; Kawamura et al., 2006; Ludányi et al., 2008; Marsicano and Kuner, 2008; Katona and Freund, 2012; De-May and Ali, 2013; Steindel et al., 2013; Hu and Mackie, 2015), is at low levels in glutamatergic synaptic terminals (Marsicano et al., 2003; Domenici et al., 2006; Katona et al., 2006; Monory et al., 2006; Takahashi and Castillo, 2006; Kamprath et al., 2009; Bellocchio et al., 2010; Puente et al., 2011; Reguero et al., 2011; Ruehle et al., 2013; Soria-Gómez et al., 2014) and in astrocytes (Navarrete and Araque, 2008, 2010; Stella, 2010; Han et al., 2012; Bosier et al., 2013; Metna-Laurent and Marsicano, 2015; Viader et al., 2015; Oliveira Da Cruz et al., 2016; Jimenez-Blasco et al., 2020). Moreover, the amount of the CB_1 receptor expression does not directly correspond with its importance in a physiological context, as low and very low CB_1 receptor levels passing

unaware in brain cell types or subcellular compartments (Katona et al., 1999, 2000; Hájos et al., 2001) have functional and behavioral relevance (Busquets-Garcia et al., 2018).

Nevertheless, the pre-embedding immunogold method has limitations: it is only semi-quantitative because labeling does not correlate with the exact localization of the antigen and not all epitopes are revealed with the technique. However, the pre-embedding method was improved by the development of ultra-small gold-labeled secondary conjugates (Nanogold®) combined with silver enhancement, making it possible to detect epitopes deeper into tissue thus reducing the intrinsic limitation of antibody penetration and molecule detection and increasing the resolution of receptor localization.

The pre-embedding immunogold method in combination with immunoperoxidase and the chromogen 3,3´-diaminobenzidine (DAB) can reveal at high resolution protein co-localizations with cell specificity. This double immunolabeling is often used to decipher the localization of CB_1 receptors in different neuronal and glial cells, together with specific protein markers expressed by particular cell types. In this manner, labeled cells filled with DAB in their cell bodies and/or projections can be distinguished from others. For example, GFAP is routinely used to identify astrocytes in the electron microscope to analyze the distribution of astrocytic CB_1 receptors (Eng, 1985; Eng et al., 2000; Hol and Penky, 2015; Gutiérrez-Rodríguez et al., 2018; Bonilla-Del Río et al., 2019). However, due to its filament nature, GFAP immunolabeling does not show the complete surface of the astrocyte. Alternatively, the glutamate aspartate transporter (GLAST) also known as the excitatory amino acid transporter 1 (EAAT1), stands as a good marker to visualize the fine astrocytic projections in the electron microscope (Storck et al., 1992; Arriza et al., 1994; Danbolt, 2001; Zhou and Danbolt, 2014, Danbolt et al., 2016), as it is the only EAAT family member selectively expressed in astroglial cells in the CNS (Danbolt, 1994; Danbolt et al., 2016). GLAST is abundantly expressed throughout membranes of astrocytic processes localized preferentially around excitatory synapses (Cholet et al., 2002), but it is also in cell bodies membranes (Sullivan et al., 2007). Besides, as both too much and too little glutamate is harmful for brain function (Zhou and Danbolt, 2014), GLAST and other EAATs are essential in CNS being widely expressed in different brain

areas. Methodologically, however, the use of GLAST versus GFAP antibodies as astroglial markers has not been assessed for the localization of CB_1 receptors in astrocytes in the electron microscope.

2.4. ECS AND SYNAPTIC PLASTICITY

The ECS is a key modulator of synaptic transmission and participates in synaptic plasticity. Synaptic transmission regulation induced by eCBs happens in both the short- and long-term. Thus, synaptic modifications occurring within seconds are eCB-mediated short-term changes, that can be depolarization-induced suppression of excitation (DSE) or inhibition (DSI) depending on whether eCBs affect glutamatergic or GABAergic terminals, respectively (Kano et al., 2009; Castillo et al., 2012). Synaptic changes taking place from minutes to hours occur in response to different forms of pre- or postsynaptic activity at both excitatory and inhibitory synapses (Araque et al., 2017). These changes can be either LTD or long-term potentiation (LTP) of synaptic transmission. Thus, eCBs are powerful mediators of synaptic function through the brain and have proved to modulate numerous brain functions like cognition, motor control, emotion, reward or feeding.

2.4.1. Hippocampal plasticity

The hippocampus is involved in the processing of declarative/explicit memories and is a key component for regulation of cognitive-related behaviors and long-term memory processing (Aggleton and Brown, 1999; Eichenbaum, 2000; Eichembaum et al., 2012; Peñasco et al., 2019, 2020). Collectively, the ECS plays a crucial role in long-term synaptic plasticity in the hippocampus and throughout the brain, and underlies learning and memory formation (Lafourcade et al., 2007; Castillo et al., 2012; Peñasco et al., 2019, 2020; Fontaine et al., 2020; Egaña-Huguet et al., 2021). Cortical inputs encoding spatial information converge into the dentate gyrus (DG) via the medial perforant path (MPP) and lateral perforant path (LPP) (Peñasco et al., 2019). The glutamatergic synapses made by the MPP axon terminals with the granule cell (GC) dendritic spines in the middle 1/3 of the dentate molecular layer (DML) (Grandes and Streit, 1991) are capable of sustaining LTD (Christie and Abraham, 1994), show paired-pulse depression at low stimulus intensities (Petersen et al., 2013) and exhibit distinct forms of eCB-dependent synaptic plasticity (Chávez et al., 2010; Peñasco et al., 2019; Fontaine et al., 2020). Our laboratory has discovered a long-lasting CB_1 receptor-dependent depression of MPP-GC excitatory synapses (eCB-eLTD) (Peñasco et al., 2019). The stimulation used

for the eCB-eLTD induction was previously used to consistently induce eCB-dependent eLTD in the prefrontal cortex and bed nucleus of the striatal terminalis (BNST) (Lafourcade et al., 2007; Puente et al., 2011). Interestingly, the eCB-eLTD magnitude was unchanged after bath application of the NMDA receptor antagonist DL-APV, unlike at other synapses (Sjöström et al., 2003; Bender et al., 2006). Finally, we also found that 2-AG was responsible for the eCB-eLTD through the activation of presynaptic CB_1 receptors located on MPP terminals (Peñasco et al., 2019).

2.4.2. Prefrontal cortex plasticity

Higher-order executive tasks depend on the PFC, the brain region most elaborated in primates (Puig and Gulledge, 2011). It participates in learning (Pasupathy and Miller, 2005; Antzoulatos and Miller, 2011), memory (Warden and Miller, 2010), categorization (Freedman et al., 2001; Antzoulatos and Miller, 2011), inhibitory control (Chudasama et al., 2003; Dalley et al., 2011) or cognitive flexibility (Clarke et al., 2004; Gruber et al., 2010; Rygula et al., 2010), among other functions. Cannabinoids have deleterious effects on PFC-mediated functions and multiple evidences link ECS, cannabis use and schizophrenia, a disease in which PFC is altered (Ujike and Morita, 2004; Lafourcade et al., 2007). Similar to other brain regions (Kano et al., 2009; Katona and Freund, 2012), the highest concentration of CB_1 mRNA was found in PFC interneurons. CB_1 receptor immunoreactivity was also present in glutamatergic fibers surrounding pyramidal neurons distributed in the deep (layers V/VI) and superficial layers (layer II/III) of the PFC (Egertová and Elphick, 2000; Lafourcade et al., 2007; Araque et al., 2017). Interestingly, a type of eCB-mediated LTD was observed in layers V/VI excitatory inputs that involved CB_1 receptors, postsynaptic mGluR5, phospholipase C, postsynaptic Ca^{2+} and 2-AG (Lafourcade et al., 2007).

2.5. ECS AND EPILEPSY

Epilepsy is a common neurological condition that causes spontaneous recurrent seizures and affects approximately 1% of the adult population (Leo et al., 2016; Reddy and Golub, 2016). Epileptic seizures are abnormal electrical discharges that can originate from a variety of brain regions and can alter behavior, consciousness and sensation (Reddy and Golub, 2016). They are classified into partial and generalized seizures (Reddy, 2014; Reddy and Golub, 2016). Epileptogenesis is the process by which a normal brain becomes progressively epileptic owing to an injury or other risk factors such as stroke, infection or prolonged seizures. The disease can also develop from abnormal neural wiring, imbalance between excitatory and inhibitory neurotransmitters, or a combination of them (Reddy and Golub, 2016).

To date, no drug therapies exist for curing epilepsy. However, symptomatic relief can be reached for up to 70% of patients (Reddy and Golub, 2016). A wide variety of antiepileptic drugs (AEDs) is used to achieve symptomatic seizure control; however, between 25% and 40% of epileptic patients suffer from refractory seizures resistant to current therapies (Sillanpää and Schmidt, 2012; Reddy and Golub, 2016). So, the search for new therapeutic targets is crucial for treating effectively the disease (Wilcox et al., 2013).

As already stated, the ECS plays a key role in the brain where it regulates many physiological and pathological conditions (Di Marzo et al., 1998; Alger, 2006; Mackie and Stella, 2006; Kano et al., 2009; Castillo et al., 2012). Cannabis has been medically used for centuries in the treatment of neurological disorders, including epilepsy (Friedman and Devinsky, 2015; Rosenberg et al., 2015; Leo et al., 2016). Some studies have focused their attention on understanding the potential role that the ECS function and dysfunction could have controlling or favoring seizures (Blair et al., 2015). Animal models have demonstrated that activation of CB_1 receptors decreases seizure severity. Hence, conditional mutant mice lacking CB_1 receptors in principal forebrain excitatory neurons (but not in interneurons) show more severe kainate-induced seizures compared to WT controls (Marsicano et al., 2003), and CB_1 receptors in hippocampal glutamatergic but not GABAergic inputs were necessary and sufficient to protect against kainate-induced seizures (Monory et al., 2006). Moreover, CB_1 receptor overexpression

reduced mortality and the severity of kainate-induced seizures in the hippocampus (Guggenhuber et al., 2010). Altogether, these results demonstrate that CB_1 receptors could control seizures and protect neurons from cell death and reactive gliosis (Rosenberg et al., 2015).

Information processing is also profoundly shaped by rapid and reciprocal astrocyte-neuron communication operating on short time scales of milliseconds to minutes. Thereby, it is intuitive that long-term changes of astrocyte structure or function over weeks and months have an impact on neuronal signaling in the brain. Astrogliosis is a prominent feature in later stages of epileptic patients and animal models (Henneberger, 2017). The term describes a number of changes in astrocyte density, morphology, biochemistry and physiology associated with epilepsy and other diseases (Sofroniew and Vinters, 2010; Pekny and Pekna, 2014). Some of the functional modifications in astrocytes (e.g., altered K^+ or glutamate clearance) can contribute to the generation of seizures. Thus, several recent studies suggest a causal role of astrogliosis in epileptogenesis, as persistent astrogliosis and ensuing changes in astrocyte function are sufficient to render neuronal networks susceptible to the development of spontaneous seizures after days or weeks (Ortinski et al., 2010; Robel et al., 2015; Henneberger, 2017). CB_1 receptors are expressed in astrocytes possibly playing important roles in the course of the disease. Therefore, CB_1 receptors in astrocytes might be considered a potential target to treat epilepsy.

WORKING HYPOTHESIS

Astrocytes are known to modulate neuronal activity playing crucial roles in brain activity (Araque et al., 1999; Haydon and Carmignoto, 2006; Perea et al., 2009; Gómez-Gonzalo et al., 2014). Astrocytes express different neurotransmitter receptors that sense synaptic activity and respond to it with the release of gliotransmitters which, in turn, regulate neuronal excitability and synaptic transmission (Perea and Araque, 2005a; Perea and Araque, 2010; Araque and Navarrete, 2010).

CB_1 receptors are expressed in astrocytes where their functional importance has been demonstrated (Rodríguez et al., 2001; Navarrete and Araque, 2008, 2010; Stella, 2010; Han et al., 2012; Bosier et al., 2013; Han et al., 2012; Bosier et al., 2013; Gómez-Gonzalo et al., 2014; Navarrete et al., 2014; Metna-Laurent and Marsicano, 2015; Viader et al., 2015; Oliveira da Cruz et al., 2016; Gutiérrez- Rodríguez et al., 2017; Bonilla-del Río et al., 2019, 2021). CB_1 receptor-mediated astrocytic functions are highly dependent on the CB_1 receptor distribution in astrocytes closely related to neuronal compartments, particularly at the synapses. However, little is known about the expression and precise localization of CB_1 receptors in astrocytes.

GFAP is a specific astrocytic cytoskeletal protein that is commonly used as astroglial marker to study at high resolution the receptor distribution in astrocytes (Gutiérrez-Rodríguez et al., 2017; Bonilla-del Río et al., 2019, 2021). On the other hand, GLAST is known to be specifically distributed throughout the astrocytic membranes (Danbolt, 1994; Sullivan et al., 2007; Danbolt et al., 2016). In this context, we hypothesized that GLAST is a better marker than GFAP for the identification of the fine astroglial processes surrounding synapses where astrocytic receptors are readily exposed to transmitters released at the synapses. Furthermore, mitochondria in astrocytes localize CB_1 receptors like mitochondria in neurons do (Bénard et al., 2012; Hebert-Chatelain et al., 2016; Gutiérrez-Rodríguez et al., 2018; Bonilla-del Río et al., 2019; Jimenez-Blasco et al., 2020). However, the density of CB_1 receptors detected in astroglial mitochondria might depend on the identification of the astroglial processes with good and specific markers like GLAST, instead of GFAP which is restricted to cell bodies and main astrocytic branches.

Finally, functional CB_1 receptors are involved in different forms of synaptic plasticity throughout the brain. In previous studies, LFS induced eCb-eLTD at excitatory synapses

in PFC and the dentate gyrus of 11–12-week-old young adult mice (Lafourcade et al., 2007; Peñasco et al., 2019, 2020). However, the eCB-dependent synaptic plasticity elicited by LFS (10 min, 10 Hz) might change when the animal ages, as the loss in hippocampal neurons caused by ageing might impact on CB_1 receptor expression. Actually, cognitive decline accelerates in mice lacking CB_1 receptors (Bilkei-Gorzo et al., 2005).

OBJECTIVES

The general goal of my thesis was to investigate de ECS in rodent brain by high resolution microscopy and electrophysiology, focusing on the hippocampal CA1 region and the prelimbic PFC. The specific objectives were to:

1.- Compare the astroglial markers GLAST versus GFAP for a better localization of CB_1 receptors in astrocytes.

2.- Study the CB_1 receptor distribution in neuronal and astrocytic compartments in the prelimbic PFC of Glu-CB_1-WT/KO and GABA-CB_1-WT/KO mice.

3.- Investigate the CB_1 receptor distribution in neuronal and astrocytic compartments in the prelimbic PFC of GFAP-CB_1-WT/KO mice.

4.- Assess the density of mtCB_1 receptors in mitochondria of neurons and astrocytes in different brain regions (CA1, PFC, nucleus accumbens, piriform cortex).

5.- Evaluate eCB-dependent excitatory synaptic plasticity at MPP and PFC synapses of 14-week-old GFAP-CB_1-WT and GFAP-CB_1-KO mice.

6.- Explore eCB-dependent synaptic plasticity in GFAP-CB_1-WT/KO mice exposed to kainate-induced seizures.

MATERIALS AND METHODS

4.1. ETHICS STATEMENT

The experiments were performed in the *Laboratory of Ultrastructural and Functional Neuroanatomy of the Synapse*, Department of Neurosciences, University of the Basque Country UPV/EHU. All protocols were approved by the Committee of Ethics for Animal Welfare of the University of the Basque Country (CEEA/M20/2015/093). The animals were treated according to the European Community Council Directive of 22nd September 2010 (2010/63/UE) and the Spanish legislation (RD/53/2013 and Ley 6/2013). All efforts were made to minimize pain and suffering and to reduce the number of animals used.

Mice were housed in pairs or groups of maximum of three littermates in standard plexiglass cages (17 cm x 14.3 cm x 36.3 cm) and were allowed to acclimate to the environment for at least 1 week. They were maintained at standard conditions with food and tap water ad libitum throughout all experiments, in a room with constant temperature (22°C) and 12 h: 12 h light/dark cycle with lights off at 9 pm.

4.2. RESEARCH ANIMALS

4.2.1 CB_1 receptor mutant lines

4.2.1.1. C57BL/6 mice

8-14-week-old C57BL/6 mice (The Jackson Laboratory and Janvier labs) received at the University of the Basque Country were available after a week of quarantine.

4.2.1.2. CB_1-KO mice

Mice lacking CB_1 receptors (CB_1-KO) were generated and genotyped as previously described (Marsicano et al., 2002). Conditional mutant mice were obtained by crossing the respective Cre expressing mouse line with $CB_1^{f/f}$ mice (Marsicano et al., 2003) using a three-step breeding protocol (Monory et al., 2006). All mice were in a predominant C57BL/6N background.

4.2.1.3. Glu-CB_1-KO: Conditional mutant mice bearing a selective deletion of the CB_1 receptor in cortical glutamatergic neurons

NEX is a helix-loop-helix transcription factor of embryonic neural progenitors of cortical glutamatergic neurons (Wu et al., 2005). In the adult brain, NEX is only expressed in mature cortical glutamatergic neurons and to a much lesser extent in neurons of subcortical regions (Barthalomä and Nave, 1994). Cre expression under the control of the regulatory sequences of NEX in mutant mice generated by knock-in into the NEX locus (NEX-Cre mice), leads to the specific deletion of “floxed” alleles in forebrain neurons (Kleppisch et al., 2003). In that way, $CB_1^{f/f,\ NEX\text{-}Cre}$ mice (Glu-CB_1-KO) (Monory et al., 2006) were obtained by crossing $CB_1^{f/f}$ with NEX-Cre mice (Schwab et al., 2000; Kleppisch et al., 2003). $CB_1^{f/f}$ females were crossed with $CB_1^{f/f,\ NEX\text{-}Cre}$ males to obtain mutant mice.

4.2.1.4. GABA-CB_1-KO: conditional mutant mice bearing a selective deletion of the CB_1 receptor in GABAergic neurons

The *Dlx5/Dlx6* genes are homeobox genes that are expressed in differentiating and migrating forebrain GABAergic neurons during the embryonic development (Stühmer, 2002). $CB_1^{f/f,\ Dlx5/6\text{-}Cre}$ mice were obtained by crossing Dlx5/6-Cre (Zerucha et al., 2000) with $CB_1^{f/f}$ mice. In this way, the expression of Cre recombinase under the control of the regulatory sequences of *Dlx5/6* genes drives to a recombination of loxP sites in GABAergic neurons, leading to GABA-CB_1-KO mice (Monory et al., 2006). Mutants were obtained by crossing $CB_1^{f/f}$ females with $CB_1^{f/f,\ Dlx5/6\text{-}Cre}$ males.

4.2.1.5. GFAP-CB_1-KO: conditional mutant mice bearing a selective deletion of CB_1 receptor in astrocytes

To obtain transgenic $CB_1^{f/f,\ GFAP\text{-}CreERT2}$ mice (GFAP-CB_1-KO) lacking CB_1 receptors in astrocytes, (Hirrlinger et al., 2006), mice carrying CB_1 receptor "floxed" sequence (Marsicano et al., 2003) were crossed with transgenic mice expressing inducible version of Cre recombinase CreERT2 under the control of the human glial fibrillary acid protein (GFAP-CreERT2 mice). This mouse model allows the on-demand control of astroglial CB_1 receptor recombination in adult mice (Han et al., 2012).

4.3. PRE-EMBEDDING IMMUNOLABELING FOR ELECTRON MICROSCOPY

The protocol published by our laboratory was used in all the experiments (Puente et al., 2019):

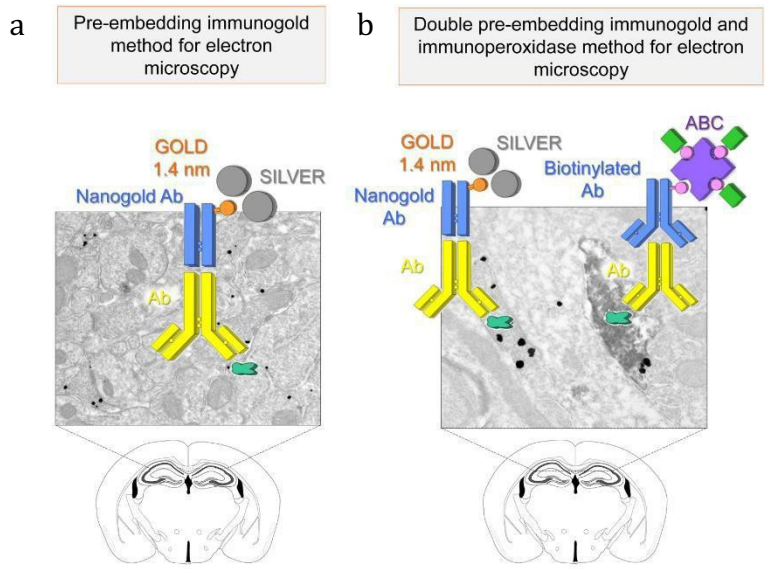

Figure 1. Immunolabeling methods used for high-resolution electron microscopy. (Adapted with permission from Puente et al., 2019).

4.3.1 Tissue preservation

1. Animals were deeply anesthetized (at least n=3) using intraperitoneal injection of a mixture of ketamine/xylazine (80/10 mg/kg body weight).
2. Mice were transcardially perfused at room temperature (RT) (20-25°C) through the left ventricle with phosphate buffered saline (PBS) (0.1 M, pH 7.4) for ~ 20 seconds, followed by the iced-cooled fixative solution made up of 4% formaldehyde (freshly depolymerized from paraformaldehyde), 0.2% picric acid and 0.1% glutaraldehyde in phosphate buffer (PB) (0.1 M, pH 7.4) for 10-15 minutes (min).
3. Brains were carefully removed from the skull and post-fixed in the fixative solution for one week at 4°C. Finally, they were stored in fixative solution diluted in 0.1 M PB (1:10) with 0.025% sodium azide at 4°C until use.

4. Coronal sections of the brains were cut at 50 μm in a vibratome, and collected in 0.1 M PB (pH 7.4) at RT. Vibrosections were stored in 12-well cell culture plates at 4°C in 0.1 M PB (pH 7.4) with 0.025% sodium azide, until use.

4.3.2. Single pre-embedding immunogold method for electron microscopy

1. Two or three vibrosections per brain containing the area of interest were selected and placed in a new 12-well cell culture plate with 0.1 M PB (pH 7.4).
2. Samples were pre-incubated in blocking solution on a shaker (300 rpm) for 30 min at RT. Blocking solution was made up of 10% bovine serum albumin (BSA), 0.02% saponin and 0.1% sodium azide in tris-hydrogen chloride buffered saline (TBS) 1X (pH 7.4; 1 ml/well).
3. Sections were incubated with guinea pig polyclonal anti-CB_1 receptor antibody, mouse monoclonal anti-GFAP antibody, or rabbit polyclonal anti-GLAST antibody. All antibodies were diluted in 10% BSA/TBS 1X containing 0.004% saponin and 0.1% sodium azide. Incubation time was 2 days at 4°C on an orbital shaker (0.5-1 ml/well).
4. They were washed in 1% BSA/TBS 1X to remove the excess of primary antibody (3 x 1 min and 2 x 10 min) on a shaker at RT (1 ml/well).
5. Sections were incubated with the corresponding 1.4 nm gold-conjugated anti-guinea pig, anti-mouse or anti-rabbit secondary antibodies. Antibodies were diluted and incubated in 1% BSA/TBS 1X with 0.004% saponin on a shaker for 3 h at RT (1 ml/well).
6. They were washed in 1% BSA/TBS 1X to remove the excess of secondary antibodies (3 x 1 min and 2 x 10 min) on a shaker at RT (1 ml/well).
7. Samples were kept in 1% BSA/TBS 1X overnight on a shaker at 4°C (1 ml/well).
8. They were post-fixated with 1% glutaraldehyde prepared in TBS 1X for 10 min at RT (1 ml/well).
9. Three washes of 10 min in 0.1 M PB were made on a shaker at RT (1 ml/well).
10. Sections were transferred to test tubes for next step.

11. Gold particles were silver intensified with the HQ Silver kit (Nanoprobes Inc., Yaphank, NY, USA) for 10-12 min in the dark (0.8-1 ml/test tube).
12. Three washes of 1 min in double distillated water were made in the dark (1 ml/test tube).
13. They were followed by three washes of 10 min in 0.1 M PB (pH 7.4; 1 ml/test tube).
14. Samples were transferred to glass vials (15 ml, 3 cm x 5 cm; 1 ml/vial).
15. Samples were osmified for 20 min with 1% osmium tetroxide in 0.1 M PB (pH 7.4; 1 ml/vial).
16. They were washed in 0.1 M PB (pH 7.4; 3 x 1 min and 2 x 10 min; 1 ml/vial).
17. Sections were dehydrated in graded ethanol (50%, 70%, 96%; 5 min each), finishing in 100% ethanol for three times (5 min each; 1 ml/vial).
18. Ethanol was cleared in propylene oxide for three times (5 min each; 1 ml/vial).
19. Sections were embedded in 1:1 mixture of propylene oxide and Epon resin 812, and kept overnight on a shaker at RT (1 ml/vial).
20. They were embedded in pure Epon resin 812 for 2 h at RT.
21. Sections were placed between two glass slides and wrapped in aluminum foil.
22. Resin-embedded sections were polymerized in an oven for 2 days at 60°C.
23. The area of interest was cut and glued to a block of pure resin Epon 812.
24. Tissue blocks were trimmed and 1 μm semi-thin sections were cut on an ultra-microtome with a diamond knife.
25. Ultra-thin sections of 50 nm were cut with another diamond knife and collected on nickel mesh grids.
26. Samples were stained with 2.5% lead citrate for 20 min at RT.
27. They were washed in double distillated water (3 x 1 min and 2 x 10 min).

28. Samples were examined under a JEOL JEM-1400 Plus transmission electron microscope (JEOL Canada).
29. Tissue was photographed by using a digital Gatan SC1000 digital camera (Gatan USA).

4.3.3. Single pre-embedding immunoperoxidase method for electron microscopy

1. Two or three sections per brain containing the area of interest were selected and placed in a new plate in 0.1 M PB.
2. Samples were pre-incubated in blocking solution on a shaker (300 rpm) for 30 min at RT. Blocking solution was composed of 10% BSA, 0.02% saponin and 0.1% sodium azide in TBS 1X (pH 7.4; 1 ml/well).
3. Sections were incubated with guinea pig polyclonal anti-CB_1 receptor antibody, mouse monoclonal anti-GFAP antibody, or rabbit polyclonal anti-GLAST antibody. All antibodies were diluted in 10% BSA/TBS 1X containing 0.004% saponin and 0.1% sodium azide. Incubation time was 2 days at 4°C on an orbital shaker (0.5-1 ml/well).
4. They were washed in 1% BSA/TBS 1X to remove the excess of primary antibody (3 x 1 min and 2 x 10 min) on a shaker at RT (1 ml/well).
5. Tissue was incubated with biotinylated anti-mouse or anti-rabbit secondary antibodies in 1% BSA/TBS 1X with 0.004% saponin on a shaker for 3 h at RT (1 ml/well).
6. It was washed in 1% BSA/TBS 1X to remove the excess of secondary antibodies (3 x 1 min and 2 x 10 min) on a shaker at RT (1 ml/well).
7. Samples were incubated in avidin-biotin-peroxidase complex (1:50; Elite, Vector Laboratories, Burlingame, CA, USA) prepared in washing solution for 1.5 h on a shaker at RT (1 ml/well).
8. Several washes were made in 1% BSA/TBS 1X (3 x 1 min and 2 x 10 min) on a shaker at RT (1 ml/well).
9. Samples were kept in 1% BSA/TBS 1X overnight on a shaker at 4°C (1 ml/well).

10. They were post-fixated with 1% glutaraldehyde prepared in TBS 1X for 10 min at RT (1 ml/well).
11. Three washes of 10 min in 0.1 M PB (pH 7.4) were made (1 ml/well).
12. Tissue was incubated in 0.05% diaminobenzidine (DAB) and 0.01% hydrogen peroxide prepared in 0.1 M PB (pH 7.4) for 3 min at RT (1 ml/well).
13. Sections were washed in 0.1 M PB (pH 7.4; 3 x 1 min and 2 x 10 min; 1 ml/well).
14. They were transferred to glass vials (15 ml, 3x5 cm).
15. Samples were osmified for 20 min with 1% osmium tetroxide in 0.1 M PB (pH 7.4; 1 ml/vial).
16. They were washed in 0.1 M PB (pH 7.4; 3 x 1 min and 2 x 10 min; 1 ml/vial).
17. Samples were dehydrated in graded ethanol (50%, 70%, 96%; 5 min/each), finishing in 100% ethanol for three times (5 min each; 1 ml/vial).
18. Ethanol was cleared in propylene oxide for three times (5 min each; 1 ml/vial).
19. Sections were embedded in 1:1 mixture of propylene oxide and Epon resin 812, and kept overnight on a shaker at RT (1 ml/vial).
20. They were embedded in pure Epon resin 812 for 2 h at RT.
21. Sections were placed between two glass slides and wrapped in aluminum foil.
22. Resin-embedded tissue was polymerized in an oven for 2 days at 60°C.
23. The area of interest was cut and glued to a block of pure resin Epon 812.
24. Tissue blocks were trimmed and 1 μm semi-thin sections were cut on ultra-microtome with a diamond knife.
25. Ultra-thin sections of 50 nm were cut with another diamond knife and collected on nickel mesh grids.
26. Samples were stained with 2.5% lead citrate for 20 min at RT.
27. They were washed in double distillated water (3 x 1 min and 2 x 10 min).

28. Samples were examined under the JEOL JEM-1400 Plus transmission electron microscope.
29. Tissue was photographed with the Gatan SC1000 digital camera.

4.3.4. Double pre-embedding immunogold and immunoperoxidase method for electron microscopy

1. Two or three sections per brain containing the area of interest were selected and placed in a new plate in 0.1 M PB.
2. Samples were pre-incubated in blocking solution on a shaker (300 rpm) for 30 min at RT. Blocking solution contained 10% BSA, 0.02% saponin and 0.1% sodium azide in TBS 1X (pH 7.4; 1 ml/well).
3. Sections were incubated with the combination of two primary antibodies: goat anti-CB_1 receptor with mouse anti-GFAP; or guinea pig anti-CB_1 receptor with rabbit anti-GLAST. All antibodies were prepared in 10% BSA/TBS 1X containing 0.004% saponin and 0.1% sodium azide. Incubation time was 2 days at 4°C on an orbital shaker (0.5-1 ml/well).
4. They were washed in 1% BSA/TBS 1X to remove the excess of primary antibody (3 x 1 min and 2 x 10 min) on a shaker at RT (1 ml/well).
5. Sections were incubated with the combination of 1.4 nm conjugated anti-goat and biotinylated anti-mouse secondary antibodies, or 1.4 nm gold-conjugated anti-guinea pig and biotinylated anti-rabbit secondary antibodies in 1% BSA/TBS 1X with 0.004% saponin on a shaker for 3 h at RT (1 ml/well).
6. They were washed in 1% BSA/TBS 1X to remove the excess of secondary antibodies (3 x 1 min and 2 x 10 min) on a shaker at RT (1 ml/well).
7. Samples were incubated in avidin-biotin-peroxidase complex (1:50) prepared in washing solution for 1.5 h at on a shaker at RT (1 ml/well).
8. Several washes in 1% BSA/TBS 1X (3 x 1 min and 2 x 10 min) were made on a shaker at RT (1 ml/well).
9. Samples were kept in 1% BSA/TBS 1X overnight on a shaker at 4°C (1 ml/well).

10. They were post-fixated with 1% glutaraldehyde prepared in TBS 1X for 10 min at RT (1 ml/well).
11. Three washes of 10 min in double distillated water were made on a shaker at RT (1 ml/well).
12. Sections were transferred to test tubes for next step.
13. Gold particles were silver intensified with the HQ Silver kit for 10-12 min in the dark (1 ml/test tube).
14. Three washes of 1 min in double distillated water were made in the dark (1 ml/test tube).
15. They were followed by three washes of 10 min in 0.1 M PB (pH 7.4).
16. Samples were transferred to glass vials (15 ml, 3x5 cm; 1 ml/vial).
17. Tissue was incubated in 0.05% DAB and 0.01% hydrogen peroxide prepared in 0.1 M PB (pH 7.4) for 3 min at RT (1 ml/vial).
18. Washes were made in 0.1 M PB (pH 7.4; 3 x 1 min and 2 x 10 min; 1 ml/vial).
19. Samples were osmified for 20 min with 1% osmium tetroxide in 0.1 M PB (pH 7.4).
20. Various washes were made in 0.1 M PB (pH 7.4; 3 x 1 min and 2 x 10 min; 1 ml/vial).
21. Sections were dehydrated in graded ethanol (50%, 70%, 96%; 5 min/each), finishing in 100% ethanol for three times (5 min each; 1 ml/vial).
22. Ethanol was cleared in propylene oxide for three times (5 min each; 1 ml/vial).
23. Sections were embedded in 1:1 mixture of propylene oxide and Epon resin 812, and kept overnight on a shaker at RT (1 ml/vial).
24. They were embedded in pure Epon resin 812 for 2 h at RT.
25. Sections were placed between two glass slides and wrapped in aluminum foil.
26. Resin-embedded sections were polymerized in an oven for 2 days at 60°C.

27. The area of interest was cut and glued to a block of pure resin Epon 812.
28. Tissue blocks were trimmed and 1 μm semi-thin sections were cut on ultra-microtome with a diamond knife.
29. Ultra-thin sections of 50 nm were cut with another diamond knife and collected on nickel mesh grids.
30. Samples were stained with 2.5% lead citrate for 20 min at RT.
31. They were washed in double distillated water (3 x 1 min, 2 x 10 min).
32. Samples were examined with the JEOL JEM-1400 Plus transmission electron microscope.
33. Tissue was photographed with the Gatan SC1000 digital camera.

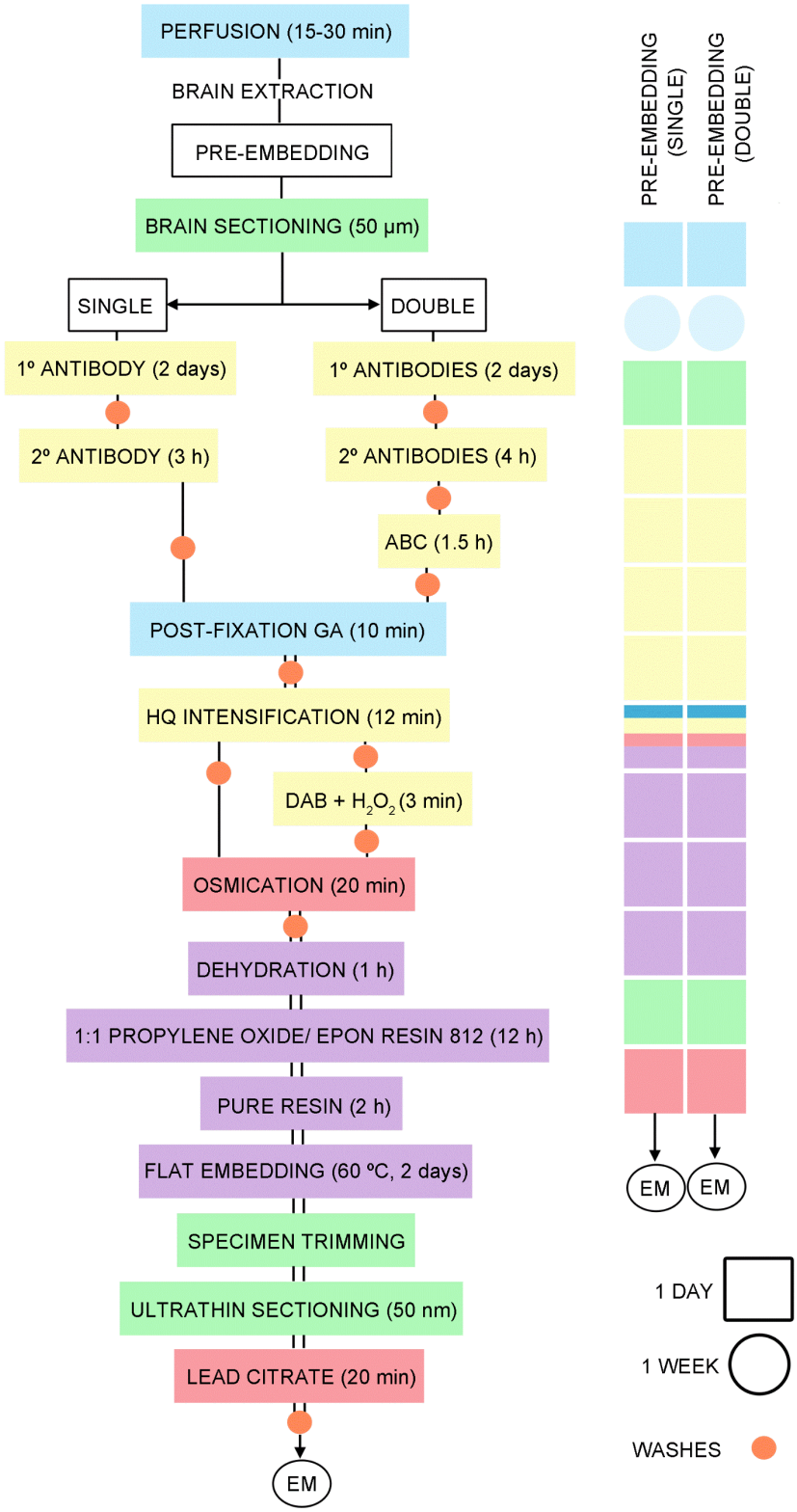

Figure 2. Timeline of the general steps for pre-embedding immunoelectron microscopy techniques (Puente et al., 2019).

Antibody	[Concentration]	Manufacturer; species; catalogue number; RRID
Anti-cannabinoid receptor type-1 (CB_1)	2 μg/ml	Frontier Institute co.; guinea pig polyclonal; CB1-GP-Af530; AB_2571593
Anti-cannabinoid receptor type-1 (CB_1)	2 μg/ml	Frontier Institute co.; goat polyclonal; CB1-Go-Af450; AB_2571592
Anti-glial fibrillary acidic protein (GFAP)	20 ng/ml	Sigma-Aldrich; mouse monoclonal; G3893; AB_257130
Anti-A522 (glutamate aspartate transporter, GLAST)	0.3 μg/ml	Prof. Niels Christian Danbolt, University of Oslo; rabbit polyclonal; Ab#314; AB_2314561

Table 1. Primary antibodies used in pre-embedding methods for electron microscopy.

Antibody	[Concentration]	Manufacturer; species; catalogue number; RRID
Biotinylated anti-mouse	7.5 μg/ml	Vector Labs, horse; BA-2000; AB_2313581
Biotinylated anti-rabbit	7.5 μg/ml	Vector Labs, goat; BA-1000; AB_2313606
1.4 nm gold-conjugated anti-guinea pig IgG (Fab´ fragment)	0.8 μg/ml	Nanoprobes, goat; #2055
1.4 nm gold-conjugated anti-mouse IgG (Fab´ fragment)	0.8 μg/ml	Nanoprobes, goat; #2002
1.4 nm gold-conjugated anti-rabbit IgG (Fab´ fragment)	0.8 μg/ml	Nanoprobes, goat; #2004

Table 2. Secondary antibodies used in pre-embedding methods for electron microscopy.

4.3.5. Semi-quantification of the CB_1 receptor labeling

It was done according to our protocol (Puente et al., 2019). The pre-embedding immunogold method was carried out simultaneously in all mice studied. Furthermore, three replicated experiments were done for each animal. In order to select tissue portions with good and reproducible CB_1 receptor labeling, samples were visualized under a light microscope to ensure the analysis of the same tissue area. In addition, to further standardize the conditions between the labeled sections from different mice, only the first 1.5 μm from section surface was collected and randomly photographed. Sampling was always done carefully and in the same way for all the animals studied.

The excitatory and inhibitory synapses were identified by their ultrastructural features (Puente et al., 2019):

- Excitatory synapses are asymmetrical with postsynaptic densities and presynaptic axon terminals containing clear, abundant and spherical synaptic vesicles.
- Inhibitory synapses are symmetrical with slim postsynaptic membranes and axon terminals containing pleomorphic synaptic vesicles.

Astrocytes and their processes were identified by GFAP or GLAST immunostaining. CB_1 immunoparticles were considered astroglial if they were located on GFAP or GLAST positive membranes.

The proportion of the CB_1 receptor labeling in different compartments was then tabulated. Positive labeling was considered when at least a single CB_1 receptor particle was within 30 nm of the membrane compartment under study. To consider a CB_1 receptor particle belonging to mitochondria, there should be at least 80 nm to the nearest membrane. Image-J software (NIH; RRID:SRC_003070) was used to analyze the distribution of CB_1 receptor immunoparticles in the different compartments. Then, CB_1 particles/100 μm^2 were calculated. The same software was used to identify astrocytic processes and to measure their area and perimeter.

All values were given as mean ± SEM using a statistical software package (GraphPad Prism 8, GraphPad Software Inc., San Diego, USA). The normality test (Kolgomorov-Smirnov normality test) was always run before statistical tests. The potential variability

between mice of the same mutant line was analyzed. Since there were not statistical differences, values of each group were pooled. Data were analyzed using parametric or non-parametric two tailed Student´s t-test or one-way ANOVA with subsequent post-hic analysis (Bonferroni post-test).

4.4. ELECTROPHYSIOLOGY

4.4.1. Research animals

Most of the experiments were done in 8- and 14-week-old C57BL/6J mice (Janvier Labs, Le Genest-Saint-Isle, France). GFAP-CB_1-WT and GFAP-CB_1-KO mice were also used.

4.4.2. Slice preparation

Mice were anesthetized with isoflurane (2-4%) and decapitated. Brains were immediately removed and placed in a sucrose-based solution at 4°C consisting of (in mM): 87 NaCl, 75 sucrose, 25 glucose, 7 $MgCl_2$, 2.5 KCl, 0.5 $CaCl_2$ and 1.25 NaH_2PO_4. 300 μm-thick coronal vibratome sections (Leica Microsistemas S.L.U.) containing the hippocampus or the prefrontal cortex were collected at 32-35°C in artificial cerebrospinal fluid (aCSF) made up of (in mM): 130 NaCl, 11 glucose, 1.2 MgCl, 2.5 KCl, 2.4 $CaCl_2$, 1.2 NaH_2PO_4 and 23 $NaHCO_3$, always equilibrated with 95% O_2/5% CO_2.

4.4.3. Extracellular field recordings

Vibroslices were placed in the recording chamber and superfused (2 ml/min) with the same aCSF also equilibrated with 95% O_2/5% CO_2. All the experiments were carried out at 32-35°C, and picrotoxin (PTX; 100 μM, Tocris Bioscience, UK) was added to aCSF to block $GABA_A$ receptors. For extracellular field recordings, a glass-recording pipette was filled with aCSF.

For recordings in the hippocampal dentate gyrus, the stimulation electrode (borosilicate glass capillaries, Harvard apparatus UK capillaries 30-0062 GC100T-10) was placed in the MPP or mossy cell fibers (MCF) and the recording pipette in the middle 1/3 of the DML. For recordings in the prefrontal cortex, both the stimulation and recording pipettes were placed in layers II/III of the prelimbic cortex.

To evoke field excitatory postsynaptic potential responses (fEPSPs), repetitive control stimuli were delivered at 0.1 Hz (Stimulus Isolater ISU 165, Cibertec, Spain; controlled by a Master-8, with an isolation unit A.M.P.I.). An Axopatch-200B (Axon

Instruments/Molecular Devices, Union City, CA, USA) was used to record the data filtered at 1-2 kHz, digitalized at 5 kHz on a DigiData 1440A interface collected on a PC using Clampex 10.0 and analyzed by using Clamfit 10.0 (all obtained from Axon Instruments/Molecular Devices, Union City, CA, USA). At first, an input-output curve was constructed to select the stimulation intensity for baseline measurements that yielded between 40-60% of the maximal amplitude response. To induce plasticity at excitatory synapses, a low frequency stimulation protocol (LFS; 10 min at 10 Hz) was applied following recording of a steady baseline, as described previously (Lafourcade et al., 2007; Puente et al., 2011; Peñasco et al., 2019).

The magnitude of the fEPSP area was calculated as the percentage change between baseline area (averaged excitatory responses for 10 min before LFS) and last 10 min of stable responses recorded 30 min after the end of LFS. At least 3 mice were used for each experimental condition, and the same mice were used to analyze MPP and PFC synaptic plasticity. The paired-pulse-ratio (PPR) was calculated by averaging the ratio of the fEPSP initial slopes (P2/P1) of 30 pulse pairs (50 msec interpulse interval), where P2 corresponded to fEPSP2 slopes (2^{nd} evoked responses) and P1 to fEPSP1 slopes (1^{st} evoked responses).

4.4.4. Data analysis

All values were given as mean SEM with *p* values and sample size (n). Shapiro-Wilk and Kolmogorov-Smirnov tests were used to confirm normality of all the data. In general, statistical significance between different conditions (baseline versus after drug or stimulation protocol or both) was tested using parametric (two-tailed Student´s t-test) or non-parametric tests (Mann-Whitney). The significance level was set at $p < 0.05$ for all comparisons. All statistical tests were performed with GraphPad Prism (GraphPad Prism 8, GraphPad software Inc, San Diego, USA).

4.4.5. Drugs

All drugs were dissolved in dimethyl sulfoxide (DMSO; Sigma-Aldrich) and were added at the final concentration to the superfusion medium.

Drug	Description	Concentration of use	Incubated time	Supplier
Picrotoxin (PTX)	$GABA_A$ receptor antagonist	[100 μM]	All recording	Tocris BioScience (Bristol, United Kingdom)
AM251	Potent CB_1 receptor antagonist and GPR55 agonist	[4 μM]	20 min of additional incubation	Tocris BioScience (Bristol, United Kingdom)
JZL 184	Potent and selective MAGL inhibitor	[50 μM]	1 h of additional pre-incubation	Tocris BioScience (Bristol, United Kingdom)
THL	Potent inhibitor of DAGLα	[10 μM]	20 min of additional incubation	Tocris BioScience (Bristol, United Kingdom)
URB597	Potent and selective FAAH inhibitor	[2 μM]	20 min of additional incubation	Tocris BioScience (Bristol, United Kingdom)
AMG9810	TRPV1 receptor antagonist	[3 μM]	All recording	Tocris BioScience (Bristol, United Kingdom)
DL-APV	Potent, selective NMDA antagonist; an active form of DL-APV	[50 μM]	All recording	Tocris BioScience (Bristol, United Kingdom)
Latrunculin-A (LAT-A)	G-actin monomer	[0.5 μM]	All recording	Tocris BioScience

	polymerization blocker			(Bristol, United Kingdom)

Table 3. Drugs used in electrophysiological experiments.

4.5. INTRAPERITONEAL KAINIC ACID MODEL OF EPILEPTIC SEIZURES

Kainic acid (KA)-induced seizures is widely used as a model of temporal lobe epilepsy (Lévesque and Avoli, 2013).

4.5.1. Intraperitoneal injection of KA

Day 1. Intraperitoneal saline injection (NaCl 0.9 %; 10 ml/kg). Mice were kept without food and water during 2 h in an unfenced cage with another cage facing down on top.

Day 2. Like day 1, except that the mouse´s nest was removed, let over the grid and put back after the 2 h.

Day 3. Intraperitoneal KA injection (20 mg/kg; 10 ml/kg). Mice were kept like in conditions of days 1 and 2, but the nest was removed and substituted by a new one of identical size and folding.

4.5.2. Behavioral scoring of seizure severity

Mice were scored during 4 hours after injection. Seizure's severity was assessed every 30 minutes according to the modified Racine´s scale (RS) (1972). Racine developed a scale based on the relationship between EEG changes and motor seizures to score seizures in the model of amygdala kindling. Nowadays, RS is still in use and often adapted for a wide variety of seizures and epilepsy models (Clement et al., 2003; Vinogradova and van Rijn, 2008; Lüttjohann et al., 2009).

Seven stages of intensity were defined in the modified Racine's scale based on the behavioral changes displayed by the animals during seizures after being recovered from the effects of the anesthesia: "staring and immobility" (stage 1); "tail extension and forelimb clonus" (stage 2); "rearing and repetitive movements" (stage 3); "rearing and falling" (stage 4); "continuous rearing and falling" (stage 5); "tonic-clonic seizures with loss of posture, jumping and wild running" (stage 6); "death" (stage 7). The maximum score reached by the mouse in each 30 min-time period was taken for the analysis. Differences between GFAP-CB_1-WT and GFAP-CB_1-KO mice were analyzed by Two-Way ANOVA test. Results were displayed as mean ± SEM using a statistical

software package (GraphPad Prism, GraphPad Software Inc, San Diego, USA). Values of $p < 0.05$ were considered statistically significant.

RESULTS

5.1. COMPARISON OF GFAP VERSUS GLAST AS ASTROGLIAL MARKERS FOR ELECTRON MICROSCOPY

5.1.1. Localization of GFAP and GLAST labeling with immunoelectron microscopy

To analyze the precise localization of GFAP and GLAST within astrocytes, I labeled WT mouse tissues with our immunogold method for electron microscopy. Gold particles intensified with silver facilitated to decipher the exact localization of both astroglial markers. I observed that while GFAP-metal particles were located in the cytoplasm of cell bodies and main thick astroglial projections (figure 1a), GLAST labeling was distributed along the plasma membrane of astrocytes, including cell bodies and the smallest astrocytic projections in close contact with neurons, capillaries and other glial cells, covering altogether a much broader labeled area than GFAP (figure 1b).

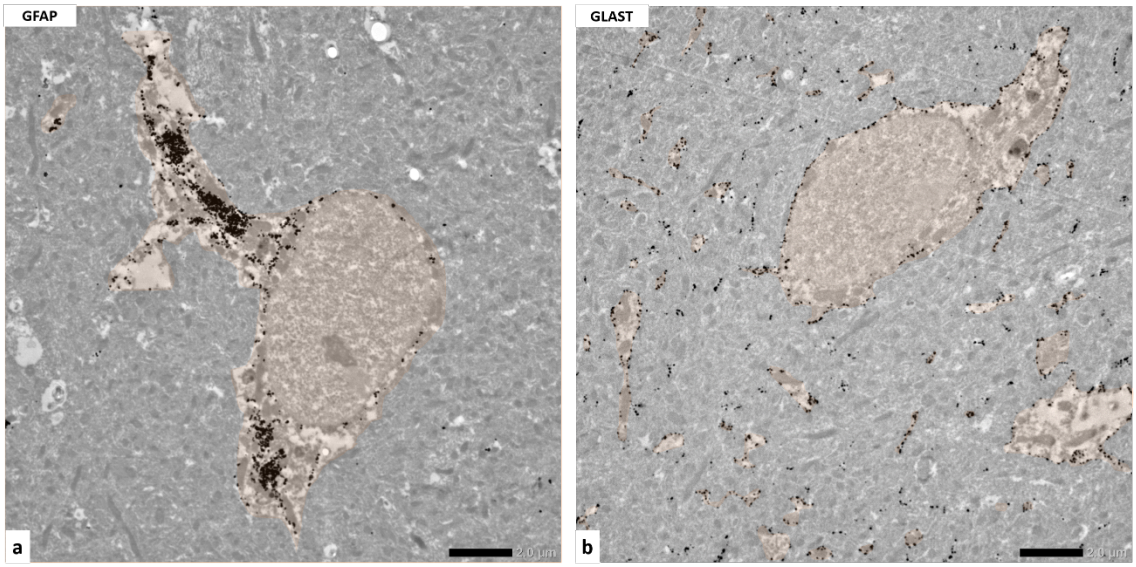

Figure 1. CA1 hippocampus of WT mice labeled with GFAP (a) or GLAST (b) antibodies in combination with an immunogold method for electron microscopy. a) Metal particles of GFAP labeling are concentrated in the cytoplasm of the soma and the main branches of astrocytes. b) Silver-intensified GLAST gold particles are located in the plasma membrane of astrocytic cell bodies, main branches as well as small and thin projections. Scale bars: 2 µm.

5.1.2. Immunoperoxidase method for electron microscopy using GFAP and GLAST antibodies

Next, I used GFAP and GLAST antibodies in combination with an immunoperoxidase method for electron microscopy to analyze the astrocytic area and plasma membrane with both astroglial markers. However, as GFAP is only expressed in

cell bodies and main branches of astrocytes, DAB immunodeposits were not observed in the smallest astrocytic projections (figure 2).

I analyzed photomontages (4 x 4) of 16 electron micrographs (x 8,000) obtained from the CA1 region of WT hippocampus. Almost three times more astroglial area was visualized with GLAST than GFAP (GLAST: 8.831 ± 0.6265 μm^2 astroglial area/100 μm^2; GFAP: 3.115 ± 0.3388; ****p < 0.0001; figure 2c). Likewise, GLAST revealed four times as much astroglial membranes as GFAP (GLAST: 96.21 ± 3.430 μm astroglial membrane/100 μm^2 area; GFAP: 21.15 ± 1.932; ****p < 0.0001; figure 2d).

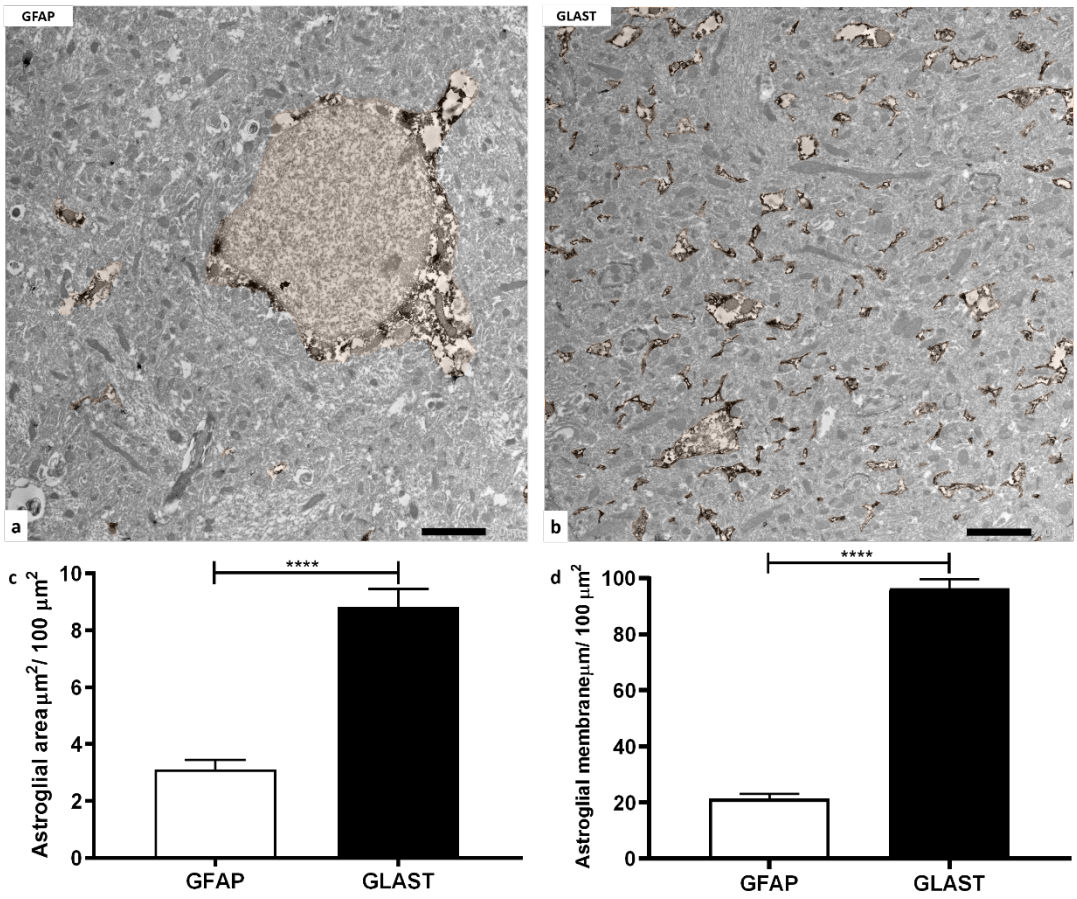

Figure 2. Electron micrographs of CA1 hippocampus showing GFAP (A) and GLAST staining (b) with an immunoperoxidase method for electron microscopy. Statistics of labeled astroglia with each marker (c, d). a) GFAP labeling is restricted to the cell body and main projections of an astrocyte. b) GLAST is distributed in numerous thin astroglial processes throughout the neuropil. c, d) Astroglial area (μm^2) and membrane (μm) labeled with GFAP or GLAST per 100 μm^2. Data were analyzed by parametric tests (Unpaired t-test, ****p < 0.0001). Scale bars: 2 μm.

5.1.3. Double immunogold and immunoperoxidase method for electron microscopy to localize astroglial CB_1 receptors

We have shown in our previous studies using GFAP antibodies that 5-6% of the total CB_1 receptor labeling is located on astroglial membranes. Here, I have compared the combination of GFAP-CB_1 versus GLAST-CB_1 using double immunogold and immunoperoxidase method for electron microscopy. I confirmed that 5-6% of total CB_1 receptors is located in GFAP-positive astrocytes. However, as much as 12% of total CB_1 particles were found to be localized in GLAST-positive astrocytes (GLAST-CB_1: 11.92 ± 0.6368 % CB_1 astroglial membrane/total CB_1; GFAP-CB_1: 4.98 ± 1.102 %; ****$p < 0.0001$; figure 3).

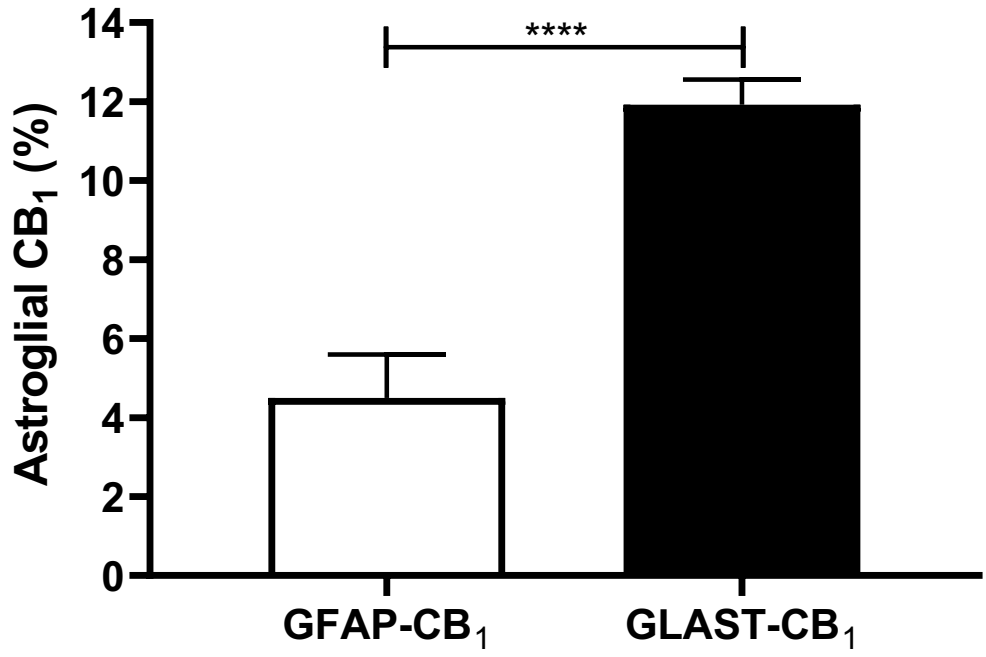

Figure 3. Percentage of astroglial CB_1 receptors using double immunoelectron microscopy for GFAP-CB_1 (4.98 ± 1.102 %) and GLAST-CB_1 (11.92 ± 0.6368 %).

5.2. DISTRIBUTION OF CB_1 RECEPTORS IN LAYERS II/III OF THE PRELIMBIC PREFRONTAL CORTEX OF GLU-CB_1-WT/KO AND GABA-CB_1-WT/KO MICE BY GLAST-CB_1 IMMUNOLABELING

Once GLAST was shown to be better marker for the localization of CB_1 receptors in astrocytes, I wanted to validate the GLAST-CB_1 receptor labeling in layers II/III of the prefrontal cortex where the receptor is known to be present. Different transgenic mice were used in this analysis: Glu-CB_1-WT, Glu-CB_1-KO, GABA-CB_1-WT, GABA-CB_1-KO and CB_1-KO (figure 4). I first studied CB_1 receptors in inhibitory and excitatory synaptic terminals as well as in astrocytes.

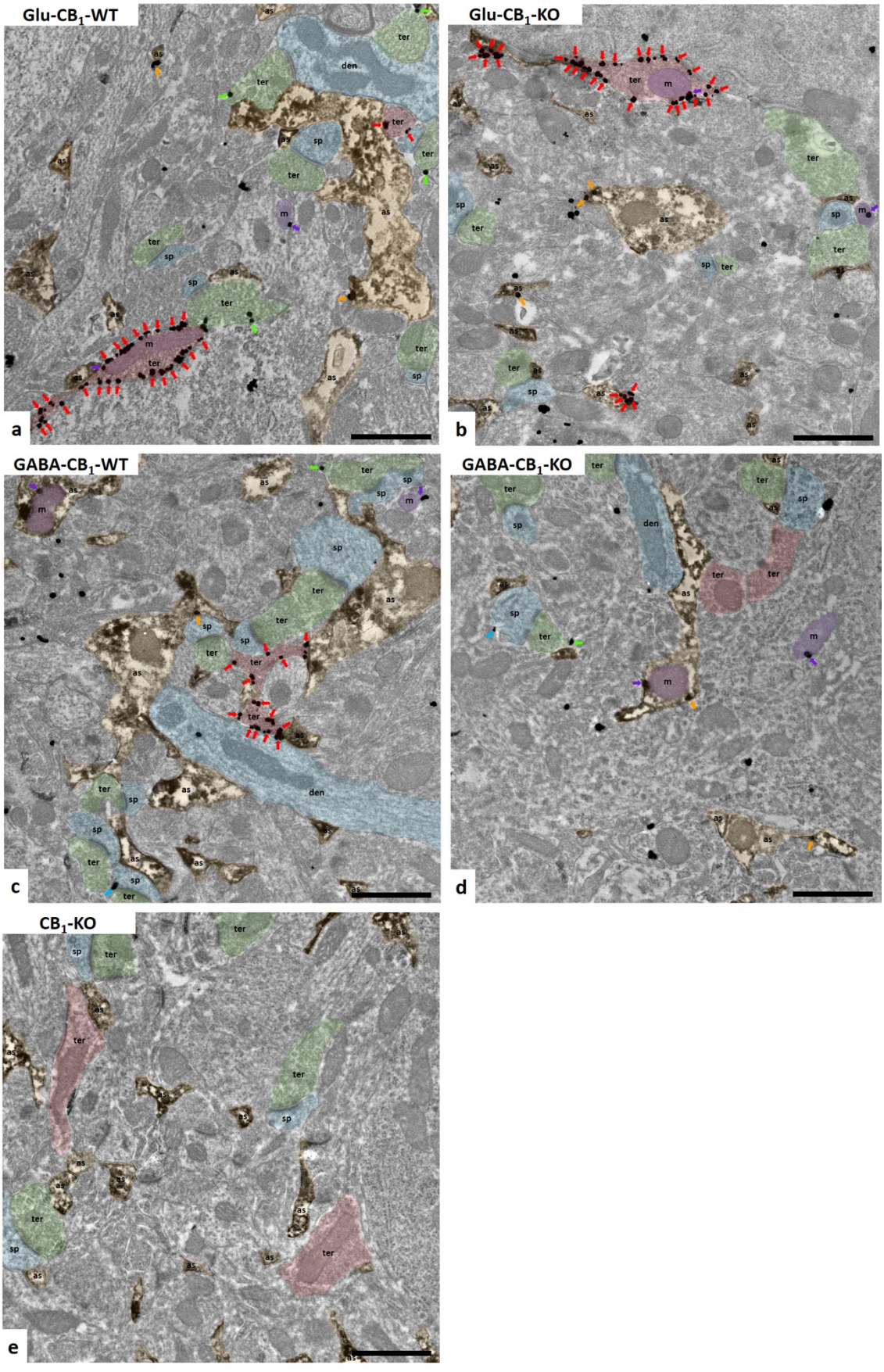
Glu-CB1-WT
Glu-CB1-KO
GABA-CB1-WT
GABA-CB1-KO
CB1-KO
a
b
c
d
e
ter
sp
as
m
den

Figure 4. CB_1 receptors in the prelimbic cortical layers II/III of several transgenic mice and in CB_1-KO. CB_1 receptor labeling (arrows) is observed in GABAergic terminals (ter, red), glutamatergic terminals (ter, green), GLAST-positive astrocytic processes (as, orange) and mitochondria (m, purple) in WT mice (a, c). However, gold particles are not detected in glutamatergic terminals of Glu-CB_1-KO (b) or in GABAergic terminals of GABA-CB_1-KO (d). Labeling for CB_1 receptors is fully absent in CB1-KO tissue (e). Dendrite (den, blue), spine (sp, blue). Scale bars: 1 μm.

As already described in different brain regions, CB_1 receptors were mostly localized to inhibitory terminals (Glu-CB_1-WT: 38.94 ± 3.923 particles/100 μm^2; Glu-CB_1-KO: 41.51 ± 6.041; GABA-CB_1-WT: 45.80 ± 6.373; GABA-CB_1-KO: 0.7895 ± 0.3337; CB_1-KO: 0.1247 ± 0.1247; figure 5a). No CB_1 receptor labeling was found in inhibitory terminals of GABA-CB_1-KO and CB_1-KO, so there were significant differences: Glu-CB_1-WT vs GABA-CB_1-KO, *p = 0.0122; Glu-CB_1-KO vs GABA-CB_1-KO, **p = 0.0064; GABA-CB_1-WT vs GABA-CB_1-KO, **p = 0.0032; Glu-CB_1-WT vs CB_1-KO, **p = 0.0017; Glu-CB_1-KO vs CB_1-KO, ***p = 0.0008; GABA-CB_1-WT vs CB_1-KO, ***p = 0.0004.

As expected, the CB_1 receptor localization was much lower in excitatory terminals (Glu-CB_1-WT: 3.919 ± 0.3544 CB_1 particles/100 μm^2; Glu-CB_1-KO: 0.1062 ± 0.08389; GABA-CB_1-WT: 4.305 ± 0.2372; GABA-CB_1-KO: 3.365 ± 0.4159; CB_1-KO: 0.3738 ± 0.08728; figure 5b). Significant differences were found with Glu-CB_1-KO and CB_1-KO: Glu-CB_1-WT vs Glu-CB_1-KO, ***p = 0.0004; GABA-CB_1-WT vs Glu-CB_1-KO, ****p < 0.0001; GABA-CB_1-KO vs Glu-CB_1-KO, **p = 0.0051; Glu-CB_1-WT vs CB_1-KO, *p = 0.0104; GABA-CB_1-WT vs CB_1-KO, **p = 0.0015.

There were more CB_1 receptors in astrocytic membranes than at excitatory terminals (Glu-CB_1-WT: 5.036 ± 0.3639 CB_1 particles/100 μm^2; Glu-CB_1-KO: 4.588 ± 0.3177; GABA-CB_1-WT: 6.028 ± 0.7241; GABA-CB_1-KO: 5.587 ± 1.111; CB_1-KO: 1.124 ± 0.1886; figure 5c). Specific labeling was absent in CB_1-KO astrocytes showing significant differences with the transgenic mice: Glu-CB_1-WT vs CB_1-KO, **p = 0.0050; Glu-CB_1-KO vs CB_1-KO, *p = 0.0289; GABA-CB_1-WT vs CB_1-KO, ****p < 0.0001; GABA-CB_1-KO vs CB_1-KO, **p = 0.0069.

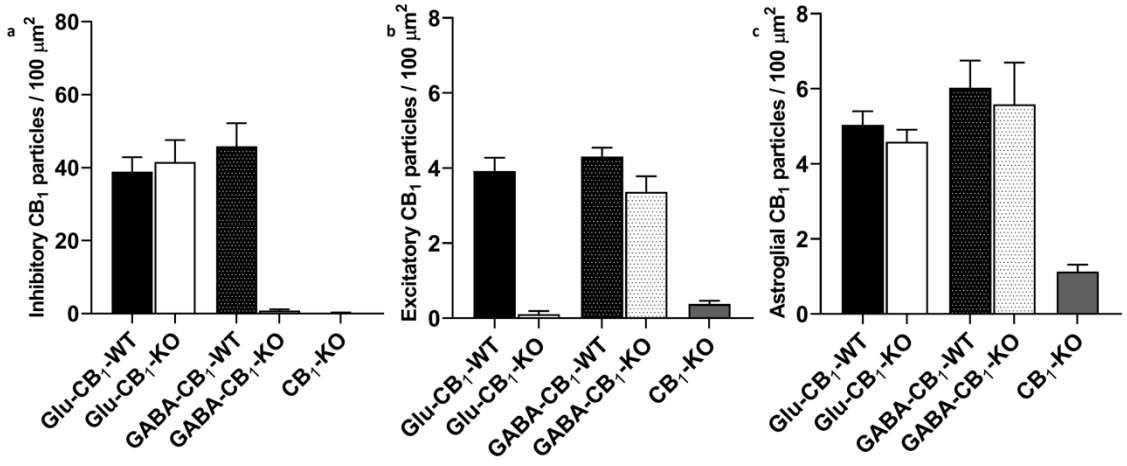

Figure 5. Statistical analysis of the CB_1 receptor distribution in cell compartments of different transgenic mice. a) CB_1 receptor localization in inhibitory terminals. b) CB_1 receptors at excitatory terminals. c) Astroglial CB_1 receptors. Kruskal-Wallis test. All data are represented as mean ± SEM.

5.2.1. Proportion of CB_1 receptor immunopositive inhibitory and excitatory terminals

As described in hippocampal CA1 (Gutiérrez-Rodríguez et al., 2017), most of the inhibitory terminals in layers II/III of the prelimbic cortex were CB_1 receptor immunopositive, except in GABA-CB_1-KO and CB_1-KO (Glu-CB_1-WT 95.17 ± 2.024 %; Glu-CB_1-KO: 95.49 ± 1.946 %; GABA-CB_1-WT: 96.71 ± 1.706 %, GABA-CB_1-KO: 2.222 ± 2.222 %; CB_1-KO: 2.778 ± 2.778 %; figure 6a). Significant differences were detected between GABA-CB_1-KO and CB_1-KO mice and the others: Glu-CB_1-WT vs GABA-CB_1-KO, $^{**}p$ = 0.0022; Glu-CB_1-KO vs GABA-CB_1-KO, $^{**}p$ = 0.0017; GABA-CB_1-WT vs GABA-CB_1-KO, $^{***}p$ = 0.0006; Glu-CB_1-WT vs CB_1-KO, $^{**}p$ = 0.0024; Glu-CB_1-KO vs CB_1-KO, $^{**}p$ = 0.0019; GABA-CB_1-WT vs CB_1-KO, $^{***}p$ = 0.0007.

On the other hand, the proportion of CB_1 receptor-labeled excitatory terminals was low, as expected (Glu-CB_1-WT: 18.74 ± 1.327 %; Glu-CB_1-KO: 1.299 ± 0.6814 %; GABA-CB_1-WT: 18.77 ± 1.387 %; GABA-CB_1-KO: 17.81 ± 1.290 %; CB_1-KO: 1.394 ± 0.6984 %; figure 6b). Glu-CB1-KO and CB1-KO mice showed significant differences with the other transgenic mice because no specific CB_1 receptor labeling was found in their excitatory terminals: Glu-CB_1-WT vs Glu-CB_1-KO, $^{**}p$ = 0.0014; GABA-CB_1-WT vs Glu-CB_1-KO, $^{**}p$ = 0.0020; GABA-CB_1-KO vs Glu-CB_1-KO, $^{**}p$ = 0.0036; Glu-CB_1-WT vs CB_1-KO, $^{**}p$ = 0.0018; GABA-CB_1-WT vs CB_1-KO, $^{**}p$ = 0.0025; GABA-CB_1-KO vs CB_1-KO, $^{**}p$ = 0.0044.

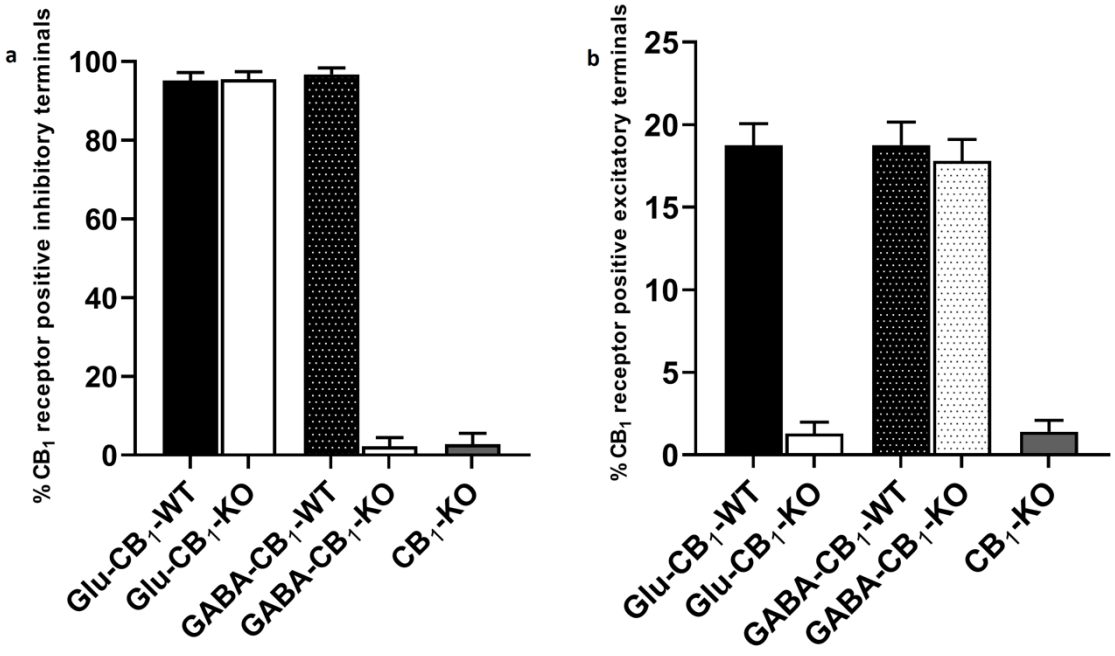

Figure 6. Percentage of inhibitory (a) and excitatory (b) terminals positive for CB_1 receptors in the mutant mice under study. Kruskal-Wallis test. All data are represented as mean ± SEM.

5.3. DENSITY OF CB_1 RECEPTORS IN MITOCHONDRIA OF ASTROCYTES AND NEURONS

An immunogold method for electron microscopy revealed the presence of mitochondrial-associated CB_1 receptors in neurons (Bernard et al., 2012; Hebert-Chatelain et al., 2014, 2016; Koch et al., 2015). Moreover, our lab has also localized CB_1 receptors in mitochondrial membranes of hippocampal astrocytes (Gutiérrez-Rodríguez et al., 2018; Jimenez-Blasco et al., 2020). I used here GLAST-CB_1 immunolabeling for electron microscopy to analyze the density of mitochondrial CB_1 receptors in neurons and astrocytes in different brain regions: hippocampal CA1 region, prefrontal cortex, piriform cortex and nucleus accumbens (figure 7). I observed that despite the lower absolute levels of CB_1 receptors in astrocytes than in neurons (Metna-Laurent et al., 2015), the density of mtCB_1 receptors in astrocytes was higher than in neurons in the four brain regions studied (figure 8). Namely, CB_1 receptors were more expressed in astroglial than neuronal mitochondria (Jimenez-Blasco et al., 2020).

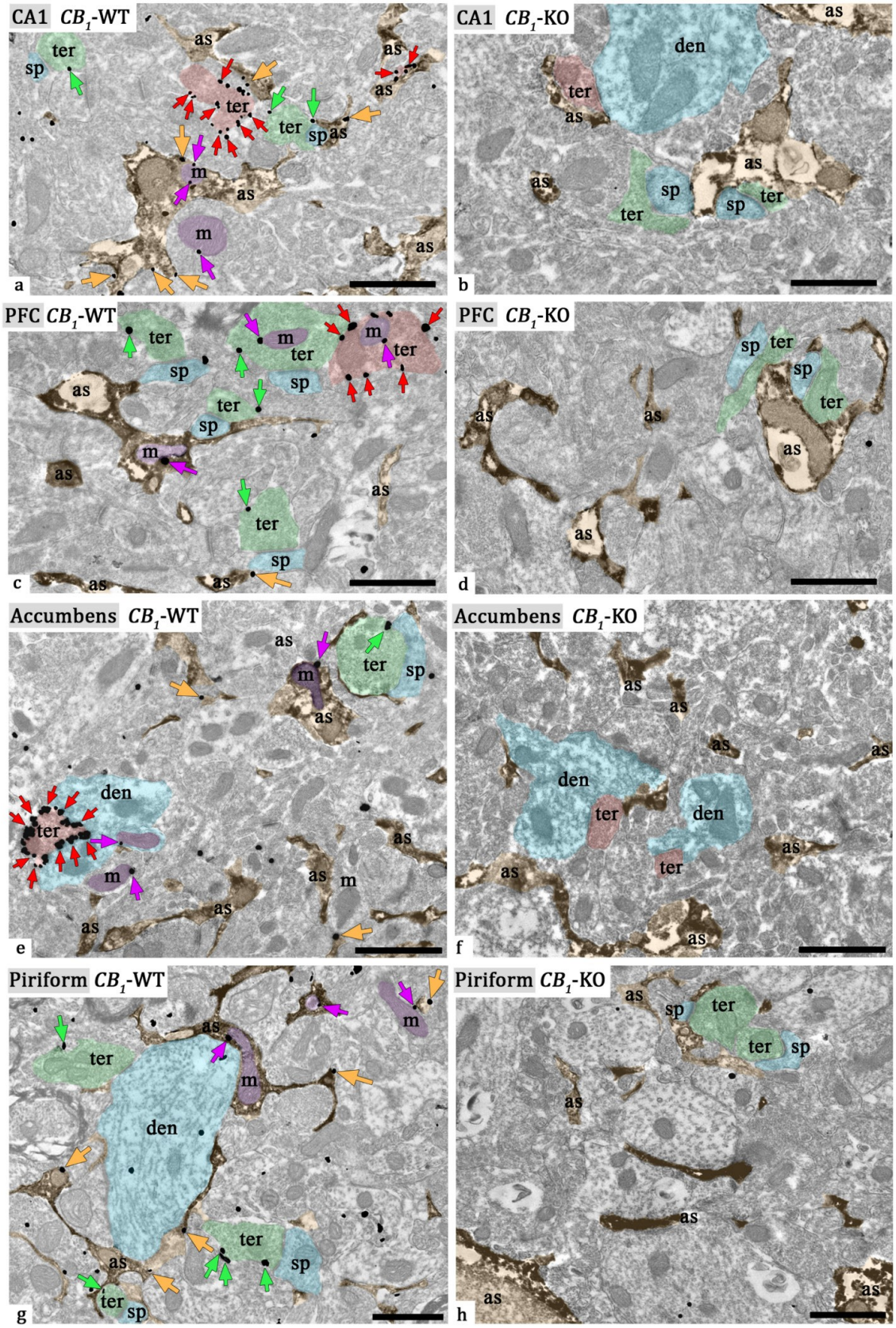

Figure 7. CB_1 receptor localization in mitochondria, astrocytes and synaptic terminals in the CA1 stratum radiatum, prefrontal cortex, nucleus accumbens and piriform cortex of WT and CB_1-KO mice. Double pre-embedding immunogold and immunoperoxidase method for electron microscopy. Representative electron microscopic images of CB_1 receptor particles (purple arrows) on mitochondrial (m, purple) membranes of astrocytes (identified with

GLAST immunoperoxidase staining (as, orange) and neurons in the hippocampus (a), prefrontal cortex (c), nucleus accumbens (e) and piriform cortex (g) of WT. CB_1 receptor labeling (color coding arrows) is also in GABAergic terminals (ter, red), glutamatergic terminals (ter, green) and astrocytic membranes (as, orange). Residual particles, if any, are seen in CB_1-KO tissues (b, d, f, h). Dendrite (den, blue), spine (sp, blue). Scale bars: 1 µm.

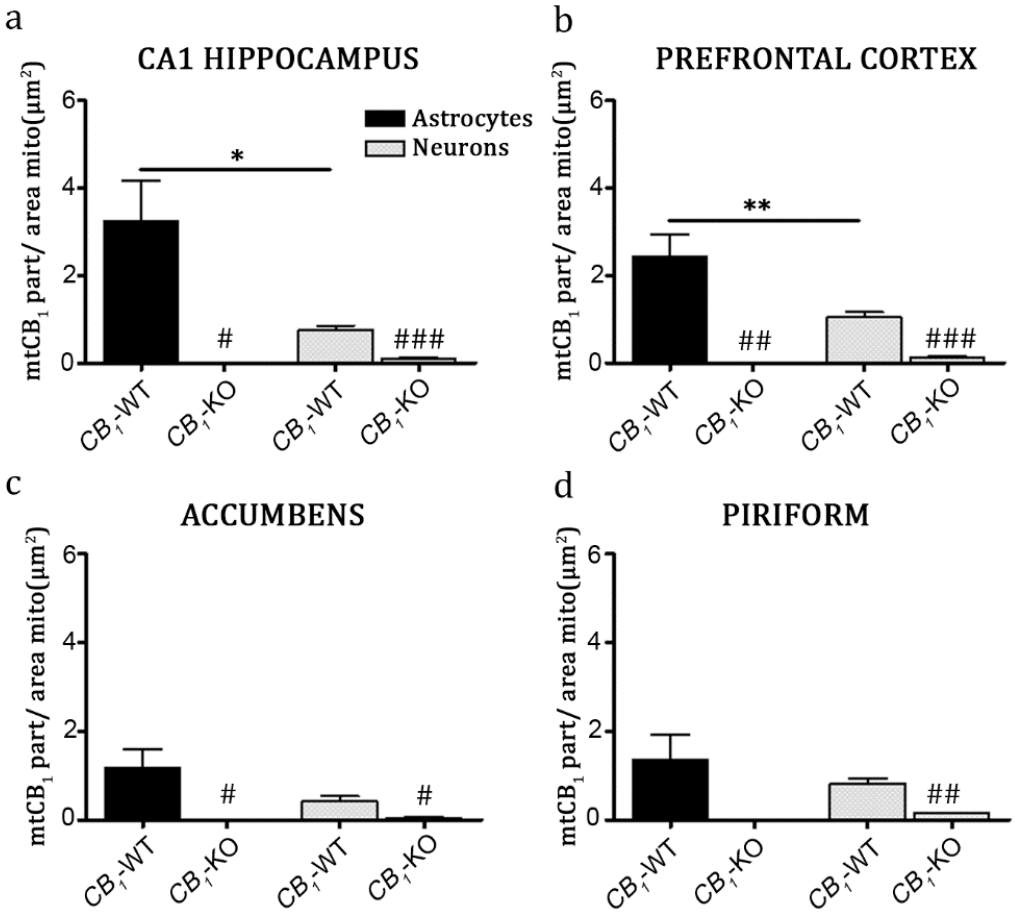

Figure 8. CB_1 receptor density in astrocytic and neuronal mitochondria. The CB_1 receptor density in astrocytic mitochondria of CA1 (3.24 ± 0.94 part/µm²), prefrontal cortex (2.45 ± 0.49 part/µm²), nucleus accumbens (1.16 ± 0.44 part/µm²) and piriform cortex (1.35 ± 0.57 part/µm²), is higher than in neuronal mitochondria of CA1 (0.76 ± 0.09 part/µm²), prefrontal cortex (1.04 ± 0.13 part/µm²), nucleus accumbens (0.42 ± 0.12 part/µm²) and piriform cortex (0.82 ± 0.12 part/µm²). Only residual particles were found in neuronal mitochondria in CA1 (0.09 ± 0.04 part/µm²), prefrontal cortex (0.13 ± 0.02 part/µm²), nucleus accumbens (0.03 ± 0.03 part/µm²) and piriform cortex (0.14 ± 0.02 part/µm²) of CB_1-KO. Data are expressed as mean ± SEM. Data were analyzed by means of non-parametric or parametric tests (Mann–Whitney U test or unpaired t-test. *$p < 0.05$; **$p < 0.01$ (WT astrocytes vs. WT neurons); #$p < 0.05$; ##$p < 0.01$; ###$p < 0.001$ (WT vs. CB_1-KO).

5.4. ULTRASTRUCTURAL AND FUNCTIONAL STUDIES IN LAYERS II/III OF THE GFAP-CB_1-WT/KO PREFRONTAL (PRELIMBIC) CORTEX

Based on the previous observations in the prefrontal cortex (PFC), I wanted to investigate the anatomy and function of the CB_1 receptor in the prelimbic subregion of 14-week-old mice lacking CB_1 receptors in astrocytes (GFAP-CB_1-KO) and their WT littermates (GFAP-CB_1-WT), in order to know whether changes in astrocytic CB_1 receptors already take place at relatively older animals than routinely used (aged 8-9 weeks) (figure 9). The CB_1 receptor distribution in layers II/III of the prelimbic PFC was studied in the main compartments of neurons and astrocytes, as well as the proportion of inhibitory and excitatory terminals positive for the CB_1 receptor. All data were compared with the CB_1-KO mice used in the previous experiments. Moreover, electrophysiological recordings were done to detect possible forms of eCB-dependent synaptic plasticity at the dentate MPP synapses and in the prelimbic PFC.

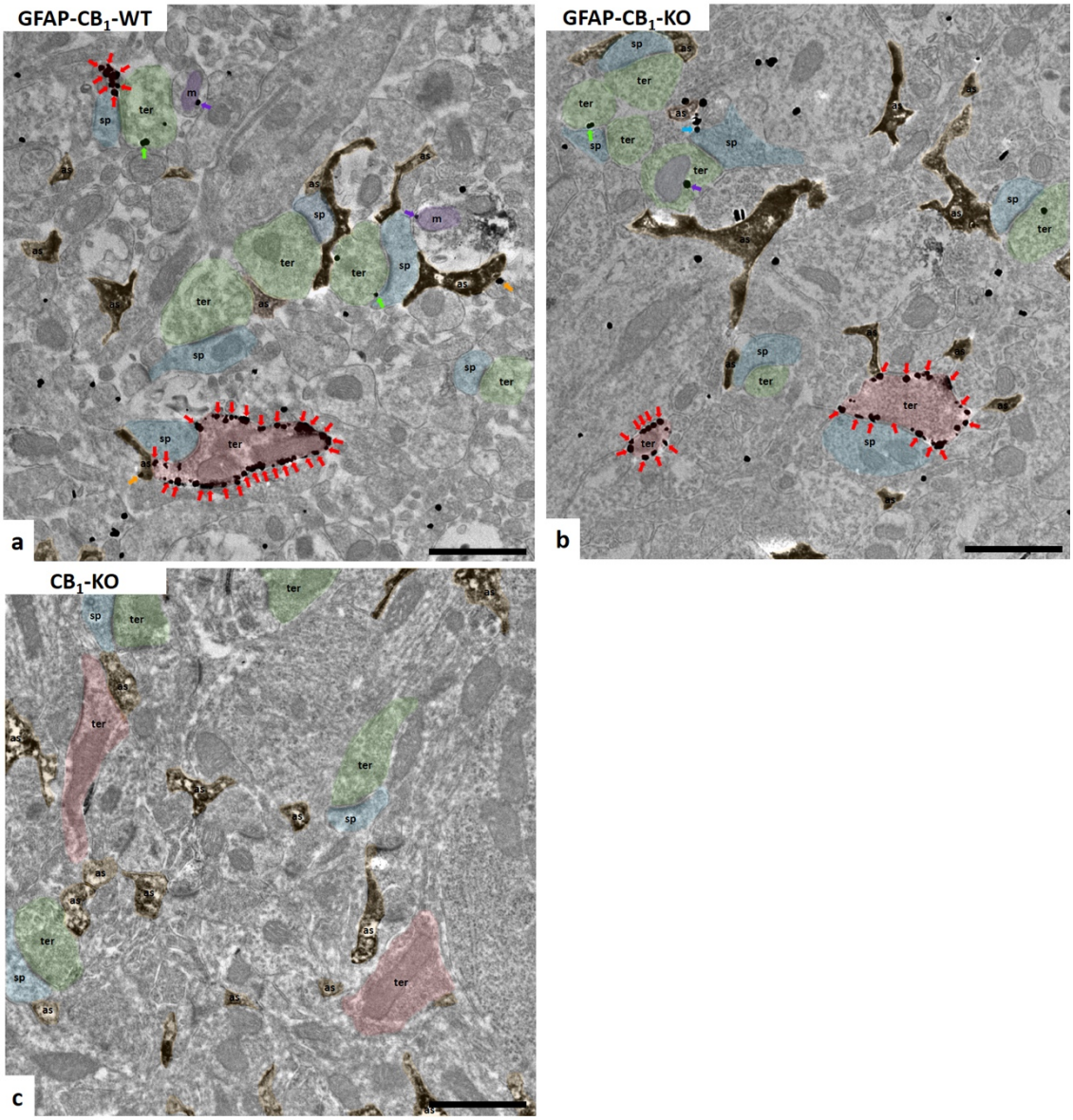

Figure 9. CB_1 receptor distribution in prefrontal (prelimbic) cortical layers II/III of GFAP-CB_1-WT/KO and CB_1-KO. (a) In GFAP-CB_1-WT, CB_1 receptor particles (color arrows) localize to inhibitory terminals (red), excitatory terminals (ter, green), astrocyte processes (as, dark brown) and mitochondria (m, purple), as expected. (b) Similar localization is observed in GFAP-CB_1-KO but astrocytes (as, dark brown) are free of CB_1 receptor labeling. (c) CB_1-KO tissue lacks CB_1 particles. Dendrite (den, blue), spine (sp, blue). Scale bars: 1 μm.

5.4.1. Distribution of CB_1 receptors in layers II/III of the prelimbic PFC of GFAP-CB_1-WT/KO mice

Regarding CB_1 receptor labeling in inhibitory terminals, I observed a similar pattern as described before (GFAP-CB_1-WT: 49.78 ± 7.010 particles/100 μm^2; GFAP-CB_1-KO: 46.95 ± 6.888; CB_1-KO: 0.1247 ± 0.1247; figure 10a). Significant differences were

found relative to CB_1-KO: GFAP-CB_1-WT vs CB_1-KO, ***p = 0.0006; GFAP-CB_1-KO vs CB_1-KO, **p = 0.0010. Kruskal-Wallis test. All data are represented as mean ± SEM.

Excitatory terminals in GFAP-CB_1-WT and GFAP-CB_1-KO also displayed their typical labeling (GFAP-CB_1-WT: 4.037 ± 0.2994 particles/100 μm^2; GFAP-CB_1-KO: 3.987 ± 0.4053; CB_1-KO: 0.3738 ± 0.08728; figure 10b). Statistically: GFAP-CB_1-WT vs CB_1-KO, ****p < 0.0001; GFAP-CB_1-KO vs CB_1-KO, ****p < 0.0001.

Finally, astroglial CB_1 receptors were not found in GFAP-CB_1-KO, as expected (GFAP-CB_1-WT, 3.934 ± 0.5558 particles/100 μm^2; GFAP-CB_1-KO: 0.4078 ± 0.1287; CB_1-KO: 1.124 ± 0.1886; figure 10c). Significant differences were detected: GFAP-CB_1-WT vs GFAP-CB_1-KO, ****p < 0.0001; GFAP-CB_1-WT vs CB_1-KO, ****p < 0.0001.

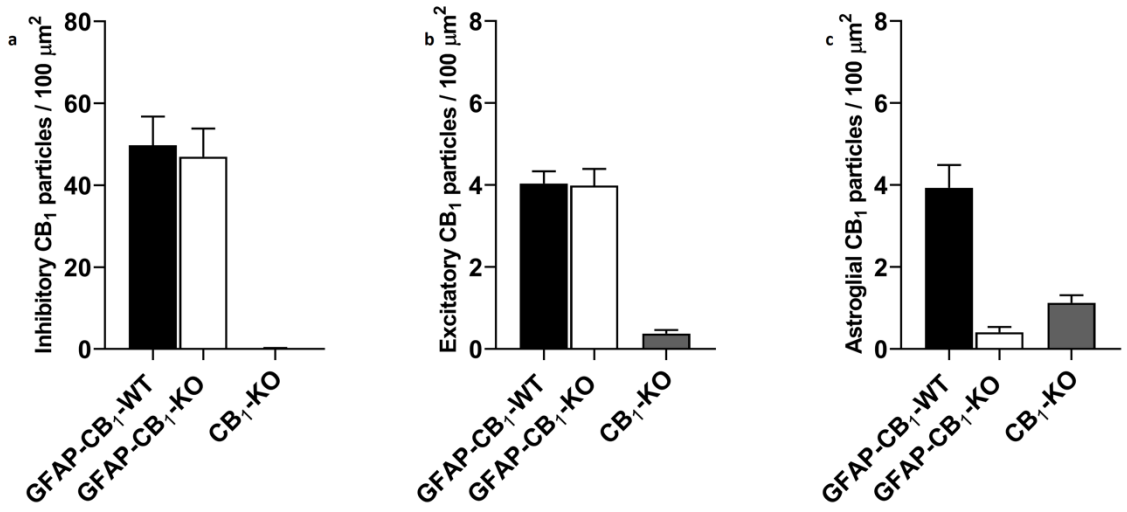

Figure 10. Statistical analysis of the CB_1 receptor distribution in main compartments in layers II/III of GFAP-CB_1-WT/KO and CB_1-KO prefrontal (prelimbic) cortex. a) CB_1 receptor localization in inhibitory terminals, b) excitatory terminals and c) astrocytes. Kruskal-Wallis and One-way ANOVA test. All data are represented as mean ± SEM.

5.4.2. Proportion of CB_1 receptor immunopositive inhibitory and excitatory terminals in layers II/III of GFAP-CB_1-WT/KO prefrontal (prelimbic) cortex

Like in Glu-CB_1-WT/KO and GABA-CB_1-WT, most inhibitory terminals in GFAP-CB_1-WT/KO were equipped with CB_1 receptors (GFAP-CB_1-WT: 93.21 ± 2.523 %; GFAP-CB_1-KO: 93.06 ± 2.560 %; CB_1-KO: 2.778 ± 2.778 %; figure 11a). Significant differences were found when compared with CB_1-KO: GFAP-CB_1-WT vs CB_1-KO, ***p = 0.0006; GFAP-CB_1-KO vs CB_1-KO, ***p = 0.0007.

The proportion of CB_1 receptor-labeled excitatory terminals was found to be similar to the described above and previously (GFAP-CB_1-WT: 18.85 ± 1.197 %; GFAP-CB_1-KO: 17.67 ± 1.135 %; CB_1-KO: 1.394 ± 0.6984 %; figure 11b). Significant differences were observed: GFAP-CB_1-WT vs CB_1-KO, ***p = 0.0003; GFAP-CB_1-KO vs CB_1-KO, **p = 0.0023.

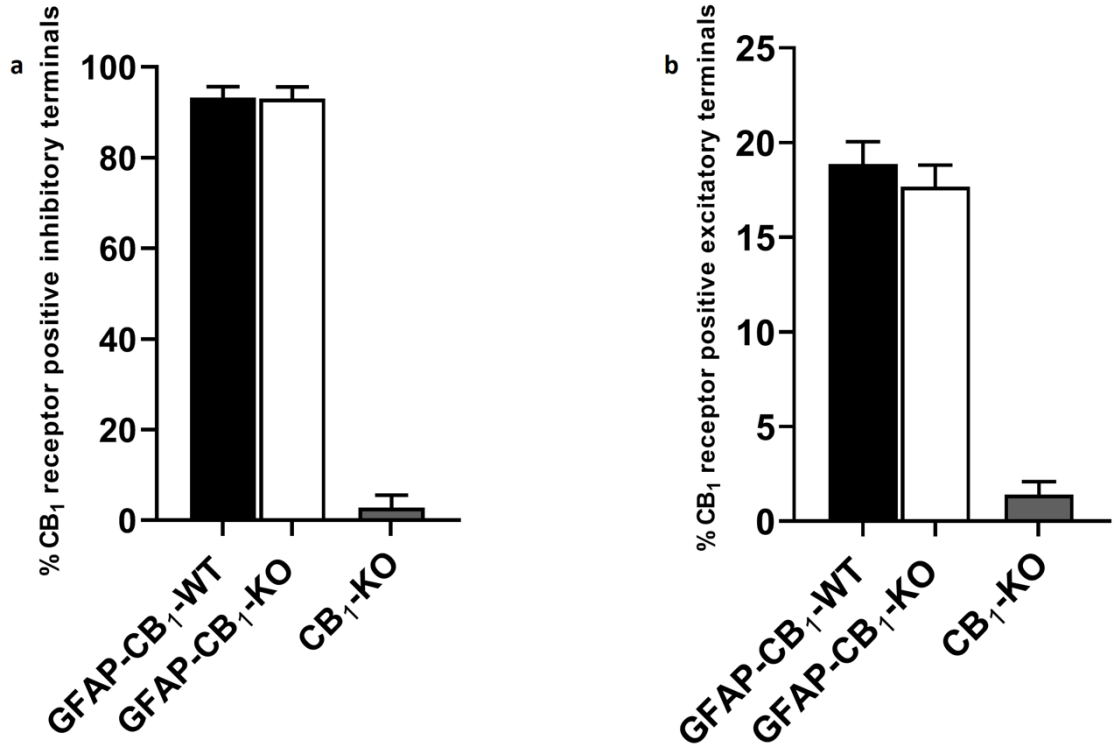

Figure 11. Statistical analysis of the percentage of inhibitory (a) and excitatory (b) terminals positive for CB_1 receptors in layers II/III of GFAP-CB_1-WT/KO and CB_1-KO prefrontal (prelimbic) cortex. Kruskal-Wallis test. All data are represented as mean ± SEM.

5.4.3. Synaptic plasticity at the excitatory MPP synapses in GFAP-CB_1-WT/KO dentate gyrus

I first wanted to characterize the synaptic plasticity elicited by LFS at the dentate MPP synapses in 14-week-old GFAP-CB_1-WT and GFAP-CB_1-KO mice. Unlike the eCB-driven LTD previously described by our laboratory (Peñasco et al., 2019), a significant LTP was found in GFAP-CB_1-WT (123 ± 6.688 %; **p = 0.0038; figure 12 a, c) but not in GFAP-CB_1-KO (108.8 ± 4.742 %; ns p = 0.1041; figure 12 a, d). However, there were not significant

differences between them suggesting that astroglial CB_1 receptors are not involved in this potentiation observed in GFAP-CB_1-WT (ns p = 0.1478; figure 12b).

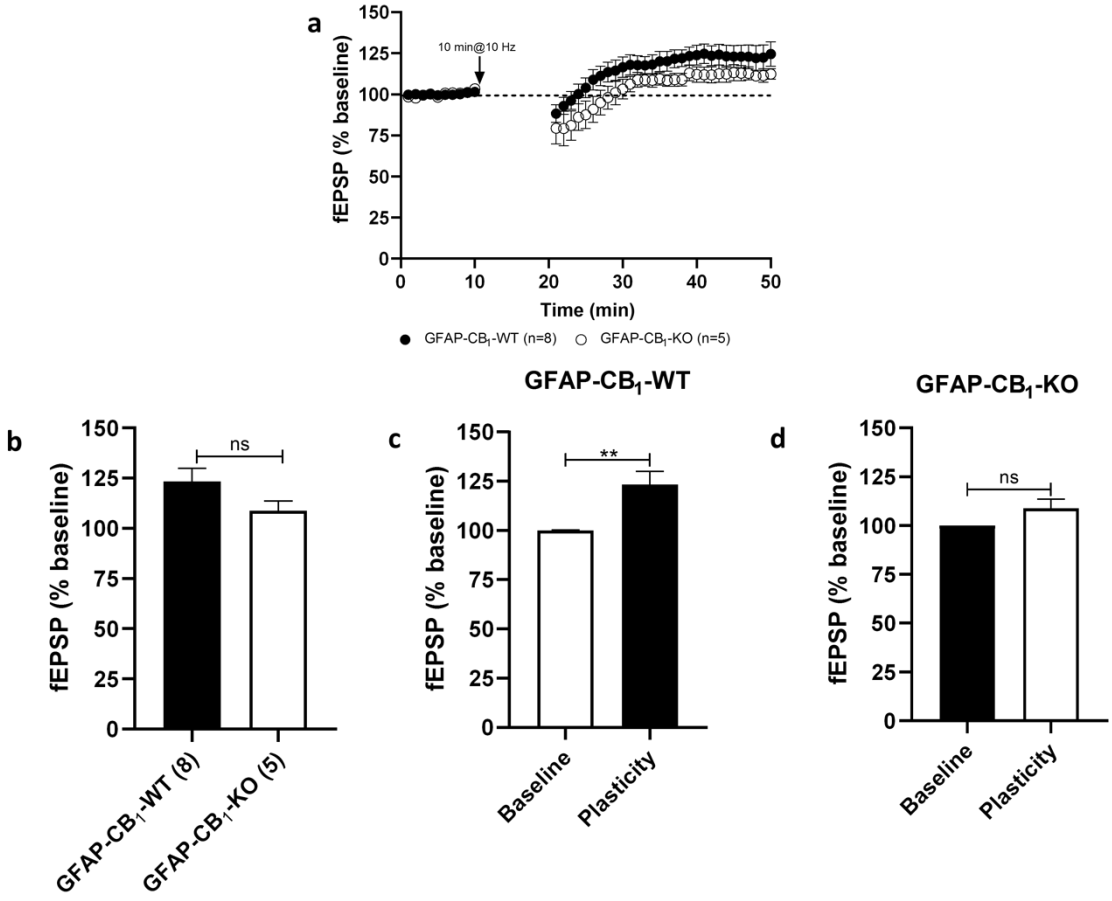

Figure 12. Excitatory long-term potentiation (eLTP) at MPP synapses (MPP-LTP) in 14-week-old GFAP-CB_1-WT mice. For representation, each experiment was normalized to its baseline. The average of the fEPSP areas is shown. A black arrow marks LFS application. a) LFS (10 min, 10 Hz) triggers LTP at MPP in GFAP-CB_1-WT (black circles) but only a non-significant potentiation in GFAP-CB_1-KO of the same age (white circles). b) Representative histogram of the last 10 min fEPSP after LFS at MPP in GFAP-CB_1-WT and GFAP-CB_1-KO. Unpaired t test. ns, p = 0.1478. c) Representative histogram of the last 10 min fEPSP after LFS at MPP in GFAP-CB_1-WT. Unpaired t test. **p = 0.0038. d) Representative histogram of the last 10 min fEPSP after LFS at MPP in GFAP-CB_1-KO. Unpaired t test. ns, p = 0.1041. All data expressed as mean ± SEM.

To find out whether CB_1 receptors participated in the MPP-LTP in GFAP-CB_1-WT, the CB_1 receptor inverse agonist AM251 was applied. Different effects were observed: MPP-LTP was abolished by AM251 ([4 μM]; 92.64 ± 12.35 %; *p = 0.0356; figure 13 a, c). However, the non-significant fEPSP potentiation in GFAP-CB_1-KO was not affected by the drug ([4

μM]; 122.5 ± 5.455 %; ns, *p* = 0.0931; figure 13 b, d). Altogether, these results indicate that CB_1 receptors are involved in the MPP-LTP observed in GFAP-CB_1-WT mice.

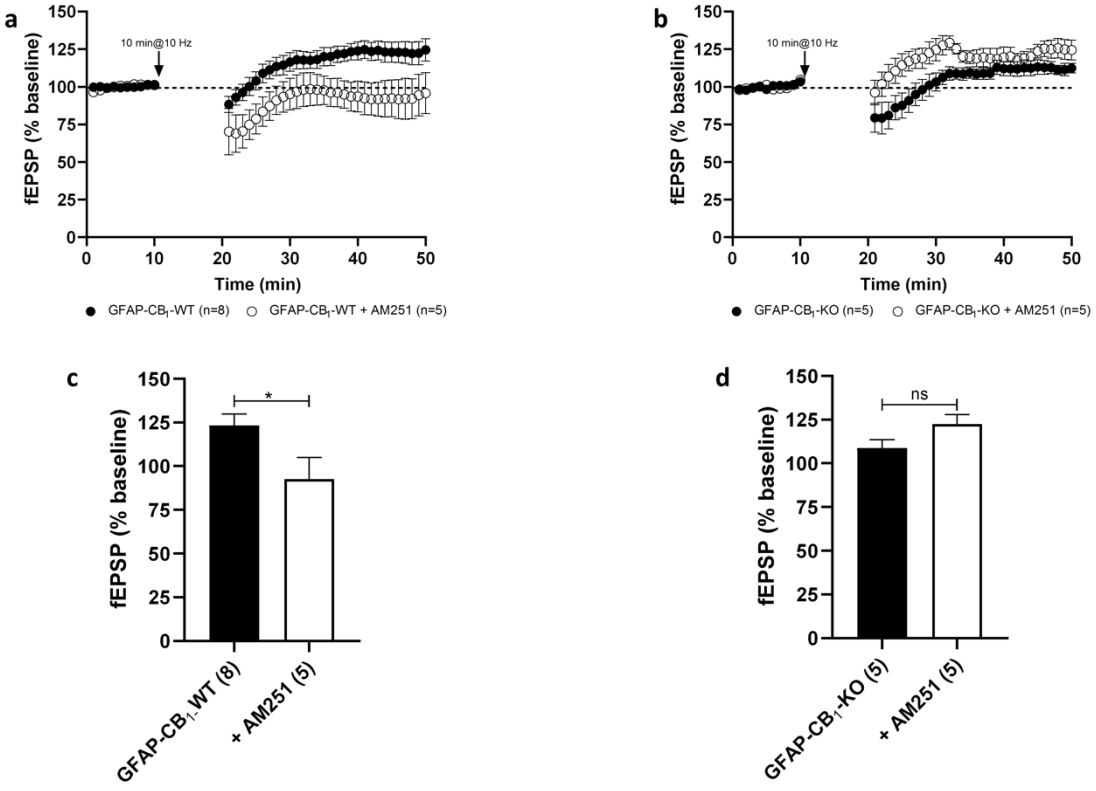

Figure 13. LTP at MPP synapses in GFAP-CB_1-WT is CB_1 receptor dependent. For representation, each experiment was normalized to its baseline. The average of the fEPSP areas is shown. A black arrow marks LFS application. a) AM251 [4 μM] has a significant effect over MPP-LTP in GFAP-CB_1-WT (white circles). b) AM251 [4 μM] has not a significant effect in GFAP-CB_1-KO (white circles). c) Representative histogram of the last 10 min fEPSP after LFS in the presence of AM251 in GFAP-CB_1-WT. Unpaired t test. **p* = 0.0356. d) Representative histogram of the last 10 min fEPSP after LFS in the presence of AM251 in GFAP-CB_1-KO. Unpaired t test. ns, *p* = 0.0931. All data expressed as mean ± SEM.

5.4.4. Synaptic plasticity in the prelimbic PFC of GFAP-CB_1-WT/KO mice

The same mice used to study synaptic plasticity at the dentate MPP synapses were used to record fEPSPs after LFS in the prelimbic cortical layers II/III of GFAP-CB_1-WT/KO PFC. As in MPP, a significant potentiation of fEPSP occurred in the 14-week-old GFAP-CB_1-WT (123.6 ± 4.480 %; ****p* = 0.0007; figure 14 a, c), but no effect was observed in GFAP-CB_1-KO (99.01 ± 17.29 %; ns, *p* > 0.9999; figure 14 a, d).

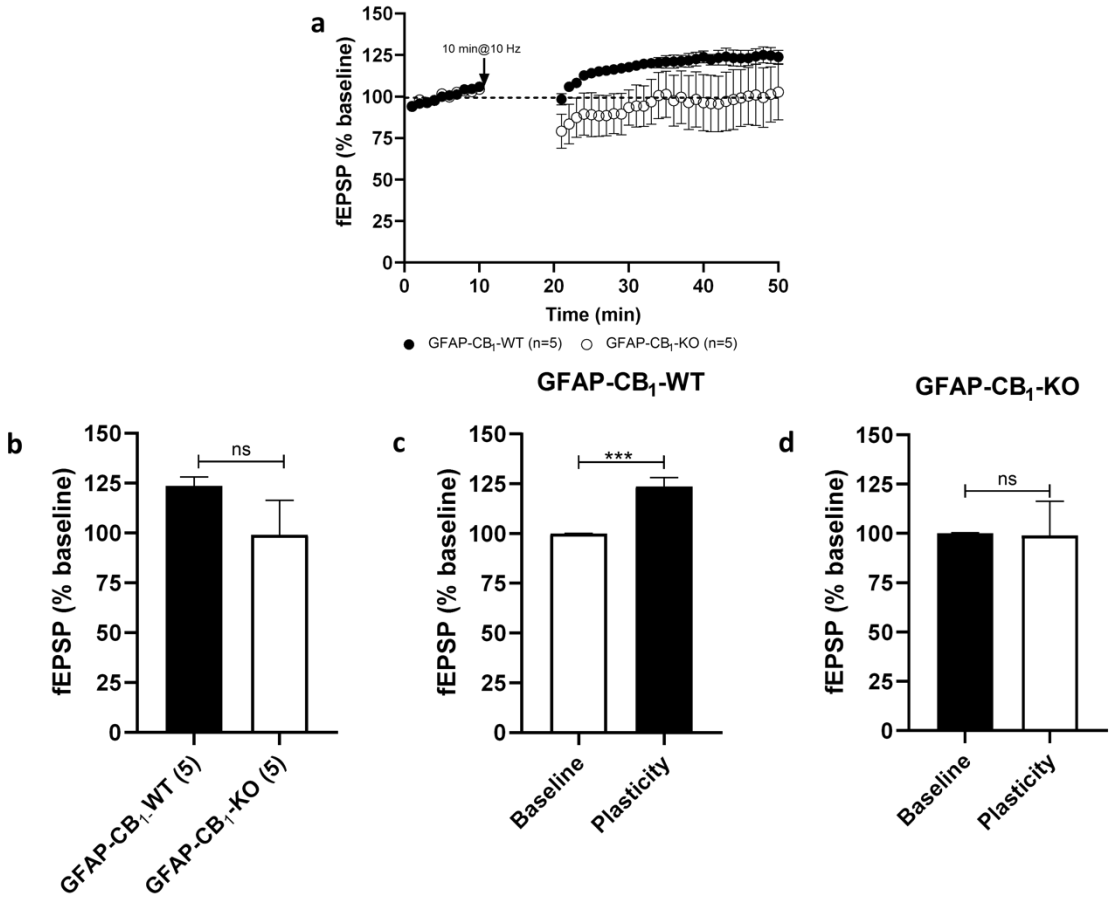

Figure 14. Excitatory long-term potentiation (eLTP) at prelimbic cortical layers II/III synapses in GFAP-CB_1-WT but not GFAP-CB_1-KO mice. For representation, each experiment was normalized to its baseline. The average of the fEPSP areas is shown. A black arrow marks LFS application. a) LFS (10 min, 10 Hz) triggers LTP in GFAP-CB_1-WT (black circles) with no effect in GFAP-CB_1-KO (white circles). b) Representative histogram of the last 10 min fEPSP after LFS at prelimbic cortical layers II/III in GFAP-CB_1-WT and GFAP-CB_1-KO. Unpaired t test. ns, p = 0.1679. c) Representative histogram of the last 10 min fEPSP after LFS in GFAP-CB_1-WT. Unpaired t test. ***p = 0.0007. d) Representative histogram of the last 10 min fEPSP after LFS in GFAP-CB_1-KO. Mann Whitney test. ns, p > 0.9999. All data expressed as mean ± SEM.

5.4.6. Effect of KA-induced epilepsy on synaptic plasticity in GFAP-CB_1-WT/KO mice

Taken into account the relevance of CB_1 receptors and astrocytes in pathological conditions, I finally wanted to investigate the possible consequences of the KA-induced epilepsy over the eCb-dependent synaptic plasticity in GFAP-CB_1-WT/KO mice. Kainate had not a significant effect on the MPP-LTP in GFAP-CB_1-WT (102.8 ± 7.928 %; ns, p = 0.0699; figure 15 a, c) nor on the slight potentiation observed in GFAP-CB_1-KO mice (100.9 ± 7.951 %; ns, p = 0.4440; figure 15 b, d).

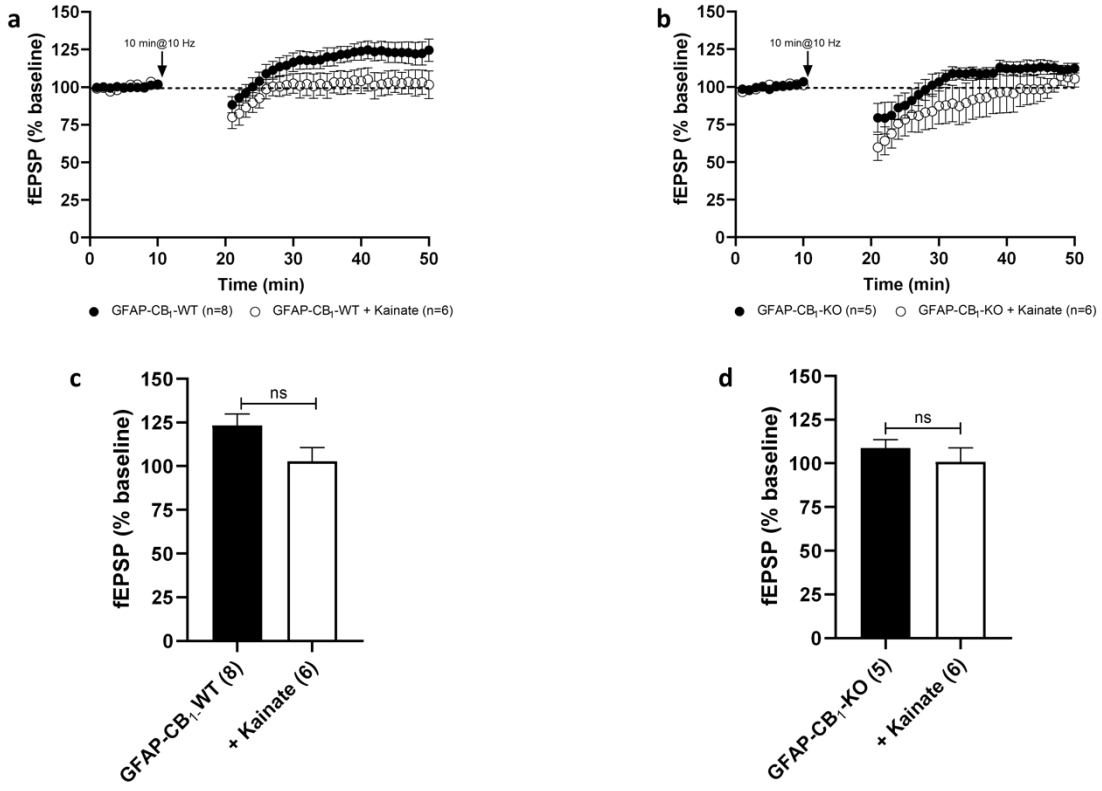

Figure 15. KA does not affect LTP at MPP synapses in GFAP-CB_1-WT mice. For representation, each experiment was normalized to its baseline. The average of the fEPSP areas is shown. A black arrow marks LFS application. a) The MPP-LTP after LFS in GFAP-CB_1-WT is not significantly blocked in KA-induced epileptic mice (white circles). b) Likewise, the slight potentiation in GFAP-CB_1-KO is not affected by KA (white circles). c) Representative histogram of the last 10 min fEPSP after LFS in KA-exposed GFAP-CB_1-WT. Unpaired t test. ns, p = 0.0699. d) Representative histogram of the last 10 min fEPSP after LFS in KA-injected GFAP-CB_1-KO mice. Unpaired t test. ns, p = 0.4440. All data expressed as mean ± SEM.

Similarly, KA did not affect fEPSPs in the prelimbic cortical layers II/III of GFAP-CB_1-WT (118.6 ± 6.613%; ns, p = 0.5586; figure 16 a, c) nor in GFAP-CB_1-KO (103.5 ± 4.638 %, ns, p > 0.9999; figure 16 b, d).

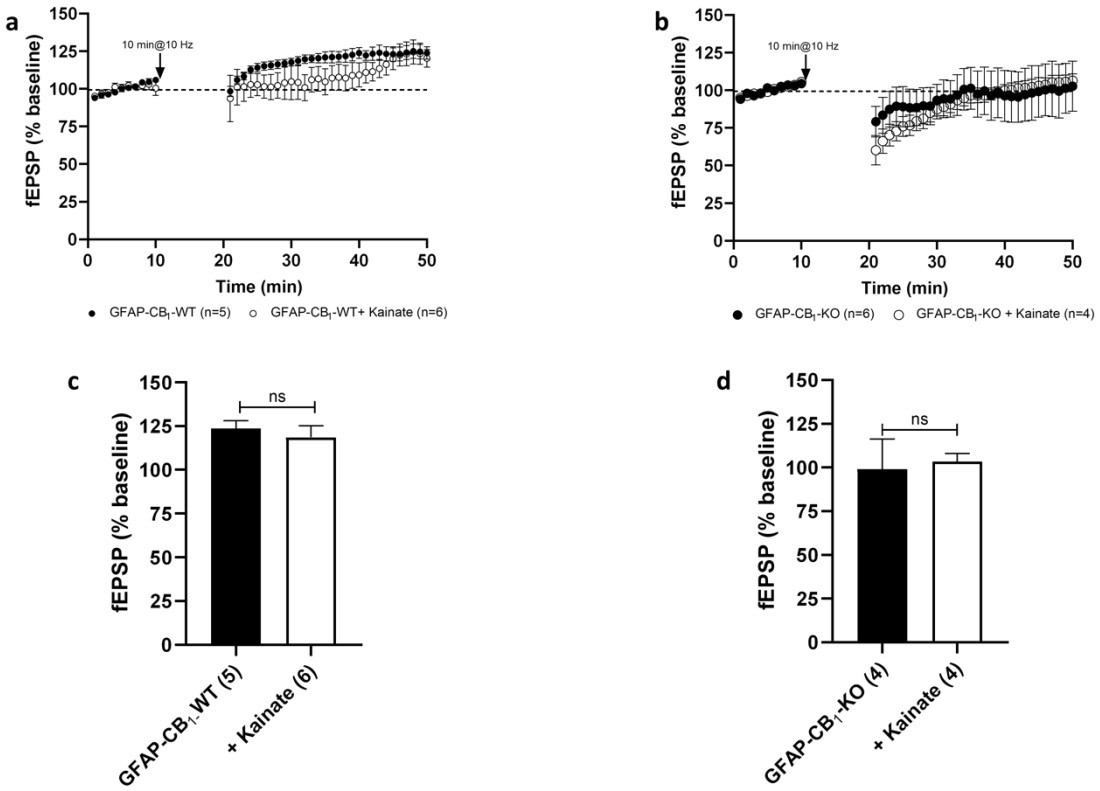

Figure 16. KA treatment does not affect LTP at prelimbic cortical layers II/III synapses in GFAP-CB_1-WT mice. For representation, each experiment was normalized to its baseline. The average of the fEPSP areas is shown. A black arrow marks LFS application. a) The PFC-LTP after LFS in GFAP-CB_1-WT remains intact after KA (white circles). b) No KA effect is seen in GFAP-CB_1-KO (white circles). c) Representative histogram of the last 10 min fEPSPs after LFS in GFAP-CB_1-WT exposed to KA. Unpaired t test. ns, p = 0.5586. d) Representative histogram of the last 10 min fEPSPs after LFS in KA-injected GFAP-CB_1-KO. Unpaired t test. ns, $p > 0.9999$. All data expressed as mean ± SEM.

5.4. SYNAPTIC PLASTICITY AT THE DENTATE MPP AND PFC SYNAPSES OF 14-WEEK-OLD MICE

5.4.1. MPP synaptic plasticity in 14-week-old mice

To confirm the results obtained in the 14-week-old GFAP-CB_1-WT and GFAP-CB_1-KO mice, I used the same LFS in 14-week-old WT mice. This stimulation protocol also caused MPP-LTP at that age (114.1 ± 5.256 %; **p* = 0.0147; figure 17a, c) but did not significantly affect fEPSPs in 8-week-old mice (figure 17a, b). The MPP-LTP was abolished by AM251 in a significant manner ([4 μM]; 92.78 ± 6.911 %; **p* = 0.0204; figure 18 a, d). These results indicated that CB_1 receptors are involved in the MPP-LTP in 14-week-old mice.

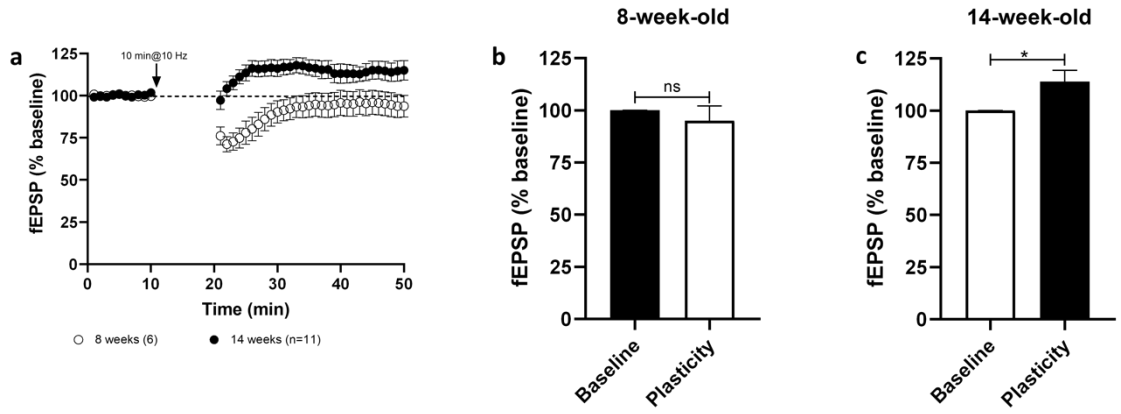

Figure 17. Excitatory long-term potentiation (eLTP) at MPP synapses in 14-week-old mice. For representation, each experiment was normalized to its baseline. The average of the fEPSP areas is shown. A black arrow marks LFS application. a) LFS (10 min, 10 Hz) triggers MPP-LTP in 14-week-old (black circles) but has no effect in 8-week-old mice. b) Representative histogram of the last 10 min fEPSP after MPP LFS in 8-week-old mice. Unpaired t test. ns, *p* = 0.4956. c) Representative histogram of the last 10 min fEPSP after MPP LFS in 14-week-old mice. Unpaired t test. **p* = 0.0147. All data expressed as mean ± SEM.

Furthermore, the NMDA receptor antagonist DL-APV ([50 μM]; 98.74 ± 7.041 %; ns, *p* = 0.0693; figure 18 c, f) and the TRPV1 receptor antagonist AMG9810 ([3 μM]; 99.06 ± 6.302 %; ns, *p* = 0.0815; figure 18 b, e) did not significantly affect fEPSPs.

We also investigated the participation of actin filaments as their phosphorylation was shown to be necessary for the LTP driven by CB_1 receptors at the lateral perforant path

synapses (Wang et al., 2018). Thus, the inhibitor of the actin filaments phosphorylation latrunculin-A (LAT-A) was applied but did not had any effect on the MPP-LTP in the 14-week-old mice ([0.5 mM]; 111.0 ± 7.163 %; ns, $p > 0.9999$; figure 18 g, h).

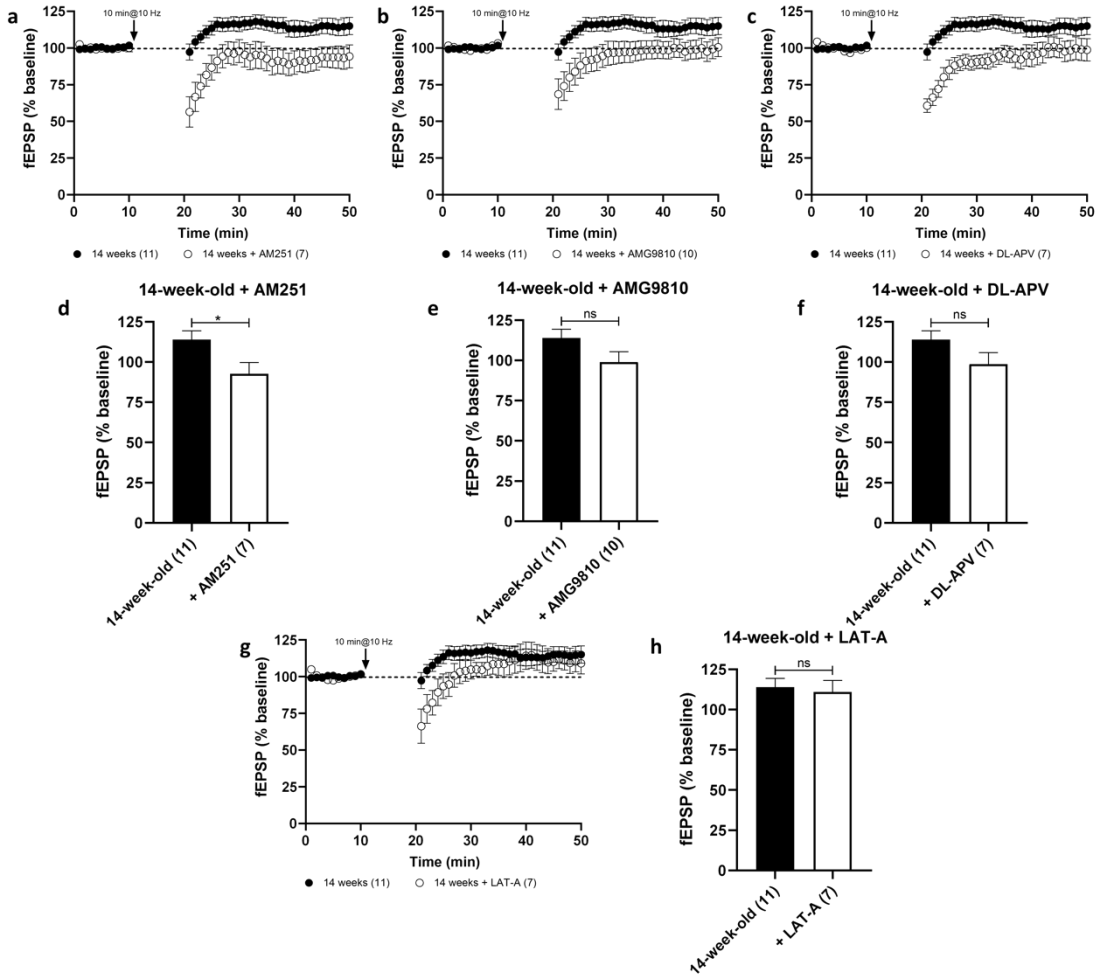

Figure 18. LTP at MPP synapses in 14-week-old mice is CB_1 receptor dependent, but NMDA, TRPV1 and actin filaments phosphorylation do not seem to participate. For representation, each experiment was normalized to its baseline. The average of the fEPSP areas is shown. A black arrow marks LFS application. a) AM251 [4 μM] has a significant effect on the LTP after LFS in 14-week-old mice (white circles). b) AMG9810 [3 μM] (white circles) and c) DL-APV [50 μM] do not significantly change fEPSPs. d) Representative histogram of the last 10 min fEPSP after LFS in the presence of AM251. Mann-Whitney test. *$p = 0.0204$. e) Representative histogram of the last 10 min fEPSP after LFS in the presence of AMG9810. Unpaired t test. ns, $p = 0.0815$. f) Representative histogram of the last 10 min fEPSP after LFS in the presence of DL-APV. Mann-Whitney test. ns, $p = 0.0693$. g) LAT-A has no effect on the LTP after LFS in 14-week-old mice (white circles). h) Representative histogram of the last 10 min fEPSP after LFS in the presence of LAT-A. Mann-Whitney test. ns, $p > 0.9999$. All data expressed as mean ± SEM.

Finally, I studied the participation of 2-AG and/or anandamide by bath application and pre-incubation with drugs affecting the synthesis and degradation of both eCBs. The

MAGL inhibitor JZL 184 ([50 μM]; 101.9 ± 3.803 %; ns, *p* = 0.0997; figure 19 a, d), the DAGLα inhibitor THL ([10 μM]; 108.3 ± 3.892 %; ns, *p* = 0.4623; figure 19 b, e) or the FAAH inhibitor URB597 ([2 μM]; 112.5 ± 4.866 %; ns, *p* = 0.8257; figure 19 c, f) did not affect MPP-LTP.

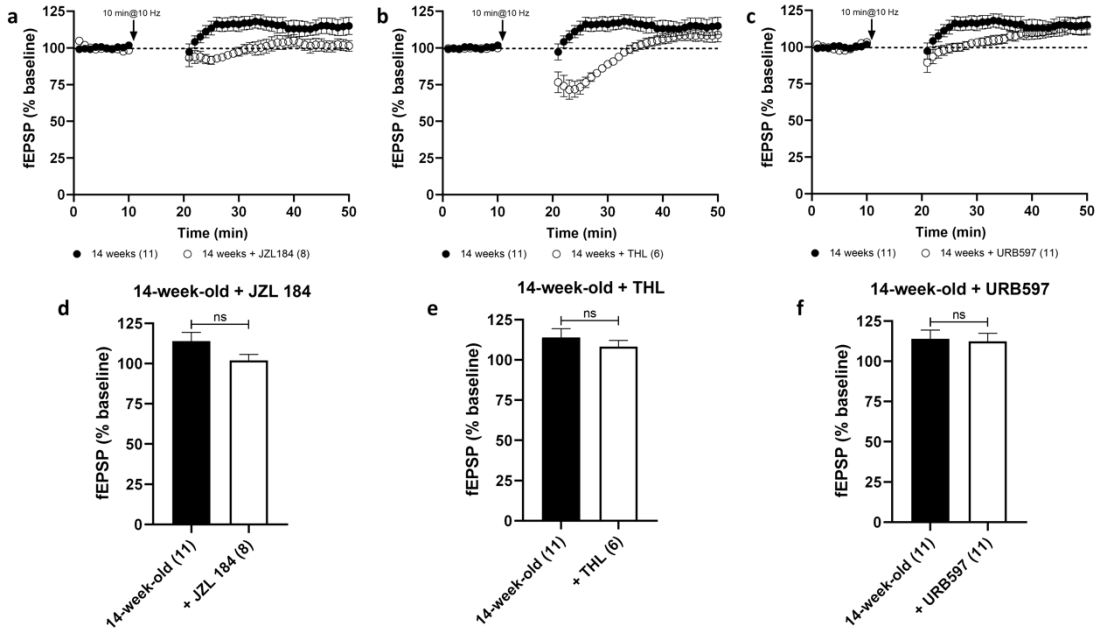

Figure 19. Changes in 2-AG and anandamide levels do not affect MPP-LTP in 14-week-old mice. For representation, each experiment was normalized to its baseline. The average of the fEPSP areas is shown. A black arrow marks LFS application. a) JZL 184 [50 μM] does not change LTP after LFS in 14-week-old mice (white circles); neither, b) THL [10 μM] (white circles) nor c) URB597 [2 μM] (white circles). d) Representative histogram of the last 10 min fEPSP after LFS in the presence of JZL 184. Unpaired t test. ns, *p* = 0.0997. e) Representative histogram of the last 10 min fEPSP after LFS in the presence of THL. Mann-Whitney test. ns, *p* = 0.4623. f) Representative histogram of the last 10 min fEPSP after LFS in the presence of URB597. Mann-Whitney test. ns, *p* = 0.8257. All data expressed as mean ± SEM.

5.4.2. Synaptic plasticity in the prelimbic PFC in 14-week-old mice.

The same mice were used to study synaptic plasticity in layers II/III of the prelimbic PFC. We described previously a CB_1 receptor-driven LTD in PFC layers V/VI elicited by LFS applied to layers II/III in 8-week-old mice (Lafourcade et al., 2007). Interestingly, the same stimulation paradigm in 14-week-old mice elicited an excitatory LTP in prelimbic cortical layers II/III (115.5 ± 4.836 %; ***p = 0.0008; figure 20 a, b).

Moreover, this LTP was not blocked by AM251 [50 μM]; 104.3 ± 6.578 %; ns, p = 0.2350; figure 20 a, c).

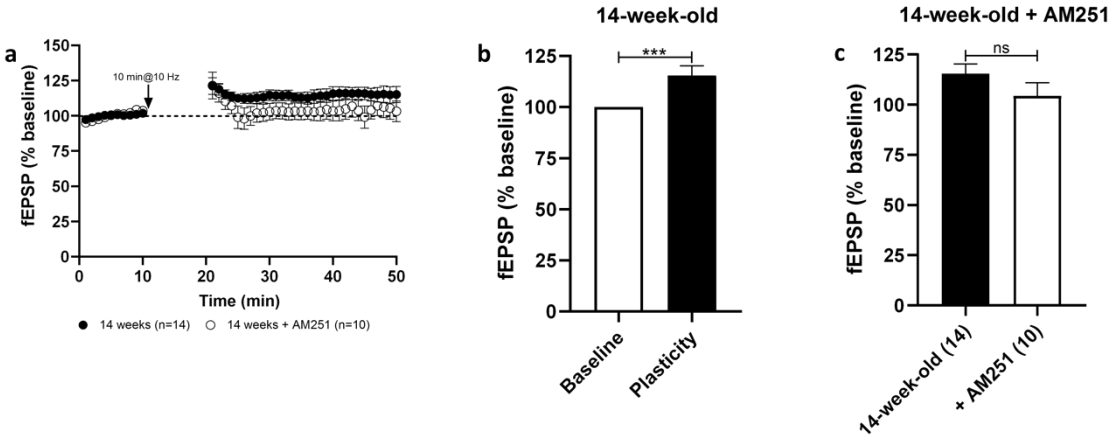

Figure 20. LTP at excitatory synapses in layers II/III of the prefrontal (prelimbic) cortex in 14-week-old mice is not reverted by AM251. For representation, each experiment was normalized to its baseline. The average of the fEPSP areas is shown. A black arrow marks LFS application. a) LFS (10 min, 10 Hz) triggers LTP (black circles) which is not blocked by AM251 [4 μM] (white circles). b) Representative histogram of the last 10 min fEPSP after LFS at prelimbic synapses in 14-week-old WT mice. Mann-Whitney test. ***p = 0.0008. c) Representative histogram of the last 10 min fEPSP after LFS in the presence of AM251. Mann-Whitney test. ns, p = 0.2350. All data expressed as mean ± SEM.

Neither DL-APV ([50 μM]; 106.5 ± 5.346 %; ns, p = 0.7267; figure 21 a, c) nor AMG9810 ([3 μM]; 117.6 ± 4.786 %; ns, p = 0.5466; figure 21 b, d) changed PFC-LTP.

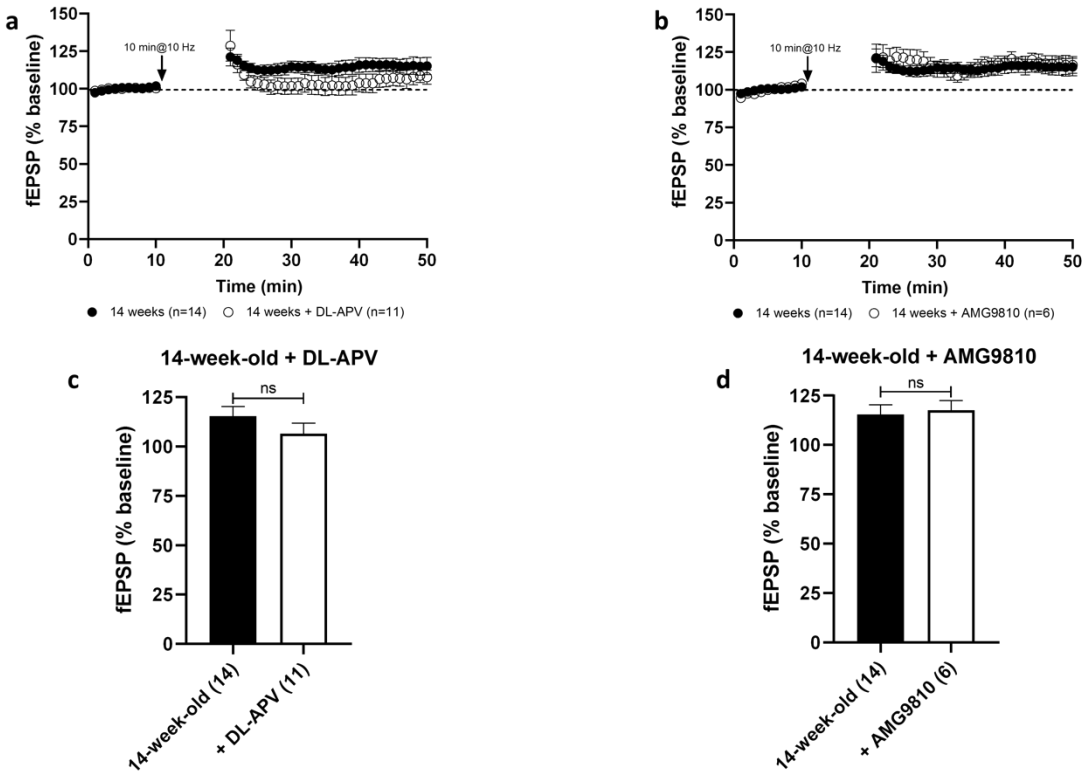

Figure 21. Neither NMDA nor TRPV1 receptors seem to be participating in layers II/III PFC-LTP in 14-week-old mice. For representation, each experiment was normalized to its baseline. The average of the fEPSP areas is shown. A black arrow marks LFS application. a) DL-APV [50 μM] and b) AMG9810 [3 μM] have no significant effect on the LTP (white circles). c) Representative histogram of the last 10 min fEPSP after LFS and with DL-APV. Mann-Whitney test. ns, p = 0.7267. d) Representative histogram of the last 10 min fEPSP after LFS and with AMG9810. Mann-Whitney test. ns, p = 0.5466. All data expressed as mean ± SEM.

Lastly, JZL 184 ([50 μM]; 118.7 ± 7.692 %; ns, p = 0.9203; figure 22 a, d), THL ([10 μM]; 117.5 ± 2.260 %; ns, p = 0.2667; figure 22 b, e) and URB597 ([2 μM]; 107.9 ± 1.2 %; ns, p = 0.0913; figure 22 c, f) did not have any significant effect either.

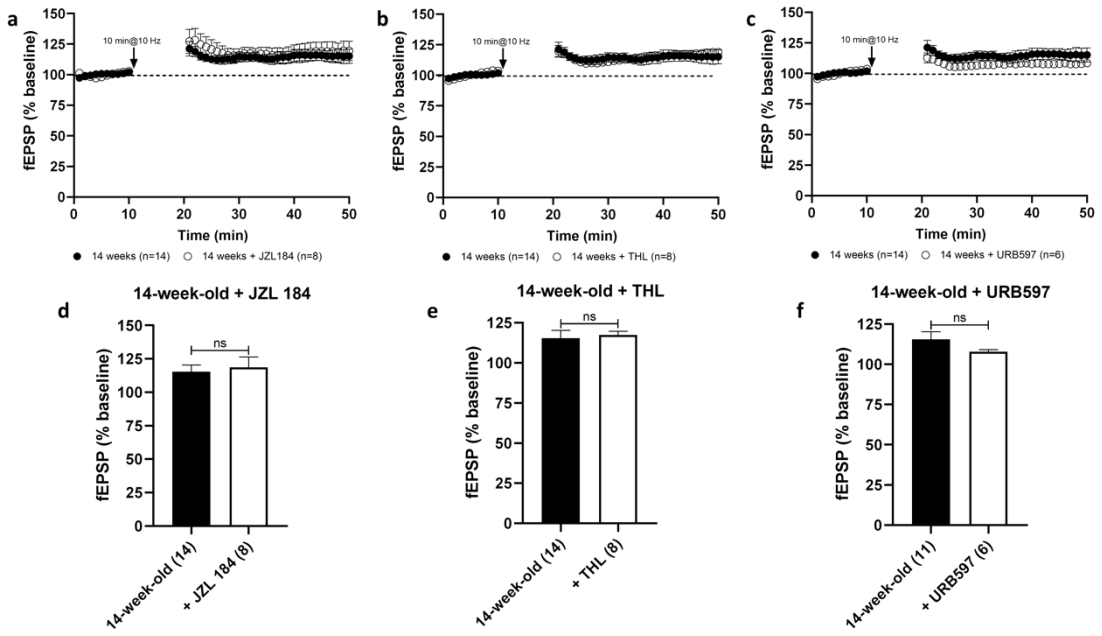

Figure 22. Changes in 2-AG and anandamide have no effect on PFC-LTP in layers II/III in 14-week-old mice. For representation, each experiment was normalized to its baseline. The average of the fEPSP areas is shown. A black arrow marks LFS application. a) JZL 184 [50 μM] (white circles), b) THL [10 μM], and c) URB597 [2 μM] are not able to inhibit the PFC-LTP in a significant manner (white circles). d) Representative histogram of the last 10 min fEPSP after LFS in the presence of JZL 184. Unpaired t test. ns, $p = 0.9203$. e) Representative histogram of the last 10 min fEPSP after LFS and with THL. Mann-Whitney test. ns, $p = 0.2667$. f) Representative histogram of the last 10 min fEPSP after LFS in the presence of URB597. Mann-Whitney test. ns, $p = 0.0913$. All data expressed as mean ± SEM.

DISCUSSION

6.1. COMPARISON OF GFAP AND GLAST AS ASTROGLIAL MARKERS FOR HIGH RESOLUTION ELECTRON MICROSCOPY

The presence of CB_1 receptors in astrocytes has been demonstrated over the last years (Navarrete and Araque, 2008, 2010; Stella, 2010; Han et al., 2012; Bosier et al., 2013; Metna-Laurent and Marsicano, 2015; Viader et al., 2015; Oliveira Da Cruz et al., 2016; Jimenez-Blasco et al., 2020; Bonilla-Del Río et al., 2019, 2021; Egaña-Huguet et al., 2021). The CB_1 receptor-mediated astrocytic functions are highly dependent on the CB_1 receptor distribution in astrocytes relative to neuronal sites, particularly at the nearby synapses, under normal or pathological conditions (Bonilla-Del Río et al., 2019, 2021). However, the whole picture of the subcellular CB_1 receptor distribution in astroglial compartments remains uncompleted due to the low CB_1 receptor expression in astrocytes (Rodríguez et al., 2001; Bosier et al., 2013; Han et al., 2012; Kovács et al., 2017). In this sense, our laboratory has estimated that about 5-6% of the total CB_1 receptors in the hippocampal CA1 stratum radiatum are localized in astrocytes (Gutiérrez-Rodríguez et al., 2018; Bonilla-Del Río et al., 2019, 2021). Similar values were obtained in the basolateral amygdala and posterior parietal association cortical layers II/III (Bonilla-Del Río et al., 2021). These percentages were obtained by double immunoelectron microscopy using GFAP antibodies to label astroglia. However, GFAP is a cytoskeleton protein assembled in intermediate filament packets (Hol and Pekny, 2015) that is mostly restricted to the astroglial cell bodies and their main branches (Sullivan et al., 2007). On the other hand, we have demonstrated previously that ~ 12% of the total CB_1 receptor labeling was in astrocytes of mice intra-hippocampally injected with an adeno-associated virus expressing humanized renilla green fluorescent protein (hrGFP) under the control of human GFAP promoter (GFAPhrGFP-CB_1-WT mice) (Gutiérrez-Rodríguez et al., 2018). These mice also had ~ 34% higher proportion of CB_1 receptor positive astrocytic processes and ~ 64% more particle density than genetic rescue mice that re-expressed CB_1 receptors exclusively in astrocytes (GFAP-*CB_1*-RS) (Gutiérrez-Rodríguez et al., 2018). As hrGFP is a diffusible protein extending into the delicate astrocytic processes that normally lack GFAP (Nolte et al., 2001), these results indicated that CB_1 receptor expression in astrocytes is higher than the one previously revealed in GFAP-positive profiles (Bosier et al., 2013; Han et al., 2012). Following this

line of reasoning, I have confirmed in my thesis by high resolution immunoelectron microscopy that GFAP is concentrated in the cytoplasm of cell bodies and main thick projections of astrocytes, whereas the smallest and fine astrocytic projections were free of GFAP-DAB immunodeposits.

GLAST (EAAT1) is also used as astroglial marker for several reasons: 1) most of the spines are contacted by astrocytes, though only a portion of the dendritic spines are covered with glia in CA1 stratum radiatum; 2) it is reckoned that 3,200 transporters are distributed per μm^3 of CA1 stratum radiatum in the adult rat hippocampus (Lehre and Danbolt, 1998); 3) as the total astroglial cell surface is estimated to be 1.4 m^2/cm^3, the average density of GLAST molecules in astrocytic membranes is ~ 2,300 μm^{-2} (Lehre and Danbolt, 1998); 4) GLAST labeling is localized on astrocytic plasma membranes along the astroglial surface (Chaudhry et al., 1995; also the present thesis). Thus, in my study, GLAST-immunoperoxidase staining detected about three-fold astroglial area and four-fold astroglial membranes than GFAP. I next combined GLAST-immunoperoxidase staining with CB_1 receptor-immunogold labeling for electron microscopy to determine the proportion of astroglial CB_1 receptors. In these conditions, the astroglial CB_1 receptors detected (~12%) was twice as high as with GFAP labeling in CA1 hippocampus (Gutiérrez-Rodríguez et al., 2018; Bonilla-Del Río et al., 2019, 2021). On top of that, the thin projections labeled with GLAST but not with GFAP are astroglial branches that are closely apposed to synapses (Cholet et al., 2002), where most of the receptors are concentrated. Noteworthy, dynamic changes that occur normally in the morphology of the dendritic spines and astrocytes (Wenzel et al., 1991; Fischer et al., 1998) impact on the density of glutamate transporters and receptors (Gegelashvilli et al., 1997; Rao and Craig, 1997). However, abnormal conditions like ethanol exposure also alters receptor expression. In this sense, we have observed in a recent study that adolescent male mice subjected over a period of 4 weeks to binge drinking, have ~ 40 % decrease in CB_1 receptor-positive astroglial processes and ~ 30 % reduction in CB_1 receptor density in CA1 stratum radiatum astrocytes in the young adulthood (Bonilla-Del Río et al., 2019). Also, the proportion of total CB_1 receptor labeling in astrocytes was much lower after ethanol intake (Bonilla-Del Río et al., 2019). These changes in CB_1 receptor expression were associated with astroglial swelling that leads to GFAP disruption (Renau-Piqueras

et al. 1989; Adermark and Bowers, 2016). Interestingly, GLAST up-regulates upon ethanol exposure (Rimondini et al. 2002) that theoretically should favor glutamate clearance. However, GLAST deficient mice with normal CB_1 receptors show less ethanol consumption, motivation and reward (Karlsson et al. 2012).

Altogether, these results indicate that GLAST is a better marker than GFAP to label astrocytes in the electron microscope. Furthermore, the more astroglial surface and membranes are labeled, the more CB_1 receptors located on astroglial processes can be visualized.

6.2. CB_1 RECEPTORS IN ASTROGLIAL AND NEURONAL MITOCHONDRIA

Recent studies have shown that a low but significant proportion of CB_1 receptors in the brain are functionally associated to mitochondrial membranes, where they mediate cannabinoid effects on cellular mitochondrial activity and on behavioral food intake and memory consolidation (Koch et al., 2015, Hebert-Chatelain et al., 2016). We have previously shown by immunoelectron microscopy that CB_1 receptors are localized to neuronal as well as astrocytic mitochondrial membranes in the hippocampus (Bénard et al., 2012; Hebert-Chatelain et al., 2014, 2016; Melser et al., 2017; Gutiérrez-Rodríguez et al., 2018; Bonilla-del Río et al., 2019, 2021; Egaña-Huguet et al., 2021). Also, CB_1 receptors were shown in muscle mitochondria (Mendizabal-Zubiaga et al., 2016). However, doubts raised as whether other brain regions were actually expressing CB_1 receptors at mitochondria, as no studies have been conducted so far to explore this possibility. Hence, I aimed in my doctoral thesis to investigate this issue in prefrontal cortex, nucleus accumbens and piriform cortex, and to compare the CB_1 receptor labeling pattern in these brain regions with the receptor distribution in CA1 hippocampus. I used GLAST labeling because it has been proven to be a good astroglial marker in combination with CB_1 receptor immunolocalization in the electron microscope (see the section before). The results demonstrated that in addition to the presence of mitochondrial CB_1 receptors in neurons already described by our laboratory in the hippocampus (Bénard et al., 2012; Hebert-Chatelain et al., 2014, 2016; Melser et al., 2017; Gutiérrez-Rodríguez et al., 2018, 2019; Bonilla-del Río et al., 2019, 2021; Egaña-Huguet et al., 2021), CB_1 receptors were specifically detected in astroglial mitochondria in the prefrontal cortex, nucleus accumbens and piriform cortex (Jimenez-Blasco et al., 2020).

Under normal conditions, CB_1 receptor expression is very high in inhibitory terminals (Katona and Freund, 2012; Lu and Mackie, 2016; Gutiérrez-Rodríguez et al., 2017), low in excitatory terminals (Katona et al., 2006; Monory et al., 2006; Gutiérrez-Rodríguez et al., 2017) and even lower in astrocytes (Gutiérrez-Rodríguez et al., 2018). We assessed in previous studies that 56% of the CB_1 receptor labeling is localized in GABAergic terminals, 12% in glutamatergic terminals, 6% in astrocytes and 15% in mitochondria (Gutiérrez-Rodríguez et al., 2018; Bonilla-Del Río et al., 2019). Noticeably, 11% of the

immunoparticles were localized elsewhere (Gutiérrez-Rodríguez et al., 2018; Bonilla-Del Río et al., 2019) that might correspond to CB_1 receptors sit at lysosomes/endosomes (Rozenfeld and Devi, 2008) or another compartments. Interestingly, despite the lower absolute CB_1 receptor levels in astrocytes than in neurons (Metna-Laurent and Marsicano, 2015), the density of mitochondrial CB_1 receptors that I found in my thesis was larger in astroglial than in neuronal mitochondria in the prefrontal cortex, nucleus accumbens, piriform cortex and CA1 hippocampus (Jimenez-Blasco et al., 2020).

Activation of mitochondrial CB_1 receptors alters energy production in neurons (Bénard et al., 2012; Hebert-Chatelain et al., 2014; Koch et al., 2015) and can cause memory impairment (Hebert-Chatelain et al., 2016). Furthermore, activation of mitochondrial CB_1 receptors in astrocytes interferes with glucose metabolism and lactate production, disrupting neuronal functions and social behavior (Jimenez-Blasco et al., 2020). The findings that astrocytes of the four brain regions studied contain more CB_1 receptors in their mitochondria than the neuronal mitochondria, and that the cannabinoid-induced reduction of oxygen consumption (Bérnard et al., 2012) is absent in mitochondria isolated from the forebrain of GFAP-CB_1-KO mice (Jimenez-Blasco et al., 2020) suggest that astroglial CB_1 receptors in mitochondria play a crucial role in the global effects of cannabinoids on brain mitochondrial respiration. Taking into account that neurons express much more absolute levels of CB_1 receptors than astrocytes (Busquets-García et al., 2018), CB_1 receptors in neuronal mitochondria might mediate other specific mitochondrial effects of cannabinoids (Hebert-Chatelain et al., 2016). In this regard, our laboratory has demonstrated that CB_1 receptors are reduced in mitochondria of CA1 hippocampus after acute THC administration (CB_1-positive mitochondria decreased by 42% in neurons and 50% in astrocytes; Bonilla-Del Río et al., 2021). Activation of mitochondrial CB_1 receptors in the hippocampus reduces mitochondrial activity and cellular respiration, inhibits soluble adenylyl cyclase and decreases cAMP and protein kinase A (PKA)-dependent phosphorylation of specific subunits of the mitochondrial electron transport system (Hebert-Chatelain et al., 2016). Consequently, mitochondrial mobility is reduced in axons and, therefore, the gathering of mitochondria at neuronal sites of high energy demands might not be achieved. Our previous findings showing more abundant but smaller mitochondria in dendrites and synaptic terminals after acute

exposure to THC (Bonilla-Del Río et al., 2021) suggest that THC is affecting their dynamics, which are crucial for mitochondrial functions. Actually, cAMP-dependent PKA modulates dynamin-related protein 1 (dRP1) activity, a mitochondrial fission enzyme playing an essential role in mitochondrial division and mitochondrial accumulation in dendrites necessary for the upkeeping of dendritic spines and synapses (Li et al., 2004; Cribbs and Strack, 2007). As Drp1 phosphorylation inhibits mitochondrial fission and reduces apoptosis (Cribbs and Strack, 2007), it is plausible that the numerous and small mitochondria found after acute THC might reflect the shutdown of mitochondrial function and the reduced cellular respiration elicited by the activation of the mitochondrial CB_1 receptors in neurons. The THC effects on mitochondrial morphology in astrocytes remain to be elucidated. However, mitochondrial mobility decreases in astrocytes by neuronal activity and astroglial glutamate uptake, and increases by tetrodotoxin (Jackson et al., 2014). Thus, the drastic reduction in CB_1 receptors in inhibitory terminals observed in CA1 after acute THC (Bonilla-Del Río et al., 2021) would facilitate network inhibition and, likely, would promote changes in mitochondrial mobility in astrocytes. Finally, the activation of the mitochondrial CB_1 receptors in astrocytes and the concomitant cAMP-dependent PKA decrease (Jimenez-Blasco et al., 2020) might also be meaning some common mechanisms of mitochondrial dynamics in astrocytes and neurons. It is also possible that the effects on respiration of cannabinoids on neuronal mitochondria are limited to specific brain regions, subcellular domains and/or neuronal types. Experiments suggest that the cell types involved in the effects of mitochondrial CB_1 receptors depend on the functions and the behavioral task, as well as on the subjects´ state (Busquets-García et al., 2015).

6.3. THE IMPORTANCE OF CB_1 RECEPTOR MUTANT MICE IN THE STUDY OF CB_1 RECEPTOR LOCALIZATION

The CB_1 receptor is expressed in various brain cell types (Marsicano and Lutz, 1999; Tsou et al., 1999; Nyíri et al., 2005b; Monory et al., 2006; Häring et al., 2007; Scavone et al., 2010; Han et al., 2012; Metna-Laurent and Marsicano, 2015). Moreover, a wide variety of intracellular effects are triggered by the activation of CB_1 receptors (Bosier et al., 2010; Pertwee, 2015). Retrograde inhibition of transmitter release is one of the most known and important result of these intracellular events (Kano et al., 2009). Consequently, the activation of CB_1 receptors modulates the release of several neurotransmitters (Kano et al., 2009).

Anatomically, the CB_1 receptor is also widely distributed in the brain with a preferential localization in motor, limbic, reward and cortical regions (Matsuda et al., 1993; Tsou et al., 1998). Its high concentration in certain brain areas is an advantage for studying the functional role of the receptor in neural circuits where it is abundantly localized (Katona et al., 1999; Kawamura et al., 2006; Ludányi et al., 2008; Marsicano and Kuner, 2008; Katona and Freund, 2012; De-May and Ali, 2013; Steindel et al., 2013; Hu and Mackie, 2015). However, CB_1 receptor density is not uniform through the regions expressing the receptor, which makes it extremely difficult to identify low CB_1 receptor expression in brain cell types and/or in subcellular compartments of wild-type animals (Busquets-Garcia et al., 2015).

The development and use of cell type specific CB_1 receptor knockout mice lacking CB_1 receptors in specific brain cell populations served to identify low CB_1 receptor expression in cellular, subcellular or intracellular compartments, as well as to understand the physiological functions of the receptor in those compartments (Marsicano et al., 2003; Monory et al., 2006, 2007; Bellocchio et al., 2010; Bénard et al., 2012; Han et al., 2012; Ruehle et al., 2013; Steindel et al., 2013; Soria-Gómez et al., 2014; Busquets-Garcia et al., 2015; Martín-García et al., 2015; Oliveira da Cruz et al., 2016). For example, in the GABA-CB_1-KO brain, a drastic decrease in CB_1 receptor immunoreactivity was observed throughout the hippocampus, but remained a noticeable immunoreactive band in the inner third of the dentate molecular layer (Martín-García et al., 2015). On the other hand, just a very low decrease in CB_1 receptor

immunostaining was noticed in the Glu-CB_1-KO hippocampus (Martín-García et al., 2015; Gutiérrez-Rodríguez et al., 2017). Yet, there was not a full disappearance of the CB_1 receptor immunoreactivity in either condition as it occurred in CB_1-KO. The reason is because the CB_1 receptor localization is mostly, but not exclusively, restricted to neuronal membrane compartments, as CB_1 receptors are also distributed in astrocytic processes (Bosier et al., 2013) and mitochondrial membranes of different cell types of the hippocampus (Bénard et al., 2012; Hebert- Chatelain et al., 2014a; b), as already discussed before. However, these conditional mutant mice have limitations as biological compensations derived from the CB_1 receptor deletion could occur. In addition, a link between the anatomical CB_1 receptor localization in some nerve cells and a certain physiological task might not be likely achievable (Ruehle et al., 2013).

The use of GFAP-CB_1-KO mice have shown that the activation of CB_1 receptors in CA1 astrocytes mediates the impairment of working memory elicited by acute cannabinoids through the modulation of hippocampal LTD (Han et al., 2012). The results obtained in my thesis on the proportion of CB_1 receptor-positive astrocytes in CA1 hippocampus is similar to the value reported in our previous work (Han et al., 2012). Furthermore, the levels of CB_1 receptor immunoparticles in terminals of GFAP-CB_1-KO mice was comparable to CB_1-WT, indicating that GFAP-CB_1-KO mice are good tools for studies based on the loss of function of astrocytic CB_1 receptors (Han et al., 2012).

6.4. CB_1 RECEPTOR DISTRIBUTION IN LAYERS II/III OF THE PRELIMBIC PREFRONTAL CORTEX OF DIFFERENT TRANSGENIC MICE

The CB_1 receptor has been reported to be present in the PFC where is mainly distributed in the layers II/III and V/VI (Lafourcade et al., 2007). However, no statistical analysis of the CB_1 distribution in different synaptic terminals or cell types has been done so far. I used in my thesis, Glu-CB_1-WT, Glu-CB_1-KO, GABA-CB_1-WT, GABA-CB_1-KO and CB_1-KO mice to study the CB_1 receptor distribution in the layers II/III of the prelimbic PFC. Actually, the labeling pattern was similar to the previously found in several brain regions using these mutant mice (Martín-García et al., 2016; Gutiérrez-Rodríguez et al., 2017). Thus, CB_1 receptor immunostaining was very low in GABA-CB_1-KO mice relative to their WT littermates, as most of the CB_1 receptors were located in GABAergic neurons in the PFC. On the contrary, the total CB_1 receptor labeling in Glu-CB_1-KO was similar to the WT mice, but in this case no CB_1 receptor particles were found in excitatory terminals. Finally, more than 90% of the inhibitory terminals and almost 20% of the excitatory terminals were CB_1 receptor immunopositive, like in CA1 hippocampus (Bonilla-Del Río et al., 2019).

The density of CB_1 receptor particles in astrocytes was quite similar or even a bit higher than in excitatory terminals. Importantly, CB_1 receptor particles were not found in GLAST-positive astroglial ramifications of GFAP-CB_1-KO mice. In our previous study, the CB_1 receptor density in the CA1 hippocampus using GFAP as astrocytic marker differed from my present findings in the prelimbic cortical layers II/III of the prefrontal cortex (Gutiérrez-Rodríguez et al., 2018). This might reflect, first, that the amount of CB_1 receptors in astrocytes varies among brain regions; second, that more CB_1 receptors are detected in astrocytes with GLAST than GFAP; or third, that the quantification method applied (particles/100 μm^2 versus particles/µm membrane) would render different density values. CB_1 receptors in astrocytes play a key role in the two-way communication between neurons and astrocytes through rising calcium in astrocytes that modulates synaptic transmission and plasticity (Navarrete and Araque, 2008, 2010; Navarrete et al., 2013; Navarrete et al., 2014; Gómez-Gonzalo et al., 2015; Araque et al., 2017; Martin-Fernandez et al., 2017). Astroglial CB_1 receptor activation regulates astrocytic D-aspartate uptake (Shivachar, 2007) and might be contributing to the brain´s energy

supply through the control of leptin receptors expression in astrocytes (Bosier et al., 2013). In addition, a strong decrease in CB_1 receptors in adult mouse CA1 astrocytes has been recently observed after adolescent drinking-in-the-dark ethanol intake patterns (Bonilla-Del Río et al., 2019).

The endocannabinoid system plays a central role in modulating dopaminergic levels in the CNS (Hermann, et al., 2002). CB_1 receptor activation increases dopamine and decreases GABA in the PFC (Pistis et al., 2002). High CB_1 receptor expression was found in large cholecystokinin (CCK)-containing basket interneurons (Marsicano and Lutz, 1999) whereas parvalbumin and somatostatin-expressing interneurons lack the receptor (Tsou et al. 1999; Bodor et al. 2005). Low but detectable CB_1 receptor mRNA levels were revealed in the glutamatergic neurons of many cortical regions (Monory et al. 2006; Hill et al. 2007). We have recently observed that the CB_1 receptor staining is noticeable in the striatum, cortex, prefrontal cortex and amygdala in rescue mice modified to express the gene exclusively in specific dorsal telencephalic glutamatergic neurons (Glu-*CB_1*-RS; Gutiérrez-Rodríguez et al., 2017). Furthermore, CB_1 receptor localization was mostly restricted to layers II/III and V/VI of the prelimbic prefrontal cortex (Egertova and Elphick 2000). Also, the vast majority of the PFC excitatory projections to the VTA are from prelimbic and cingular neurons that make excitatory synapses with GABAergic interneurons and also dopaminergic neurons (Carr and Sesack, 2000; Geisler et al., 2007). Cannabis derivatives impair prefrontal-based functions and evidences suggest that cannabis can develop and increase the risk of schizophrenia, as the ECS alteration in the PFC may also be contributing to this mental illness (Andreasson et al., 1988; Mathers and Ghodse, 1992). In this context, the knowledge of the subcellular localization of the CB_1 receptor reported in this doctoral thesis, opens new lines of investigation on how cannabis alters functional performance of the prefrontal cortex.

6.5. CB_1 RECEPTOR-DEPENDENT MPP-LTP IN 14-WEEK-OLD MICE

Brain functions regulated by the ECS rely on the regional distribution of the system (Busquets-Garcia et al., 2018; Castillo et al., 2012; Hu and Mackie, 2015; Katona and Freund, 2012). The hippocampus is required for declarative/episodic memory and is involved in spatial and context-dependent learning (Eichenbaum et al., 2012). Inputs from the postrhinal cortex convey spatial information to the dorsolateral medial entorhinal cortex that projects to the dorsal hippocampus through the MPP (Fyhn et al., 2004; Hargreaves et al., 2005). On the other hand, the perirhinal cortex projects to the lateral entorhinal cortex, which gives rise to the LPP (Burwell, 2000). The LPP pathway transmits non-spatial information, and, together with information about spatial clues forwarded by the MPP into the DG, representations for object-place or event-place scenarios are thought to be built (Suzuki et al., 1997; Gaffan, 1998; Hargreaves et al., 2005). At the same time, signal integration by granule cells related to environment or context is under control of hilar mossy cells, which are critical in the learning of information sequences (Lisman et al., 2005). The mossy cells receive glutamatergic granule mossy fiber collaterals, and in turn send commissural/associational fibers that travel long distances giving innervation to multiple DG cells forming mossy-granule cell synapses (Amaral and Witter, 1989; Scharfman and Myers, 2013). The glutamatergic synapses of the three excitatory pathways targeting the dentate granule cells contain CB_1 receptors (Marsicano and Lutz, 1999; Katona et al., 2006; Kawamura et al., 2006; Monory et al., 2006; Uchigashima et al., 2011; Katona and Freund, 2012; Wang et al., 2016; Gutiérrez-Rodríguez et al., 2017) and display different forms of eCB dependent-synaptic plasticity (Chiu and Castillo, 2008; Chávez et al., 2010; Wang et al., 2016, 2018), which correlate with the distinct information processed by each pathway.

As the LTP observed in 14-week-old GFAP-CB_1-WT mice was CB_1 receptor dependent, we aimed to analyze other possible participants in this synaptic plasticity. As in the MPP-LTP of GFAP-CB_1-WT mice, the potentiation of fEPSP observed in 14-week-old WT mice was blocked with the CB_1 receptor inverse agonist AM251, confirming the participation of CB_1 receptors. However, there was not found any change after applying DL-APV, suggesting that the CB_1 receptor-mediated LTP was NMDA receptor-independent. However, although there was not statistical significance, the potentiation seemed to be

reverted in absolute numbers by the NMDA receptor antagonist, so further experiments will be needed to confirm that this is actually the case. We observed previously that the magnitude of eCB-LTD elicited by LFS at the MPP-GC synapses was unaffected by DL-APV (Peñasco et al., 2019), indicating that NMDA receptors were neither involved in the eCB-LTD despite the fact that eCB-LTD may require NMDA receptors at other synapses (Sjöström et al., 2003; Bender et al., 2006; Lutzu and Castillo 2020).

TRPV1 has been shown to participate in synaptic plasticity (Marsch et al., 2007; Gibson et al., 2008; Kauer and Gibson, 2009; Maione et al., 2009; Chávez et al., 2010, 2014; Grueter et al., 2010; Puente et al., 2011), learning and memory (Marsch et al., 2007; Li et al., 2008), fear and anxiety (Marsch et al., 2007; Micale et al., 2009), and to modulate cortical excitability in humans (Mori et al., 2012). TRPV1 and its endogenous agonist AEA participate in synaptic LTD in several brain regions (Di Marzo et al., 2001; 2002; 2008; Ross, 2003; Gibson et al., 2008; Kauer and Gibson, 2009; Maione et al., 2009; Grueter et al., 2010; Chávez et al., 2011). Also, TRPV1 has been shown to participate in NMDA receptor-dependent LTP in CA1 hippocampus that increases after TRPV1 activation (Marsch et al. 2007; Li et al. 2008). We applied the TRPV1 receptor antagonist AMG9810 to analyze the possible implication of this receptor in our MPP-LTP observed in 14-week-old mice. Although it was not statistically significant, AMG9810 eliminated the fEPSP potentiation observed.

The CB_1 receptor activation at LPP synaptic terminals was seen to cause the assembly of latrunculin-sensitive actin filaments, the reorganization of the actin cytoskeleton by an integrin-associated kinase (FAK) and its downstream effector ROCK, resulting in the enhancement of glutamate release and LTP (Wang et al., 2018). Thus, we tested whether this mechanism was playing a role in the CB_1 receptor-dependent MPP-LTP revealed in 14-week-old mice. However, the potentiation was unaltered by the inhibitor of actin polymerization LAT-A. Very recently, our laboratory has reported the existence of MPP-LTP in TRPV1 deficient mice that significantly decreased with LAT-A (Egaña-Huguet et al., 2021), suggesting similar mechanism to LPP-LTP elicited by HFS (100Hz) (Wang et al., 2016, 2018). Also, the NO donor SNAP blocked the MPP-LTP in $TRPV1^{-/-}$ mice (Egaña-Huguet et al., 2021). As TRPV1 is highly permeable to calcium (Caterina et al., 1997; Caterina and Julius, 2001), it is plausible that reduced intracellular calcium

caused by the absence of TRPV1 at the MPP–GC dendritic spine synapses would damp postsynaptic NO synthase and, therefore, decrease NO production needed to support presynaptic LTD in the hippocampus (Reyes-Harde et al., 1999). Under normal conditions, NO activates the presynaptic cGMP-dependent protein kinase (PKG) known to phosphorylate and inactivate the small GTPase RhoA (Sawada et al., 2001), as well as to regulate actin cytoskeleton (Francis et al., 2010). Thus, the lack of NO in the absence of TRPV1 would eventually lead to the signaling of presynaptic molecular pathways that ultimately would enhance the release of glutamate endorsing MPP-LTP (Egaña-Huguet et al., 2021).

The possibility of indirect effects on MPP-LTP by CB_1 receptors in other cells like astrocytes should also be considered, as astroglial CB_1 receptors promote excitatory LTD by favoring local glutamate availability (Han et al., 2012) and endorse LTP at distant excitatory synapses (Araque et al., 2017). In this regard, I have also used 14-week-old mice lacking CB_1 receptors in astrocytes (GFAP-CB_1-KO) and their WT littermates (GFAP-CB_1-WT). I could observe LTP after LFS in GFAP-CB_1-WT, but not significant differences were seen in GFAP-CB_1-KO, meaning that astroglial CB_1 receptors are not playing a key role in the MPP-LTP of 14-week-old mice. Nevertheless, AM251 blocked the potentiation indicating the participation of CB_1 receptors localized in non-astroglial cells.

Altogether, more experiments will be needed to decipher whether TRPV1 receptors are involved in the MPP-LTP in 14-week-old mice. Also, the above-mentioned signaling pathways remain to be assessed.

Different drugs affecting the synthesis and degradation of eCBs were also used to figure out whether 2-AG or AEA were involved. None of the drugs affected significantly the fEPSP potentiation observed in 14-week-old mice. However, the potentiation was reverted by the MAGL inhibitor JZL 184 in a non-significant manner. Consequently, CB_1 receptor desensitization caused by the high 2-AG concentration reached after the JZL 184 incubation time before recordings could be responsible for the CB_1 receptor-LTP blockade, like the JZL 184 effect we reported on eCB-eLTD at the MPP-GC synapses of younger mice (Peñasco et al., 2019). Furthermore, this is in line with previous studies showing that the long-term increase in 2-AG elicits CB_1 receptor desensitization (Chanda et al., 2010; Schlosburg et al., 2010).

As a conclusion, the shift from CB_1 receptor-dependent MPP-LTD to MPP-LTP in 14-week-old-mice might be affecting memory, as the hippocampus in general (Eichenbaum et al., 2012), and the MPP synapses in particular, are involved in spatial memory processing (Fyhn et al., 2004; Hargreaves et al., 2005).

6.6. CB_1 RECEPTOR-DEPENDENT LTP AT PFC SYNAPSES OF 14-WEEK-OLD MICE

The PFC is involved in working memory, self-regulatory and goal-directed behaviors, and displays remarkable structural and functional plasticity over the life course. Neural circuitry, molecular profiles and neurochemistry can be changed by experience, which also influences behavior as well as neuroendocrine and autonomic functions. LFS elicited LTP at layers II/III excitatory synapses in the prelimbic PFC of 14-week-old mice that was blocked by AM251. Interestingly, the significant potentiation in the GFAP-CB_1-WT was not observed in GFAP-CB_1-KO mice. However, the number of experiments done in GFAP-CB_1-KO mice was not sufficient. Therefore, more mutants are required to test the participation in prelimbic PFC-LTP of CB_1 receptors in astrocytes.

NMDA and TRPV1 antagonists were unable to affect the potentiation, indicating that these receptors were not involved in the PFC-LTP. As in MPP-LTP, neither JZL 184 nor THL affected the fEPSP potentiation seen in 14-week-old WT mice PFC. However, the FAAH inhibitor URB597 reverted partially that LTP, although not significantly. Therefore, more experiments will be needed to confirm the plausible implication of AEA in PFC-LTP.

Both, the PFC and the endocannabinoid system are key players in the extinction of aversive memories (Marsicano et al., 2002; Myers and Davis, 2002) and emotional learning plasticity (Laviolette and Grace, 2006). CB_1 receptors are highly expressed in the PFC (Mackie 2005; Eggan and Lewis 2007; Hu and Mackie, 2015) that mediates fear memory extinction as well as an increase in dopaminergic transmission (Diana et al., 1998; Lin et al., 2009). We observed presynaptic CB_1 receptors facing postsynaptic metabotropic glutamate receptor type-5 (mGluR5) in dendritic elements that also contained DAGLα (Lafourcade et al., 2007). This molecular arrangement was responsible for the eCB (2-AG) long-term depression (LTD) elicited by prolonged synaptic stimulation of excitatory inputs to layers V/VI (Lafourcade et al., 2007). Altogether, I observed CB_1-receptor mediated LTP at prelimbic PFC excitatory synapses in 14-week-old mice, in contrast to the LTD elicited by similar LFS in 8-10-week-old-mice (Lafourcade et al., 2007; Peñasco et al., 2019). It remains to be studied the components of the ECS with immunoelectron microscopy in order to figure out the molecular events underlying the PFC-LTP in 14-week-old mice.

CONCLUSIONS

1. While GFAP particles is localized in the cytoplasm of cell bodies and main thick processes of astrocytes, GLAST labeling is distributed along astrocytic plasma membranes, including cell bodies and the smallest astrocytic projections in close contact with neurons, capillaries and other glial cells.
2. About three-fold larger astroglial area and four-fold more astroglial membranes are visualized with GLAST than with GFAP.
3. As much as 12% of the total CB_1 receptor particles localize to GLAST-positive astrocytes, while only about 5% of the total CB_1 receptor labeling is visualized in astrocytes using GFAP.
4. GLAST is an excellent marker for the accurate detection of CB_1 receptors in mitochondria of astrocytes, as demonstrated in this thesis in several brain regions: hippocampus, prefrontal cortex, nucleus accumbens and piriform cortex.
5. The density of mitochondrial CB_1 receptors is higher in astrocytes than in neurons.
6. The proportion of CB_1 receptor-positive compartments and the receptor particle distribution in layers II/III of the prefrontal (prelimbic) cortex of GFAP-CB_1-WT and GFAP-CB_1-KO, are similar to the previously described localization of CB_1 receptors in the hippocampus.
7. Significant LTP is observed at the medial perforant path and in layers II/III prefrontal (prelimbic) excitatory synapses in 14-week-old mice. Moreover, this LTP is CB_1 receptor. NMDA and TRPV1 receptors do not seem to participate.
8. Astroglial CB_1 receptors are not involved in the LTP because is not affected in GFAP-CB_1-KO mice.

BIBLIOGRAPHY

Acin-Perez, R., Salazar, E., Kamenetsky, M., Buck, J., Levin, L. R., & Manfredi, G. (2009). Cyclic AMP produced inside mitochondria regulates oxidative phosphorylation. *Cell metabolism*, 9(3), 265–276.

Acin-Perez, R., Russwurm, M., Günnewig, K., Gertz, M., Zoidl, G., Ramos, L., Buck, J., Levin, L. R., Rassow, J., Manfredi, G., & Steegborn, C. (2011). A phosphodiesterase 2A isoform localized to mitochondria regulates respiration. *Journal of Biological Chemistry*, *286*(35), 30423–30432.

Adermark, L., & Bowers, M. S. (2016). Disentangling the Role of Astrocytes in Alcohol Use Disorder. *Alcoholism, clinical and experimental research*, 40(9), 1802–1816.

Aggleton, J. P., & Brown, M. W. (1999). Episodic memory, amnesia, and the hippocampal-anterior thalamic axis. *The Behavioral and brain sciences*, 22(3), 425–489.

Aguado, T., Palazuelos, J., Monory, K., Stella, N., Cravatt, B., Lutz, B., Marsicano, G., Kokaia, Z., Guzmán, M., & Galve-Roperh, I. (2006). The endocannabinoid system promotes astroglial differentiation by acting on neural progenitor cells. *Journal of Neuroscience*, *26*(5), 1551–1561.

Aguado, T., Romero, E., Monory, K., Palazuelos, J., Sendtner, M., Marsicano, G., Lutz, B., Guzmán, M., & Galve-Roperh, I. (2007). The CB_1 cannabinoid receptor mediates excitotoxicity-induced neural progenitor proliferation and neurogenesis. *Journal of Biological Chemistry*, *282*(33), 23892–23898.

Alger B. E. (2002). Retrograde signaling in the regulation of synaptic transmission: focus on endocannabinoids. *Progress in neurobiology*, 68(4), 247–286.

Alger, B. E. (2006). Not too excited? Thank your endocannabinoids. *Neuron*, 51(4), 393–395.

Alhouayek, M., Masquelier, J., & Muccioli, G. G. (2014). Controlling 2-arachidonoylglycerol metabolism as an anti-inflammatory strategy. *Drug Discovery Today*, *19*(3), 295–304.

Allen, N. J., & Barres, B. A. (2009). How do glia differ from neurons? *Nature Q&A*, *457*(February), 675–677.

Amaral, D. G., & Witter, M. P. (1989). The three-dimensional organization of the hippocampal formation: a review of anatomical data. *Neuroscience*, *31*(3), 571–591.

Ameri A. (1999). The effects of cannabinoids on the brain. *Progress in neurobiology*, 58(4), 315–348.

Andre, C. M., Hausman, J. F., & Guerriero, G. (2016). Cannabis sativa: The plant of the thousand and one molecules. *Frontiers in Plant Science*, *7*(FEB2016), 1–17.

Andréasson, S., Allebeck, P., Engström, A., & Rydberg, U. (1988). *Cannabis and schizophrenia. Lancet (London, England), 1(8592),* 1000–1001.

Andreeva, A. V., Kutuzov, M. A., & Voyno-Yasenetskaya, T. A. (2008). Gα12 is targeted to the mitochondria and affects mitochondrial morphology and motility. *The FASEB Journal*, *22*(8), 2821–2831.

Angulo, M. C., Kozlov, A. S., Charpak, S., & Audinat, E. (2004). Glutamate released from glial cells synchronizes neuronal activity in the hippocampus. *Journal of Neuroscience*, *24*(31), 6920–6927.

Antzoulatos, E. G., & Miller, E. K. (2011). Differences between neural activity in prefrontal cortex and striatum during learning of novel abstract categories. *Neuron*, *71*(2), 243–249.

Aquila, S., Guido, C., Santoro, A., Perrotta, I., Laezza, C., Bifulco, M., & Sebastiano, A. (2010). Human sperm anatomy: Ultrastructural localization of the cannabinoid1 receptor and a potential role of anandamide in sperm survival and acrosome reaction. *Anatomical Record*, *293*(2), 298–309.

Araque, A., Parpura, V., Sanzgiri, R. P., & Haydon, P. G. (1999). Tripartite synapses: glia, the unacknowledged partner. *Trends in neurosciences*, 22(5), 208–215.

Araque, A., Carmignoto, G., & Haydon, P. G. (2001). Dynamic signaling between astrocytes and neurons. *Annual review of physiology*, 63, 795–813.

Araque, A., & Navarrete, M. (2010). Glial cells in neuronal network function. *Philosophical Transactions of the Royal Society B: Biological Sciences*, *365*(1551), 2375–2381.

Araque, A., Castillo, P. E., Manzoni, O. J., & Tonini, R. (2017). Synaptic functions of endocannabinoid signaling in health and disease. *Neuropharmacology*, *124*, 13–24.

Arriza, J. L., Fairman, W. A., Amara, S. G., Kavanaugh, P., Wadiche, I., & Murdoch, H. (1994). Functional Comparisons of Three Glutamate Cloned from Human Motor Cortex Transporter. *The Journal of Neuroscience : The Official Journal of the Society for Neuroscience*, *14*(9), 5559–5569.

Ashton, J. C., Friberg, D., Darlington, C. L., & Smith, P. F. (2006). Expression of the cannabinoid CB_2 receptor in the rat cerebellum: An immunohistochemical study. *Neuroscience Letters*, *396*(2), 113–116.

Attwell, D., & Laughlin, S. B. (2001). An energy budget for signaling in the grey matter of the brain. *Journal of Cerebral Blood Flow and Metabolism*, *21*(10), 1133–1145.

Atwood, B. K., & MacKie, K. (2010). CB_2: A cannabinoid receptor with an identity crisis. *British Journal of Pharmacology*, *160*(3), 467–479.

Azad, S. C., Kurz, J., Marsicano, G., Lutz, B., Zieglgänsberger, W., & Rammes, G. (2008). Activation of CB_1 specifically located on GABAergic interneurons inhibits LTD in the lateral amygdala. *Learning and Memory*, *15*(3), 143–152.

Barros, L. F., & Weber, B. (2018). CrossTalk proposal: an important astrocyte-to-neuron lactate shuttle couples neuronal activity to glucose utilisation in the brain. *Journal of Physiology*, *596*(3), 347–350.

Bartholomä, A., & Nave, K. A. (1994). NEX-1: a novel brain-specific helix-loop-helix protein with autoregulation and sustained expression in mature cortical neurons. *Mechanisms of development*, 48(3), 217–228.

Bélanger, M., & Magistretti, P. J. (2009). The role of astroglia in neuroprotection. *Dialogues in Clinical Neuroscience*, *11*(3), 281–296.

Bélanger, M., Allaman, I., & Magistretti, P. J. (2011). Brain energy metabolism: Focus on Astrocyte-neuron metabolic cooperation. *Cell Metabolism*, *14*(6), 724–738.

Bellocchio, L., Lafentre, P., Cannich, A., Cota, D., Puente, N., Grandes, P., Chaouloff, F., Piazza, P. V., & Marsicano, G. (2010). Bimodal control of stimulated food intake by the endocannabinoid system. *Nature Neuroscience*, *13*(3), 281–283.

Bénard, G., Massa, F., Puente, N., Lourenço, J., Bellocchio, L., Soria-Gómez, E., Matias, I., Delamarre, A., Metna-Laurent, M., Cannich, A., Hebert-Chatelain, E., Mulle, C., Ortega-Gutiérrez, S., Martín-Fontecha, M., Klugmann, M., Guggenhuber, S., Lutz, B., Gertsch, J., Chaouloff, F., López-Rodríguez, M. L., … Marsicano, G. (2012). Mitochondrial CB_1 receptors regulate neuronal energy metabolism. *Nature neuroscience*, 15(4), 558–564.

Bender, V. A., Bender, K. J., Brasier, D. J., & Feldman, D. E. (2006). Two coincidence detectors for spike timing-dependent plasticity in somatosensory cortex. *Journal of Neuroscience*, *26*(16), 4166–4177.

Bilkei-Gorzo, A., Racz, I., Valverde, O., Otto, M., Michel, K., Sastre, M., & Zimmer, A. (2005). Early age-related cognitive impairment in mice lacking cannabinoid CB_1 receptors. *Proceedings of the National Academy of Sciences of the United States of America*, 102(43), 15670–15675.

Bisogno, T., Berrendero, F., Ambrosino, G., Cebeira, M., Ramos, J. A., Fernandez-Ruiz, J. J., & Di Marzo, V. (1999). Brain regional distribution of endocannabinoids: Implications for their biosynthesis and biological function. *Biochemical and Biophysical Research Communications*, *256*(2), 377–380.

Blair, R. E., Deshpande, L. S., & Delorenzo, R. J. (2015). Cannabinoids: Is there a potential treatment role in epilepsy? *Expert Opinion on Pharmacotherapy*, *16*(13), 1911–1914.

Bodor, A. L., Katona, I., Nyíri, G., Mackie, K., Ledent, C., Hájos, N., & Freund, T. F. (2005). Endocannabinoid signaling in rat somatosensory cortex: laminar differences and involvement of specific interneuron types. *The Journal of neuroscience : the official journal of the Society for Neuroscience*, 25(29), 6845–6856.

Bolaños, J. P. (2016). Bioenergetics and redox adaptations of astrocytes to neuronal activity. *Journal of Neurochemistry*, *139*, 115–125.

Bonilla-Del Río, I., Puente, N., Peñasco, S., Rico, I., Gutiérrez-Rodríguez, A., Elezgarai, I., Ramos, A., Reguero, L., Gerrikagoitia, I., Christie, B. R., Nahirney, P., & Grandes, P. (2019). Adolescent ethanol intake alters cannabinoid type-1 receptor localization in astrocytes of the adult mouse hippocampus. *Addiction Biology*, *24*(2), 182–192.

Bonilla-Del Río, I., Puente, N., Mimenza, A., Ramos, A., Serrano, M., Lekunberri, L., Gerrikagoitia, I., Christie, B. R., Nahirney, P. C., & Grandes, P. (2021). Acute Δ9-tetrahydrocannabinol prompts rapid changes in cannabinoid CB_1 receptor immunolabeling and subcellular structure in CA1 hippocampus of young adult male mice. *Journal of Comparative Neurology*, *529*(9), 2332–2346.

Bonini, S. A., Premoli, M., Tambaro, S., Kumar, A., Maccarinelli, G., Memo, M., & Mastinu, A. (2018). Cannabis sativa: A comprehensive ethnopharmacological review of a medicinal plant with a long history. *Journal of Ethnopharmacology*, *227*(September), 300–315.

Bosier, B., Bellocchio, L., Metna-Laurent, M., Soria-Gomez, E., Matias, I., Hebert-Chatelain, E., Cannich, A., Maitre, M., Leste-Lasserre, T., Cardinal, P., Mendizabal-Zubiaga, J., Canduela, M. J., Reguero, L., Hermans, E., Grandes, P., Cota, D., & Marsicano, G. (2013). Astroglial CB_1 cannabinoid receptors regulate leptin signaling in mouse brain astrocytes. *Molecular Metabolism*, *2*(4), 393–404.

Bouaboula, M., Bourrié, B., Rinaldi-Carmona, M., Shire, D., Le Fur, G., & Casellas, P. (1995). Stimulation of cannabinoid receptor CB_1 induces krox-24 expression in human astrocytoma cells. *Journal of Biological Chemistry*, *270*(23), 13973–13980.

Burwell R. D. (2000). The parahippocampal region: corticocortical connectivity. *Annals of the New York Academy of Sciences*, 911, 25–42.

Busquets-Garcia, A., Desprez, T., Metna-Laurent, M., Bellocchio, L., Marsicano, G., & Soria-Gomez, E. (2015). Dissecting the cannabinergic control of behavior: The where matters. *BioEssays : news and reviews in molecular, cellular and developmental biology*, 37(11), 1215–1225.

Busquets-Garcia, A., Bains, J., & Marsicano, G. (2018). CB_1 Receptor Signaling in the Brain: Extracting Specificity from Ubiquity. *Neuropsychopharmacology*, *43*(1), 4–20.

Cabral, G. A., Rogers, T. J., & Lichtman, A. H. (2015). Turning Over a New Leaf: Cannabinoid and Endocannabinoid Modulation of Immune Function. *Journal of neuroimmune pharmacology: the official journal of the Society on NeuroImmune Pharmacology*, 10(2), 193–203.

Carr, D. B., & Sesack, S. R. (2000). Dopamine terminals synapse on callosal projection neurons in the rat prefrontal cortex. *The Journal of comparative neurology*, 425(2), 275–283.

Castillo, P. E., Younts, T. J., Chávez, A. E., & Hashimotodani, Y. (2012). Endocannabinoid signaling and synaptic function. *Neuron*, 76(1), 70–81.

Caterina, M. J., Schumacher, M. A., Tominaga, M., Rosen, T. A., Levine, J. D., & Julius, D. (1997). The capsaicin receptor: a heat-activated ion channel in the pain pathway. *Nature*, 389(6653), 816–824.

Caterina, M. J., & Julius, D. (2001). The vanilloid receptor: a molecular gateway to the pain pathway. *Annual review of neuroscience*, 24, 487–517.

Chanda, P. K., Gao, Y., Mark, L., Btesh, J., Strassle, B. W., Lu, P., Piesla, M. J., Zhang, M. Y., Bingham, B., Uveges, A., Kowal, D., Garbe, D., Kouranova, E. V., Ring, R. H., Bates, B., Pangalos, M. N., Kennedy, J. D., Whiteside, G. T., & Samad, T. A. (2010). Monoacylglycerol lipase activity is a critical modulator of the tone and integrity of the endocannabinoid system. *Molecular pharmacology*, 78(6), 996–1003.

Chaudhry, F. A., Lehre, K. P., van Lookeren Campagne, M., Ottersen, O. P., Danbolt, N. C., & Storm-Mathisen, J. (1995). Glutamate transporters in glial plasma membranes: highly differentiated localizations revealed by quantitative ultrastructural immunocytochemistry. *Neuron*, 15(3), 711–720.

Chávez, A. E., Chiu, C. Q., & Castillo, P. E. (2010). TRPV1 activation by endogenous anandamide triggers postsynaptic long-term depression in dentate gyrus. *Nature Neuroscience*, *13*(12), 1511–1519.

Chen, C., Ko, Y., Delannoy, M., Ludtke, S. J., Chiu, W., & Pedersen, P. L. (2004). Mitochondrial ATP synthasome. Three-dimensional structure by electron microscopy of the ATP synthase in complex formation with carriers for P i and ADP/ATP. *Journal of Biological Chemistry*, *279*(30), 31761–31768.

Chiu, C. Q., & Castillo, P. E. (2008). Input-specific plasticity at excitatory synapses mediated by endocannabinoids in the dentate gyrus. *Neuropharmacology*, 54(1), 68–78.

Cholet, N., Pellerin, L., Magistretti, P. J., & Hamel, E. (2002). Similar perisynaptic glial localization for the Na+,K+-ATPase α2 subunit and the glutamate transporters GLAST and GLT-1 in the rat somatosensory cortex. *Cerebral Cortex*, *12*(5), 515–525.

Christie, B. R., & Abraham, W. C. (1994). L-type voltage-sensitive calcium channel antagonists block heterosynaptic long-term depression in the dentate gyrus of anaesthetized rats. *Neuroscience letters*, 167(1-2), 41–45.

Chudasama, Y., Baunez, C., & Robbins, T. W. (2003). Functional disconnection of the medial prefrontal cortex and subthalamic nucleus in attentional performance: Evidence for corticosubthalamic interaction. *Journal of Neuroscience*, *23*(13), 5477–5485.

Clarke, H. F., Dalley, J. W., Crofts, H. S., Robbins, T. W., & Roberts, A. C. (2004). Cognitive inflexibility after prefrontal serotonin depletion. *Science*, 304(5672), 878–880.

Clement, A. B., Hawkins, E. G., Lichtman, A. H., & Cravatt, B. F. (2003). Increased seizure susceptibility and proconvulsant activity of anandamide in mice lacking fatty acid amide hydrolase. *Journal of Neuroscience*, *23*(9), 3916–3923.

Cravatt, B. F., Giang, D. K., Mayfield, S. P., Boger, D. L., Lerner, R. A., & Gilula, N. B. (1996). Molecular characterization of an enzyme that degrades neuromodulatory fatty-acid amides. *Nature*, 384(6604), 83–87.

Cribbs, J. T., & Strack, S. (2007). Reversible phosphorylation of Drp1 by cyclic AMP-dependent protein kinase and calcineurin regulates mitochondrial fission and cell death. *EMBO reports*, 8(10), 939–944.

Cristino, L., Starowicz, K., De Petrocellis, L., Morishita, J., Ueda, N., Guglielmotti, V., & Di Marzo, V. (2008). Immunohistochemical localization of anabolic and catabolic enzymes for anandamide and other putative endovanilloids in the hippocampus and cerebellar cortex of the mouse brain. *Neuroscience*, *151*(4), 955–968.

Dalley, J. W., Everitt, B. J., & Robbins, T. W. (2011). Impulsivity, Compulsivity, and Top-Down Cognitive Control. *Neuron*, *69*(4), 680–694.

Danbolt, N. C. (1994). The high affinity uptake system for excitatory amino acids in the brain. *Progress in neurobiology*, 44(4), 377–396.

Danbolt, N. C. (2001). Glutamate uptake. *Progress in neurobiology*, 65(1), 1–105.

Danbolt, N. C., Furness, D. N., & Zhou, Y. (2016). Neuronal vs glial glutamate uptake: Resolving the conundrum. *Neurochemistry International*, *98*, 29–45.

De Petrocellis, L., Vellani, V., Schiano-Moriello, A., Marini, P., Magherini, P. C., Orlando, P., Di Marzo, V. (2008). Plant-derived cannabinoids modulate the activity of transient receptor potential channels of ankyrin type-1 and melastatin type-8. *The Journal of pharmacology and experimental therapeutics*, 325(3), 1007-1015.

De Petrocellis, L., & Di Marzo, V. (2009). Role of endocannabinoids and endovanilloids in Ca^{2+} signalling. *Cell Calcium*, *45*(6), 611–624.

De-May, C. L., & Ali, A. B. (2013). Cell type-specific regulation of inhibition via cannabinoid type 1 receptors in rat neocortex. *Journal of Neurophysiology*, *109*(1), 216–224.

Devane, W. A., Hanus, L., Breuer, A., Pertwee, R. G., Stevenson, L. A., Griffin, G., Gibson, D., Mandelbaum, A., Etinger, A., Mechoulam, R. (1992). Isolation and structure of a brain constituent that binds to the cannabinoid receptor. *Science*, 18, 258(5090), 1946-9.

Di Marzo, V., Melck, D., Bisogno, T., & De Petrocellis, L. (1998). Endocannabinoids: endogenous cannabinoid receptor ligands with neuromodulatory action. *Trends in neurosciences*, 21(12), 521–528.

Di Marzo, V., Bisogno, T., De Petrocellis, L., Brandi, I., Jefferson, R. G., Winckler, R. L., Davis, J. B., Dasse, O., Mahadevan, A., Razdan, R. K., & Martin, B. R. (2001). Highly selective CB(1) cannabinoid receptor ligands and novel CB(1)/VR(1) vanilloid receptor "hybrid" ligands. *Biochemical and biophysical research communications*, 281(2), 444–451.

Di Marzo, V., De Petrocellis, L., Fezza, F., Ligresti, A., & Bisogno, T. (2002). Anandamide receptors. *Prostaglandins, leukotrienes, and essential fatty acids*, 66(2-3), 377–391.

Di Marzo, V., Gobbi, G., & Szallasi, A. (2008). Brain TRPV1: a depressing TR(i)P down memory lane?. *Trends in pharmacological sciences*, 29(12), 594–600.

Di Marzo, V., Stella, N., & Zimmer, A. (2015). Endocannabinoid signalling and the deteriorating brain. Nature reviews. *Neuroscience*, 16(1), 30–42.

Diana, M., Melis, M., Muntoni, A. L., & Gessa, G. L. (1998). Mesolimbic dopaminergic decline after cannabinoid withdrawal. *Proceedings of the National Academy of Sciences of the United States of America*, 95(17), 10269–10273.

Domenici, M. R., Azad, S. C., Marsicano, G., Schierloh, A., Wotjak, C. T., Dodt, H. U., Zieglgänsberger, W., Lutz, B., & Rammes, G. (2006). Cannabinoid receptor type 1 located on presynaptic terminals of principal neurons in the forebrain controls glutamatergic synaptic transmission. *Journal of Neuroscience*, *26*(21), 5794–5799.

Durkee, C. A., & Araque, A. (2019). Diversity and Specificity of Astrocyte-neuron Communication. *Neuroscience*, 396, 73–78.

Egaña-Huguet, J., Bonilla-Del Río, I., Gómez-Urquijo, S. M., Mimenza, A., Saumell-Esnaola, M., Borrega-Roman, L., García del Caño, G., Sallés, J., Puente, N., Gerrikagoitia, I., Elezgarai, I., & Grandes, P. (2021). The Absence of the Transient Receptor Potential Vanilloid 1 Directly Impacts on the Expression and Localization of the Endocannabinoid System in the Mouse Hippocampus. *Frontiers in Neuroanatomy*, *15*(February), 1–17.

Egertova, M., Giang, D. K., Cravatt, B. F., & Elphick, M. R. (1998). A new perspective on cannabinoid signalling: Complementary localization of fatty acid amide hydrolase and the CB_1 receptor in rat brain. *Proceedings of the Royal Society B: Biological Sciences*, *265*(1410), 2081–2085.

Egertová, M., & Elphick, M. R. (2000). Localisation of cannabinoid receptors in the rat brain using antibodies to the intracellular C-terminal tail of CB_1. *Journal of Comparative Neurology*, *422*(2), 159–171.

Eggan, S. M., & Lewis, D. A. (2007). Immunocytochemical distribution of the cannabinoid CB_1 receptor in the primate neocortex: a regional and laminar analysis. *Cerebral cortex (New York, N.Y. : 1991)*, 17(1), 175–191.

Eichenbaum, H. (2000). Hippocampus: Mapping or memory? *Current Biology*, *10*(21), 785–787.

Eichenbaum, H., Sauvage, M., Fortin, N., Komorowski, R., & Lipton, P. (2012). Towards a functional organization of episodic memory in the medial temporal lobe. *Neuroscience and biobehavioral reviews*, 36(7), 1597–1608.

Elphick, M. R., & Egertová, M. (2005). The phylogenetic distribution and evolutionary origins of endocannabinoid signalling. *Handbook of experimental pharmacology*, (168), 283–297.

Eng L. F. (1985). Glial fibrillary acidic protein (GFAP): the major protein of glial intermediate filaments in differentiated astrocytes. *Journal of neuroimmunology*, 8(4-6), 203–214.

Eng, L. F., Ghirnikar, R. S., & Lee, Y. L. (2000). Glial fibrillary acidic protein: GFAP-thirty-one years (1969-2000). *Neurochemical research*, 25(9-10), 1439–1451.

Felder, C. C., & Glass, M. (1998). Cannabinoid receptors and their endogenous agonists. *Annual review of pharmacology and toxicology*, 38, 179–200.

Fellin, T. (2009). Communication between neurons and astrocytes: Relevance to the modulation of synaptic and network activity. *Journal of Neurochemistry*, *108*(3), 533–544.

Fezza, F., Bari, M., Florio, R., Talamonti, E., Feole, M., & Maccarrone, M. (2014). Endocannabinoids, related compounds and their metabolic routes. *Molecules*, *19*(11), 17078–17106.

Fischer, M., Kaech, S., Knutti, D., & Matus, A. (1998). Rapid actin-based plasticity in dendritic spines. *Neuron*, 20(5), 847–854.

Flores, Á., Maldonado, R., & Berrendero, F. (2013). Cannabinoid-hypocretin cross-talk in the central nervous system: What we know so far. *Frontiers in Neuroscience*, *7*(7 DEC), 1–17.

Fontaine, C. J., Gräfe, E. L., Pinar, C., Bonilla-Del Río, I., Grandes, P., & Christie, B. R. (2020). Endocannabinoid receptors contribute significantly to multiple forms of long-term depression in the rat dentate gyrus. *Learning & memory*, 27(9), 380–389.

Francis, S. H., Busch, J. L., Corbin, J. D., & Sibley, D. (2010). cGMP-dependent protein kinases and cGMP phosphodiesterases in nitric oxide and cGMP action. *Pharmacological reviews*, 62(3), 525–563.

Freedman, D. J., Riesenhuber, M., Poggio, T., & Miller, E. K. (2001). Categorical representation of visual stimuli in the primate prefrontal cortex. *Science*, 291(5502), 312–316.

Friedman, D., & Devinsky, O. (2015). Cannabinoids in the Treatment of Epilepsy. *The New England journal of medicine*, 373(11), 1048–1058.

Fyhn, M., Molden, S., Witter, M. P., Moser, E. I., & Moser, M. B. (2004). Spatial representation in the entorhinal cortex. *Science (New York, N.Y.)*, 305(5688), 1258–1264.

Gaffan D. (1998). Idiothetic input into object-place configuration as the contribution to memory of the monkey and human hippocampus: a review. *Experimental brain research*, 123(1-2), 201–209.

Galiègue, S., Mary, S., Marchand, J., Dussossoy, D., Carrière, D., Carayon, P., Bouaboula, M., Shire, D., LE Fur, G., & Casellas, P. (1995). Expression of Central and Peripheral Cannabinoid Receptors in Human Immune Tissues and Leukocyte Subpopulations. *European Journal of Biochemistry*, *232*(1), 54–61.

Galve-Roperh, I., Palazuelos, J., Aguado, T., & Guzmán, M. (2009). The endocannabinoid system and the regulation of neural development: Potential implications in psychiatric disorders. *European Archives of Psychiatry and Clinical Neuroscience*, *259*(7), 371–382.

Gegelashvili, G., Danbolt, N. C., & Schousboe, A. (1997). Neuronal soluble factors differentially regulate the expression of the GLT1 and GLAST glutamate transporters in cultured astroglia. *Journal of neurochemistry*, 69(6), 2612–2615.

Geisler, S., Derst, C., Veh, R. W., & Zahm, D. S. (2007). Glutamatergic afferents of the ventral tegmental area in the rat. *The Journal of neuroscience: the official journal of the Society for Neuroscience*, 27(21), 5730–5743.

Gerdeman, G. L., & Lovinger, D. M. (2003). Emerging roles for endocannabinoids in long-term synaptic plasticity. *British journal of pharmacology*, 140(5), 781–789.

Gibson, H. E., Edwards, J. G., Page, R. S., Van Hook, M. J., & Kauer, J. A. (2008). TRPV1 channels mediate long-term depression at synapses on hippocampal interneurons. *Neuron*, 57(5), 746–759.

Golech, S. A., McCarron, R. M., Chen, Y., Bembry, J., Lenz, F., Mechoulam, R., Shohami, E., & Spatz, M. (2004). Human brain endothelium: Coexpression and function of vanilloid and endocannabinoid receptors. *Molecular Brain Research*, *132*(1), 87–92.

Gómez-Gonzalo, M., Navarrete, M., Perea, G., Covelo, A., Martín-Fernández, M., Shigemoto, R., Luján, R., & Araque, A. (2015). Endocannabinoids induce lateral long-term potentiation of transmitter release by stimulation of gliotransmission. *Cerebral Cortex*, *25*(10), 3699–3712.

Gómez-Gonzalo, M., Martin-fernandez, M., Martínez-murillo, R., Hernández-vivanco, A., Jamison, S., Fernandez, A. P., Calero, P., Futch, H. S., Corpas, R., Sanfeliu, C., & Araque, A. (2018). Neuron.-astrocye signaling is preserved in the ageing brain. *Glia*, *65*(4), 612–624.

Gonsiorek, W., Lunn, C., Fan, X., Narula, S., Lundell, D., & Hipkin, R. W. (2000). Endocannabinoid 2-arachidonyl glycerol is a full agonist through human type 2 cannabinoid receptor: Antagonism by anandamide. *Molecular Pharmacology*, *57*(5), 1045–1050.

Grandes, P., & Streit, P. (1991). Effect of perforant path lesion on pattern of glutamate-like immunoreactivity in rat dentate gyrus. *Neuroscience*, 41(2-3), 391–400.

Gruber, A. J., Calhoon, G. G., Shusterman, I., Schoenbaum, G., Roesch, M. R., & O'Donnell, P. (2010). More is less: A disinhibited prefrontal cortex impairs cognitive flexibility. *Journal of Neuroscience*, *30*(50), 17102–17110.

Grueter, B. A., Brasnjo, G., & Malenka, R. C. (2010). Postsynaptic TRPV1 triggers cell type-specific long-term depression in the nucleus accumbens. *Nature neuroscience*, 13(12), 1519–1525.

Guggenhuber, S., Monory, K., Lutz, B., & Klugmann, M. (2010). AAV vector-mediated overexpression of CB_1 cannabinoid receptor in pyramidal neurons of the hippocampus protects against seizure-induced excitoxicity. *PloS one*, 5(12), e15707.

Gutiérrez-Rodríguez, A., Puente, N., Elezgarai, I., Ruehle, S., Lutz, B., Reguero, L., Gerrikagoitia, I., Marsicano, G., & Grandes, P. (2017). Anatomical characterization of the cannabinoid CB_1 receptor in cell-type–specific mutant mouse rescue models. *Journal of Comparative Neurology*, *525*(2), 302–318.

Gutiérrez-Rodríguez, A., Bonilla-Del Río, I., Puente, N., Gómez-Urquijo, S. M., Fontaine, C. J., Egaña-Huguet, J., Elezgarai, I., Ruehle, S., Lutz, B., Robin, L. M., Soria-Gómez, E., Bellocchio, L., Padwal, J. D., van der Stelt, M., Mendizabal-Zubiaga, J., Reguero, L., Ramos, A., Gerrikagoitia, I., Marsicano, G., & Grandes, P. (2018). Localization of the cannabinoid type-1 receptor in subcellular astrocyte compartments of mutant mouse hippocampus. *Glia*, *66*(7), 1417–1431.

Guzmán, M., Galve-Roperh, I., & Sánchez, C. (2001). Ceramide: a new second messenger of cannabinoid action. *Trends in pharmacological sciences*, 22(1), 19–22.

Hájos, N., Ledent, C., & Freund, T. F. (2001). Novel cannabinoid-sensitive receptor mediates inhibition of glutamatergic synaptic transmission in the hippocampus. *Neuroscience*, *106*(1), 1–4.

Halassa, M. M., Fellin, T., Takano, H., Dong, J. H., & Haydon, P. G. (2007). Synaptic islands defined by the territory of a single astrocyte. *Journal of Neuroscience*, *27*(24), 6473–6477.

Han, J., Kesner, P., Metna-Laurent, M., Duan, T., Xu, L., Georges, F., Koehl, M., Abrous, D. N., Mendizabal-Zubiaga, J., Grandes, P., Liu, Q., Bai, G., Wang, W., Xiong, L., Ren, W., Marsicano, G., & Zhang, X. (2012). Acute cannabinoids impair working memory through astroglial CB_1 receptor modulation of hippocampal LTD. *Cell*, *148*(5), 1039–1050.

Hargreaves, E. L., Rao, G., Lee, I., & Knierim, J. J. (2005). Major dissociation between medial and lateral entorhinal input to dorsal hippocampus. *Science (New York, N.Y.)*, 308(5729), 1792–1794.

Häring, M., Marsicano, G., Lutz, B., & Monory, K. (2007). Identification of the cannabinoid receptor type 1 in serotonergic cells of raphe nuclei in mice. *Neuroscience*, *146*(3), 1212–1219.

Haydon, P. G., & Carmignoto, G. (2006). Astrocyte control of synaptic transmission and neurovascular coupling. *Physiological Reviews*, *86*(3), 1009–1031.

Haydon P. G. (2017). Astrocytes and the modulation of sleep. *Current opinion in neurobiology*, 44, 28–33.

Hirrlinger, P. G., Scheller, A., Braun, C., Hirrlinger, J., & Kirchhoff, F. (2006). Temporal control of gene recombination in astrocytes by transgenic expression of the tamoxifen-inducible DNA recombinase variant CreERT2. *Glia*, 54(1), 11–20.

Hebert-Chatelain, E., Reguero, L., Puente, N., Lutz, B., Chaouloff, F., Rossignol, R., Piazza, P. V., Benard, G., Grandes, P., & Marsicano, G. (2014). Studying mitochondrial CB_1 receptors: Yes we can. *Molecular Metabolism*, *3*(4), 339.

Hebert-Chatelain, E., Reguero, L., Puente, N., Lutz, B., Chaouloff, F., Rossignol, R., Piazza, P. V., Benard, G., Grandes, P., & Marsicano, G. (2014). Cannabinoid control of brain bioenergetics: Exploring the subcellular localization of the CB_1 receptor. *Molecular Metabolism*, *3*(4), 495–504.

Hebert-Chatelain, E., Desprez, T., Serrat, R., Bellocchio, L., Soria-Gomez, E., Busquets-Garcia, A., Pagano Zottola, A. C., Delamarre, A., Cannich, A., Vincent, P., Varilh, M., Robin, L. M., Terral, G., García-Fernández, M. D., Colavita, M., Mazier, W., Drago, F., Puente, N., Reguero, L., … Marsicano, G. (2016). A cannabinoid link between mitochondria and memory. *Nature*, *539*(7630), 555–559.

Heifets, B. D., & Castillo, P. E. (2009). Endocannabinoid signaling and long-term synaptic plasticity. *Annual review of physiology*, 71, 283–306.

Helling, S., Vogt, S., Rhiel, A., Ramzan, R., Wen, L., Marcus, K., & Kadenbach, B. (2008). Phosphorylation and kinetics of mammalian cytochrome c oxidase. *Molecular and Cellular Proteomics*, *7*(9), 1714–1724.

Henneberger, C. (2017). Does rapid and physiological astrocyte–neuron signalling amplify epileptic activity? *Journal of Physiology*, *595*(6), 1917–1927.

Herkenham, M., Lynn, A. B., Little, M. D., Johnson, M. R., Melvin, L. S., de Costa, B. R., & Rice, K. C. (1990). Cannabinoid receptor localization in brain. *Proceedings of the National Academy of Sciences of the United States of America*, 87(5), 1932–1936.

Hermann, H., Marsicano, G., & Lutz, B. (2002). Coexpression of the cannabinoid receptor type 1 with dopamine and serotonin receptors in distinct neuronal subpopulations of the adult mouse forebrain. *Neuroscience*, *109*(3), 451–460.

Hill, E. L., Gallopin, T., Férézou, I., Cauli, B., Rossier, J., Schweitzer, P., & Lambolez, B. (2007). Functional CB_1 receptors are broadly expressed in neocortical GABAergic and glutamatergic neurons. *Journal of neurophysiology*, 97(4), 2580–2589.

Hillard, C. J. (2014). Stress regulates endocannabinoid-CB_1 receptor signaling. *Seminars in Immunology*, *26*(5), 380–388.

Hol, E. M., & Pekny, M. (2015). Glial fibrillary acidic protein (GFAP) and the astrocyte intermediate filament system in diseases of the central nervous system. *Current opinion in cell biology*, 32, 121–130.

Howlett, A. C., Barth, F., Bonner, T. I., Cabral, G., Casellas, P., Devane, W. A., Felder, C. C., Herkenham, M., Mackie, K., Martin, B. R., Mechoulam, R., & Pertwee, R. G. (2002). International Union of Pharmacology. XXVII. Classification of cannabinoid receptors. *Pharmacological Reviews*, *54*(2), 161–202.

Hu, S. S., & Mackie, K. (2015). Distribution of the Endocannabinoid System in the Central Nervous System. *Handbook of experimental pharmacology*, 231, 59–93.

Ishac, E. J. N., Jiang, L., Lake, K. D., Varga, K., Abood, M. E., & Kunos, G. (1996). Inhibition of exocytotic noradrenaline release by presynaptic cannabinoid CB_1 receptors on peripheral sympathetic nerves. *British Journal of Pharmacology*, *118*(8), 2023–2028.

Jackson, J. G., O'Donnell, J. C., Takano, H., Coulter, D. A., & Robinson, M. B. (2014). Neuronal activity and glutamate uptake decrease mitochondrial mobility in astrocytes and position mitochondria near glutamate transporters. *The Journal of neuroscience: the official journal of the Society for Neuroscience*, 34(5), 1613–1624.

Jimenez-Blasco, D., Busquets-Garcia, A., Hebert-Chatelain, E., Serrat, R., Vicente-Gutierrez, C., Ioannidou, C., Gómez-Sotres, P., Lopez-Fabuel, I., Resch-Beusher, M., Resel, E., Arnouil, D., Saraswat, D., Varilh, M., Cannich, A., Julio-Kalajzic, F., Bonilla-Del Río, I., Almeida, A., Puente, N., Achicallende, S., Lopez-Rodriguez, M. L., … Marsicano, G. (2020). Glucose metabolism links astroglial mitochondria to cannabinoid effects. *Nature*, 583(7817), 603–608.

Kamprath, K., Plendl, W., Marsicano, G., Deussing, J. M., Wurst, W., Lutz, B., & Wotjak, C. T. (2009). Endocannabinoids mediate acute fear adaptation via glutamatergic neurons independently of corticotropin-releasing hormone signaling. *Genes, Brain and Behavior*, *8*(2), 203–211.

Kano, M., Ohno-Shosaku, T., Hashimotodani, Y., Uchigashima, M., & Watanabe, M. (2009). Endocannabinoid-mediated control of synaptic transmission. *Physiological Reviews*, *89*(1), 309–380.

Karlsson, R. M., Adermark, L., Molander, A., Perreau-Lenz, S., Singley, E., Solomon, M., Holmes, A., Tanaka, K., Lovinger, D. M., Spanagel, R., & Heilig, M. (2012). Reduced alcohol intake and reward associated with impaired endocannabinoid signaling in mice with a deletion of the glutamate transporter GLAST. *Neuropharmacology*, 63(2), 181–189.

Katona, I., Sperlágh, B., Sík, A., Käfalvi, A., Vizi, E. S., Mackie, K., & Freund, T. F. (1999). Presynaptically located CB_1 cannabinoid receptors regulate GABA release from axon terminals of specific hippocampal interneurons. *Journal of Neuroscience*, *19*(11), 4544–4558.

Katona, I., Sperlágh, B., Maglóczky, Z., Sántha, E., Köfalvi, A., Czirják, S., Mackie, K., Vizi, E. S., & Freund, T. F. (2000). GABAergic interneurons are the targets of cannabinoid actions in the human hippocampus. *Neuroscience*, *100*(4), 797–804.

Katona, I., Urbán, G. M., Wallace, M., Ledent, C., Jung, K. M., Piomelli, D., Mackie, K., & Freund, T. F. (2006). Molecular composition of the endocannabinoid system at glutamatergic synapses. *Journal of Neuroscience*, *26*(21), 5628–5637.

Katona, I., & Freund, T. F. (2012). Multiple functions of endocannabinoid signaling in the brain. *Annual review of neuroscience*, 35, 529–558.

Katona I. (2015). Cannabis and Endocannabinoid Signaling in Epilepsy. *Handbook of experimental pharmacology*, 231, 285–316.

Kauer, J. A., & Gibson, H. E. (2009). Hot flash: TRPV channels in the brain. *Trends in neurosciences*, 32(4), 215–224.

Kawamura, Y., Fukaya, M., Maejima, T., Yoshida, T., Miura, E., Watanabe, M., Ohno-Shosaku, T., & Kano, M. (2006). The CB_1 cannabinoid receptor is the major cannabinoid receptor at excitatory presynaptic sites in the hippocampus and cerebellum. *Journal of Neuroscience*, *26*(11), 2991–3001.

Kleppisch, T., Wolfsgruber, W., Feil, S., Allmann, R., Wotjak, C. T., Goebbels, S., Nave, K. A., Hofmann, F., & Feil, R. (2003). Hippocampal cGMP-dependent protein kinase I supports an age- and protein

synthesis-dependent component of long-term potentiation but is not essential for spatial reference and contextual memory. *Journal of Neuroscience*, *23*(14), 6005–6012.

Koch, M., Varela, L., Kim, J. G., Kim, J. D., Hernández-Nuño, F., Simonds, S. E., Castorena, C. M., Vianna, C. R., Elmquist, J. K., Morozov, Y. M., Rakic, P., Bechmann, I., Cowley, M. A., Szigeti-Buck, K., Dietrich, M. O., Gao, X. B., Diano, S., & Horvath, T. L. (2015). Hypothalamic POMC neurons promote cannabinoid-induced feeding. *Nature*, 519(7541), 45–50.

Kofuji, P., & Araque, A. (2021). G-Protein-Coupled Receptors in Astrocyte–Neuron Communication. *Neuroscience*, *456*, 71–84.

Kovács, A., Bordás, C., Bíró, T., Hegyi, Z., Antal, M., Szücs, P., & Pál, B. (2017). Direct presynaptic and indirect astrocyte-mediated mechanisms both contribute to endocannabinoid signaling in the pedunculopontine nucleus of mice. *Brain structure & function*, 222(1), 247–266.

Lafourcade, M., Elezgarai, I., Mato, S., Bakiri, Y., Grandes, P., & Manzoni, O. J. (2007). Molecular Components and Functions of the Endocannabinoid System in Mouse Prefrontal Cortex. *PLoS ONE*, *2*(8), 1–11.

Laughlin, S. B., de Ruyter van Steveninck, R. R., & Anderson, J. C. (1998). The metabolic cost of neural information. *Nature neuroscience*, 1(1), 36–41.

Laviolette, S. R., & Grace, A. A. (2006). Cannabinoids Potentiate Emotional Learning Plasticity in Neurons of the Medial Prefrontal Cortex through Basolateral Amygdala Inputs. *The Journal of neuroscience : the official journal of the Society for Neuroscience*, 26(24), 6458–6468.

Lehre, K. P., & Danbolt, N. C. (1998). The number of glutamate transporter subtype molecules at glutamatergic synapses: chemical and stereological quantification in young adult rat brain. The Journal of neuroscience: the official journal of the *Society for Neuroscience*, 18(21), 8751–8757.

Leo, A., Russo, E., & Elia, M. (2016). Cannabidiol and epilepsy: Rationale and therapeutic potential. *Pharmacological Research*, *107*, 85–92.

Lévesque, M., & Avoli, M. (2013). The kainic acid model of temporal lobe epilepsy. *Neuroscience and biobehavioral reviews*, 37(10 Pt 2), 2887–2899.

Li, Z., Okamoto, K., Hayashi, Y., & Sheng, M. (2004). The importance of dendritic mitochondria in the morphogenesis and plasticity of spines and synapses. *Cell*, 119(6), 873–887.

Li, H. B., Mao, R. R., Zhang, J. C., Yang, Y., Cao, J., & Xu, L. (2008). Antistress effect of TRPV1 channel on synaptic plasticity and spatial memory. *Biological psychiatry*, 64(4), 286–292.

Lin, H. C., Mao, S. C., Su, C. L., & Gean, P. W. (2009). The role of prefrontal cortex CB_1 receptors in the modulation of fear memory. *Cerebral cortex (New York, N.Y. : 1991)*, 19(1), 165–175.

Lisman, J. E., Talamini, L. M., & Raffone, A. (2005). Recall of memory sequences by interaction of the dentate and CA3: a revised model of the phase precession. *Neural networks : the official journal of the International Neural Network Society*, 18(9), 1191–1201.

López, A., Aparicio, N., Pazos, M. R., Grande, M. T., Barreda-Manso, M. A., Benito-Cuesta, I., Vázquez, C., Amores, M., Ruiz-Pérez, G., García-García, E., Beatka, M., Tolón, R. M., Dittel, B. N., Hillard, C. J., & Romero, J. (2018). Cannabinoid CB_2 receptors in the mouse brain: Relevance for Alzheimer's disease. *Journal of Neuroinflammation*, *15*(1), 1–11.

Lu, H. C., & Mackie, K. (2016). An Introduction to the Endogenous Cannabinoid System. *Biological psychiatry,* 79(7), 516–525.

Ludányi, A., Eross, L., Czirják, S., Vajda, J., Halász, P., Watanabe, M., Palkovits, M., Maglóczky, Z., Freund, T. F., & Katona, I. (2008). Downregulation of the CB_1 cannabinoid receptor and related molecular elements of the endocannabinoid system in epileptic human hippocampus. *Journal of Neuroscience*, *28*(12), 2976–2990.

Luk, T., Jin, W., Zvonok, A., Lu, D., Lin, X. Z., Chavkin, C., Makriyannis, A., & Mackie, K. (2004). Identification of a potent and highly efficacious, yet slowly desensitizing CB_1 cannabinoid receptor agonist. *British Journal of Pharmacology*, *142*(3), 495–500.

Lüttjohann, A., Fabene, P. F., & van Luijtelaar, G. (2009). A revised Racine's scale for PTZ-induced seizures in rats. *Physiology and Behavior*, *98*(5), 579–586.

Lutz, B., Marsicano, G., Maldonado, R., & Hillard, C. J. (2015). The endocannabinoid system in guarding against fear, anxiety and stress. *Nature reviews. Neuroscience*, 16(12), 705–718.

Lutzu, S., & Castillo, P. E. (2021). Modulation of NMDA Receptors by G-protein-coupled receptors: Role in Synaptic Transmission, Plasticity and Beyond. *Neuroscience*, 456, 27–42.

Lyssand, J. S., & Bajjalieh, S. M. (2007). The heterotrimeric [corrected] G protein subunit G alpha i is present on mitochondria. *FEBS letters*, 581(30), 5765–5768.

MacAskill, A. F., & Kittler, J. T. (2010). Control of mitochondrial transport and localization in neurons. *Trends in cell biology*, 20(2), 102–112.

Maccarrone, M., Rossi, S., Bari, M., De Chiara, V., Fezza, F., Musella, A., Gasperi, V., Prosperetti, C., Bernardi, G., Finazzi-Agrò, A., Cravatt, B. F., Centonze, D. (2008). Anandamide inhibits metabolism and physiological actions of 2-arachidonoylglycerol in the striatum. *Nature Neuroscience,* 11, 152–159.

Maccarone, R., Rapino, C., Zerti, D., Di Tommaso, M., Battista, N., Di Marco, S., Bisti, S., & Maccarrone, M. (2016). Modulation of Type-1 and Type-2 cannabinoid receptors by saffron in a rat model of retinal neurodegeneration. *PLoS ONE*, *11*(11), 1–20.

Mackie K. (2005). Distribution of cannabinoid receptors in the central and peripheral nervous system. *Handbook of experimental pharmacology*, (168), 299–325.

Mackie, K., & Stella, N. (2006). Cannabinoid receptors and endocannabinoids: Evidence for new players. *The AAPS Journal*, *8*(2), E298–E306.

Magistretti, P. J., & Pellerin, L. (1999). Astrocytes couple synaptic activity to glucose utilization in the brain. *News in Physiological Sciences*, *14*(5), 177–182.

Magistretti, P. J., & Allaman, I. (2018). Lactate in the brain: from metabolic end-product to signalling molecule. *Nature reviews. Neuroscience*, 19(4), 235–249.

Mailleux, P., & Vanderhaeghen, J. J. (1992). Age-related loss of cannabinoid receptor binding sites and mRNA in the rat striatum. *Neuroscience letters*, 147(2), 179–181.

Maione, S., Cristino, L., Migliozzi, A. L., Georgiou, A. L., Starowicz, K., Salt, T. E., & Di Marzo, V. (2009). TRPV1 channels control synaptic plasticity in the developing superior colliculus. *The Journal of physiology*, 587(Pt 11), 2521–2535.

Marsch, R., Foeller, E., Rammes, G., Bunck, M., Kössl, M., Holsboer, F., Zieglgänsberger, W., Landgraf, R., Lutz, B., & Wotjak, C. T. (2007). Reduced anxiety, conditioned fear, and hippocampal long-term potentiation in transient receptor potential vanilloid type 1 receptor-deficient mice. *The Journal of neuroscience : the official journal of the Society for Neuroscience*, 27(4), 832–839.

Marsicano, G., & Lutz, B. (1999). Expression of the cannabinoid receptor CB_1 in distinct neuronal subpopulations in the adult mouse forebrain. *European Journal of Neuroscience*, *11*(12), 4213–4225.

Marsicano, G., Wotjak, C. T., Azad, S. C., Bisogno, T., Rammes, G., Cascioll, M. G., Hermann, H., Tang, J., Hofmann, C., Zieglgänsberger, W., Di Marzo, V., & Lutz, B. (2002). The endogenous cannabinoid system controls extinction of aversive memories. *Nature*, *418*(6897), 530–534.

Marsicano, G., Goodenough, S., Monory, K., Hermann, H., Eder, M., Cannich, A., Azad, S. C., Cascio, M. G., Gutiérrez, S. O., van der Stelt, M., López-Rodriguez, M. L., Casanova, E., Schütz, G., Zieglgänsberger, W., Di Marzo, V., Behl, C., & Lutz, B. (2003). CB_1 cannabinoid receptors and on-demand defense against excitotoxicity. *Science*, 302(5642), 84–88.

Marsicano, G. & Lutz, B. (2006). Neuromodulatory functions of the endocannabinoid system. *Journal of endocrinological investigation*, 29(3), 27.

Marsicano, G. & Kuner, R. (2008). Anatomical distribution of receptors, ligands and enzymes in the brain and in the spinal cord: circuitries and neurochemistry. In *Cannabinoids and the Brain, Springer, Boston, MA.*, 161-201.

Martin-Fernandez, M., Jamison, S., Robin, L. M., Zhao, Z., Martin, E. D., Aguilar, J., Benneyworth, M. A., Marsicano, G., & Araque, A. (2017). Synapse-specific astrocyte gating of amygdala-related behavior. *Nature neuroscience*, 20(11), 1540–1548.

Martín-García, E., Fernández-Castillo, N., Burokas, A., Gutiérrez-Cuesta, J., Sánchez-Mora, C., Casas, M., Ribasés, M., Cormand, B., & Maldonado, R. (2015). Frustrated expected reward induces differential transcriptional changes in the mouse brain. *Addiction Biology*, *20*(1), 22–27.

Mathers, D. C., & Ghodse, A. H. (1992). Cannabis and psychotic illness. *The British journal of psychiatry : the journal of mental science, 161*, 648–653.

Matsuda, L. A., Lolait, S. J., Brownstein, M. J., Young, A. C., & Bonner, T. I. (1990). Structure of a cannabinoid receptor and functional expression of the cloned cDNA. *Nature*, *346*(6284), 561–564.

Matsuda, L. A., Bonner, T. I. & Lolait, S. J. (1993). Localization of cannabinoid receptor mRNA in rat brain. *Journal of Comparative Neurology*, 327(4), 535-550.

Mattson, M. P., Gleichmann, M., & Cheng, A. (2008). Mitochondria in neuroplasticity and neurological disorders. *Neuron*, 60(5), 748–766.

Mechoulam, R., Ben-Shabat, S., Hanus, L., Ligumsky, M., Kaminski, N. E., Schatz, A. R., Gopher, A., Almog, S., Martin, B. R., Compton, D. R., Pertwee, R. G., Griffin, G., Bayewitch, M., Barg, J., & Vogel, Z. (1995). Identification of an endogenous 2-monoglyceride, present in canine gut, that binds to cannabinoid receptors. *Biochemical Pharmacology*, *50*(1), 83–90.

Melser, S., Pagano Zottola, A. C., Serrat, R., Puente, N., Grandes, P., Marsicano, G., & Hebert-Chatelain, E. (2017). Functional Analysis of Mitochondrial CB_1 Cannabinoid Receptors ($mtCB_1$) in the Brain. *Methods in enzymology*, 593, 143–174.

Mendizabal-Zubiaga, J., Melser, S., Bénard, G., Ramos, A., Reguero, L., Arrabal, S., Elezgarai, I., Gerrikagoitia, I., Suarez, J., De Fonseca, F. R., Puente, N., Marsicano, G., & Grandes, P. (2016). Cannabinoid CB_1 receptors are localized in striated muscle mitochondria and regulate mitochondrial respiration. *Frontiers in Physiology*, *7*(OCT), 1–10.

Metna-Laurent, M., & Marsicano, G. (2015). Rising stars: Modulation of brain functions by astroglial type-1 cannabinoid receptors. *Glia*, *63*(3), 353–364.

Micale, V., Cristino, L., Tamburella, A., Petrosino, S., Leggio, G. M., Drago, F., & Di Marzo, V. (2009). Anxiolytic effects in mice of a dual blocker of fatty acid amide hydrolase and transient receptor potential vanilloid type-1 channels. *Neuropsychopharmacology : official publication of the American College of Neuropsychopharmacology*, 34(3), 593–606.

Moldrich, G., & Wenger, T. (2000). Localization of the CB_1 cannabinoid receptor in the rat brain. An immunohistochemical study. *Peptides*, *21*(11), 1735–1742.

Molina-Holgado, F., Molina-Holgado, E., Guaza, C., & Rothwell, N. J. (2002). Role of CB_1 and CB_2 receptors in the inhibitory effects of cannabinoids on lipopolysaccharide-induced nitric oxide release in astrocyte cultures. *Journal of Neuroscience Research*, *67*(6), 829–836.

Monory, K., Massa, F., Egertová, M., Eder, M., Blaudzun, H., Westenbroek, R., Kelsch, W., Jacob, W., Marsch, R., Ekker, M., Long, J., Rubenstein, J. L., Goebbels, S., Nave, K. A., During, M., Klugmann, M., Wölfel, B., Dodt, H. U., Zieglgänsberger, W., Wotjak, C. T., … Lutz, B. (2006). The endocannabinoid system controls key epileptogenic circuits in the hippocampus. *Neuron*, 51(4), 455–466.

Monory, K., Blaudzun, H., Massa, F., Kaiser, N., Lemberger, T., Schütz, G., Wotjak, C. T., Lutz, B., & Marsicano, G. (2007). Genetic dissection of behavioural and autonomic effects of Delta(9)-tetrahydrocannabinol in mice. *PLoS biology*, 5(10), e269.

Mori, F., Ribolsi, M., Kusayanagi, H., Monteleone, F., Mantovani, V., Buttari, F., Marasco, E., Bernardi, G., Maccarrone, M., & Centonze, D. (2012). TRPV1 channels regulate cortical excitability in humans. *The Journal of neuroscience : the official journal of the Society for Neuroscience*, 32(3), 873–879.

Morozov, Y. M., Torii, M., & Rakic, P. (2009). Origin, early commitment, migratory routes, and destination of cannabinoid type 1 receptor-containing interneurons. *Cerebral Cortex*, *19*(SUPPL. 1).

Munro, S., Thomas, K. L., & Abu-Shaar, M. (1993). Molecular characterization of a peripheral receptor for cannabinoids. *Nature*, *365*(6441), 61–65.

Myers, K. M., & Davis, M. (2002). Systems-level reconsolidation: reengagement of the hippocampus with memory reactivation. *Neuron*, 36(3), 340–343.

Navarrete, M., & Araque, A. (2008). Endocannabinoids Mediate Neuron-Astrocyte Communication. *Neuron*, *57*(6), 883–893.

Navarrete, M., & Araque, A. (2010). Endocannabinoids potentiate synaptic transmission through stimulation of astrocytes. *Neuron*, *68*(1), 113–126.

Navarrete, M., Perea, G., Maglio, L., Pastor, J., García De Sola, R., & Araque, A. (2013). Astrocyte calcium signal and gliotransmission in human brain tissue. *Cerebral Cortex*, *23*(5), 1240–1246.

Navarrete, M., Díez, A., & Araque, A. (2014). Astrocytes in endocannabinoid signalling. *Philosophical Transactions of the Royal Society B: Biological Sciences*, *369*(1654).

Nicholls, D. G., and Ferguson, S. J. (2002). Bioenergetics. *Biochemistry*, 69, 818–819.

Nolte, C., Matyash, M., Pivneva, T., Schipke, C. G., Ohlemeyer, C., Hanisch, U. K., Kirchhoff, F., & Kettenmann, H. (2001). GFAP promoter-controlled EGFP-expressing transgenic mice: a tool to visualize astrocytes and astrogliosis in living brain tissue. *Glia*, 33(1), 72–86.

Nyíri, G., Szabadits, E., Cserép, C., Mackie, K., Shigemoto, R., & Freund, T. F. (2005). GABAB and CB_1 cannabinoid receptor expression identifies two types of septal cholinergic neurons. *The European journal of neuroscience*, 21(11), 3034–3042.

Oliveira, J. F., Sardinha, V. M., Guerra-Gomes, S., Araque, A., & Sousa, N. (2015). Do stars govern our actions? Astrocyte involvement in rodent behavior. *Trends in neurosciences*, 38(9), 535–549.

Oliveira da Cruz, J. F., Robin, L. M., Drago, F., Marsicano, G., & Metna-Laurent, M. (2016). Astroglial type-1 cannabinoid receptor (CB_1): A new player in the tripartite synapse. *Neuroscience*, *323*, 35–42.

Oropeza, V. C., Mackie, K., & Van Bockstaele, E. J. (2007). Cannabinoid receptors are localized to noradrenergic axon terminals in the rat frontal cortex. *Brain research*, 1127(1), 36–44.

Pasupathy, A., & Miller, E. K. (2005). Different time courses of learning-related activity in the prefrontal cortex and striatum. *Nature*, *433*(7028), 873–876.

Pekny, M., & Pekna, M. (2014). Astrocyte reactivity and reactive astrogliosis: Costs and benefits. *Physiological Reviews*, *94*(4), 1077–1098.

Peñasco, S., Rico-Barrio, I., Puente, N., Gómez-Urquijo, S. M., Fontaine, C. J., Egaña-Huguet, J., Achicallende, S., Ramos, A., Reguero, L., Elezgarai, I., Nahirney, P. C., Christie, B. R., & Grandes, P. (2019). Endocannabinoid long-term depression revealed at medial perforant path excitatory synapses in the dentate gyrus. *Neuropharmacology*, 153, 32–40.

Peñasco, S., Rico-Barrio, I., Puente, N., Fontaine, C. J., Ramos, A., Reguero, L., Gerrikagoitia, I., de Fonseca, F. R., Suarez, J., Barrondo, S., Aretxabala, X., García del Caño, G., Sallés, J., Elezgarai, I., Nahirney, P. C., Christie, B. R., & Grandes, P. (2020). Intermittent ethanol exposure during adolescence impairs cannabinoid type 1 receptor-dependent long-term depression and recognition memory in adult mice. *Neuropsychopharmacology*, *45*(2), 309–318.

Perea, G., & Araque, A. (2002). Communication between astrocytes and neurons: A complex language. *Journal of Physiology, Paris*, *96*(3–4), 199–207.

Perea, G., & Araque, A. (2005). Synaptic regulation of the astrocyte calcium signal. *Journal of Neural Transmission*, *112*(1), 127–135.

Perea, G., & Araque, A. (2005). Properties of synaptically evoked astrocyte calcium signal reveal synaptic information processing by astrocytes. *Journal of Neuroscience*, *25*(9), 2192–2203.

Perea, G., Navarrete, M., & Araque, A. (2009). Tripartite synapses: astrocytes process and control synaptic information. *Trends in neurosciences*, 32(8), 421–431.

Perea, G., & Araque, A. (2010). GLIA modulates synaptic transmission. *Brain research reviews*, 63(1-2), 93–102.

Pertwee R. G. (2001). Cannabinoid receptors and pain. *Progress in neurobiology*, 63(5), 569–611.

Pertwee, R. G. (2009). Emerging strategies for exploiting cannabinoid receptor agonists as medicines. *British Journal of Pharmacology*, *156*(3), 397–411.

Pertwee, R. G., Howlett, A. C., Abood, M. E., Alexander, S. P. H., Di Marzo, V., Elphick, M. R., Greasley, P. J., Hansen, H. S., Kunos, G., Mackie, K., Mechoulam, R., & Ross, R. A. (2010). International Union of Basic and Clinical Pharmacology. LXXIX. Cannabinoid receptors and their ligands: Beyond CB_1 and CB_2. *Pharmacological Reviews*, *62*(4), 588–631.

Pertwee R. G. (2015). Endocannabinoids and Their Pharmacological Actions. *Handbook of experimental pharmacology*, 231, 1–37.

Petersen, R. P., Moradpour, F., Eadie, B. D., Shin, J. D., Kannangara, T. S., Delaney, K. R., & Christie, B. R. (2013). Electrophysiological identification of medial and lateral perforant path inputs to the dentate gyrus. *Neuroscience*, *252*, 154–168.

Petit, J. M., & Magistretti, P. J. (2016). Regulation of neuron-astrocyte metabolic coupling across the sleep-wake cycle. *Neuroscience*, *323*, 135–156.

Piazza, P. V., Cota, D., & Marsicano, G. (2017). The CB_1 Receptor as the Cornerstone of Exostasis. *Neuron*, *93*(6), 1252–1274.

Piluzza, G., Delogu, G., Cabras, A., Marceddu, S., & Bullitta, S. (2013). Differentiation between fiber and drug types of hemp (Cannabis sativa L.) from a collection of wild and domesticated accessions. *Genetic Resources and Crop Evolution*, *60*(8), 2331–2342.

Piomelli, D. (2003). The molecular logic of endocannabinoid signalling. *Nature Reviews Neuroscience*, *4*(11), 873–884.

Piomelli D. (2014). More surprises lying ahead. The endocannabinoids keep us guessing. *Neuropharmacology*, 76 Pt B, 228–234.

Pistis, M., Muntoni, A. L., Pillolla, G., & Gessa, G. L. (2002). Cannabinoids inhibit excitatory inputs to neurons in the shell of the nucleus accumbens: an in vivo electrophysiological study. *The European journal of neuroscience*, 15(11), 1795–1802.

Puente, N., Cui, Y., Lassalle, O., Lafourcade, M., Georges, F., Venance, L., Grandes, P., & Manzoni, O. J. (2011). Polymodal activation of the endocannabinoid system in the extended amygdala. *Nature Neuroscience*, *14*(12), 1542–1547.

Puente, N., Bonilla-Del Río, I., Achicallende, S., Nahirney, P., & Grandes, P. (2019). High-resolution Immunoelectron Microscopy Techniques for Revealing Distinct Subcellular Type 1 Cannabinoid Receptor Domains in Brain. *Bio-Protocol*, *9*(2).

Puig, M. V., & Gulledge, A. T. (2011). Serotonin and prefrontal cortex function: neurons, networks, and circuits. *Molecular Neurobiology*, *44*(3), 449–464.

Ortinski, P. I., Dong, J., Mungenast, A., Yue, C., Takano, H., Watson, D. J., Haydon, P. G., & Coulter, D. A. (2010). Selective induction of astrocytic gliosis generates deficits in neuronal inhibition. *Nature neuroscience*, 13(5), 584–591.

Racine R. J. (1972). Modification of seizure activity by electrical stimulation. II. Motor seizure. *Electroencephalography and clinical neurophysiology*, 32(3), 281–294.

Rao, A., & Craig, A. M. (1997). Activity regulates the synaptic localization of the NMDA receptor in hippocampal neurons. *Neuron*, 19(4), 801–812.

Reddy D. S. (2014). Neurosteroids and their role in sex-specific epilepsies. *Neurobiology of disease*, 72 Pt B, 198–209.

Reddy, D. S., & Golub, V. M. (2016). The pharmacological basis of cannabis therapy for epilepsy. *Journal of Pharmacology and Experimental Therapeutics*, *357*(1), 45–55.

Reguero, L., Puente, N., Elezgarai, I., Mendizabal-Zubiaga, J., Canduela, M. J., Buceta, I., Ramos, A., Suárez, J., de Fonseca, F. R., Marsicano, G., & Grandes, P. (2011). GABAergic and cortical and subcortical glutamatergic axon terminals contain CB_1 cannabinoid receptors in the ventromedial nucleus of the hypothalamus. *PLoS ONE*, *6*(10).

Renau-Piqueras, J., Zaragoza, R., De Paz, P., Baguena-Cervellera, R., Megias, L., & Guerri, C. (1989). Effects of prolonged ethanol exposure on the glial fibrillary acidic protein-containing intermediate filaments of astrocytes in primary culture: a quantitative immunofluorescence and immunogold electron microscopic study. *The journal of histochemistry and cytochemistry: official journal of the Histochemistry Society,* 37(2), 229–240.

Reyes-Harde, M., Potter, B. V., Galione, A., & Stanton, P. K. (1999). Induction of hippocampal LTD requires nitric-oxide-stimulated PKG activity and Ca2+ release from cyclic ADP-ribose-sensitive stores. *Journal of neurophysiology*, 82(3), 1569–1576.

Rimondini, R., Arlinde, C., Sommer, W., & Heilig, M. (2002). Long-lasting increase in voluntary ethanol consumption and transcriptional regulation in the rat brain after intermittent exposure to alcohol. *FASEB journal: official publication of the Federation of American Societies for Experimental Biology*, 16(1), 27–35.

Robel, S., Buckingham, S. C., Boni, J. L., Campbell, S. L., Danbolt, N. C., Riedemann, T., Sutor, B., & Sontheimer, H. (2015). Reactive astrogliosis causes the development of spontaneous seizures. *Journal of Neuroscience*, *35*(8), 3330–3345.

Robin, L. M., Oliveira da Cruz, J. F., Langlais, V. C., Martin-Fernandez, M., Metna-Laurent, M., Busquets-Garcia, A., Bellocchio, L., Soria-Gomez, E., Papouin, T., Varilh, M., Sherwood, M. W., Belluomo, I., Balcells, G., Matias, I., Bosier, B., Drago, F., Van Eeckhaut, A., Smolders, I., Georges, F., … Marsicano, G. (2018). Astroglial CB_1 Receptors Determine Synaptic D-Serine Availability to Enable Recognition Memory. *Neuron*, *98*(5), 935-944.e5.

Rodríguez, J. J., Mackie, K., & Pickel, V. M. (2001). Ultrastructural localization of the CB_1 cannabinoid receptor in μ-opioid receptor patches of the rat caudate putamen nucleus. *Journal of Neuroscience*, *21*(3), 823–833.

Rosenberg, E. C., Tsien, R. W., Whalley, B. J., & Devinsky, O. (2015). Cannabinoids and Epilepsy. *Neurotherapeutics*, *12*(4), 747–768.

Ross, R. A. (2003). Anandamide and vanilloid TRPV1 receptors. *British Journal of Pharmacology*, *140*(5), 790–801.

Rossi, S., Motta, C., Musella, A., & Centonze, D. (2015). The interplay between inflammatory cytokines and the endocannabinoid system in the regulation of synaptic transmission. *Neuropharmacology*, *96*(PA), 105–112.

Rozenfeld, R., & Devi, L. A. (2008). Regulation of CB1 cannabinoid receptor trafficking by the adaptor protein AP-3. *FASEB journal: official publication of the Federation of American Societies for Experimental Biology*, 22(7), 2311–2322.

Ruehle, S., Remmers, F., Romo-Parra, H., Massa, F., Wickert, M., Wörtge, S., Häring, M., Kaiser, N., Marsicano, G., Pape, H. C., & Lutz, B. (2013). Cannabinoid CB_1 receptor in dorsal telencephalic glutamatergic neurons: Distinctive sufficiency for hippocampus-dependent and amygdala-dependent synaptic and behavioral functions. *Journal of Neuroscience*, *33*(25), 10264–10277.

Russo, E. B. (2007). History of cannabis and its preparations in saga, science, and sobriquet. *Chemistry and Biodiversity*, *4*(8), 1614–1648.

Ryberg, E., Larsson, N., Sjögren, S., Hjorth, S., Hermansson, N. O., Leonova, J., Elebring, T., Nilsson, K., Drmota, T., & Greasley, P. J. (2007). The orphan receptor GPR55 is a novel cannabinoid receptor. *British Journal of Pharmacology*, *152*(7), 1092–1101.

Rygula, R., Walker, S. C., Clarke, H. F., Robbins, T. W., & Roberts, A. C. (2010). Differential contributions of the primate ventrolateral prefrontal and orbitofrontal cortex to serial reversal learning. *Journal of Neuroscience*, *30*(43), 14552–14559.

Ryu, H., Lee, J., Impey, S., Ratan, R. R., & Ferrante, R. J. (2005). Antioxidants modulate mitochondrial PKA and increase CREB binding to D-loop DNA of the mitochondrial genome in neurons. *Proceedings of the National Academy of Sciences of the United States of America*, *102*(39), 13915–13920.

Sagan, S. (1999). Anandamide and WIN 55212-2 inhibit cyclic AMP formation through G-protein-coupled receptors distinct from CB1 cannabinoid receptors in cultured astrocytes. *European Journal of Neuroscience*, *11*(2), 691–699.

Salio, C., Doly, S., Fischer, J., Franzoni, M. F., & Conrath, M. (2002). Neuronal and astrocytic localization of the cannabinoid receptor-1 in the dorsal horn of the rat spinal cord. *Neuroscience letters*, 329(1), 13–16.

Sánchez, C., Galve-Roperh, I., Canova, C., Brachet, P., & Guzmán, M. (1998). Δ9-Tetrahydrocannabinol induces apoptosis in C6 glioma cells. *FEBS Letters*, *436*(1), 6–10.

Sawada, N., Itoh, H., & Nakao, K. (2001). [Novel actions of HMG-CoA reductase inhibitors(statins)--vascular and cerebral protection through inhibition of small GTPase Rho]. *Nihon rinsho. Japanese journal of clinical medicine*, 59(12), 2470–2475.

Scavone, J. L., Mackie, K., & Van Bockstaele, E. J. (2010). Characterization of cannabinoid-1 receptors in the locus coeruleus: relationship with mu-opioid receptors. *Brain research*, 1312, 18–31.

Scharfman, H. E., & Myers, C. E. (2013). Hilar mossy cells of the dentate gyrus: a historical perspective. *Frontiers in neural circuits*, 6, 106.

Schatz, A. R., Lee, M., Condie, R. B., Pulaski, J. T., & Kaminski, N. E. (1997). Cannabinoid receptors CB1 and CB2: a characterization of expression and adenylate cyclase modulation within the immune system. *Toxicology and applied pharmacology*, 142(2), 278–287.

Schlosburg, J. E., Blankman, J. L., Long, J. Z., Nomura, D. K., Pan, B., Kinsey, S. G., Nguyen, P. T., Ramesh, D., Booker, L., Burston, J. J., Thomas, E. A., Selley, D. E., Sim-Selley, L. J., Liu, Q. S., Lichtman, A. H., & Cravatt, B. F. (2010). Chronic monoacylglycerol lipase blockade causes functional antagonism of the endocannabinoid system. *Nature neuroscience*, 13(9), 1113–1119.

Schwab, M. H., Druffel-Augustin, S., Gass, P., Jung, M., Klugmann, M., Bartholomae, A., Rossner, M. J., & Nave, K. A. (1998). Neuronal basic helix-loop-helix proteins (NEX, neuroD, NDRF): spatiotemporal expression and targeted disruption of the NEX gene in transgenic mice. *The Journal of neuroscience: the official journal of the Society for Neuroscience*, 18(4), 1408–1418.

Sheng, W. S., Hu, S., Min, X., Cabral, G. A., Lokensgard, J. R., & Peterson, P. K. (2005). Synthetic cannabinoid WIN55,212-2 inhibits generation of inflammatory mediators by IL-1β-stimulated human astrocytes. *Glia*, *49*(2), 211–219.

Shivachar A. C. (2007). Cannabinoids inhibit sodium-dependent, high-affinity excitatory amino acid transport in cultured rat cortical astrocytes. *Biochemical pharmacology*, 73(12), 2004–2011.

Showalter, V. M., Compton, D. R., Martin, B. R., & Abood, M. E. (1996). Evaluation of binding in a transfected cell line expressing a peripheral cannabinoid receptor (CB_2): identification of cannabinoid receptor subtype selective ligands. *The Journal of pharmacology and experimental therapeutics*, 278(3), 989–999.

Sillanpää, M., & Schmidt, D. (2012). Is incident drug-resistance of childhood-onset epilepsy reversible? A long-term follow-up study. *Brain*, *135*(7), 2256–2262.

Sjöström, P. J., Turrigiano, G. G., & Nelson, S. B. (2003). Neocortical LTD via coincident activation of presynaptic NMDA and cannabinoid receptors. *Neuron*, *39*(4), 641–654.

Sofroniew, M. V., & Vinters, H. V. (2010). Astrocytes: Biology and pathology. *Acta Neuropathologica*, *119*(1), 7–35.

Soria-Gómez, E., Bellocchio, L., Reguero, L., Lepousez, G., Martín, C., Bendahmane, M., ... & Wiesner, T. (2014). The endocannabinoid system controls food intake via olfactory processes. *Nature neuroscience*, 17(3), 407.

Soria-Gómez, E., Busquets-Garcia, A., Hu, F., Mehidi, A., Cannich, A., Roux, L., Louit, I., Alonso, L., Wiesner, T., Georges, F., Verrier, D., Vincent, P., Ferreira, G., Luo, M., & Marsicano, G. (2015). Habenular CB_1 Receptors Control the Expression of Aversive Memories. *Neuron*, *88*(2), 306–313.

Steindel, F., Lerner, R., Häring, M., Ruehle, S., Marsicano, G., Lutz, B., & Monory, K. (2013). Neuron-type specific cannabinoid-mediated G protein signalling in mouse hippocampus. *Journal of Neurochemistry*, *124*(6), 795–807.

Stella N. (2010). Cannabinoid and cannabinoid-like receptors in microglia, astrocytes, and astrocytomas. *Glia*, 58(9), 1017–1030.

Storck, T., Schulte, S., Hofmann, K., & Stoffel, W. (1992). Structure, expression, and functional analysis of a Na+-dependent glutamate/aspartate transporter from rat brain. *Proceedings of the National Academy of Sciences of the United States of America*, *89*(22), 10955–10959.

Stühmer, T., Puelles, L., Ekker, M., & Rubenstein, J. L. R. (2002). Expression from a Dlx gene enhancer marks adult mouse cortical GABAergic neurons. *Cerebral Cortex*, *12*(1), 75–85.

Suárez, J., Romero-Zerbo, S. Y., Rivera, P., Bermúdez-Silva, F. J., Pérez, J., De Fonseca, F. R., & Fernández-Llebrez, P. (2010). Endocannabinoid system in the adult rat circumventricular areas: An immunohistochemical Study. *Journal of Comparative Neurology*, *518*(15), 3065–3085.

Sugiura, T., Kondo, S., Kishimoto, S., Miyashita, T., Nakane, S., Kodaka, T., Suhara, Y., Takayama, H., & Waku, K. (2000). Evidence that 2-arachidonoylglycerol but not N-palmitoylethanolamine or anandamide is the physiological ligand for the cannabinoid CB_2 receptor. Comparison of the agonistic activities of various cannabinoid receptor ligands in HL-60 cells. *Journal of Biological Chemistry*, *275*(1), 605–612.

Sugiura, T., Kishimoto, S., Oka, S., & Gokoh, M. (2006). Biochemistry, pharmacology and physiology of 2-arachidonoylglycerol, an endogenous cannabinoid receptor ligand. *Progress in Lipid Research*, *45*(5), 405–446.

Sullivan, S. M., Lee, A., Björkman, S. T., Miller, S. M., Sullivan, R. K. P., Poronnik, P., Colditz, P. B., & Pow, D. V. (2007). Cytoskeletal anchoring of GLAST determines susceptibility to brain damage: An identified role for GFAP. *Journal of Biological Chemistry*, *282*(40), 29414–29423.

Sun, Y., Alexander, S. P., Kendall, D. A., & Bennett, A. J. (2006). Cannabinoids and PPARalpha signalling. *Biochemical Society Transactions*, 34, 1095-1097.

Suzuki, F., Makiura, Y., Guilhem, D., Sørensen, J. C., & Onteniente, B. (1997). Correlated axonal sprouting and dendritic spine formation during kainate-induced neuronal morphogenesis in the dentate gyrus of adult mice. *Experimental neurology*, 145(1), 203–213.

Suzuki, A., Stern, S. A., Bozdagi, O., Huntley, G. W., Ruth, H., Magistretti, P. J., & Alberini, C. M. (2012). Memory Formation. *Encyclopedia of Exercise Medicine in Health and Disease*, *144*(5), 557–557.

Takahashi, K. A., & Castillo, P. E. (2006). The CB_1 cannabinoid receptor mediates glutamatergic synaptic suppression in the hippocampus. *Neuroscience*, *139*(3), 795–802.

Taura, F., Sirikantaramas, S., Shoyama, Y., Shoyama, Y., & Morimoto, S. (2007). Phytocannabiniods in Cannabis sativa: Recent studies on biosynthetic enzymes. *Chemistry and Biodiversity*, *4*(8), 1649–1663.

Theodosis, D. T., Poulain, D. A., & Oliet, S. H. R. (2008). Activity-dependent structural and functional plasticity of astrocyte-neuron interactions. *Physiological Reviews*, *88*(3), 983–1008.

Tsou, K., Brown, S., Sañudo-Peña, M. C., Mackie, K., & Walker, J. M. (1998). Immunohistochemical distribution of cannabinoid CB_1 receptors in the rat central nervous system. *Neuroscience*, 83(2), 393–411.

Twitchell, W., Brown, S., & Mackie, K. (1997). Cannabinoids inhibit n- and p/q-type calcium channels in cultured rat hippocampal neurons. *Journal of Neurophysiology*, *78*(1), 43–50.

Uchigashima, M., Yamazaki, M., Yamasaki, M., Tanimura, A., Sakimura, K., Kano, M., & Watanabe, M. (2011). Molecular and morphological configuration for 2-arachidonoylglycerol-mediated retrograde signaling at mossy cell-granule cell synapses in the dentate gyrus. *The Journal of neuroscience : the official journal of the Society for Neuroscience*, 31(21), 7700–7714.

Ujike, H., & Morita, Y. (2004). New perspectives in the studies on endocannabinoid and cannabis: Cannabinoid receptors and schizophrenia. *Journal of Pharmacological Sciences*, *96*(4), 376–381.

Viader, A., Blankman, J. L., Zhong, P., Liu, X., Schlosburg, J. E., Joslyn, C. M., Liu, Q. S., Tomarchio, A. J., Lichtman, A. H., Selley, D. E., Sim-Selley, L. J., & Cravatt, B. F. (2015). Metabolic Interplay between Astrocytes and Neurons Regulates Endocannabinoid Action. *Cell Reports*, *12*(5), 798–808.

Vinogradova, L. V., & Van Rijn, C. M. (2008). Anticonvulsive and antiepileptogenic effects of levetiracetam in the audiogenic kindling model. *Epilepsia*, *49*(7), 1160–1168.

Yi, C. X., Habegger, K. M., Chowen, J. A., Stern, J., & Tschöp, M. H. (2011). A role for astrocytes in the central control of metabolism. *Neuroendocrinology*, 93(3), 143–149.

Walter, L., & Stella, N. (2003). Endothelin-1 increases 2-arachidonoyl glycerol (2-AG) production in astrocytes. *Glia*, *44*(1), 85–90.

Wang, W., Trieu, B. H., Palmer, L. C., Jia, Y., Pham, D. T., Jung, K. M., Karsten, C. A., Merrill, C. B., Mackie, K., Gall, C. M., Piomelli, D., & Lynch, G. (2016). A Primary Cortical Input to Hippocampus Expresses

a Pathway-Specific and Endocannabinoid-Dependent Form of Long-Term Potentiation. *eNeuro*, 3(4), ENEURO.0160-16.2016.

Wang, W., Jia, Y., Pham, D. T., Palmer, L. C., Jung, K. M., Cox, C. D., Rumbaugh, G., Piomelli, D., Gall, C. M., & Lynch, G. (2018). Atypical Endocannabinoid Signaling Initiates a New Form of Memory-Related Plasticity at a Cortical Input to Hippocampus. *Cerebral cortex (New York, N.Y. : 1991)*, 28(7), 2253–2266.

Warden, M. R., & Miller, E. K. (2010). Task-dependent changes in short-term memory in the prefrontal cortex. *Journal of Neuroscience*, *30*(47), 15801–15810.

Wenzel, J., Lammert, G., Meyer, U., & Krug, M. (1991). The influence of long-term potentiation on the spatial relationship between astrocyte processes and potentiated synapses in the dentate gyrus neuropil of rat brain. *Brain research*, 560(1-2), 122–131.

Whiting, P. F., Wolff, R. F., Deshpande, S., Di Nisio, M., Duffy, S., Hernandez, A. V., Keurentjes, J. C., Lang, S., Misso, K., Ryder, S., Schmidlkofer, S., Westwood, M., & Kleijnen, J. (2015). Cannabinoids for Medical Use: A Systematic Review and Meta-analysis. *JAMA*, 313(24), 2456–2473.

Wilcox, K. S., Dixon-Salazar, T., Sills, G. J., Ben-Menachem, E., White, H. S., Porter, R. J., Dichter, M. A., Moshé, S. L., Noebels, J. L., Privitera, M. D., & Rogawski, M. A. (2013). Issues related to development of new antiseizure treatments. *Epilepsia*, *54*(SUPPL.4), 24–34.

Wu, S. X., Goebbels, S., Nakamura, K., Nakamura, K., Kometani, K., Minato, N., Kaneko, T., Nave, K. A., & Tamamaki, N. (2005). Pyramidal neurons of upper cortical layers generated by NEX-positive progenitor cells in the subventricular zone. *Proceedings of the National Academy of Sciences of the United States of America*, *102*(47), 17172–17177.

Zerucha, T., Stühmer, T., Hatch, G., Park, B. K., Long, Q., Yu, G., Gambarotta, A., Schultz, J. R., Rubenstein, J. L. R., & Ekker, M. (2000). A highly conserved enhancer in the Dlx5/Dlx6 intergenic region is the site of cross-regulatory interactions between Dlx genes in the embryonic forebrain. *Journal of Neuroscience*, *20*(2), 709–721.

Zhou, Y., & Danbolt, N. C. (2014). Glutamate as a neurotransmitter in the healthy brain. *Journal of Neural Transmission*, *121*(8), 799–817.

Zippin, J. H., Chen, Y., Nahirney, P., Kamenetsky, M., Wuttke, M. S., Fischman, D. A., Levin, L. R., & Buck, J. (2003). Compartmentalization of bicarbonate-sensitive adenylyl cyclase in distinct signaling microdomains. *The FASEB Journal : Official Publication of the Federation of American Societies for Experimental Biology*, *17*(1), 82–84.

Zou, S., & Kumar, U. (2018). Cannabinoid receptors and the endocannabinoid system: Signaling and function in the central nervous system. *International Journal of Molecular Sciences*, *19*(3).

Zygmunt, P. M., Petersson, J., Andersson, D. A., Chuang, H. H., Sørgård, M., Di Marzo, V., Julius, D., & Högestätt, E. D. (1999). Vanilloid receptors on sensory nerves mediate the vasodilator action of anandamide. *Nature*, *400*(6743), 452–457.

ASTROZITOETAN KOKATUTAKO CB_1 HARTZAILE KANNABINOIDEAREN ANALISI ULTRAESTRUKTURALA ETA FISIOLOGIKOA

DOKTOREGO TESIA

Svein Achicallende Urcaregui

Leioa, 2021

Universidad del País Vasco
Euskal Herriko Unibertsitatea

NEUROZIENTZIAK SAILA
DEPARTAMENTO DE NEUROCIENCIAS
MEDIKUNTZA ETA ERIZAINTZA FAKULTATEA
FACULTAD DE MEDICINA Y ENFERMERÍA

SVEIN ACHICALLENDE URCAREGUI
aurkeztutako doktorego tesia

Autorea Euskal Herriko Unibertsitateko (UPV/EHU) ikertzaile-aurredoktore kontratu baten hartzailea (PIF 16/251) izan zen
Lan hau babestuta egon zen: Eusko Jaurlaritza (IT1230-19); MINECO/FEDER, UE (SAF2015-65034-R); Zientzia eta Berrikuntza sailburua (PID2019-107548RBI00)

Zuzendariak:

Pedro Rolando Grandes Moreno, MD PhD
María Inmaculada Gerrikagoitia Marina, PhD

Neurozientziak saila
Medikuntza eta Erizaintza fakultatea
Euskal Herriko Unibertsitatea (UPV/EHU) Leioa, 2021

AURKIBIDEA

LABURDURAK

2-AG: 2-arakidonoilglizerola

A1R: 1-motako adenosina-hartzailea
A2AR: 2A-motako adenosina-hartzailea
AA: azido arakidonikora
ABC: abidina-biotina konplexua
aCSF: likido zefalorrakideo artifizialean (*artificial cerebrospinal fluid*)
AEA: N-arakidonoiletanolamina edo anandamida
AED: anti-epilepsia botika (*antiepileptic drug*)
AMG: amigdala
AMP: adenosina monofosfatoa
AMPA: azido D-amino-3-hidroxi-5-metil-4-isoxazole-propionikoa
ANOVA: bariantzaren analisia (*analysis of variance*)
AR: adenosina-hartzailea
ARNm: azido erribonukleiko mezularia
ATP: adenosina trofosfatoa

BNST: bukaera ildaskaren nukleoan (*bed nucleus of the striatal terminalis*)
BSA: behi-serum albumina (*bovine serum albumine*)

CA: Cornu ammonis edo *Ammon´s horn*
CA1: Cornu ammonis 1 eremua
Ca^{2+}: kaltzioa
cAMP: adenosine monofosfato ziklikoa (*cyclic adenosine monophosphate*)
CB_1 hartzailea: 1-motako kannabinoide-hartzailea
CB_2 hartzailea: 2-motako kannabinoide-hartzailea
CCK: kolezistokinina (*cholecystokinin*)
CPu: putamen kaudoa (*caudate putamen*)
Ctx: kortexa (*cortex*)

D1R: 1-motako dopamina-hartzailea
DAB: 3,3´-diaminobentzidina
DAG: diazilglizerola
DAGL: α eta β diazilglizerol lipasak (*diacylglycerol lipases*)
DG: bihurgune horzduna (*dentate gyrus*)
DML: horzdun molekula-geruza (*dentate gyrus molecular layer*)
DMSO: dimetil sulfoxidoa
DRN: bizkarraldeko errafe-nukleoa (*dorsal raphe nucleus*)
DSE: depolarizazioak eragindako kitzikapenaren murriztea
DSI: depolarizazioak eragindako inhibizioaren murriztea

EAAT1: aminoazido kitzikatzaileen 1-motako garraiatzailea (*excitatory amino acid transporter 1*)
EGFP: proteina fluoreszente berde hobetua (*enhanced green fluorescent protein*)
eKB: endokannabinoideek
eKB-LTD: endokannabinoideek bideratutako epe-luzeko inhibizioa (*endocannabinoid-mediated long-term depression*)

eKB-LTP: endokannabinoideek bideratutako epe-luzeko indartzea (*endocannabinoid-mediated long-term potentiation*)

EKS: endokannabinoide sistema
EM: mikroskopia elektronikoa
EtNH2: etanolaminara

FAAH: gantz azidoen amida hidrolasa (*fatty acid amide hydrolase*)
fEPSP: Neurona-eremu bateko potentzial postsinaptiko kitzikagarrien erantzunak (*field excitatory postsynaptic potential*)
FIJI: Fiji is just IMAGE J

GABA: azido gamma-aminobutirikoa
$GABA_AR$: A-motako GABA-hartzailea
$GABA_BR$: B-motako GABA-hartzailea
GC: pikor-zelula (*granule cell*)
GFAP: glia proteina harikara azidoa (*glial fibrillary acidic protein*)
GLAST: aspartato-glutamato garraiatzailea (*glutamate aspartate transporter*)
GP: nukleo zurbila (*globus pallidus*)
GPCR: G-proteinatara akoplaturiko hartzailea
GPR55: G-proteinetara aklopaturiko 55. Hartzailea

HIF-1: hipoxiak eragindako 1-faktorea (*hypoxia-induced factor-1)*

I**P_3:** inositol (1,4,5)-trifosfatoaren

KO: knock-out saguak

LC: locus coeruleus (*locus coeruleus*)
LFS: maiztasun txikiko estimulazio tetanikoko protokolo bat (*low frequency stimulation*)
LPP: alboko bide-zulatzailea (*lateral perforant path*)
LTD: epe-luzeko depresioa (*long-term depression*)
LTP: epe-luzeko indartzea (*long-term potentiation*)

MAGL: monoazilglizerol lipasa (*monoacylglycerol lipase*)
MCFL: (*mossy cell fiber layer*)
mGluR: glutamato-hartzaile metabotropikoa
MOR: m-motako opioide-hartzailea
MPP: erdiko bide-zulatzailearen (*medial perforant path*)
$mtCB_1$ hartzailea: mitokondriatako CB_1 hartzailea

NAc: accumbens nukleo (*nucleus accumbens*)
NAPE-PLD: N-azilfosfatidiletanolamina hidrolizatzeko D fosfolipasa (*phospholipase D selective N-acylphosphatidylethanolamine*)
NMDAR: N-metil-D-aspartato-hartzailea

NSZ: nerbio sistema zentrala
NT: neurotransmisorea
NTS: traktu bakartiaren nukleoa (*nucleus of the solitary tract*)

OB: usaimen-erraboila (*olfactory bulb*)
OT: usaimen-tuberkulua (*olfactory tubercle*)

P2XR: P2X-motako purina-hartzailea
P2YR: 2-motako purina-hartzailea
PAG: ubide inguruko gai grisa (*periaqueductal gray*)
PB: fosfato tanpoia (*phosphate buffer*)
PBS: gatz-fosfato tanpoia (*phosphate buffered saline*)
PFC: kortex prefrontala (*prefrontal kortex*)
PKA: proteina kinasa A
PKG: cGMP mendeko proteina kinasa (*cGMP-dependent protein kinase*)
PLC: C-fosfolipasa
PPAR-α: peroxisomen proliferazio bidez aktibaturiko hartzailea (*peroxisome proliferator-activated receptors*)
PPR: pultsu-parekatuen ratioa
PrL: kortex prelinbikoa
PTX: pikrotoxina

RS: Racineren eskala
RT: giro-tenperatura (*room temperature*)

SEM: batezbestekoaren errore estandarra (*standard error mean*)
SNr: gai beltzaren erretikulu-zatia (*substantia nigra pars reticulata*)

TBS: tris-hidrogeno kloruroarekin bahetutako gatz-tanpoia (*tris-hydrogen chloride buffered saline*)
TNFα: tumore nekrosiaren alfa faktorea
TRPA1: potentzial aldakorreko lehen motako ankirina hartzailea (*transient receptor potential ankyrin 1*)
TRPV1: potentzial aldakorreko lehen motako kanal baniloidea (*transient receptor potential vanilloid 1*)

VTA: sabelaldeko tegmentu eremua (*ventral tegmental area*)

WT: sagu basatiak (*wild-type mice*)

Δ9-THC: trans-Δ-9-tetrahidrokannabinola

LABURPENA

CB_1 hartzaile kannabinoideak astrozitoetan dituen funtzioak, glia-zelula horietan CB_1 hartzaileak neuronen inguruan duen banaketaren oso mende daude, batez ere sinapsietatik hurbil baldintza normal eta patologikoetan. Hala ere, CB_1 hartzailearen kokapen subzelularraren irudi osoa ez dago osatuta, CB_1 hartzailearen adierazpena sakabanatua baita, eta, ondorioz, astrozitoetan detektatzeko zaila. Gure laborategiak aurreko ikerketetan zenbatetsi zuen hipokanpoko CA1 *stratum radiatum*-ean CB_1 hartzaileen % 5-6 inguru GFAP markatzailea erabiliz identifikatutako astrozitoetan kokatzen direla. Antzeko balioak lortu ziren amigdalaren oinalde-alboko nukleoan eta atzeko asoziazio pareta-kortexeko II/III geruzan. Hala ere, GFAP zitoeskeletoko proteina bat da, batez ere astrozitoen gorputzera eta beraien adarkadura nagusietara mugatzen dena. Baliteke honek astrozitoetako CB_1 hartzaileen benetako proportzioa eta kantitate osoa desitxuratzea.

GLAST hainbat arrazoirengatik erabiltzen da astrozitoen markatzaile gisa: 1) arantza dendritiko gehienak astrozitoekin kontaktuan daude; 2) arratoi helduen hipokanpoko CA1-eko *stratum radiatum*-ean μm^3-ko 3.200 garraiatzaile daudela kalkulatzen da; 3) astrozitoen azalera totala 1,4 m^2/cm^3 dela uste denez, GLAST molekulen batezbesteko dentsitatea astrozitoen mintzean ~ 2.300 μm^2; 4) GLAST markaketa astrozitoen plasma-mintzean kokatzen da astrozitoen azalera osoan zehar. Hori dela eta, GLAST astrozitoak markatzeko hautagai gisa agertu da CB_1 hartzailearen banaketa xehetasunez ikertzeko glia-zelula horietan. Hipotesi hau frogatzeko, mikroskopio elektronikorako erretxinan murgildu aurreko immunourre metodoa erabili dut, lehenik eta behin GLAST eta GFAP markatzaileek astrozitoetan duten banaketa aztertzeko. GLAST markaketa astrozitoen plasma-mintzean zehar zegoen, bai gorputz zein neurona, kapilar eta beste glia-zelula batzuekin kontaktuan zeuden proiekzio txikienetan. Horrela, GLAST markaketa GFAParenak baino askoz ere eremu zabalagoan agertzen zen. Gainera, mikroskopio elektronikorako immunoperoxidasa metodoa erabiliz ikusi da GLAST markatzaileak GFAPk baino hiru aldiz astrozitoen azalera gehiago ikusarazten duela, eta era berean, lau aldiz astrozito-mintz gehiago. Azkenik, erretxinan murgildu aurreko immunourre/immunoperoxidasa metodo bikoitzari esker, CB_1 hartzaileen % 12 GLAST-positibo ziren astrozitoetan kokatzen zela zenbatetsi zen, aldiz GFAP-positibo ziren astrozitoetan % 5-6 baino ez, lehenago gure laborategiak

deskribatu bezala.

Aurkikuntza horiek egin ondoren, zehaztasun handiagoz aztertu nuen CB_1 hartzaileen kokapena astrozitoen mitokondriatan. CB_1 hartzaile funtzionalen presentzia aurkitu genuen hipokanpoko neuronen eta astrozitoen mitokondria-mintzetan. Hala ere, zalantzak agertu ziren komunitate zientifikoan, ea CB_1 hartzaileak garuneko beste eremu batzuetako mitokondriatan zeuden, izan ere, orain arte ez da egin ikerketarik hau argitzeko. Horren ondorioz, GLAST-CB_1 immunomarkaketa bikoitza erabili nuen mikroskopio elektronikoan neurona eta astrozitoen mitokondriatako CB_1 hartzailearen dentsitateak kalkulatzeko garuneko lau eskualdetan: hipokanpoko CA1, kortex prefrontala, kortex piriformea eta accumbens nukleoa. Emaitzek erakutsi zuten CB_1 hartzailearen dentsitatea astrozitoen mitokondriatan, CA1 eremuan (3,24 ± 0,94 part/μm^2), kortex prefrontalean (2,45 ± 0,49 part/μm^2), accumbens nukleoan (1,16 ± 0,44 part/μm^2) eta kortex piriformean (1,35 ± 0,57 part/μm^2), neuronen mitokondriatako dentsitatea baino handiagoa zela, CA1 eremua (0,76 ± 0,09 part/μm^2), kortex prefrontala (1,04 ± 0,13 part/μm^2), accumbens nukleoa (0,42 ± 0,12 part/μm^2) eta kortex piriformea (0,82 ± 0,12 part/μm^2). Oro har, astrozitoetako CB_1 hartzaileen maila absolutuak neuronetakoak baino baxuagoak diren arren, astrozitoetako CB_1 hartzailearen mitokondria-dentsitatea neuronetakoa baino handiagoa da aztertutako lau garun-eskualdetan. Hau da, CB_1 hartzaileak gehiago adierazten dira astrozitoen mitokondriatan neuronenetan baino. Mitokondriatako CB_1 hartzaileen aktibazioak neuronen energia-ekoizpena aldatzen du eta memoria kaltetu dezake. Era berean, astrozitoen mitokondriatako CB_1 hartzaileen aktibazioak eragina du glutamatoaren metabolismoan eta laktato-ekoizpenean, neurona-funtzioak eta jokabide soziala asaldatuz.

Beraz, aztertutako lau garun-eskualdetan astrozitoen mitokondriak neuronen mitokondriak baino CB_1 hartzaile gehiago adierazteak, eta GFAP-CB_1-KO saguen aurre-garunetik isolatutako mitokondriatan kannabinoideek eragindako oxigeno-kontsumoaren murrizpena ez emateak, astrozitoen mitokondriatako CB_1 hartzaileek garuneko mitokondria-arnasketan kannabinoideek duten ondorioetan funtsezko zeregina dutela iradokitzen da.

Astrozitoen mitokondriatako CB_1 hartzailearen nire tesiko aurkikuntza anatomikoak

Nature aldizkarian argitaratu dira (Jimenez-Blasco et al., 2020).

SARRERA

2.1. ENDOKANNABINOIDE SISTEMA

Cannabis sativa L. gizakiak landaturiko landare zaharrenetako bat da ziurrenik, baina historian zehar eztabaida-iturri izan da (Russo, 2007). Urteroko landare dioiko honek, Asiako lehen nekazari-elkarteen hasierarekin partekatzen du bere jatorria (Bonini et al., 2018). *C. sativa* zuntz-, elikagai-, olio- eta medikuntza-iturri gisa erabili izan da mendeetan zehar, baita jolas- eta erlijio-helburuetarako ere (Piluzza et al., 2013). Kimikoki aktiboak diren zenbait osagai ditu, hala nola kannabinoideak, terpenoideak, flabonoideak eta alkaloideak (Andre et al., 2016). Osagai aktiboenak kannabinoideak dira, konposatu terpenofenoliko mota bat, batez ere lore emeen trikomakaren barrunbean metatuak (Taura et al., 2007; Bonini et al., 2018). Orain arte identifikatutako 100 kannabinoide baino gehiagotatik, ahaltsuena trans-Δ-9-tetrahidrokannabinola (Δ9-THC) da, marihuanaren efektu psikoaktiboen arduradun nagusia (Whiting et al., 2015).

Endokannabinoide sistemaren (EKS) aurkikuntzak, prozesu fisiologiko askotan parte hartzen duen sistema konplexu eta multimodal bat ezagutarazi zuen. Sistema hau honako hauek osatzen dute: kannabinoide-hartzaileak, estekatzaile lipofiliko endogenoak edo endokannabinoideak (eKB), eta horiek ekoizteko, askatzeko eta degradatzeko entzimak (Piomelli, 2003; Marsicano eta Lutz, 2006; Kano et al., 2009; Navarrete eta Araque, 2008; Katona eta Freund, 2012; Lu eta Mackie, 2016; Oliveira Da Cruz et al., 2016).

EKS oso banatuta dago ugaztunen organismoen zehar eta, beste organo batzuetan presente dagoen arren (Piazza et al., 2017), oso hedatuta dago nerbio sistema zentral (NSZ) eta periferikoan (Katona eta Freund et al., 2012; Lu eta Mackie et al., 2016). Sistema honek hainbat garun-funtzio erregulatzen ditu, neurona eta glia-zelulen konpartimentu espezifikoetan eraginez (Katona eta Freund et al., 2012; Lu eta Mackie et al., 2016; Gutiérrez-Rodríguez et al., 2017; Busquets-García et al., 2018). Gainera, EKSk garuneko hainbat prozesu ezberdinetan parte hartzen du, jatetik kogniziora (Marsicano eta Kuner, 2008; Bellocchio et al., 2010; Katona eta Freund, 2012). eKB-ak mekanismo zelular eta molekular konplexuen eta sinapsi-plastikotasunaren partaide dira, garun-zirkuitoei konputazio-propietate garrantzitsuak emanez, esaterako kontzientzia eta input-espezifikotasuna, garuneko prozesu gorenetarako beharrezkoak

direnak (Castillo et al., 2012). Ondorioz, EKSren asaldura hainbat gaitz neurologiko eta neuropsikiatrikoren patogenesiaren parte da (Pertwee, 2009).

2.1.1. Kannabinoide-hartzaileak

Jakina da kannabinoide-hartzaileak ornodunen espezie askotan daudela, karraskarietatik primateetara, tximino eta gizakia barne (Elphick eta Egertová, 2005). Bi kannabinoide-hartzaile nagusiak klonatu izan dira: 1-motako kannabinoide-hartzailea (CB_1 hartzailea) (Matsuda et al., 1990; Matsuda et al., 1993) eta 2-motako kannabinoide-hartzailea (CB_2 hartzailea) (Munro et al., 1993). CB_1 eta CB_2 hartzaileak G-proteinatara akoplaturiko hartzaileen (GPCR) superfamiliakoak dira, mintzean-zeharreko proteinen familiarik handiena giza-genoman, eta ezinbestekoak dira hainbat funtsezko prozesu fisiologikotan. GPCRak honakoaz osatuta daude: mintzean zeharreko zazpi segmentu hidrofobiko zelularen kanpoalde eta barrualdeko bihurguneei esker loturik, glikosilazio-guneak dituen N-terminal zelula kanpoko domeinua, eta G-proteinara akoplaturiko C-terminal zelula barruko domeinua (Howlett et al., 2002).

2.1.1.1. CB_1 hartzailea

NSZeko G-proteinatara akoplaturiko hartzaile ugarienetako bat da eta neurona eta zelula ez-neuronaletan dago (Herkenham et al., 1990; Tsou et al., 1998; Moldrich eta Wenger, 2000). Hartzailearen adierazpena zabala eta heterogeneoa da, eta ezinbesteko eginkizunak ditu garuneko funtzio, disfuntzio eta kognizioan (Marsicano et al., 2002; Monory et al., 2006; Marsicano eta Kuner, 2008; Bellocchio et al., 2010; Puente et al., 2011; Castillo, 2012; Katona eta Freund, 2012; Steindel et al., 2013; Ruehle et al., 2013; Soria-Gómez et al., 2014, 2015; Hu eta Mackie, 2015; Katona, 2015; Martín-García et al., 2015; Gutiérrez-Rodríguez et al., 2017, 2018; Bonilla-Del Río et al., 2019, 2021). Lokomozioan, hautematean edo memorian dituzten ondorio kaltegarriak, eta konbultsioak arintzean edo jateko gogoa handitzean kannabinoideek dituzten efektu positiboak, bat datoz CB_1 hartzailearen banaketarekin NSZean. Beraz, hartzaileak adierazpen handia du kortex prefrontalean (PFC), bihurgune zingulatuan, hipokanpoan, oinaldeko nukleoetan, gai beltzan eta garuntxoan (Mackie, 2005; Hillard, 2014;

Gutiérrez-Rodríguez et al., 2017), baina baxua hipotalamoan, entzefalo-enborrean eta bizkarrezur-muinean (Tsou et al., 1998). Entzefalo-enborrean dagoen CB_1 hartzaile dentsitate txiki hori, marihuanaren toxizitate eta hilkortasun baxuarekin lotuta dago.

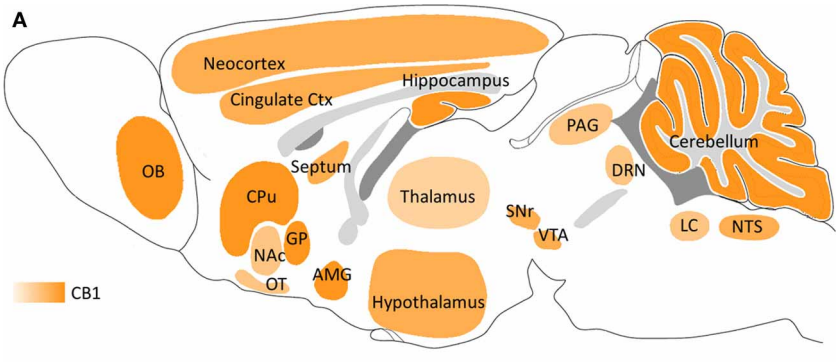

1. irudia. CB_1 hartzaileak adierazten dituzten garun-eremu nagusien adierazpen eskematikoa. AMG, amigdala; CPu, putamen kaudatua; Ctx, kortexa; DRN, bizkarraldeko errafe-nukleoa; GP, nukleo zurbila; LC, locus coeruleus; NAc, accumbens nukleoa; NTS, traktu bakartiaren nukleoa; OB, usaimen-erraboila; OT, usaimen-tuberkulua; PAG, ubide inguruko gai grisa; SNr, gai beltzaren erretikulu-zatia; VTA, sabelaldeko tegmentu eremua. Flores et al., 2013 lanetik hartua.

CB_1 hartzailea batez ere bukaera presinaptikoetan kokatzen da eta bere aktibazioak neurotransmisoreen askapena oztopatzen du (Kano et al., 2009). NSZean, CB_1 hartzaileak GABA-, glutamato-, serotonina-, noradrenalina- eta azetilkolina-neuronetan adierazten dira, EKSk neurotransmisore guzti horien askapenaren inhibizioan parte hartzen duela aditzera emanez (Hermann et al., 2002; Oropeza et al., 2007; Azad et al., 2008; Kano et al., 2009; Morozov et al., 2009; Lutz et al., 2015; Soria-Gómez et al., 2015; Gutierrez-Rodriguez et al., 2017). eKB-seinaleztapenaren eragin handienak GABA- eta glutamato-sinapsietan ematen dira (Katona eta Freund, 2012). Astrozito (Salio et al., 2002; Navarrete eta Araque, 2008, 2010; Han et al., 2012; Gutiérrez-Rodríguez et al., 2017; Bonilla-Del Río et al., 2019, 2021) eta oligodendrozito (Moldrich eta Wegner, 2000) bezalako glia-zelulek eta garuneko zelula baskularrek (Golech et al., 2004) ere adierazten dute CB_1 hartzailea. Gainera, CB_1 hartzailea bukaera presinaptiko eta postsinaptikoen eta astrozitoen kanpoko mitokondria-mintzean ere agertzen da (Hebert-Chatelain et al., 2014a, 2014b, 2016; Koch et al., 2015; Lutz et al., 2015; Gutiérrez-Rodríguez et al., 2018, Jimenez-Blasco et al., 2020). Mitokondriako CB_1 hartzailearen aktibazioak energiaren metabolismoa modulatzen du fosforilazio

oxidatzailea eta ATParen produkzioa inhibituz, memoria narraiadura (Hebert-Chatelain et al., 2016) neurona-funtzio asaldatuak eta interakzio sozial kaltetua (Jimenez-Blasco et al., 2020) eraginez. Azkenik, CB_1 hartzailea hainbat organo eta ehun periferikotan ere adierazten da: gantz-ehunean, muskuluan, gibelean, bihotzean, urdail-hesteetan, arean, barean, amigdaletan, prostatan, barrabiletan, umetokian, obarioan, azalean, begietan eta sistema periferiko sinpatikoko nerbio-terminaletan (Galiègue et al., 1995; Ishac et al., 1996; Pertwee, 2001; Maccarone et al., 2016; Zou eta Kumar, 2018). Muskulu eskeletikoen eta miokardioen mitokondrietan ere adierazten dira, zeinen Δ9-THC bidezko aktibazioak mitokondriari-akoplaturiko arnasketa murrizten du (Mendizabal-Zubiaga et al., 2016).

EKSk funtzio garrantzitsuak betetzen ditu garunean CB_1 hartzaileen aktibazioari esker, esaterako, neurotransmisoreen askapenaren atzerazko inhibizioa (Alger, 2002; Marsicano eta Lutz, 2006; Heifets eta Castillo, 2009; Kano et al., 2009), neuronen kitzikapenaren kontrola (Marsicano et al., 2003), hainbat epe-labur eta -luzeko sinapsi-plastikotasun motaren erregulazioa (Gerdeman eta Lovinger, 2003; Marsicano eta Lutz, 2006; Heifets eta Castillo, 2009; Kano et al., 2009, Puente et al., 2011), neurona-astrozito komunikazioa (Navarre eta Araque, 2008, 2010), neuronen ama-zelulen bikoizketa eta exzitotoxizitateak eragindako neurogenesia (Aguado et al., 2006, 2007), edo neuronen biziraupenaren kontrola (Galve-Roperh et al., 2009).

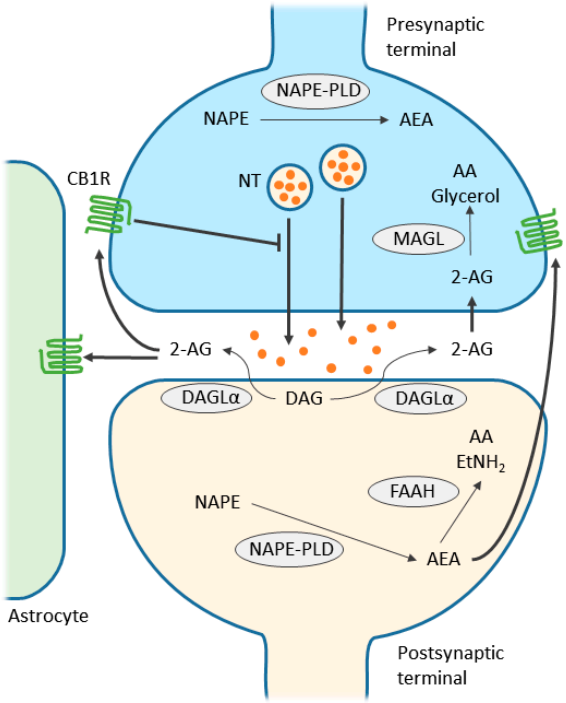

2. irudia. Endokannabinoideek bideratutako atzerazko sinapsi-transmisioa adierazten duen eskema sinplifikatua. eKBak bukaera postsinaptikoetan sintetizatzen dira neurona-aktibazio baten ondorioz. Lipidoak izanik, eKB-ek, batez ere 2-AGak, erraz zeharkatzen dute mintza eta atzerazko bidea egiten dute CB_1 hartzaileak aktibatuz bukaera presinaptikoetan. Aktibatutako CB_1 hartzaileek neurotransmisoreen (NT) askapena inhibitzen duten kaltzioaren jarioa bertan behera utziz. 2-AGak astrozitoetan dauden CB_1 hartzaileak ere aktiba ditzake, glutamatoaren askapena eraginez. Sinapsi-tartean dagoen gehiegizko 2-AGa bukaera-presinaptikoek barneratzen dituzte, oraindik argi ez dagoen mekanismo bati esker, eta MAGL entzima bidez azido arakidonikora (AA) eta glizerolera degradatuko da. Beste alde batetik, bukaera postsinaptikoetan sintetizatzen den AEAk, zelula barneko CB_1 hartzaileak eta kannabinoideak ez diren beste hartzaile batzuk aktibatzen ditu, hala nola TRPV1 hartzailea. Nahiz eta eKB-en atzerazko seinaleztapena batez ere 2-AGak bideratuta egon, AEAk ere aktibatu ditzake CB_1 hartzaile presinaptikoak. FAAH batez ere bukaera postsinaptikoetan aurkitzen da, eta AEA AAra eta etanolaminara (EtNH2) degradatzen du. Garuneko hainbat eremutan NAPE-PLD bukaera presinaptikoetan adierazten den arren, ez dago argi EKSren aurrerazko seinaleztapenaren arduraduna AEA ote den. Kontuan hartu behar da bestelako bide batzuk daudela eKB-en metabolismorako, garun-eremu eta egoera fisiologikoen arabera. Zou eta Kumar 2018 lanetik hartua.

2.1.1.2. CB_2 hartzailea

CB_2 hartzailea barean deskribatu zen lehen aldiz (Munro et al., 1993), eta, horretaz gain, sistema immunologikoko hartzaile espezifikoa zela uste zen (amigdalak, B eta T linfozitoak, ZK zelulak, makrofagoak eta T CD8 eta CD4 linfozitoak) (Galiègue et al., 1995; Ameri, 1999). Hala ere, CB_2 hartzailea bihotzean, endotelioan, hezurrean, gibelean, pankrean eta barrabiletan ere agertzen dela ikusi zen gero (Zou eta Kumar, 2018). Antigorputz espezifikorik ez dagoenez, CB_2 hartzailearen adierazpena NSZean gai eztabaidagarria da (Atwood eta Mackie, 2010; Lu eta Mackie, 2016). Ondorioz, arazo hori saihesteko, estrategia genetiko berriak garatu dira, CB_2 promotorearen kontrolpean proteina fluoreszente berde hobetua (*enhanced green fluorescent protein*, EGFP) adierazten duten sagu mutanteen anduietan oinarrituta (López et al., 2018).

2.1.1.3. Beste kannabinoide-hartzaileak

Kannabinoide-hartzaile klasikoez gain, badira beste hartzaile batzuk eKB-en efektuak bideratzen dituztenak (Pertwee, 2015), hala nola, potentzial aldakorreko lehen motako hartzaile baniloidea (*transient potential vanilloid*, TRPV1), anandamidak aktibatua (Maccarrone et al., 2008; De Petrocellis eta Di Marzo, 2009b; Tóth et al., 2009; Alhouayek et al., 2014; Rossi et al., 2015). Horretaz gain, eKB-ek beste hartzaile batzuk ere aktibatzen dituzte: potentzial aldakorreko lehen motako ankirina hartzaileak

(*transient receptor potential ankyrin 1*, TRPA1) (De Petrocellis et al., 2008), peroxisomen proliferazio bidez aktibaturiko hartzailea (*peroxisome proliferator-activated receptors*, PPAR-α) (Sun et al., 2006; Alhouayek et al., 2014) eta G-proteinetara aklopaturiko 55. hartzailea (GPCR55) (Ryberg et al., 2007).

2.1.2. Endokannabinoideak

eKB-ak molekula promiskuotzat hartzen diren mezulari lipidikoak dira, CB_1 eta CB_2 hartzaileak aktibatzen baitituzte, baina baita beste hartzaile batzuk ere (Piomelli, 2003; Kano et al., 2009; Katona eta Freund, 2012; Lutz et al., 2015; Lu eta Mackie, 2016; Zou eta Kumar, 2018). Sistemaren osagai eta funtzioen banaketa zabalaren ondorioz, eKB-en fisiologia eta farmakologia konplexua da. Bere funtzioak era parakrino eta autokrinoan egiten dituzte, eta beraien natura lipidikoa dela eta, mintzean zehar sar daitezkenez eta zeharkatu dezaketenez, ziur aski baita modu endokrinoan ere. Neurotransmisoreak ez bezala, eKB-ak ez dira metatzen besikula jariatzaileetan (adiposometan metatzen direla uste da); aitzitik, eskariz sintetizatzen dira zelula kanpora askatuz estimulu fisiologiko edo patologiko baten ostean (Piomelli, 2003; Kano et al., 2009; Pertwee et al., 2010; Katona eta Freund, 2012; Lutz et al., 2015; Lu eta Mackie, 2016; Zou eta Kumar, 2018).

eKB-ak zelula-mintzetik sintetizatzen diren konposatu lipidiko endogenoak dira. Horien artean, N-arakidonoiletanolamina (anandamida ere deitzen zaio, AEA) (Devane et al., 1992) eta 2-arakidonoilglizerola (2-AG ere esaten zaio) (Mechoulam et al., 1995) dira bi eKB nagusiak, hobekien identifikatu eta karakterizatu direnak. AEAk kannabinoideen "tetrada" efektuak (katalepsia, anti-nozizepzioa, hipolokomozioa eta hipotermia) eragiten ditu karraskarietan; 2-AGa, berriz, funtsezkoa da CB_1 hartzaileen-menpeko transmisioaren eta sinapsi-plastikotasunaren modulazio gehienetan (Kano et al., 2009).

Garunean kontzentrazio handiena duen eKB-a 2-AGa da (AEA baino 200 aldiz handiagoa) (Bisogno et al., 1999), eta bertako kannabinoide-hartzaileen dentsitatearekin bat dator (Sugiura et al., 2006). Bestalde, AEA modu berean metatzen da kannabinoide-hartzaileen adierazpen handiko (hipokanpoa, kortexa, gorputz ildaxkatua) eta txikiko garuneko eskualdeetan (talamoa, entzefalo-enborra) (Felder eta Glass, 1998). 2-AGak

eraginkortasun handiz aktibatzen ditu CB_1 eta CB_2 hartzaileak; AEAren eraginkortasuna, berriz, txikia da CB_1 hartzaileetan, eta oso txikia CB_2 hartzaileetan (Showalter et al., 1996; Gonsiorek et al., 2000; Sugiura et al., 2000; Luk et al., 2004).

Dagoeneko, eKB-en sintesi, garraio, askapen eta degradazio bidezidor ezberdinak deskribatu dira. Ondorioz, sintesi eta degradazio entzimak eKB-en funtzio fisiologiko eta patologiko bereizgarrien arduradun dira: 2-AG-ren kasuan α eta β diazilglizerol lipasak (*diacylglycerol lipases*, DAGL), eta AEA-ren kasuan N-azilfosfatidiletanolamina hidrolizatzeko D fosfolipasa (*phospholipase D selective N-acylphosphatidylethanolamine*, NAPE-PLD) sintesirako entzimak; eta 2-AG-ren kasuan monoazilglizerol lipasa (*monoacylglycerol lipase*, MAGL), eta AEA-ren kasuan gantz azidoen amida hidrolasa (*fatty acid amide hydrolase*, FAAH) degradazio entzimak (Kano et al., 2009; Fezza et al., 2014; Piomelli, 2014; Lu eta Mackie, 2016; Zou eta Kumar, 2018).

Zenbait egoeratan, AEAk GABA eta glutamato presinaptikoak askatzea inhibitzen du, eta TRPV1 hartzailea aktibatzen du (Zygmunt et al., 1999; Ross, 2003; Chávez et al., 2010; Puente et al., 2011; Lu eta Mackie, 2016; Zou eta Kumar, 2018). 2-AGak atzerantz seinaleztatzen du eta CB_1 hartzaile presinaptikoak aktibatzen ditu neurotransmisoreen askapena murrizteko. 2-AGak TRPV1 hartzailea ere aktibatzen du, baina kontzentrazio handiagoa behar da AEAk egindako antzeko efektua lortzeko. Gainera, FAAH eta MAGL, gune subzelular ezberdinetan kokatzen dira, AEA eta 2-AGarentzako seinalaztapen mekanismo ezberdinak daudela iradokiz, hurrenez hurren (Cravatt et al., 1996; Cristino et al, 2008; Kano et al., 2009).

2.2. ASTROZITOAK

Glia-zelulak, garuneko zelula-populazio ugariena, Rudolf Virchowek deskribatu zituen lehen aldiz 1846an, burmuinaren “kola” funtzioa zuten zelula ez-neuronal gisa. Ondorengo ikerketek NSZeko glia-zelulak bi taldetan sailkatu zituzten, mikroglia eta makroglia. Mikroglia funtzio fagozitikoak dituzten makrofagoen antzeko zelulek osatzen dute, eta makroglia taldea bi zelula-motek osatzen dute: oligodendrozitoek, NSZeko mielinizazioaren arduradunak, eta astrozitoek. Astrozitoak ezinbestekoak dira NSZaren garapen eta fisiologian, garrantzi handiko funtzioetan parte hartuz, esaterako laguntza trofikoa, biziraupen eta bereizketa neuronala, orientazio neuronala, neuriten hazkuntza edo sinapsi-eraginkortasuna (Perea eta Araque, 2002). Are gehiago, astrozitoek garuneko homeostasia mantentzen laguntzen dute tokiko ioi eta sustantzia neuroaktiboen kontzentrazioak erregulatuz (Perea eta Araque, 2002).

Astrozitoek maila ezberdinetan elkarrekiten dute neuronekin eta NSZeko lesio baten aurrean osagai babesle gisa jokatzeagatik eta neuronen energia-iturri izateagatik ezagutu izan dira (Magistretti eta Pellerin, 1999; Bélanger eta Magistretti, 2009; Bélanger et al., 2011; Yi et al., 2011; Oliveira da Cruz et al., 2015; Bolaños, 2016). Hala ere, pentsaera hau aldatu egin da dagoeneko, izan ere, neuronen jarduera modulatzen duten hainbat seinaleztapen-bidek, astrozito-neurona komunikazioa ere erregulatzen dute (Araque et al., 1999; Haydon eta Carmignoto, 2006; Perea et al., 2009; Gómez-Gonzalo et al., 2014). Gainera, aurkikuntza horiek “hiruko sinapsia ” kontzeptua sortzea ekarri zuten, zeina neuronen presinapsi eta postsinapsi atalez eta hauek inguratzen dituzten astrozitoen prozesuez osatuta dagoen (Araque et al., 1999). Testuinguru horretan, zeinbait autorek erakutsi dute hiruko sinapsiak funtsezko zeregina duela neurona eta astrozitoen arteko noranzko biko komunikazioan (Navarrete eta Araque, 2008, 2010; Navarrete et al., 2013, 2014; Gómez-Gonzalo et al., 2014). Astrozitoak funtsezkoak dira baita garuneko energiaren metabolismoa eta garuneko jarduera erregulatzeko, garuneko homeostasiari eragiten dioten aldaketa metaboliko zentral eta periferikoak hautemanez (Bélanger et al., 2011; Barros eta Weber, 2018; Magistretti eta Allaman, 2018; Jimenez-Blasco et al., 2020). Morfologia bereziki konplexua dute, egitura sinaptikoetatik hurbil daude eta dozenaka mila sinapsirekin kontaktuan daude (Halassa et al., 2007).

Funtsezko ioi-kanal batzuen adierazpen-maila nahiko txikia da astrozitoetan, elektrikoki kitzikatu ezin diren zelulatan bihurtuz, mintz-potentziala nahiko egonkorra izanez (Perea eta Araque, 2002; Araque eta Navarrete, 2010). Astrozitoek adierazitako boltai-menpeko kanal gehienek zelulaz kanpoko ioi-maila homeostatikoa mantentzeko mekanismo gisa jarduten dute nagusiki (Araque eta Navarrete, 2010). Era berean, neurotransmisore askorentzako hartzaile funtzionalak adierazten dituzte, zelula barneko kaltzio-mailan (Ca^{2+}) aldaketak eta oszilazioak eragiten dituztenak (Araque et al., 2001). Hartzaile horietako asko GPCRak dira, zeinek aktibatzean C fosfolipasa eta inositol (1,4,5)-trifosfatoaren (IP3) osaketa estimulatzen duten, eta honek zelula barneko Ca^{2+} kontzentrazioa handitzen du, barneko kaltzio-metaketetatik Ca^{2+} askatuz. Astrozitoek, batez ere, erretikulu endoplasmatikoan metatutako Ca^{2+} erabiltzen dute zitosoleko kaltzio-iturri gisa, zelulako seinaleztapen bezala jokatuz (Perea eta Araque, 2005a).

Astrozitoek berezko Ca^{2+} aldaketak erakusten dituzte neurotransmisore ezberdinek eraginda. Zelula barneko seinale bezala jokatzen dute, zelularen eskualde desberdinetara iritsiz eta astrozitoen artean eskala luzeko komunikazioak ezarriz, NSZean ondorio funtzional garrantzitsuekin; izan ere, astrozito batean ematen den Ca^{2+} gorakada alboko astrozitoetara hedatzen da "Ca^{2+} olatu" bat sortuz, ehunka mikrometrotan zabaltzen dena (Perea and Araque, 2005a, Araque and Navarrete, 2010).

Ikerketa ugarik aditzera eman dute neurona eta astrozitoen arteko bi noranzko seinaleztapen baten existentzia. Astrozitoek erakutsitako kaltzioan oinarritutako kitzikagarritasun zelularra jarduera neuronal eta sinaptikoak eragin dezake, astrozitoek adierazitako neurotransmisore-hartzaileak aktibatuz (Perea eta Araque, 2005a, Araque eta Navarrete, 2010). Era berean, astrozitoetako kaltzio gorakadek sustantzia neuroaktibo ezberdinen askapena eragiten dute, gliotransmisore deituak, adibidez, glutamatoa, ATP, tumore nekrosiaren alfa faktorea (TNFα), prostraglandinak, GABA edo D-serina, zeinek neurona-kitzikagarritasuna eta sinapsi-transmisioa arautzen duten (Perea eta Araque, 2009; Araque eta Navarrete, 2010). Hala, astrozitoak sinapsiaren osoko parte dira, eta sinapsi-funtzioetarako baldintza egokien kontrol homeostatikoan era pasiboan jarduteaz gain, sinapsi-funtzioan era aktiboan hartzen du parte (Perea et al., 2009).

Astrozito bakar bat milaka sinapsirekin kontaktuan dagoenez, eta astrozitoak elkarrekin komunika daitezkeenez, beharbada astrozitoen eraginik sinpleena neurona-sareetan, aldi berean neurona-populazioak aktibatzeko gaitasuna da. Beraz, astrozitoen kaltzio olatuek eta ondorengo glutamato askatzeak, hipokanpoko neurona piramidal multzoen kitzikapen sinkronoa eragiten dute, gliotransmisioak sinkronizazio neuronala lagun dezakeela iradokiz (Angulo et al., 2004; Fellin, 2009). Gainera, gliotransmisore bakar batek eragin ugari izan ditzake neurona-sarean, itu diren neuronen eta neurona-elementuen (presinaptikoak edo postsinaptikoak) arabera, bai eta aktibatutako hartzaileen azpimoten arabera ere, zeinak konplexutasun handia ematen duen glia-neurona sarearen jardueran astrozitoek izan dezaketen eraginei (Araque eta Navarrete, 2010).

Astrozitoek hainbat denbora-eskalatan eragiten dute neurotransmisioan; izan ere, indar sinaptikoa aldi baterako kontrolatzen dute (segundo batzuetan edo minutu gutxitan), baina sinapsi-transmisioa epe-luzera aldatzen ere laguntzen dute, zelula-mailako ikaskuntza- eta memoria-mekanismoa delakoan. Astrozitoek epe-luzeko indartzean (*long-term potentiation*, LTP) dituzten efektuen arduradun diren hainbat mekanisko deskribatu dira (Perea eta Araque, 2009). Astrozitoak sinapsi-elementu dinamikoak dira, egitura eta funtzio aldaketa nabarmenak erakusten dituztenak (Theodosis et al., 2008). Izan ere, mintzean adierazten dituzten neurotransmisore-hartzaile eta -garraiatzaileen bidez ematen diren astrozitoen erantzun sinaptikoak, epe-labur eta -luzeko plastikotasunaren antzeko eraldaketak eragiten dituzte (Perea eta Araque, 2009). Hortaz, garrantzitsua da astrozitoetako hartzaile ezberdinen kokapen zehatza aztertzeko beharrezkoak diren lanabes berriak garatzea.

2.2.1. Astrozitoak eta EKS

Luzaroan eztabaidatu izan da CB_1 hartzaileen adierazpena astrozitoetan. Zelula hauetan hartzailearen presentziari buruzko lehen ikerketak giza-zelula eta karraskarien zelula kultiboetan egin ziren (Bouaboula et al., 1995a; Sánchez et al., 1998; Molina-Holgado et al., 2002b; Sheng et al., 2005). Hala ere, saguetan kontrako emaitzak lortu ziren (Sagan et al., 1999; Walter eta Stella, 2003), astrozitoen CB_1 hartzailearen adierazpena animalia espezie, andui-mota edo zelula-kultiboen baldintzen arabera alda

daitekeela iradokiz. Are gehiago, CB_1 hartzaile astroglialaren adierazpen maila txikia denez, zaila da *in situ* hibridazioaren edo immunohistokimikaren bidez hautematea.

Zorionez, mikroskopia immunoelektronikoari esker, CB_1 hartzaile astrozitikoaren presentzia frogatu zen (Rodriguez et al., 2001; Han et al., 2012; Bosier et al., 2013). Gainera, eKB-en sintesi- eta degradazio-entzima nagusiak, glia proteina harikara azidoarekin (*glial fibrillary acidic protein*, GFAP) kolokalizatzen zutela ikusi zen (Suárez et al., 2010). Garrantzitsua da nabarmentzea lan askok frogatu dutela CB_1 hartzaile astrogliala eta haren garrantzi funtzionala (Navarrete eta Araque, 2008, 2010; Stella, 2010; Han et al., 2012; Bosier et al., 2013; Gómez-Gonzalo et al., 2014; Navarrete et al., 2014; Metna-Laurent eta Marsicano, 2015; Viader et al., 2015; Oliveira da Cruz et al., 2016; Gutiérrez- Rodríguez et al., 2017; Robin et al., 2018; Bonilla-del Río et al., 2019, 2021). Horrenbestez, zenbait autorek seinaleztapen-bide ezberdinak proposatu dituzte astrozitoetan CB_1 hartzailea aktibatu ondoren. Esaterako, batzuek iradoki dute CB_1 hartzaile astroglialak $G_{\alpha i/o}$-proteinari akoplatuta daudela (Guzmán et al., 2001); beste autore batzuek, ordea, astrozitoen CB_1 hartzaileak $G_{\alpha q}$-proteinari akoplatuta zelula barneko kaltzio maila erregulatzen dutela (Navarrete eta Araque, 2008; Navarrete et al., 2014). Ildo horretatik, eKB-ek modulatutako zelula barneko seinaleztapen-bide ezberdinek, astrozitoei funtsezko funtzio malgutasun bakarra ematen die (Metna-Laurent eta Marsicano, 2015). Gainera, astrozitoetan CB_1 hartzailea aktibatzeak, urruneko sinapsietan neuronetan glutamatoa askatzen du (Navarrete eta Araque, 2008, 2010), baina baita lokalki, hipokanpoan sinapsi-transmizio kitzikatzaileen epe-luzeko depresioa (*long-term depression*, LTD) erdietsiz, THCak eragindako lan-memoriaren narraiadura emanez (Han et al., 2012). Astrozitoetako CB_1 hartzaileak garunaren energia hornitzen laguntzen dute, leptina-hartzailearen adierazpena kontrolatuz glia-zelula hauetan (Bosier et al., 2013). Gainera, astrozitoek laktatoa ekoizten eta askatzen dute, eta hori da neuronen energia-iturri nagusietako bat (Bélanger et al., 2011; Suzuki et al., 2011; Barros eta Weber, 2018; Magistretti eta Allaman, 2018; Jimenez-Blasco et al., 2020). Izan ere, ikerketa askok frogatu dute astrozitoek laktatoa askatzeak eta neuronek hartzeak, hainbat portaeratan funtsezko zeregina dutela, besteak beste, loan (Petit eta Magistretti, 2015; Haydon, 2017), ikasketan eta memorian (Suzuki et al., 2011) edo jokabide sozialean (Jimenez-Blasco et al., 2020). Gaur egun, argi dago astrozitoen

bioenergiaren modulazioa garuneko aktibitate, plastikotasun eta portaerarako seinaleztapen-bide ahaltsu eta oinarrizko bat dela (Allen eta Barres, 2009; Bélanger et al., 2011; Suzuki et al., 2011; Oliveira et al., 2015; Magistretti eta Allaman, 2018; Robin et al., 2018; García-Cáceres et al., 2019).

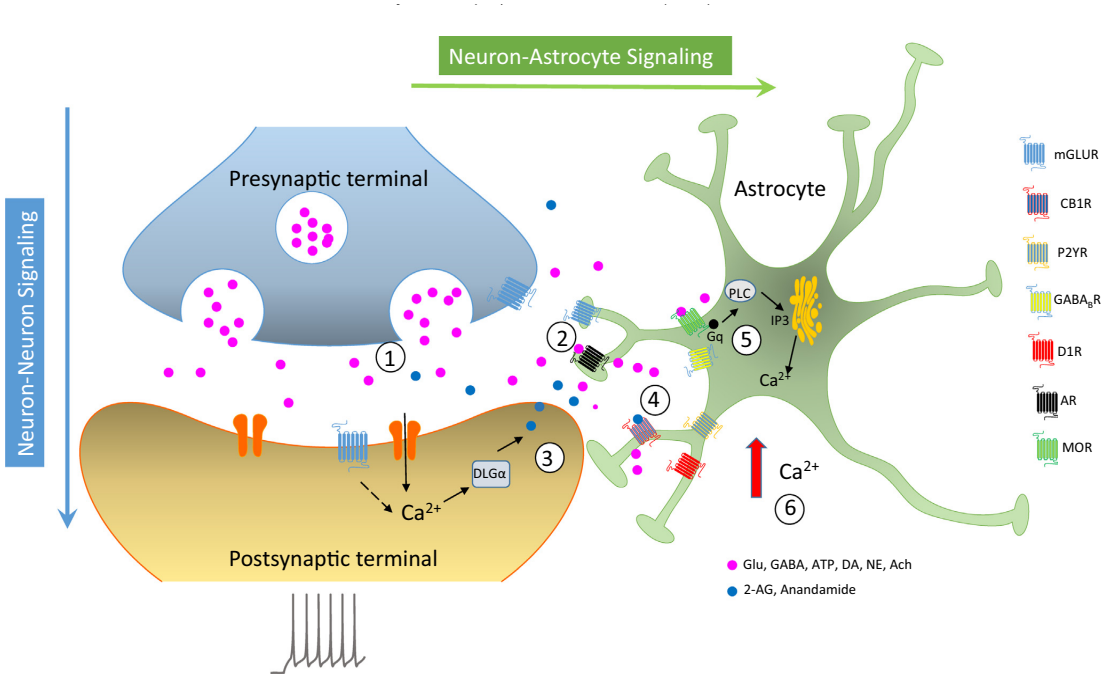

3. irudia. Neurona-astrozito seinaleztapena hiruko sinapsietan. Neurona presinaptikoek neurotransmisoreak askatzen dituzte (1), zeinak zelula postsinaptiko eta astrozitoen GPCR-ei lotzen zaizkien (2). Astrozitoen GPCR-en aktibazioak PLC-aren seinaleztapen-jauzia aktibatzen du (5) eta, ondorioz, zelula barneko Ca^{2+}-aren igoera ematen da (6). Postsinapsiko Ca^{2+} igoerak eKBen askapena eragiten du (3), zeinek CB_1 hartzailea aktibatzen duten (4). mGluR, glutamato-hartzaile metabotropikoa; CB_1 hartzailea, 1-motako kannabinoide-hartzailea; P2YR, 2-motako purina-hartzailea; GABABR, B-motako GABA-hartzailea; D1R, 1-motako dopamina-hartzailea; AR, adenosina-hartzailea; MOR, m-motako opioide-hartzailea; DLGα, alfa diazilglizerol lipasa; PLC, C-fosfolipasa. Kofuji eta Araque, 2021etik hartua.

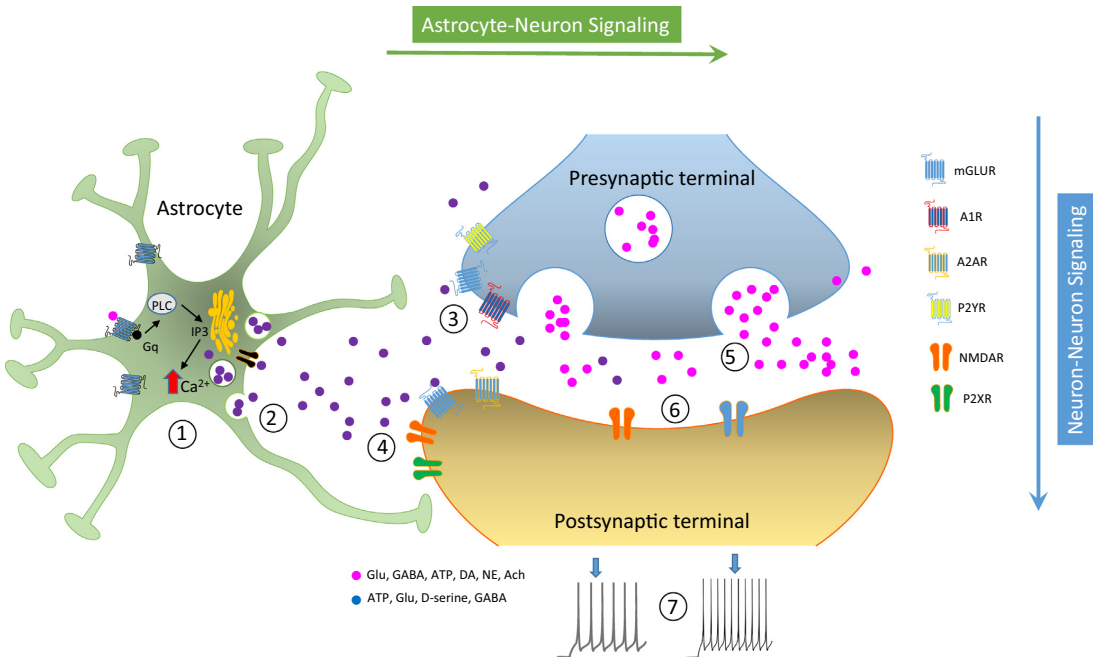

4. irudia. Astrozito-neurona seinaleztapena hiruko sinapsietan. PLCaren seinaleztapen-jauziaren aktibazioak eta ondoriozko zelula-barneko Ca^{2+}-aren igoerak (1), gliotransmisoreen askapena eragiten du (2), zeinek GPCR edo kanal presinaptiko (3) edo postsinaptikoetan (4) eragiten duten. Beraz, askapen presinaptikoa edo kitzikapen-postsinaptikoa gliotransmisoreek erregulatzen dituzte. mGluR, glutamato-hartzaile metabotropikoa; P2YR, 2-motako purina-hartzailea; A1R, 1-motako adenosina-hartzailea; A2AR, 2A-motako adenosina-hartzailea; NMDAR, N-metil-D-aspartato-hartzailea; P2XR, P2X-motako purina-hartzailea; PLC, C-fosfolipasa. Kofuji eta Araque, 2021etik hartua.

Nahiz eta oro har onartua den neuronen CB_1 hartzaileen adierazpen-maila handiak direla kanabinoideek eragindako garuneko efektuen erantzule nagusiak, berriki egindako azterketek CB_1 hartzaile astroglialaren funtsezko zeregina azpimarratu dute, bai sinapsi-mailan eta bai jokabide-mailan (Araque et al., 2017; Martín-Fernandez et al., 2017; Busquets-Garcia et al., 2018; Robin et al., 2018; Jimenez-Blasco et al., 2020). Zinez, aktibitate presinaptiko gabeko maiztasun txikiko astrozitoen aktibazioa, nahikoa da hipokanpoko CA1 eremuan AMPA-hartzaileak postsinapsitik kentzeko eta LTD bat eragiteko (Gómez-Gonzalo et al., 2015; Navarrete et al., 2019). Beraz, astrozitoen CB_1 hartzailea aktibatzeak, eta astrozitoen bereizketa sustatzeak (Aguado et al., 2006), eragina du sinapsi-plastikotasunean, memorian eta portaeran (Navarrete eta Araque, 2008, 2010; Han et al., 2012; Araque et al., 2014; Navarrete et al., 2014; Gómez-Gonzalo et al., 2015; Metna- Laurent eta Marsicano, 2015; Olivera da Cruz et al., 2016; Robin et

al., 2018; Durkee eta Araque, 2019). Hala ere, baldintza patologikoek CB_1 astroglialaren adierazpenean eta funtzioan izan dezaketen eragina gutxi ezagutzen da.

2.2.2. Mitokondriatako CB_1 ($mtCB_1$) hartzailea eta astrozitoak

Bioenergia funtsezkoa da garunean; izan ere, gorputz-pisuaren % 2 baino ez da organo hau, baina gorputzeko energiaren % 20 kontsumitzen du (Attwell eta Laughlin, 2001; MacAskill eta Kittler, 2010). Mitokondrioek zelulen energia hornidura bermatzen eta arautzen dute (Nicholls eta Ferguson, 2002; MacAskil eta Kittler, 2010). Ondorioz, mitokondrien fosforilazio oxidatzaileak, elikagaietara atxikitako energia gehiena ATP bihurtzen du. Beste zenbait prozesu fisiologiko garrantzitsu ere modulatzen dituzte, hala nola, kaltzio homeostasia, apoptosia, oxidazio-estresa eta esteroidogenesia. Mitokondrioen egitura eta funtzioak etengabe egokitzen ari dira, zelulen metabolismo-homeostasia mantentzeko (Hebert-Chatelain et al., 2014). Neuronen bioenergiak garunaren patofisiologian duen eragina ikerketa sakoneko gaia izan da (Laughlin et al., 1998; Mattson et al., 2008; MacAskill eta Kittler, 2010), nahiz eta mitokondrioen jarduera garuneko funtzioekin lotzen dituzten mekanismo molekularrak oraindik gutxi ulertuta dauden.

GPCRak garunaren jarduera erregulatzen duten proteina-familia handienetako bat dira. Gainera, frogatuta dago mitokondrioek G proteinak dituztela (Lyssand eta Bajjalieh, 2007; Andreeva et al., 2008), eta zenbait ikerketak frogatu dute G proteinen seinaleztapenean behetik dauden molekulak mitokondria barruan daudela, hala nola, adenilil ziklasa disolbagarria (Zippin et al., 2003), fosfodiesterasa (Acin-Pérez et al., 2009, 2011) eta proteina kinasa A (PKA) (Ryu et al., 2005). Era berean, mitokondriak AMP ziklikoa sortzeko gai dira (Chen et al., 2004; Helling et al., 2008; Acin-Pérez et al., 2009, 2011). Hala, $mtCB_1$ hartzailearen bidezko mitokondrio barneko $G_{\alpha i}$-proteinaren aktibazioak adenilil ziklasa disolbagarriaren inhibizioa eragiten du, eta beraz, PKA-ren mitokondria barruko aktibitatea murrizten du (Hebert-Chatelain et al., 2016). Hala, $mtCB_1$ hartzaile funtzionalak ehun desberdinetan agertzeak (Aquila et al., 2010; Koch et al., 2015; Hebert-Chatelain et al., 2016; Mendizabal-Zubiaga et al., 2016; Gutiérrez-Rodríguez et al., 2018), EKSk NSZeko prozesu bionergetikoetan duen ekarpena onesten du. Izan ere, $mtCB_1$ hartzaileek zelula-arnasketaren aktibazioa eta energia-ekoizpena

arautzen dute saguen hipokanpoko neuronetan (Hebert-Chatelain et al., 2016). Mitokondrio-disfuntzioak endekapen-gaixotasunak, garun-isuriak edo zahartzearekin lotutako nahasteak eragin ditzake, eta ondorioz, garrantzitsua litzateke kannabinoideek mitokondrietan dituzten efektuak zehaztea, kannabinoideen erabilera terapeutiko potentzialari ikuspegi berriak zabaltzeko. Horrenbestez, funtsezkoa da CB_1 hartzaileen adierazpena eta kokapena ikertzea garun osasuntsu eta gaixoen neurona eta astrozitoen mitokondrietan. Zentsu honetan, saguen astrozitoen mitokondria-mintzarekin lotutako CB_1 hartzaileen aktibazioak glukosaren metabolismoa eta laktatoaren ekoizpena eragozten du, neurona-funtzio asaldatuak agertuz, eta, ondorioz, jokabide-erantzun kaltetuak agertzen dira (Jimenez-Blasco et al., 2020). Garunej¡ko egitura ezberdinetan $mtCB_1$ astroglialaren ebidentzia anatomikoan lagundu dugun argitalpen honek iradokitzen duenez, $mtCB_1$ hartzailearen seinaleztapenak zuzenean eragin dezake astrozitoen glukosa-metabolismoa, neurona-aktibitatea eta saguen portaera doitzeko (Jimenez-Blasco et al., 2020).

2.3. BEREIZMEN HANDIKO MIKROSKOPIO ELEKTRONIKOA

CB_1 hartzailea garunaren zelula-mota eta gune-subzelular ezberdinetan lokalizatzea oso zaila da, ez dagoelako banatuta era uniformean hura adierazten den eskualdeetan (Busquets-Garcia et al., 2015). 1990eko hamarkadan, erradioligandoen autoerradiografia loteslea ([3H]CP55,940) erabili zen garuneko kannabinoide-hartzaileak kualitatiboki eta kuantitatiboki ikertzeko (Herkenham et al., 1990). CB_1 hartzailea klonatu zenean, *in situ* hibridazio teknikak erabili ziren CB_1 ARNm-aren banaketa aztertzeko NSZean (Mailleux eta Vanderhaeghen, 1992; Matsuda et al., 1993; Marsicano eta Lutz, 1999). Gero, Mackieren laborategiak antigorputz poliklonalak sortu zituen CB_1 hartzailearen N-terminaleko aminoazidoen sekuentzia espezifiko baten kontra (Twitchell et al., 1997), eta laster, arratoiaren CB_1 hartzailearen C-terminaleko aminoazido sekuentzia baten kontra antiserum berri bat egin zen (Egertova et al., 1998). Tresna immunologiko horiek argi-mikroskopiorako teknika histokimiko egokiekin konbinatuz, CB_1 hartzailearen immunoerreaktibotasunaren adierazpen-patroia ikusi ahal izan zen (Egertova et al., 1998; Tsou et al., 1998). Hala ere, ez zen ezagutzen CB_1 hartzailearen adierazpen-patroi zelular eta subzelular zehatza garai hartan. Ondoren, mikroskopia elektronikorako erretxinan murgildu-aurreko teknika immunohistokimikoa oso tresna baliagarria izan zen CB_1 hartzaileek garunean eta organo periferikoetan duten kokapen zehatza aztertzeko. Metodo horren bidez frogatu ahal izan zen CB_1 hartzaileak ez zirela era homogeneoan banatzen garuneko zelula-mota eta zelulen konportamendu ezberdinetan, izan ere, CB_1 hartzailea GABA-bukaera inhibitzaileetan kontzentratzen da (Katona et al., 1999, 2000; Kawamura et al., 2006; Ludányi et al., 2008; Marsicano eta Kuner, 2008; Katona eta Freund, 2012; De-May eta Ali, 2013; Steindel et al., 2013; Hu eta Mackie, 2015), eta maila baxuan adierazten da glutamato-bukaera kitzikatzaileetan (Marsicano et al., 2003; Domenici et al., 2006; Katona et al., 2006; Monory et al., 2006; Takahashi eta Castillo, 2006; Kamprath et al., 2009; Bellocchio et al., 2010; Puente et al., 2011; Reguero et al., 2011; Ruehle et al., 2013; Soria-Gómez et al., 2014) eta astrozitoetan (Navarrete eta Araque, 2008, 2010; Stella, 2010; Han et al., 2012; Bosier et al., 2013; Metna-Laurent eta Marsicano, 2015; Viader et al., 2015; Oliveira Da Cruz et al., 2016; Blasco-Jimenez et al., 2020). Are gehiago, CB_1 hartzailearen adierazpen-maila eta kontestu-fisiologikoan izan dezakeen garrantzia ez datoz bat; hau da, zelula-mota

eta konpartimentu subzelular batzuetan oharkabean pasatzen diren CB_1 hartzailearen adierazpen-maila baxu eta oso baxuak (Katona et al., 1999, 2000; Hacerjos et al., 2000), funtzio eta portaera egokiari eusteko garrantzitsuak dira (Busquets-Garcia et al., 2018).

Hala eta guztiz ere, erretxinan murgildu-aurreko immunourre metodoak mugak ditu: erdi-kuantitatiboa baino ez da, hau da, markaketak ez du korrelazio zuzena antigenoaren kokapen zehatzarekin eta teknikak ez ditu erakusten epitopo guztiak. Haatik, erretxinan murgildu-aurreko metodoa hobetu zen, urre ultra-txikiz markatutako bigarren konjugatuen (Nanogold®) garapena urre partikulen zilarrezko handipen kimikoarekin konbinatuz, zundek ehunean epitopoak sakonago detektatzea posible egin zuen, ondorioz, antigorputzen sartze eta molekulak detektatzeko berezko mugak murriztuz, eta hartzaileen lokalizazio-bereizmena handituz.

Erretxinan murgildu-aurreko immunourre metodoak, immunoperoxidasa eta 3,3´-diaminobentzidina (DAB) kromogenoarekin konbinatuta, bereizmen-maila handian erakutsi ditzake proteinen arteko kolokalizazioak zelula-espezifikotasunarekin. Immunomarkaketa bikoitz hori askotan CB_1 hartzailea bezalako hartzaile ezberdinen kokapena aztertzeko erabiltzen da neurona eta glia-zelula ezberdinetan, zelula jakin batek adierazitako markatzaile espezifiko bat erabiliz immunoperoxidasa metodoaren itu gisa. Hala, tindatutako zelula-populazioen gorputz edo/eta zelula-zatiak DAB erreakzio ekoizkinez betea agertzen dira, besteetatik bereiztea ahalbideratuz. Esaterako, mikroskopia elektronikorako prestaketetan astrozitoen CB_1 hartzailearen adierazpena aztertzeko GFAP erabiltzen da ohituraz astrozitoak identifikatzeko (Eng, 1985; Eng et al., 2000; Hol eta Penky, 2015; Gutiérrez-Rodríguez et al., 2018; Bonilla-Del Río et al., 2019). Hala ere, GFAPren izaera harikara dela eta, bere immunomarkaketak ez du erakusten astrozitoen azalera osoa. Bestalde, aspartato-glutamato garraiatzailea (*glutamate aspartate transporter*, GLAST), aminoazido kitzikatzaileen 1-motako garraiatzailea (*excitatory amino acid transporter 1*, EAAT1) bezala ere deitua, immunoperoxidasa metodorako balizko itu gisa agertzen da, mikroskopio elektronikoan astrozitoen proiekzio finak hobeto ikusteko (Storck et al., 1992; Arriza et al., 1994; Danbolt, 2001; Zhou eta Danbolt, 2014, Danbolt et al., 2016), izan ere, NSZean, GLAST astrozitoetan era selektiboan adierazten den EAAT familiako garraiatzaile bakarra da (Danbolt, 1994; Danbolt et al., 2016). GLAST asko adierazten da astrozitoen mintz osoan

zehar, eta batez ere sinapsi kitzikatzaileen inguruan dauden astrozitoen proiekzioetan (Cholet et et al., 2002), baina baita zelula-gorputzeko mintzean ere (Sullivan et al., 2007). Gainera, glutamato gehiegi edo gutxiegi, biak, garun-funtzioetarako kaltegarriak direnez (Zhou eta Danbolt, 2014), GLAST eta beste EAATen aktibitatea ezinbestekoa da NSZean, eta aise adierazten dira garuneko eskualde ezberdinetan. Metodologikoki, hala ere, ez da inoiz aztertu GLAST *versus* GFAP antigorputzen erabilera astrozitoen markatzaile bezala, CB_1 hartzaileak astrozitoetan lokalizatzeko mikroskopio elektronikoan.

2.4. EKS ETA SINAPSI-PLASTIKOTASUNA

EKSk sinapsi-transmisioaren funtsezko modulatzaile gisa jarduten du, sinapsi-plastikotasunean parte hartuz. Horrenbestez, eKB-ek eragindako sinapsi-transmisioaren erregulazioa epe laburrean nahiz luzean bietan gertatzen da. Segundotan ematen diren sinapsi-aldaketak eKB-ek-bideratutako epe-laburreko aldaketak dira, zeinak depolarizazioak eragindako kitzikapenaren murriztea (DSE) edo inhibizioaren murriztea (DSI) izan daitezke, eKB-ek GABA edo glutamato-bukaerei eragiten badiote, hurrenez hurren (Kano et al., 2009; Castillo et al., 2012). Minututik ordura gertatzen diren sinapsi-aldaketak bukaera kitzikatzaile eta inhibitzaileetan, bietan eman daitezke, presinapsi-edo postsinapsi-aktibitate bati erantzunez (Araque et al., 2017). Aldaketa hauek sinapsi-transmisioaren epe-luzeko depresioa (LTD) edo epe-luzeko indartzea (LTP) izan daitezke. Hala, eKB-ak garuneko sinapsi-funtzioaren bitartekari ahaltsuak dira eta hainbat garun-funtzio arautzeko gai direla frogatu da, hala nola, kognizioa, kontrol motorra, emozioa, saria eta elikadura.

2.4.1. Hipokanpoko plastikotasuna

Hipokanpoak memoria adierazle/esplizituaren prozesamenduan parte hartzen du, eta funtsezko osagaia da kognizioari lotutako portaerak erregulatzeko eta epe-luzeko memoriaren prozesamenduan (Aggleton eta Brown, 1999; Eichenbaum, 2000; Eichembaum et al., 2012; Peñasco et al., 2019, 2020). EKSk eginkizun erabakigarria du epe-luzeko sinapsi-plastikotasunean, hipokanpoan eta garun osoan, ikasketa- eta memoria-sorkuntzan eraginez (Lafourcade et al., 2007; Castillo et al., 2012; Peñasco et al., 2019, 2020; Fontaine et al., 2020; Egaña-Huguet et al., 2021). Informazio espaziala kodetzen duten input-kortikalak bihurgune horzdunera doaz erdiko bide-zulatzailearen (*medial perforant path*, MPP) eta alboko bide-zulatzailearen (*lateral perforant path*, LPP) bidez (Peñasco et al., 2019). MPPko axoi-bukaerak pikor-zelulen (*granule cells*, GC) dendrita-arantzekin horzdun bihurguneko molekula-geruzaren erdiko 1/3an eratzen dituen glutamato-sinapsiak (Grandes eta Streit, 1991) LTDa mantentzeko gai dira (Christie eta Abraham, 1994), pultsu-parekatuen murriztea erakusten dute estimulu-intentsitate baxuetan (Petersen et al., 2013) eta eKB-menpeko plastikotasun sinaptiko ezberdinak dauzkate (Chávez et al., 2010; Peñasco et al., 2019; Fontaine et al., 2020).

Gure laborategiak CB_1 hartzailearen-menpeko iraupen-luzeko depresioa aurkitu zuen MPP-GC arteko sinapsi kitzikatzaileetan (eKB-LTD) (Peñasco et al., 2019). Lan honetan eKB-LTD induzitzeko erabilitako estimulazio-protokoloa arinago ere erabili zen garuneko beste eskualde batzuetan baita eKB-menpeko eLTD eragiteko, hala nola kortex prefrontalean eta bukaerako ildaskaren nukleoan (*bed nucleus of the striatal terminalis*, BNST) (Lafourcade et al., 2007; Puente et al., 2011). Interesgarria da plastikotasun-mota honetako eKB-eLTD-aren tamaina ez dela aldatzen DL-APV, NMDA hartzaileen antagonista, bainuan jartzean, beste sinapsi batzuetan ez bezala (Sjöström et al., 2003; Bender et al., 2006). Azkenik, MPP terminaletan kokatzen diren sinapsi kitzikatzaile hauetan CB_1 hartzaile presinaptikoa aktibatzean eKB-LTD eragiten duen eKB-a 2-AGa zela aurkitu genuen (Peñasco et al., 2019).

2.4.2. Kortex prefrontaleko plastikotasuna

Goi-mailako zeregin betearazleak PFCaren, primateetan gehien lantzen den garun eskualdearen, menpe daude (Puig eta Gulledge, 2011). Ikasketan parte hartzen du (Pasupathy eta Miller, 2005; Antzoulatos eta Miller, 2011), eta baita memorian (Warden eta Miller, 2010), kategorizazioan (Freedman et al., 2001; Antzoulatos eta Miller, 2011), inhibizio-kontrolean (Chudasama et al., 2003; Dalley et al., 2011) edo kognizio-malgutasunean Clarke et al., 2004; Gruber et al., 2010; Rygula et al., 2010). Kannabinoideek ondorio kaltegarriak dituzte PFCak bideratutako funtzioetan, eta era askotako adierazgarrik lotzen dituzte EKS, kannabisaren kontsumoa eta eskizofrenia, PFCeko funtzio asko asaldatuta dituen gaixotasuna (Ujike eta Morita, 2004; Lafourcade et al., 2007). Garuneko beste eskualde batzuetan bezala (Kano et al., 2009; Katona eta Freund, 2012), CB_1 hartzailearen ARNm kontzentrazio handienak interneuronatan daude. CB_1 hartzailearen immunoerreaktibitatea zuntz glutamatergikoetan ere hautematen da, PFCeko geruza sakonetako (V/VI geruzak) eta azaleko geruzetako (II/III geruzak) neurona piramidalak inguratuz (Egertová eta Elphick, 2000; Lafourcade et al., 2007; Araque et al., 2017). Era aipagarrian, V/VI geruzetako sinapsi kitzikatzaileetan eKB-ek bideratutako LTD mota bat ikusi zen (Lafourcade et al., 2007) non CB_1 hartzailearen partaidetza behar den, baita mGluR5 postsinaptikoa, 2-AG, fosfolipasa C, eta Ca^{2+} gehikuntza postsinaptikoa (Lafourcade et al., 2007).

2.5. EKS ETA EPILEPSIA

Epilepsia gaixotasun neurologiko arrunta da, bat-bateko konbultsio errepikakorrak eragiten dituena eta helduen % 1 ingururi eragiten diona (Leo et al., 2016; Reddy eta Golub, 2016). Krisi epileptikoak garuneko eskualde askotatik sor daitezkeen deskarga elektriko anormalak dira eta portaera, kontzientzia eta sentzazioak alda ditzakete (Reddy eta Golub, 2016). Konbultsioak partzial eta orokor gisa sailkatzen dira (Reddy, 2014; Reddy eta Golub, 2016). Epileptogenesi prozesuaren bidez garun normala pixkanaka epileptiko bihurtzen doa lesio baten edo beste arrisku-faktore batzuen ondorioz, hala nola garun-isuri, infekzio edo konbultsio luze baten ondorioz. Gaixotasuna neuronen seinaleztapen anormal baten ondorioz ere garatu daiteke, neurotransmisore kitzikatzaile eta inhibitzaileen arteko desorekagatik, edo bien konbinazioagatik (Reddy eta Golub, 2016).

Orain arte ez dago epilepsia sendatzeko terapia farmakologikorik. Hala ere, pazienteen % 70aren arintze sintomatikoa lor daiteke (Reddy eta Golub, 2016). Epilepsiaren aurkako botika ugari (*antiepileptic drug*, AED) erabiltzen dira krisien kontrol sintomatikoa lortzeko, baina, hala ere, gaixo epileptikoen % 25-40ak gaur egungo terapiei aurre egiten dieten konbultsio errefraktarioak dituzte (Sillanpää eta Schmidt, 2012; Reddy eta Golub, 2016). Beraz, ezinbestekoa da gaixotasuna modu eraginkor batean tratatzeko helburu terapeutiko berriak bilatzea (Wilcox et al., 2013).

Esan bezala, EKSk funtsezko zeregina du garunean, non hainbat funtzio fisiologiko eta patologiko asko erregulatzen dituen (Di Marzo et al., 1998; Alger, 2006; Mackie eta Stella, 2006; Kano et al., 2009; Castillo et al., 2012). Kannabisa aspalditik erabili izan da arazo neurologikoen tratamenduan, epilepsia barne (Friedman eta Devinsky, 2015; Rosenberg et al., 2015; Leo et al., 2016). Zenbait ikerketek arreta jarri dute aztertzen EKSren funtzio eta disfuntzioaren parte hartzea konbultsioak kontrolatzen edo laguntzen (Blair et al., 2015). Animalia-ereduek frogatu dute CB_1 hartzaileen aktibazioak konbultsioen larritasuna gutxitzen duela. Horrela, CB_1 hartzailearen gabezia duten sagu mutanteen garun-aurreko neurona kitzikatzaile nagusietan (baina ez interneuronetan) kainatoak eragindako konbultsio arinagoak jasaten dituzte, sagu basatiekin alderatuz (Marsicano et al., 2003), eta, beraz, hipokanpoko CB_1 hartzaile glutamatergikoak baina ez GABAergikoak dira beharrezkoak eta nahikoa kainatoak eragindako konbultsioetatik

babesteko (Monory et al., 2006). Gainera, CB_1 hartzaileen gainadierazpenak kainatoak hipokanpoan eragindako konbultsioen larritasuna eta hilkortasuna gutxitzen du (Guggenhuber et al., 2010). Oro har, emaitza hauek erakusten dute CB_1 hartzaillek konbultsioak kontrola ditzaketela eta neuronak zelulen heriotzatik eta gliosi erreaktibotik babes ditzaketela (Rosenberg et al., 2015).

Informazioaren prozesamendua ere oso baldintzatua astrozito-neurona arteko elkarrekiko komunikazio azkar batez, milisegundotik minuturako eskala laburretan lan egiten duena. Beraz, intuitiboa da astrozitoen egiturak eta funtzioak aste eta hilabeteetan zehar izan ditzaketen epe-luzeko aldaketek eragina izatea garuneko neuronen seinaleztapenean. Astrogliosia ezaugarri nabarmena da epilepsia paziente eta animalia-ereduen azkenengo aldietan (Henneberger, 2017). Epilepsiarekin eta beste gaixotasun batzuekin lotutako zenbait aldaketa deskribatu dira astrozitoen dentsitatean, morfologian, biokimikan eta fisiologian (Sofroniew eta Vinters, 2009; Pekny eta Pekna, 2014). Astrozitoetako funtzio aldaketa batzuek (esaterako, K^+ eta glutamatoaren garbiketa asaldatua) konbultsioak sortzen lagun dezakete. Hala, hainbat ikerketa berrik iradokitzen dute astrogliosiaren parte hartzea epileptogenesian, izan ere, astrogliosi iraunkorra eta astrozitoen funtzioetan emandako aldaketak nahiko dira neurona-sareetan krisi espontaneoak garatzeko, egun edo aste batzuen ondoren (Ortinski et al., 2010; Robel et al., 2015; Henneberger, 2017). CB_1 hartzaileak astrozitoetan adierazten dira, eta litekeena da zeregin garrantzitsuak betetzea gaixotasunean. Beraz, astrozitoetako CB_1 hartzaileak epilepsia tratatzeko itu potentzialtzat har daitezke.

LAN HIPOTESIA

Jakina da astrozitoek neuronen jarduera modulatzen dutela, zeregin garrantzitsuak betez garunaren jardueran (Araque et al., 1999; Haydon and Carmignoto, 2006; Perea et al., 2009; Gómez-Gonzalo et al., 2014). Astrozitoek sinapsi-jarduerak hautematen dituen neurotransmisore-hartzaileak adierazten dituzte eta gliotransmisoreak askatuz erantzuten diote, zeinek neurona-kitzikagarritasuna eta sinapsi-transmisioa arautzen dituzte (Perea eta Araque, 2005a; Perea eta Araque, 2009; Araque eta Navarrete, 2010).

CB_1 hartzaileak astrozitoetan adierazten dira eta haien funtzioaren garrantzia frogatu da (Rodriguez et al., 2001; Navarrete eta Araque, 2008, 2010; Stella, 2010; Han et al., 2012; Bosier et al., 2013; Han et al., 2012; Bosier et al., 2013; Gómez-Gonzalo et al., 2014; Navarrete et al., 2014; Metna-Laurent and Marsicano, 2015; Viader et al., 2015; Oliveira da Cruz et al., 2016; Gutiérrez- Rodríguez et al., 2017; Bonilla-del Río et al., 2019, 2021). CB_1 hartzaileek bideratutako astrozitoen funtzioak estuki lotuta daude CB_1 hartzaileen banaketarekin neuronen konpartimentuetatik hurbil dauden astrozitoetan, batez ere sinapsietatik gertu. Hala ere, ezer gutxi dakigu astrozitoetako CB_1 hartzaileen adierazpen eta kokapen zehatzari buruz.

GFAP astrozitoen proteina zitoeskeletiko espezifikoa da, eta markatzaile astroglial gisa erabiltzen da hartzaileen banaketa aztertzeko astrozitoetan erresoluzio handiaren bidez (Gutiérrez- Rodríguez et al., 2017; Bonilla-del Río et al., 2019, 2021). Bestalde, jakina da GLAST astrozitoen mintzean zehar kokatzen dela espezifikoki (Danbolt, 1994; Sullivan et al., 2007; Danbolt et al., 2016). Testuinguru horretan, hipotesi hau planteatzen dugu: GLAST GFAP baino markatzaile hobea da sinapsien inguruko prozesu astroglial finak identifikatzeko, non astrozitoen hartzaileek errez antzematen dituzten sinapsietatik askatutako neurotrnasmisoreak. Gainera, astrozitoen mitokondriek neuronen mitokondriek bezala CB_1 hartzaileak adierazten dituzte (Bénard et al., 2012; Hebert-Chatelain et al., 2016; Gutiérrez-Rodríguez et al., 2018; Bonilla-del Río et al., 2019; Jimenez-Blasco et al., 2020). Hala ere, astrozitoen mitokondriatan detektatutako CB_1 hartzaileen dentsitatea identifikatutako prozesu astroglialen araberakoa izan daiteke, GLAST bezalako markatzaile on eta espezifikoak erabiliz, GFAP erabili beharrean, zeina zelula-gorputzetara eta astrozitoen adar nagusietara mugatzen baita.

Azkenik, CB_1 hartzaile funtzionalek hainbat sinapsi-plastikotasun motatan parte hartzen dute garun osoan. Aurrez egindako azterketetan ikusi da, 11-12 aste bitarteko saguen sinapsi kitzikatzaileetan LFSak eKB-LTD-a eragiten duela PFCean eta horzdun bihurgunean (Lafourcade et al., 2007; Peñasco et al., 2019, 2020). Hala ere, LFSak eragindako eKB-menpeko sinapsi plastikotasuna aldatu egin daiteke animalia zahartzean, zahartzeak eragindako hipokanpoko neuronen galtzeak CB_1 hartzailearen adierazpena aldatu dezakeelako. Berez, kognizio narraiadura azkartu egiten da CB_1 hartzailerik ez duten saguetan (Bilkei-Gorzo et al., 2005).

HELBURUAK

Nire tesiaren helburu orokorra karraskariaren garuneko EKS ikertzea izan zen, bereizmen handiko mikroskopiaren eta elektrofisiologiaren bidez, hipokanpoko CA1 eskualdean eta PFC prelinbiikoan arreta jarriz. Helburu zehatzak hauek ziren:

1.- GLAST markatzaile astroglialak GFAPrekin konparatu, astrozitoetan CB_1 hartzaileak hobeto identifikatzeko.

2.- Glu-CB_1-WT/KO eta GABA-CB_1-WT/KO saguen neurona eta astrozitoen konpartimentuetan CB_1 hartzaileen banaketa aztertzea PFC prelinbikoan.

3.- CB_1 hartzaileen banaketa ikertzea GFAP-CB_1-WT/KO saguen neurona eta astrozitoen konpartimentuetan PFC prelinbikoan.

4.- Neurona eta astrozitoen mtCB_1 hartzaileen dentsitatea aztertzea garuneko zenbait eskualdetan (CA1, PFC, accumbens nukleoa, kortex piriformea).

5.- 14 asteko GFAP-CB_1-WT eta GFAP-CB_1-KO saguetako eKB-menpeko sinapsi-plastikotasun kitzikagarria ikertzea.

6.- eKB-menpeko sinapsi-plastikotasuna aztertzea kainatoak eragindako konbultsioen eraginpean dauden GFAP-CB_1-WT/KO saguetan.

MATERIALAK ETA METODOAK

4.1. ETIKA-BATZORDEA

Esperimentuak Euskal Herriko Unibertsitateko UPV/EHU, Neurozientziak Saileko *Laboratory of ultrastructural and functional neuroanatomy of the synapse* laborategian egin ziren. Protokolo guztiak Animalien Ongizaterako etika-batzordeak onartu zituen (CEEA/M20/2015/093) eta bat zetozen Europar Batasunaren Kontseiluaren 2010eko irailaren 22ko zuzentarauarekin (2010/63/EU) eta Espainiako araudiarekin (ED/53/2013 eta 6/2013 Legea). Ahalegin guztiak egin ziren mina eta sufrimendua gutxitzeko eta erabilitako animalia-kopurua murrizteko.

Saguak bi edo gehienez hiru sabelaldi berdineko anaiekin taldekatuta eduki ziren, plexiglaseko kaiola orokorretan (17 cm x 14,3 cm x 36,3 cm) eta gutxienez aste batez ingurumenera ohitzeko utzi zitzaien. Baldintza orokorretan mantendu ziren tenperatura konstantea duen geletan (22°C), nahi besteko elikagai eta urarekin esperimentu guztietan. Saguak 12 h: 12 h argi/iluntasun zikloan egon ziren, argiak 21:00etan itzaltzen zirelarik.

4.2. ESPERIMENTAZIO-ANIMALIAK

4.2.1 CB_1 hartzailearen andui mutanteak

4.2.1.1. C57BL/6 saguak

8-14 astetako C57BL/6 saguak (*The Jackson Laboratory* eta *Janvier labs*) Euskal Herriko Unibertsitatean jasotzen ziren eta aste beteko berrogeialdiaren ostean erabilgarri zeuden.

4.2.1.2. CB_1-KO saguak

CB_1 hartzailerik gabeko saguak (CB_1-KO), lehenago deskribatu bezala sortu eta genotipatu ziren (Marsicano et al., 2002). Baldintzapeko sagu mutanteak Cre adierazten duten sagu-anduia eta $CB_1^{f/f}$ saguak gurutzatuz lortu ziren (Marsicano et al., 2003), hiru urratsetako ugaltze-protokoloa erabiliz (Monory et al., 2006). Sagu guztiek C57BL/6N oinarri genetikoa zuten.

4.2.1.3. Glu-CB_1-KO: Neurona glutamatergiko kortikaletan baldintzapeko CB_1 hartzailea selektiboki ezabatuta duten sagu mutanteak

NEX helize-bihurgune-helize motako glutamato-neurona kortikalen neurona-ama enbrionarioen transkripzio-faktore bat da (Wu et al., 2005). Garun helduan, NEX bakarrik neurona glutamatergiko kortikaletan adierazten da, eta, neurri txikiagoan, eskualde subkortikaletako neuronetan (Barthalomä eta Nave, 1994). NEX locusean "knock-in" bidez sortutako sagu mutanteetan (NEX-Cre saguak), Cre-ren adierazpena NEX-en erregulazio-sekuentziaren kontrolpean izateak, garun-aurrekoan "floxeatutako" aleloa berariaz ezabatzen ditu (Kleppisch et al., 2003). Horrela, $CB_1^{f/f,\ NEX\text{-}Cre}$ saguak, Glu-CB_1-KO saguak (Monory et al., 2006), $CB_1^{f/f}$ saguak NEX-Cre saguekin gurutzatuz lortu ziren (Schwab et al., 2000; Kleppisch et al., 2003). $CB_1^{f/f}$ sagu emeak eta $CB_1^{f/f,\ NEX\text{-}Cre}$ sagu arrak gurutzatu ziren sagu mutantean lortzeko.

4.2.1.4. GABA-CB_1-KO: GABA-neuronetan baldintzapeko CB_1 hartzailea selektiboki ezabatuta duten sagu mutanteak

Dlx5/Dlx6 geneak *homeobox* geneak dira, garapen-enbrionarioan bereizten eta migratzen ari diren garun-aurreko GABA-neuronek adierazten dituztenak (Stuhmer, 2002). $CB_1^{f/f,\ Dlx5/6\text{-}Cre}$ saguak, Dlx5/6-Cre saguak (Zerucha et al., 2000) $CB_1^{f/f}$ saguekin gurutzatuz lortu ziren. Hala, Dlx5/6 geneen erregulazio-sekuentzien kontrolpeko Cre errekonbinasaren adierazpenak, loxP geneen errekonbinazioa eragiten du GABA-neuronetan, GABA-CB_1-KO saguak sortuz (Monory et al., 2006). Sagu mutanteak $CB_1^{f/f}$ emeak $CB_1^{f/f,\ Dlx5/6\text{-}Cre}$ arrekin gurutzatuz lortu ziren.

4.2.1.5. GFAP-CB_1-KO: Astrozitoetan baldintzapeko CB_1 hartzailea selektiboki ezabatuta duten sagu mutanteak

Astrozitoetan CB_1 hartzailea adierazten ez duten sagu mutanteak lortzeko, $CB_1^{f/f,\ GFAP\text{-}CreERT2}$ saguak (GFAP-CB_1-KO) (Hirrlinger et al., 2006), CB_1 hartzailearen sekuentzia "floxeatuta" duten saguak (Marsicano et al., 2003), GFAP proteinaren kontrolpean dagoen CreERT2 Cre-aren bertsio induzigarria adierazten duten saguekin (GFAP-CreERT2 saguak) gurutzatu ziren. Sagu transgeniko honek eskaeraren araberako astrozitoen CB_1 hartzailearen errekonbinazioa baimentzen du sagu helduetan (Han et al., 2012).

4.3. ERRETXINAN MURGILDU-AURREKO IMMUNOMARKAKETA MIKROSKOPIO ELEKTRONIKORAKO

Gure laborategiak argitaratutako protokoloa jarraitu zen esperimentu guztietan (Puente et al., 2019):

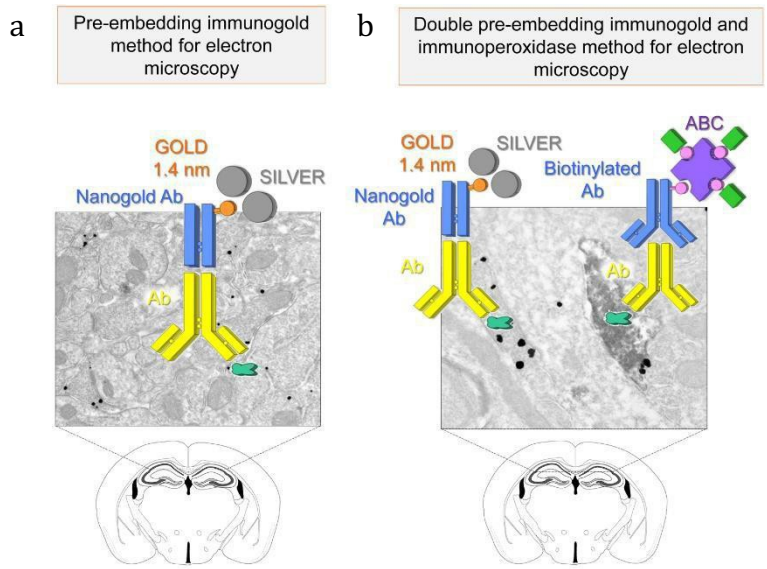

1. irudia. Bereizmen handiko mikroskopia elektronikorako erabilitako immunomarkaketa metodoak. Puente et al., 2019 lanetik egokitua.

4.3.1 Ehunaren kontserbazioa

1. Saguak ketamina/xilazina (80/10 mg/kg gorputz-pisua) nahasketa peritoneoan barnean txertatuz sakonki anestesiatu ziren.
2. Saguak bihotzean-zeharreko perfusioaz sakrifikatu ziren giro-tenperaturan (*room temperature,* RT) (20-25°C), ezkerreko bentrikulutik gatz-fosfato tanpoia (*phosphate buffered saline*, PBS) (0,1 M, pH 7,4) erabiliz 20 segundotan, eta ondoren, hoztutako disoluzio finkatzaile bat pasarazi zen 15 minutuz (min): % 4 formaldehido (unean paraformaldehidotik despolimerizatua), % 0,2 azido pikrikoa eta % 0,1 glutaraldehido fosfato tanpoian (*phosphate buffer*, PB) (0,1 M pH 7,4) disolbatuta.
3. Garunak kontu handiz atera ziren garezurretik eta disoluzio finkatzailean post-finkatu ziren aste betez 4°Ctan. Azkenik, 4°Ctan gorde ziren, disoluzio finkatzailea 0,1 M PB-tan (1:10) diluituz % 0,025 sodio azidarekin.

4. Garunak bibratomoz moztu ziren 50 μm-tako koroa-ebaketetan , eta 0,1M PB-tan (pH 7,4) batu ziren RTn. Bibro-ebaketak 12-putzutako zelula-hazkuntza plaketan mantendu ziren erabili arte 4°C-tan 0,1 M PBtan (pH 7,4) % 0,025 sodio azidarekin.

4.3.2. Erretxinan murgildu-aurreko immunourre metodo bakuna mikroskopia elektronikorako

1. Garun bakoitzeko intereseko-eremuko bi edo hiru bibro-ebaketa aukeratu ziren eta 12-putzutako zelula-hazkuntza plaketan jarri ziren 0,1 M PBtan (pH 7,4).
2. Laginak aurre-inkubatu ziren, 30 minutuz irabiatuta mantenduz (300 rpm) RT-n, blokeo-disoluzioan: % 10 behi-albumina (*bovine serum albumine*, BSA), % 0,02 saponina eta % 0,1 sodio azida, tris-hidrogeno kloruroarekin bahetutako gatz-tanpoian 1X (*tris-hydrogen chloride buffered saline*, TBS) (pH 7,4, 1 ml/putzu).
3. Ebakinak akurian eginiko anti-CB_1 hartzailearen antigorputz poliklonala, edo saguan eginiko anti-GFAP antigorputz monoklonala, edo untxian eginiko anti-GLAST antigorputz poliklonalarekin inkubatu ziren. Antigorputz guztiak % 0,004 saponina eta % 0,1 sodio azida zuen % 10 BSA/TBS 1X-tan diluitu ziren. Inkubazio-denbora 2 egunekoa izan zen, 4°Ctan irabiagailu orbital batean (0,5-1 ml/putzu).
4. % 1 BSA/TBS 1X disoluzioan garbitu ziren (3 x 1 min eta 2 x 10 min), gehiegizko antigorputz primarioaren soberakina kentzeko, irabiagailu batean RTn (1 ml/putzu).
5. Laginak dagozkien 1,4 nm-tako urre-partikulari atxikitutako anti-akuri, anti-sagu edo anti-untxi antigorputz sekundarioekin inkubatu ziren. Antigorputzak % 0,004 saponina zuen % 1 BSA/TBS 1X disoluzioan diluitu eta inkubatu ziren 3 orduz RTn (1 ml/putzu).

6. % 1 BSA/TBS 1X disoluzioan garbitu ziren (3 x 1 min eta 2 x 10 min), gehiegizko bigarren antigorputzaren soberakina kentzeko, irabiagailu batean RTn (1 ml/putzu).
7. Laginak gau osoan zehar % 1 BSA/TBS 1X disoluzioan utzi ziren 4°Ctan irabiagailu batean (1 ml/putzu).
8. TBS 1X-tan preparatutako % 1 glutaraldehidoarekin post-finkatu ziren 10 min-z RTn (1 ml/putzu).
9. 10 min-ko hiru garbiketa 0,1 M PB disoluzioan irabiagailu batean RTn (1 ml/putzu).
10. Ebakinak saiodietara aldatu ziren hurrengo pausurako.
11. Urre partikulen seinalea areagotu zen HQ zilar-kitarekin (HQ Silver kit, Nanoprobes Inc., Yaphank, NY, AEB) iluntasunean 10-12 min-z (0,8-1 ml/saiodi).
12. 1 min-ko hiru garbiketa ur ultrapuruan iluntasunean (1 ml/putzu).
13. 10 min-ko hiru garbiketa 0,1 M PBtan (pH 7,4; 1 ml/putzu).
14. Laginak kristalezko-flaskoetara aldatu ziren (15 ml, 3 x 5 cm; 1 ml/flasko).
15. Ebakinak 20 min-z osmifikatu ziren % 1 osmio tetroxidoa duen 0,1 M PBtan (pH 7,4; 1 ml/flasko).
16. 0,1 M PB (pH 7.4) disoluzioan garbitu ziren (3 x 1 min eta 2 x 10 min; 1 ml/flasko).
17. Laginak deshidratatu egin ziren alkohol gradiente gorakor bat erabiliz (% 50, % 70, % 96; 5 min bakoitza). Ebakinak deshidratatzen bukatu % 100 etanolean hiru aldiz (5 min bakoitza; 1 ml/flasko).
18. Etanola garbitu oxido propilenoan hiru aldiz (5 min bakoitza; 1 ml/flasko).
19. Laginak oxido propileno eta Epon erretxina 812 nahasketan (1:1) murgildu ziren, eta gau osoan zehar utzi ziren irabiagailu batean (1 ml/flasko).
20. Laginak Epon erretxina 812 puruan murgildu ziren 2 orduz RTn.

21. Ebakinak bi kristalezko portaobjetuen artean jarri ziren, eta aluminio-paperaz bildu ziren.
22. Erretxinan murgildutako laginak labean polimerizatu ziren 2 egunez 60°Ctan.
23. Ebakinetatik intereseko eremua moztu zen, eta Epon erretxina 812 puruaz bloketan itsatsi zen.
24. Blokeetatik 1 μm-tako ebakin semi-finak lortu ziren ultramikrotomoarekin diamantezko hortza erabiliz.
25. Ondoren 50 nm-tako ebakin ultra-finak ere diamantezko hortza erabiliz lortu ziren eta nikelezko sareetan batu ziren.
26. Laginak % 2,5 berunezko zitratoan kontrastatu ziren 20 min-z RTn.
27. Ur ultrapuruarekin garbitu ziren (3 x 1 min eta 2 x 10 min).
28. Laginak JEOL JEM-1400 Plus transmisiozko mikroskopio elektroniko batean behatu ziren (JEOL Canada).
29. Ehunari argazkiak atera zitzaizkion Gatan SC1000 kamera digitala erabiliz.

4.3.3. Erretxinan murgildu-aurreko immunoperoxidasa metodo bakuna mikroskopia elektronikorako

1. Garun bakoitzeko intereseko eremuko bi edo hiru bibro-ebaketa aukeratu ziren eta 12-putzutako zelula-hazkuntza plaketan jarri ziren 0,1 M PBtan (pH 7,4).
2. Laginak aurre-inkubatu ziren 30 minutuz irabiatuz (300 rpm), RTn eta blokeo-soluzio batean: % 10 BSA, % 0,02 saponina eta % 0,1 sodio azida, 1X TBStan (pH 7,4; 1 ml/putzu).
3. Ebakinak saguan eginiko anti-GFAP antigorputz monoklonalarekin edo untxian eginiko anti-GLAST antigorputz poliklonalarekin inkubatu ziren. Antigorputz guztiak % 0,004 saponina eta % 0,1 sodio azida zuen % 10 BSA/TBS 1Xtan diluitu ziren. Inkubazio-denbora 2 egunekoa izan zen, 4°Ctan irabiagailu orbital batean (0,5-1 ml/putzu).
4. % 1 BSA/TBS 1X disoluzioan irabiatuz garbitu ziren (3 x 1 min eta 2 x 10 min), gehiegizko antigorputz primarioa kentzeko RTn (1 ml/putzu).
5. Laginak dagozkien anti-sagu edo anti-untxi bigarren antigorputz biotinilatuekin inkubatu ziren % 0,004 saponina zuen % 1 BSA/TBS 1X disoluzioan 3 orduz RTn (1 ml/putzu).
6. % 1 BSA/TBS 1X disoluzioan garbitu ziren (3 x 1 min eta 2 x 10 min) irabiatuz, gehiegizko bigarren antigorputza kentzeko RTn (1 ml/putzu).
7. Laginak abidina-biotina-peroxidasa konplexuarekin (Elite, Vector Laboratories, Burlingame, CA, AEB) inkubatu ziren % 1 BSA/TBS 1X disoluzioan 1,5 h-z irabiatuz RTn (1 ml/putzu).
8. % 1 BSA/TBS 1X disoluzioan garbitu ziren (3 x 1 min eta 2 x 10 min) irabiatuz RTn (1 ml/putzu).
9. Laginak gau osoan zehar %1 BSA/TBS 1Xean utzi ziren 4°Ctan irabiagailu batean (1 ml/putzu).
10. TBS 1Xtan preparatutako % 1 glutaraldehidoarekin post-finkapena 10 min-z RTn (1 ml/putzu).

11. 10 min-ko hiru garbiketa 0,1 M PB disoluzioan irabiagailu batean RTn (1 ml/putzu).
12. Laginak % 0,05 diaminobentzidina (DAB) eta % 0,01 hidrogeno peroxidoarekin inkubatu ziren 0,1 M PBtan 3 min-z RTn (1ml/putzu).
13. Hainbat garbiketa 0,1 M PBtan (pH 7,4; 3 x 1 min eta 2 x 10 min; 1 ml/putzu).
14. Laginak kristalezko-flaskoetara aldatu ziren (15 ml, 3 x 5 cm; 1 ml/flasko).
15. Ebakinak 20 min-z osmifikatu ziren % 1 osmio tetroxidoa duen 0,1 M PBtan (pH 7,4; 1 ml/flasko).
16. 0,1 M PB (pH 7.4) disoluzioan garbitu ziren (3 x 1 min eta 2 x 10 min; 1 ml/flasko).
17. Laginak deshidratatzeko alkohol gradiente gorakorrak erabili ziren (% 50, % 70, % 96; 5 min bakoitza). Ebakinak deshidratzen bukatu % 100 etanolean hiru aldiz (5 min bakoitza; 1 ml/flasko).
18. Etanola garbitu oxido propilenoan hiru aldiz (5 min bakoitza; 1 ml/flasko).
19. Laginak oxido propileno eta Epon erretxina 812 nahasketa (1:1) batean murgildu ziren, eta gau osoan zehar utzi ziren irabiagailu batean (1 ml/flasko).
20. Laginak Epon erretxina 812 puruan murgildu ziren 2 orduz RTn.
21. Ebakinak bi kristalezko portaobjeturen artean jarri ziren, eta aluminio-paperaz bildu ziren.
22. Erretxinan murgildutako laginak labean polimerizatu ziren 2 egunez 60°Ctan.
23. Ebakinetatik intereseko eremua moztu zen eta Epon erretxina 812 puruaz eginiko bloketan itsatsi zen.
24. Blokea moztu eta 1 μm-tako ebakin semi-finak lortu ziren ultramikrotomoarekin diamantezko hortza erabiliz.
25. Ondoren, 50 nm-tako ebakin ultra-finak lortu ziren eta nikelezko sareetan batu ziren.
26. Laginak % 2,5 berunezko zitratoan kontrastatu ziren 20 min-z RTn.

27. Ur ultrapuruarekin garbitu ziren (3 x 1 min eta 2 x 10 min).
28. Laginak JEOL JEM-1400 Plus transmisiozko mikroskopio elektronikoan behatu ziren (JEOL Canada).
29. Ehunari argazkiak atera zitzaizkion Gatan SC1000 kamera-digitala erabiliz.

4.3.4. Erretxinan murgildu-aurreko immunourre eta immunoperoxidasa metodo bikoitza mikroskopia elektronikorako

1. Garun bakoitzeko intereseko-eremuako bi edo hiru bibro-ebaketa aukeratu ziren eta 12-putzutako zelula-hazkuntza plaketan jarri ziren 0,1 M PBtan (pH 7,4).
2. Laginak aurre-inkubatu ziren blokeo-soluzio batean 30 minutuz irabiatuz (300 rpm), RTn: % 10 BSA, % 0,02 saponina eta % 0,1 sodio azida, 1X TBStan (pH 7,4, 1 ml/putzu).
3. Laginak bi antigorputz primarioren konbinazioarekin inkubatu ziren: ahuntzean eginiko anti-CB_1 hartzailea gehi saguan eginiko anti-GFAP; edo akurian eginiko anti-CB_1 hartzailea gehi untxian eginiko anti-GLAST. Antigorputz guztiak % 0,004 saponina eta % 0,1 sodio azida zuen %10 BSA/TBS 1Xtan diluitu ziren. Inkubazio-denbora 2 egunekoa izan zen, 4°Ctan irabiagailu orbital batean (0,5-1 ml/putzu).
4. % 1 BSA/TBS 1X disoluzioan garbitu ziren (3 x 1 min eta 2 x 10 min), gehiegizko antigorputz primarioa kentzeko irabiatuz RTn (1 ml/putzu).
5. Laginak 1,4 nm-tako urre-partikulari atxikitutako anti-ahuntz eta biotinilatutako anti-sagu bigarren antigotputz, edo 1,4 nm-tako urre-partikulari atxikitutako anti-akuri eta biotinilatutako anti-untxi bigarren antigotputzen konbinazioekin inkubatu ziren % 0,004 saponina zuen % 1 BSA/TBS 1X disoluzioan 3 orduz RTn. (1 ml/putzu)
6. % 1 BSA/TBS 1X disoluzioan garbitu ziren (3 x 1 min eta 2 x 10 min), gehiegizko bigarren antigorputzak kentzeko irabiatuz RTn (1 ml/putzu).

7. Laginak abidina-biotina-peroxidasa konplexuarekin (Elite, Vector Laboratories, Burlingame, CA, USA) (1:50) inkubatu ziren % 1 BSA/TBS 1X disoluzioan 1,5 h-z irabiagailuan RTn (1 ml/putzu).
8. % 1 BSA/TBS 1X disoluzioan garbitu ziren (3 x 1 min eta 2 x 10 min) irabiatuz RTn (1 ml/putzu).
9. Laginak gau osoan zehar % 1 BSA/TBS 1X-etan utzi ziren 4°Ctan irabiatuz (1 ml/putzu).
10. TBS 1X-tan preparatutako % 1 glutaraldehidoarekin post-finkapena 10 min-z RTn (1 ml/putzu).
11. 10 min-ko hiru garbiketa 0,1 M PB disoluzioan irabiatuz RTn (1 ml/putzu).
12. Ebakinak saiodietara aldatu ziren hurrengo pausurako.
13. Urre partikulen seinalea areagotu zen HQ zilar-kitarekin (HQ Silver kit, Nanoprobes Inc., Yaphank, NY, AEB) iluntasunean 10-12 min-z (0,8-1 ml/saiodi).
14. 1 min-ko hiru garbiketa ur ultrapuruan iluntasunean (1 ml/putzu).
15. 10 min-ko hiru garbiketa 0,1 M PB disoluzioan irabiagailu batean RTn (1 ml/putzu).
16. Laginak kristalezko-flaskoetara aldatu ziren (15 ml, 3 x 5 cm; 1 ml/flasko).
17. Laginak % 0,05 DAB eta % 0,01 hidrogeno peroxidoarekin inkubatu ziren 0,1 M PBtan 3 min-z RTn (1 ml/flasko).
18. Hainbat garbiketa 0,1 M PBtan (pH 7,4) (3 x 1 min eta 2 x 10 min; 1 ml/flasko).
19. Ebakinak 20 min-z osmifikatu ziren % 1 osmio tetroxidoa duen 0,1 M PBtan (pH 7,4; 1 ml/flasko).
20. Hainbat garbiketa (3 x 1 min eta 2 x 10 min) 0,1 M PB (pH 7.4) disoluzioan (1 ml/flasko).
21. Laginak deshidratatzeko alkohol gradiente gorakorrak erabili ziren (% 50, % 70, % 96; 5 min bakoitza; 1 ml/flasko). Ebakinak deshidratzen bukatu % 100 etanolean hiru aldiz (5 min bakoitza; 1 ml/flasko).

22. Etanola garbitu oxido propilenoan hiru aldiz (5 min bakoitza; 1 ml/flasko).
23. Laginak oxido propileno eta Epon erretxina 812 nahasketa (1:1) batean murgildu ziren, eta gau osoan zehar utzi ziren irabiagailu batean (1 ml/flasko).
24. Laginak Epon erretxina 812 puruan murgildu ziren 2 orduz RTn.
25. Ebakinak bi kristalezko portaobjeturen artean jarri ziren, eta aluminio-paperaz bildu ziren.
26. Erretxinan murgildutako laginak labean polimerizatu ziren 2 egunez 60°Ctan.
27. Ebakinetatik intereseko-eremua moztu zen, eta Epon erretxina 812 puruaz eginiko bloketan itsatsi zen.
28. Blokea moztu eta 1 μm-tako ebakin semi-finak lortu ziren ultramikrotomoarekin diamantezko-hortza erabiliz.
29. Ondoren, 50 nm-tako ebakin ultra-finak beste diamantezko-hortz batekin lortu ziren eta nikelezko sareetan batu ziren.
30. Laginak % 2,5 berunezko zitratoan kontrastatu ziren 20 min-z RTn.
31. Hainbat garbiketa ur ultrapuruarekin (3 x 1 min eta 2 x 10 min).
32. Laginak JEOL JEM-1400 Plus transmisiozko mikroskopio elektronikoan behatu ziren (JEOL Canada).
33. Ehunari argazkiak atera zitzaizkion Gatan SC1000 kamera-digitala erabiliz.

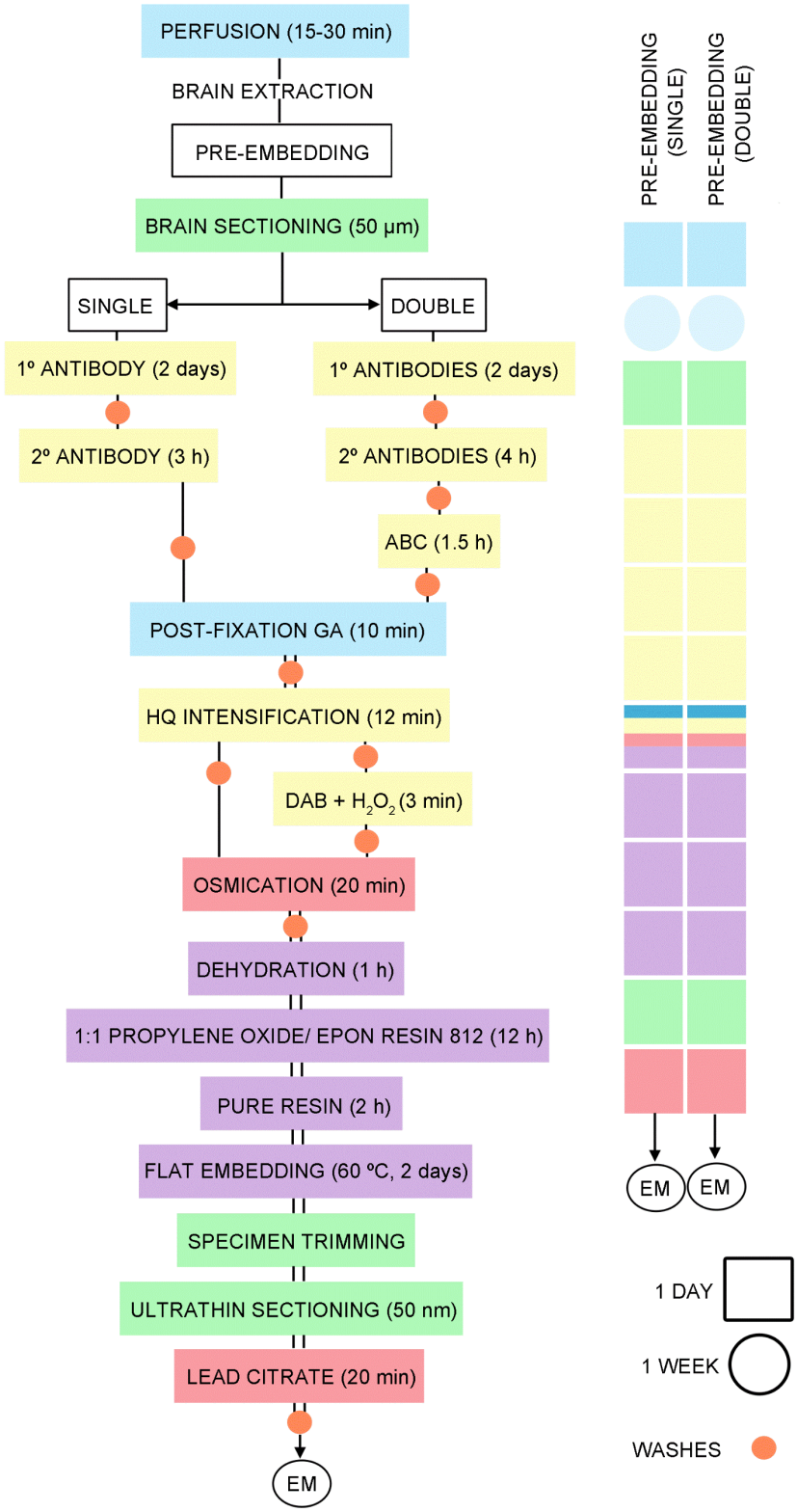

2. irudia. Erretxinan murgildu-aurreko mikroskopia elektronikorako teknikaren urrats orokorren irudikapena (Puente et al., 2019).

Antigorputza	[Kontzentrazioa]	Fabrikatzailea; espeziea; katalogo-zenbakia; RRID
Anti-1-motako kannabinoide-hartzailea (CB_1)	2 µg/ml	Frontier Institute co.; akuria poliklonala; CB1-GP-Af530; AB_2571593
Anti-1-motako kannabinoide-hartzailea (CB_1)	2 µg/ml	Frontier Institute co.; ahuntza poliklonala; CB1-Go-Af450; AB_2571592
Anti-glia proteina harikara azidoa (*glial fibrillary acidic protein,* GFAP)	20 ng/ml	Sigma-Aldrich; sagua monoklonala; G3893; AB_257130
Anti-A522 (Glutamato-aspartato garraiatzailea, *glutamate aspartate transporter*, GLAST)	0,3 µg/ml	Prof. Niels Christian Danbolt, University of Oslo; untxia poliklonala; Ab#314; AB_2314561

1. taula. Mikroskopia elektronikorako erretxinan murgildu-aurreko metodoan erabilitako antigorputz primarioak.

Antigorputza	[Kontzentrazioa]	Fabrikatzailea; espeziea; katalogo-zenbakia; RRID
Anti-sagu biotinilatua	7,5 µg/ml	Vector Labs, zaldia; BA-2000; AB_2313581
Anti-untxi biotinilatua	7,5 µg/ml	Vector Labs, ahuntza; BA-1000; AB_2313606
1,4 nm-tako urre-partikulari atxikitutako anti-akuri IgG (Fab´ fragmentua)	0,8 µg/ml	Nanoprobes, ahuntza; #2055
1,4 nm-tako urre-partikulari atxikitutako anti-sagu IgG (Fab´ fragmentua)	0,8 µg/ml	Nanoprobes, ahuntza; #2002
1,4 nm-tako urre-partikulari atxikitutako anti-untxi IgG (Fab´ fragmentua)	0,8 µg/ml	Nanoprobes, ahuntza; #2004

2. taula. Mikroskopia elektronikorako erretxinan murgildu-aurreko metodoan erabilitako bigarren antigorputzak.

4.3.5. CB_1 hartzailearen markaketaren semi-kuantifikazioa

Aldez aurretik argitaratutako protokoloaren arabera egin zen (Puente et al., 2019). Erretxinan murgildu-aurreko immunourre metodoa ikertutako sagu guztietan aldi berean burutu zen. Are gehiago, animalia bakoitzaren hiru esperimentu-erreplika erabili ziren. Intereseko eremuaren CB_1 hartzailearen markaketa ona eta erreproduzigarria duten eskualdeak aukeratzeko, laginak argi-mikroskopioz behatu ziren, lagin guztietan eremu beraren azterketa ziurtatuz. Gainera, sagu desberdinetatik lortutako lagin immunomarkatuen arteko baldintzak are gehiago estandarizatzeko, laginen azaleko lehen 1,5 μm-ak bakarrik erabiltzen ziren. Laginketa beti egiten da kontu handiz eta modu berean aztertutako animalia guztientzat.

Sinapsi kitzikatzaile eta inhibitzaileak beren ezaugarri ultra-estrukturalengatik identifikatu ziren (Puente et al., 2019):

- Sinapsi kitzikatzaileak asimetrikoak dira, dentsitate postsinaptikoarekineta axoi-bukaera presinaptikoetan besikula sinaptiko argiak, ugariak eta esferikoak dituzte.
- Sinapsi inhibitzaileak simetrikoak dira, mintz postsinaptiko meheekin eta axoi-bukaeratan besikula sinaptiko pleomorfikoak dituzte.

Astrozitoek eta beraien prozesuak GFAP edo GLAST immunomarkaketaz identifikatu ziren. CB_1 immunourre partikulak astroglialtzat hartu ziren GLAST- edo GFAP-positibo ziren mintzetan kokatuta bazeuden.

Gero, lehen deskribatu bezala konpartimentu ezberdinetan identifikatu ziren CB_1 hartzaileen proportzioak taularatu ziren. CB_1 hartzailearen markaketa positibotzat hartu zen, gutxienez immunopartikula bat ikertutako konpartimentu espezifikoaren mintzetik 30 nm-tara egonez gero. CB_1 hartzailea mitokondriari dagokiola kontsideratzeko, metal-partikula beste mintzetatik 80 nm-tara egon behar da gutxienez. CB_1 hartzailearen immunopartikulen banaketa konpartimentu ezberdinetan aztertzeko Image-J softwarea (NIH; RRID:SRC_003070) erabili zen, ondoren, CB_1 partikula/100 μm^2 kalkulatu zen eta software bera erabili zen astrozitoen prozesu guztiak identifikatzeko eta beraien azalera eta perimetroa neurtzeko.

Balio guztiak batezbesteko ± SEM gisa erakutsi ziren, horretarako estatistika-softwarea erabili zen (GraphPad Prism 8, GraphPad Software Inc., San Diego, AEB). Normaltasun-proba (Kolgomorov-Smirnov normaltasun-proba) egin zen estatistika-probak burutu aurretik. Andui mutante bereko saguen arteko desberdintasun posibleen estatistika-azterketa egin zen eta alderik ez zegoenez, talde bereko saguen datuak batu ziren. Datuak analisi parametriko edo ez-parametrikoak erabiliz analizatu ziren.

4.4. ELEKTROFISIOLOGIA

4.4.1. Esperimentazio-animaliak

Esperimentu gehienak 8 astetako eta 14 astetako C57BL/6J saguetan burutu ziren (Janvier Labs, Le Genest-Saint-Isle, France). GFAP-CB_1-WT and GFAP-CB_1-KO saguak ere erabili ziren.

4.4.2. Ehun-xerren prestaketa

Saguak isofluranoarekin (% 2-4) anestesiatu ziren eta burua moztu zitzaien. Garunak berehala atera eta sakarosaz egindako disoluzioan murgildu ziren 4°Ctan: (mM-tan) 87 NaCl, 75 sakarosa, 25 glukosa, 7 $MgCl_2$, 2,5 KCl, 0,5 $CaCl_2$ eta 1,25 NaH_2PO_4. hipokanpoko eta kortex prefrontaleko bibratomoz (Leica Microsistemas S.L.U.) egindako 300 µm lodierako koroa-ebaketak 32-35°Ctan bildu ziren honakoaz osatutako likido zefalorrakideo artifizialean (*artificial cerebrospinal fluid*, aCSF): (mM) 130 NaCl, 11 glukosa, 1,2 MgCl, 2,5 KCl, 2,4 $CaCl_2$, 1,2 NaH_2PO_4 eta 23 $NaHCO_3$, beti 95 % O_2/5 % CO_2-rekin orekatuta.

4.4.3. Zelulaz kanpoko jarduera elektrikoaren erregistroa

Garun-xerrak grabazio-ganberan jarri ziren aCFS berean murgilduta 2 ml/minko fluxuarekin, baita % 95 O_2/% 5 CO_2-rekin orekatuta. Esperimentu guztiak 32-35°Ctan egin ziren eta $GABA_A$ hartzaileak blokeatzeko pikrotoxina (PTX; 100 µM, Tocris Bioscience, UK) gehitu zen . Zelulaz kanpoko jarduera elektrikoaren erregistrorako borosilikatozko beira-kapilarra aCFS-z bete zen.

Hipokanpoko horzdun bihurguneko grabazioetan, estimulazio-elektrodoa (borosilikatozko beira-kapilarrak, Harvard apparatus UK capillaries 30-0062 GC100T-10) MPP geruzan jarri zen eta erregistratzeko beira-kapilarra goroldio-zelula axoien amaiera-eremua (*mossy cell fiber layer*, MCFL) geruzan. Kortex prefrontaleko erregistroetan, estimulazio- eta erregistro-elektrodoak, biak, kortex prelinbikoaren II/III geruzetan jarri ziren.

Neurona-eremu bateko potentzial postsinaptiko kitzikagarrien erantzunak (*field excitatory postsynaptic potential responses*, fEPSPs) eragiteko, 0,1 Hz-tako kontrol-estimulu errepikakorrak aplikatu ziren (Stimulus Isolater ISU 165, Cibertec, Espainia; Master-8 kontrolatua, A.M.P.I. isolamendu-unitate batekin). Axopatch-200B (Axon Instruments/Molecular Devices, Union City, CA, AEB) erabili zen 1-2 kHz-ra iragazitako datuak erregistratzeko, 5 kHz-ra DigiData 1440A interfazean digitalizatuak, PC batean jasoak Clampex 10.0 softwarea erabiliz eta Clampfit 10.0 softwarea baliatuz aztertuak (guztiak Axon Instruments/Molecular Devices-tik lortuak, Union City, CA, AEB) izan ziren. Esperimentu bakoitzaren hasieran sarrera-irteera kurba bat ezarri zen. Kurba hori kontrol estimuluaren intentsitatea aukeratzeko erabili zen, intentsitate ezberdinetan sortzen ziren erantzunak aztertuz, kontrol estimulua erantzunaren intentsitate handienaren % 40 eta % 60 artean egokituz. Sinapsi kitzikatzaileen eKB-menpeko plastikotasuna eragiteko, maiztasun txikiko estimulazio tetanikoko protokoloa (*low frequency stimulation*, LFS; 10 min 10 Hz-tan) aplikatu zen, 10 minututako "oinarrizko-lerro" egonkor bat lortu ostean (Lafourcade et al., 2007; Peñasco et al., 2019).

Estimulazio tetanikoaren ondorengo, fEPSP azaleraren magnitudea honela kalkulatu zen: oinarrizko lerroaren azaleraren (LFS baino 10 minutu lehenago emandako oinarrizko erantzun kitzikagarrien batezbestekoa) eta tetanizazioaren osteko erantzun egonkorren azken 10 minutuen (LFS-a amaitu eta ondorengo 30 minututara erregistratuak) arteko aldaketak, ehunekotan adierazita. Gutxienez 3 sagu erabili ziren esperimentu-baldintza bakoitzerako eta sagu berak erabili ziren hipokanpoko eta PFCeko plastikotasuna aztertzeko. Pultsu-parekatuen (PPR) ratioa kalkulatzeko, binakako 30 estimuluen (50 ms-ko pultsu arteko tartea) fEPSP-en (P2/P1) hasierako eta bukaerako malden batezbestekoa egin zen, non P2, fEPSP2 maldei zegokien (eragindako 2. erantzuna) eta P1, fEPSP1 maldei (eragindako 1. erantzuna).

4.4.4. Datuen analisia

Balio guztiak batezbestekoa $\pm$ SEM gisa ematen dira, *p* balioekin eta lagin-tamainarekin (n). Datu guztien normaltasuna bermatzeko Shapito-Wilk eta Kolmogorov-Smirnov probak erabili ziren. Oro har, egoera ezberdinen arteko

desberdintasun esanguratsuak aztertzeko (oinarrizko-lerroa *versus* botika edo/eta estimulazio-protokoloa eta gero), analisi parametrikoak (Student-en t proba) edo ez parametrikoak (Mann-Whitney proba) erabili ziren. Adierazgarritasun-maila $p < 0,05$ izan zen konparazio guztietarako. Estatistika-proba guztiak GraphPad Prism-ekin egin ziren (GraphPad Prism 8, GraphPad software Inc., AEB).

4.4.5. Botikak

Botika guztiak dimetil sulfoxidoan (DMSO; Sigma-Aldrich) disolbatu ziren, eta amaierako kontzentrazioan gainperfusio-medioari gehitu zitzaizkion (3. taula).

Botika	Deskripzioa	Erabilerako kontzentrazioa	Inkubazio-denbora	hornitzailea
Pikrotoxina (PTX)	$GABA_A$ hartzaileen antagonista	[100 μM]	Neurketa osoan zehar	Tocris BioScience (Bristol, United Kingdom)
AM251	CB_1 hartzailearen antagonista indartsua eta GPR55 agonista	[4 μM]	20 min inkubazio gehigarria neurketa baino lehen	Tocris BioScience (Bristol, United Kingdom)
JZL 184	MAGL inhibitzaile indartsu eta selektiboa	[50 μM]	Ordu bateko inkubazio gehigarria neurketa baino lehen	Tocris BioScience (Bristol, United Kingdom)
THL	DAGLα–ren inhibitzaile indartsua	[10 μM]	20 min inkubazio gehigarria neurketa baino lehen	Tocris BioScience (Bristol, Erresuma Batua)
URB597	FAAH inhibitzaile indartsu eta selektiboa	[2 μM]	20 min inkubazio gehigarria	Tocris BioScience (Bristol,

			neurketa baino lehen	Erresuma Batua)
AMG9810	TRPV1 hartzaileen antagonista	[3 μM]	Neurketa osoan zehar	Tocris BioScience (Bristol, Erresuma Batua)
DL-APV	NMDA hartzaileen antagonista indartsu eta selektiboa; DL-APV-ren forma aktiboa	[50 μM]	Neurketa osoan zehar	Tocris BioScience (Bristol Erresuma Batua)
Latrunculin-A (LAT-A)	G-aktina monomeroen polimerizazioaren inhibitzailea	[0,5 μM]	Neurketa osoan zehar	Tocris BioScience (Bristol, Erresuma Batua)

4.5. AZIDO KAINIKOAREN KONBULTSIO EPILEPTIKOEN EREDUA

Azido kainikoak (KA) eragindako konbultsioak lobulu tenporaleko epilepsia eredu gisa asko erabilitakoak dira (Lévesque and Avoli, 2013).

4.5.1. KAren peritoneo barneko txertaketa

1. eguna. Peritoneo barneko gatz txertaketa (NaCl % 0,9; 10 ml/kg) saguak janari eta ur gabe mantendu ziren 2 orduz hesirik gabeko kaiolan, beste kaiola bat gainean jarrita.

2. eguna. 1. eguna bezala, salbu saguaren habia kendu, hesiaren gainean mantendu eta 2 ordu ostean bueltatu zelako.

3. eguna. KAren peritoneo barneko txertaketa (20 mg/kg; 10 ml/kg). Saguak 1 eta 2 egunetako baldintzekin mantendu ziren baina habia kendu zen eta berri bat jarri zen, guztiek tamaina eta toleste bera zutelarik.

4.5.2. Konbultsioen larritasunaren portaera-puntuazioa

Arratoiei txertatu eta 4 ordutan zehar puntuatu ziren. Krisien larritasuna 30 minuturo ebaluatu zen, Racineren eskala (RS) (1972) eraldatuaren arabera . Racineren eskala EEG-aren aldaketen eta konbultsio motorren arteko erlazioan oinarrituta dago, amigdalaren piztearen ereduan konbultsioak puntuatzeko. Gaur egun, RS oraindik erabiltzen da eta, sarritan, krisi-mota eta epilepsia-eredu askotarako egokitua dago (Clement et al., 2003; Vinogradova eta van Rijn, 2008; Lüttjohann et al., 2009).

Intentsitate ezberdinetako zazpi etapa zehaztu ziren RS egokituan, anestesiatik berreskuratu ostean konbultsioetan animaliek izandako portaera-aldaketetan oinarrituta: “begirada finkoa eta mugiezintasuna” (1. etapa); “isatsaren luzapena eta aurreko gorputz-adarren agitazioa” (2. etapa); “zutiketa eta mugimendu errepikakorrak” (3. etapa); “zutiketa eta erorketa” (4. etapa); eta “zutiketa jarraitua eta erorketa” (5. etapa); “jarrera galketa duten konbultsio toniko-klonikoak, jauziak eta korrika” (6. etapa); “heriotza” (7. etapa). 30 minututako denbora-tarte bakoitzean saguak lortutako puntuazio maximoa hartu zen kontuan analisian. GFAP-CB_1-WT eta GFAP-CB_1-KO saguen arteko ezberdintasunak bi bideko ANOVA testa erabiliz aztertu

ziren. Emaitzak batezbestekoa ± SEM gisa adierazi ziren software estatistiko bat erabiliz (GraphPad Prism, GraphPad Software Inc, San Diego, AEB). $p < 0,05$ ziren balioak konsideratu ziren estatistikoki esanguratsuak.

EMAITZAK

5.1. GFAP ETA GLAST-AREN ARTEKO KONPARAKETA ASTROZITOEN MARKATZAILE GISA MIKROSKOPIA ELEKTRONIKORAKO PRESTAKINETAN

5.1.1. GFAP eta GLASTaren markaketaren kokapena mikroskopia immunoelektrikoan

Astrozitoen barruan GFAP eta GLAST zehazki non adierazten diren aztertzeko, WT saguen ehunak mikroskopia elektronikorako immunourre metodoarekin markatu nituen. Zilarrez biziagotutako urrezko partikulek bi markatzaile astroglialen kokapen zehatza argitzen laguntzen dute. GFAP-metal partikulak zelula-gorputzen zitoplasman eta astrozitoen adarkadura lodi eta nagusietan kokatzen diren bitartean (1a irudia), GLAST markaketa astrozitoen mintz plasmatiko osoan zehar dago banatuta (1b irudia), baita neuronekin, kapilarrekin eta beste glia-zelula batzuekin kontaktu estuan dauden proiekzio txikienetan ere, GFAP-k baino askoz azalera handiagoa estaltzen duelarik.

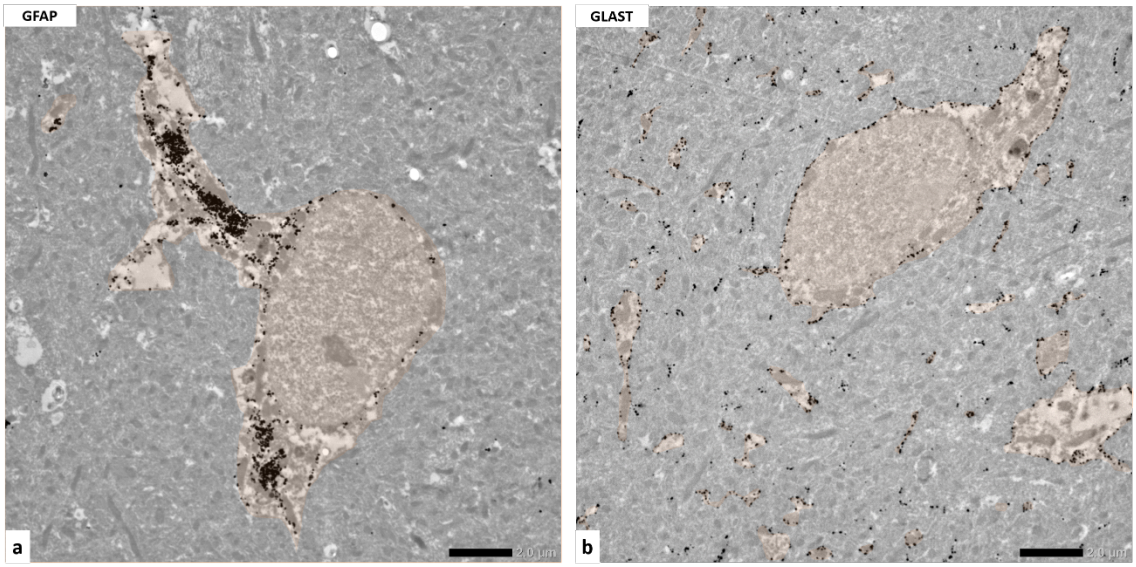

1. irudia. Anti-GFAP (a) edo anti-GLAST (b) antigorputzak erabiliz mikroskopia elektronikorako immunourre metodoaz markaturiko WT saguen hipokanpoko CA1 eremua. a) GFAP markaketaren metal-partikulak astrozitoen soma eta adarkadura nagusien zitoplasman kontzentratzen dira. b) Anti-GLAST antigorputza erabiliz, zilarrez biziagotutako urre partikulak astrozitoen plasma-mintzean kokatzen dira, bai zelula-gorputzean eta adarkadura nagusietan, eta baita proiekzio txiki eta meheetan. Eskala barrak: 2 µm.

5.1.2. Mikroskopia elektronikorako immunoperoxidasa metodoa anti-GFAP eta anti-GLAST antigorputzak erabiliz

Ondoren, GFAP eta GLASTaren aurkako antigorputzak erabili nituen mikroskopia elektronikorako immunoperoxidasa metodoarekin konbinatuta, bi markatzaile

astroglialek detektatutako astrozitoen azalera eta mintz plasmatikoa aztertzeko. Bi proteina hauek astrozitoetan bakarrik daudenez, astrozitoen zitoplasma DAB-z beterik egongo da, astrozitoen azalera eta mintza antzematea ahalbideratuz. Hala ere, GFAP astrozitoen zelula-gorputzean eta adarkadura nagusietan bakarrik adierazten denez, DAB immunosedimentuak ez ziren ikusten beraien proiekzio txikienetan.

WT saguen hipokanpoko CA1 eremuko (4x4) 16 mikrografiaren (8000 x) muntaiak ImageJ softwarearen bidez aztertu ziren. GLAST erabiliz GFAP-rekin baino ia hiru aldiz astrozitoen azalera gehiago ikusten da (GLAST: 8,831 ± 0,6265 μm^2 azalera astrozitikoa/100 μm^2 azalera ± SEM; GFAP: 3,115 ± 0,3388; ****, $p < 0,0001$; 2c irudia). Era berean, GLAST-ak GFAP-ak baino lau aldiz mintz astroglial gehiago hauteman zuen, (GLAST: 96,21 ± 3,430 μm mintz astrogliala/100 μm^2 azalera ± SEM; GFAP: 21,15 ± 1,932; ****, $p < 0,0001$; 2d irudia).

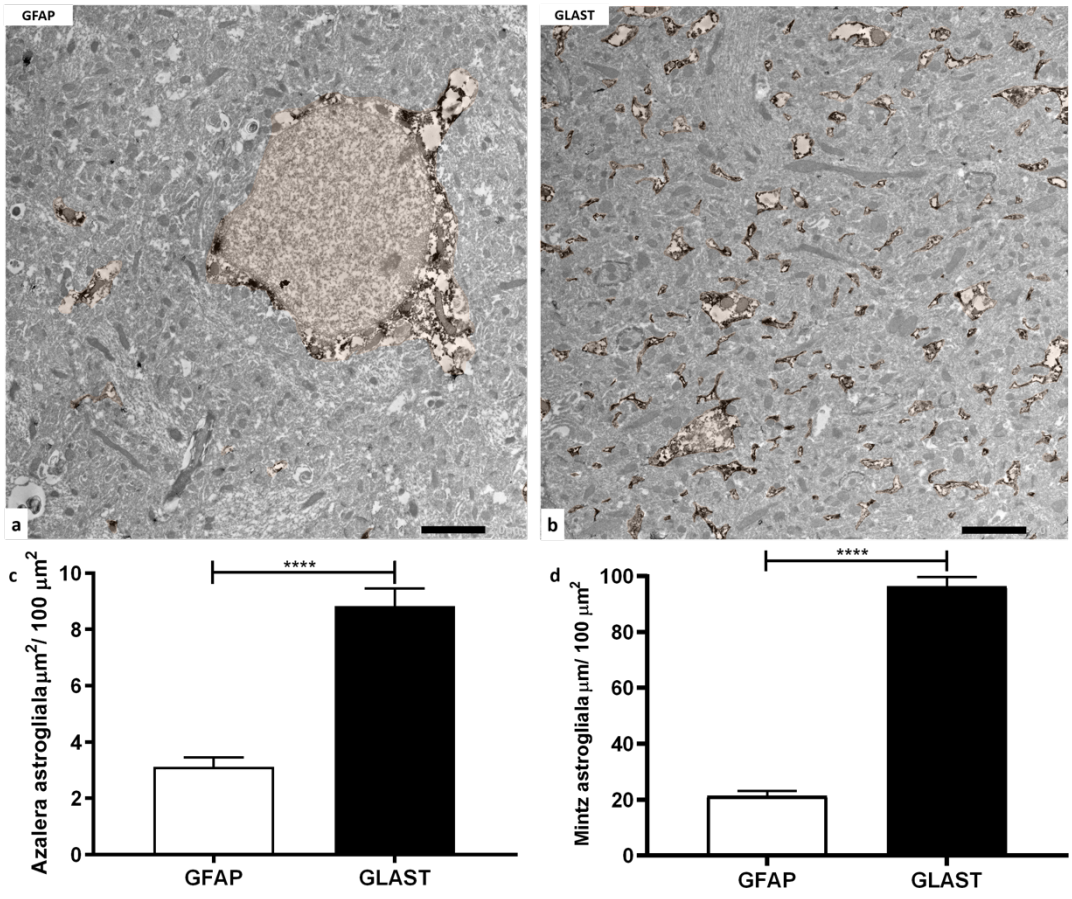

2. irudia. WT saguen hipokanpoko CA1 eremuko mikrografiak GFAP (a) eta GLAST (b) markaketa erakutsiz, mikroskopia elektronikorako immunoperoxidasa metodoarekin Markatzaile bakoitzarekin markatutako astrozitoen analisi estatistikoa (c, d). a) GFAP markaketa zelula-gorputzera eta astrozitoen adarkadura nagusietara mugatuta dago. b) GLAST markaketa astrozitoen adarkadura txikienetan ere agertzen da. c eta d) GFAP edo GLAST

erabiliz markatutako astrozitoen azalera (μm^2) eta mintza (μm) analizatutako 100 μm^2 areako. Datuak proba parametrikoen bidez aztertu ziren (parekatu gabeko t-proba, ****, $p < 0,0001$). Eskala-barra: 2 μm.

5.1.3. Mikroskopia elektronikorako immunourre eta immunoperoxidasa metodo bikoitza astrozitoen CB_1 hartzaileen kokapena aztertzeko

Gure laborategiko aurreko ikerketetan anti-GFAP antigorputzak erabiliz frogatu dugu, CB_1 hartzailearen markaketaren % 5-6 astrozitoen mintzetan dagoela. Hemen GFAP-CB_1 eta GLAST-CB_1 konbinazioak konparatu ditut mikroskopia elektronikorako immunourre eta immunoperoxidasa metodo bikoitza erabiliz. CB_1 hartzaile guztien % 5-6 GFAP-positibo diren astrozitoetan kokatzen dela egiaztatu nuen. Hala ere, CB_1 hartzaileen partikula totalaren % 12 adina GLAST-positibo ziren astrozitoetan kokatzen zela ikusi genuen (GLAST-CB_1: % 11,92 ± 0,6368 CB_1 hartzailea astrozitoen mintzean/zenbatutako CB_1 hartzaile totala ± SEM; GFAP-CB_1: % 4,98 ± 1,102; ****, $p < 0,0001$; 3. irudia).

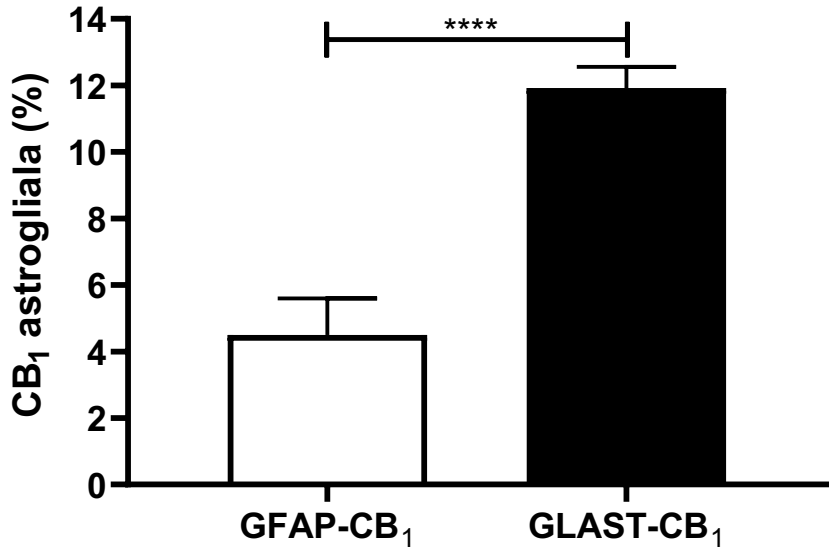

3. irudia. GFAP-CB_1 (% 4,98 ± 1,102) eta GLAST-CB_1 (% 11,92 ± 0,6368) immunomarkaketa bikoitzak mikroskopia elektronikorako erabiliz kalkulatutako CB_1 hartzaile astroglialaren ehunekoa.

5.2. KORTEX PREFRONTALEKO EREMU PRELINBIKOAREN II/III GERUZETAKO CB_1 HARTZAILEAREN BANAKETA GLU-CB_1-WT/KO ETA GABA-CB_1-WT/KO SAGUETAN GLAST-CB_1 IMMUNOMARKAKETAREKIN

Astrozitoetan CB_1 hartzaileak lokalizatzeko GLAST markatzaile hobea dela frogatu ondoren, GLAST-CB_1 markaketa balioztatu nahi izan nuen kortex prefrontaleko II/III geruzetan, non CB_1 hartzailea bertan dagoela jakina den. Analisi horretan zenbait sagu transgeniko erabili ziren: Glu-CB_1-WT, Glu-CB_1-KO, GABA-CB_1-WT, GABA-CB_1-KO eta CB_1-KO (4. irudia). Lehenik, CB_1 hartzaileak sinapsi-bukaera kitzikagarri eta inhibitzaileetan aztertu nituen, baita astrozitoetan ere.

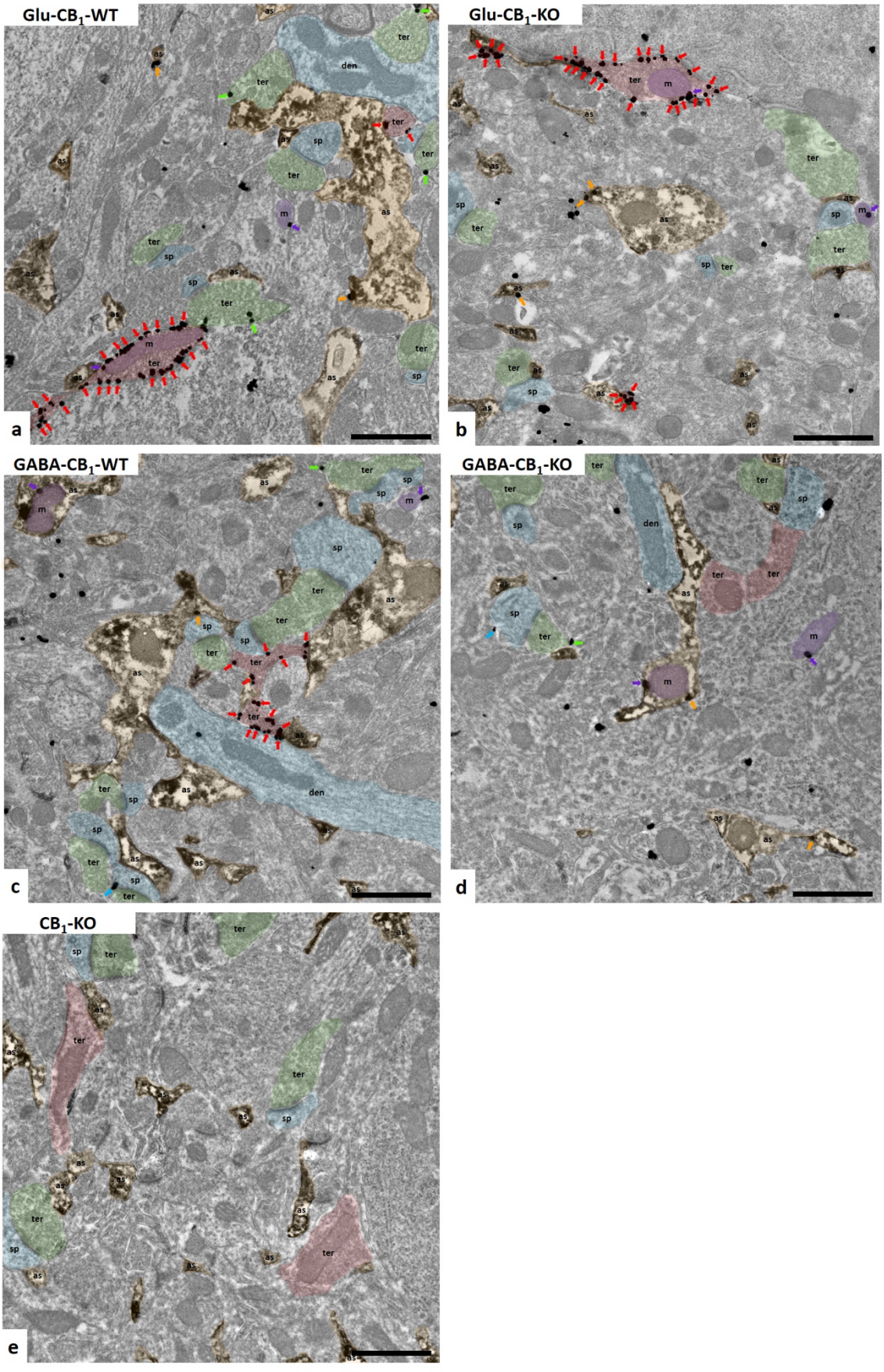
Glu-CB1-WT
Glu-CB1-KO
GABA-CB1-WT
GABA-CB1-KO
CB1-KO
a
b
c
d
e
ter
as
sp
m
den

4. irudia. CB_1 hartzaileak hainbat sagu transgenikoen eta CB_1-KO saguen kortex prelinbikoaren II/III geruzetan. CB_1 hartzailearen markaketa (geziak), GABA-bukaera presinaptikoak (ter, gorria), glutamato-bukaera presinaptikoak (ter, berdea), dendrita (den, urdina), arantza (sp, urdina), mitokondria (m, morea), eta astrozitoak (as, laranja). Eskala barrak: 1 μm.

Lehenago garuneko zenbait eskualdetan dagoeneko deskribatu bezala, CB_1 hartzaileak nagusiki bukaera inhibitzaileetan kokatzen ziren (Glu-CB_1-WT: 38,94 ± 3,923 CB_1 partikula/100 μm^2; Glu-CB_1-KO: 41,51 ± 6,041; GABA-CB_1-WT: 45,80 ± 6,373; GABA-CB_1-KO: 0,7895 ± 0,3337; CB_1-KO: 0,1247 ± 0,1247; 5a irudia). Ezberdintasun esanguratsuak aurkitu ziren GABA-CB_1-KO eta CB_1-KO saguekin alderatuz, sagu hauen bukaera inhibitzaileetan ez baitzen CB_1 hartzailearen markaketarik aurkitu: Glu-CB_1-WT vs GABA-CB_1-KO, **p* = 0,0122; Glu-CB_1-KO vs GABA-CB_1-KO, ***p* = 0,0064; GABA-CB_1-WT vs GABA-CB_1-KO, ***p* = 0,0032; Glu-CB_1-WT vs CB_1-KO, ***p* = 0,0017; Glu-CB_1-KO vs CB_1-KO, ****p* = 0,0008; GABA-CB_1-WT vs CB_1-KO, ****p* = 0,0004.

Espero zitekeen bezala, CB_1 hartzaileen adierazpena askoz txikiagoa zen bukaera kitzikatzaileetan (Glu-CB_1-WT: 3,919 ± 0,3544 CB_1 CB_1 partikula/100 μm^2; Glu-CB_1-KO: 0,1062 ± 0,08389; GABA-CB_1-WT: 4,305 ± 0,2372; GABA-CB_1-KO: 3,365 ± 0,4159; CB_1-KO: 0,3738 ± 0,08728; 5b irudia). Desberdintasun esanguratsuak aurkitu ziren Glu-CB_1-KO eta CB_1-KO saguekin: Glu-CB_1-WT vs Glu-CB_1-KO, ****p* = 0,0004; GABA-CB_1-WT vs Glu-CB_1-KO, *****p* < 0,0001; GABA-CB_1-KO vs Glu-CB_1-KO, ***p* = 0,0051; Glu-CB_1-WT vs CB_1-KO, **p* = 0,0104; GABA-CB_1-WT vs CB_1-KO, ***p* = 0,0015.

CB_1 hartzaileen adierazpena astrozitoen mintzetan, bukaera kitzikatzaileetan baino pixka bat handiagoa zen (Glu-CB_1-WT: 5,036 ± 0,3639 CB_1 partikula/100 μm^2; Glu-CB_1-KO: 4,588 ± 0,3177; GABA-CB_1-WT: 6,028 ± 0,7241; GABA-CB_1-KO: 5,587 ± 1,111; CB_1-KO: 1,124 ± 0,1886; 5c irudia). CB_1-KO saguen astrozitoetan ez zegoen markaketa espezifikorik, ezberdintasun esanguratsuak erakutsiz gainerako sagu transgenikoekin: Glu-CB_1-WT vs CB_1-KO, ***p* = 0,0050; Glu-CB_1-KO vs CB_1-KO, **p* = 0,0289; GABA-CB_1-WT vs CB_1-KO, *****p* < 0,0001; GABA-CB_1-KO vs CB_1-KO, ***p* = 0,0069.

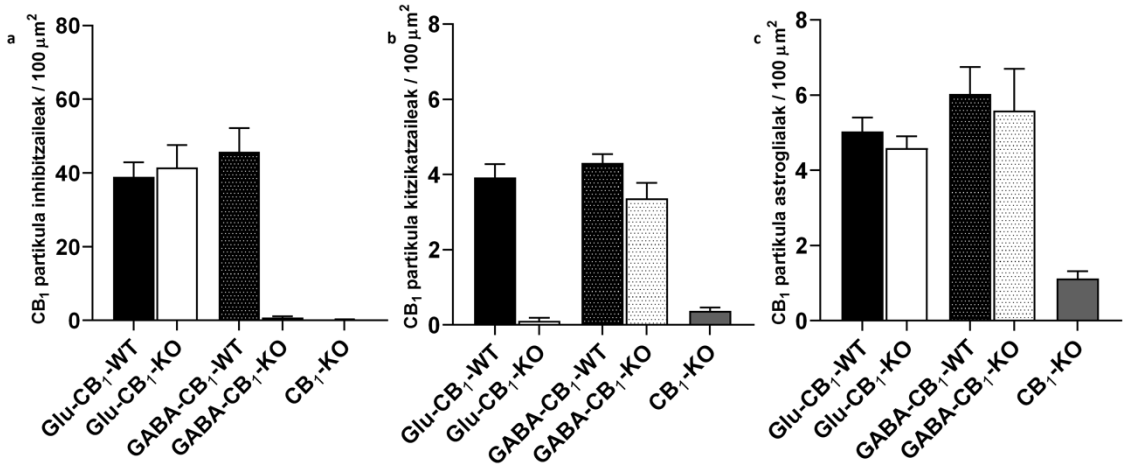

5. irudia. Sagu transgeniko ezberdinen zelula-konpartimentuetako CB_1 hartzailearen banaketaren analisi estatistikoa. a) CB_1 hartzailea bukaera-inhibitzaileetan. b) CB_1 hartzaileak bukaera-kitzikatzaileetan. c) CB_1 hartzaile astroglialak. Kruskal-Wallis proba. Datu guztiak batezbestekoa ± SEM gisa adierazten dira.

5.2.1. CB_1 hartzailearekiko immunopositibo diren bukaera-inhibitzaile eta kitzikatzaileen proportzioak

Hipokanpoko CA1 eremuan deskribatu bezala (Gutiérrez-Rodríguez et al., 2017), kortex prelinbikoko II/III geruzetako bukaera inhibitzaile gehienak CB_1 hartzailearekiko immunopositiboak ziren, GABA-CB_1-KO eta CB_1-KO saguetan izan ezik (Glu-CB_1-WT: % 95,17 ± 2,024; Glu-CB_1-KO: % 95,49 ± 1,946; GABA-CB_1-WT: % 96,71 ± 1,706; GABA-CB_1-KO: % 2,222 ± 2,222; CB_1-KO: % 2,778 ± 2,778; 6a irudia). Desberdintasun esanguratsuak aurkitu ziren GABA-CB_1-KO eta CB_1-KO saguetan besteekin alderatuz: Glu-CB_1-WT vs GABA-CB_1-KO, $^{**}p$ = 0,0022; Glu-CB_1-KO vs GABA-CB_1-KO, $^{**}p$ = 0,0017; GABA-CB_1-WT vs GABA-CB_1-KO, $^{***}p$ = 0,0006; Glu-CB_1-WT vs CB_1-KO, $^{**}p$ = 0,0024; Glu-CB_1-KO vs CB_1-KO, $^{**}p$ = 0,0019; GABA-CB_1-WT vs CB_1-KO, $^{***}p$ = 0,0007.

Beste alde batetik, espero bezela, CB_1 hartzailearekin markatutako bukaera kitzikatzaileen proportzioa baxua zen (Glu-CB_1-WT: % 18,74 ± 1,327; Glu-CB_1-KO: % 1,299 ± 0,6814; GABA-CB_1-WT: % 18,77 ± 1,387; GABA-CB_1-KO: % 17,81 ± 1,290; CB_1-KO: % 1,394 ± 0,6984; 6b irudia). Glu-CB_1-KO eta CB_1-KO saguek ezberdintasun esanguratsuak erakutsi zituzten beste sagu transgenikoekin alderatuz, ez baitzen CB_1 hartzailerik aurkitu beraien bukaera kitzikatzaileen mintzetan: Glu-CB_1-WT vs Glu-CB_1-KO, $^{**}p$ = 0,0014; GABA-CB_1-WT vs Glu-CB_1-KO, $^{**}p$ = 0,0020; GABA-CB_1-KO vs Glu-CB_1-

KO, **p = 0,0036; Glu-CB_1-WT vs CB_1-KO, **p = 0,0018; GABA-CB_1-WT vs CB_1-KO, **p = 0,0025; GABA-CB_1-KO vs CB_1-KO, **p = 0,0044.

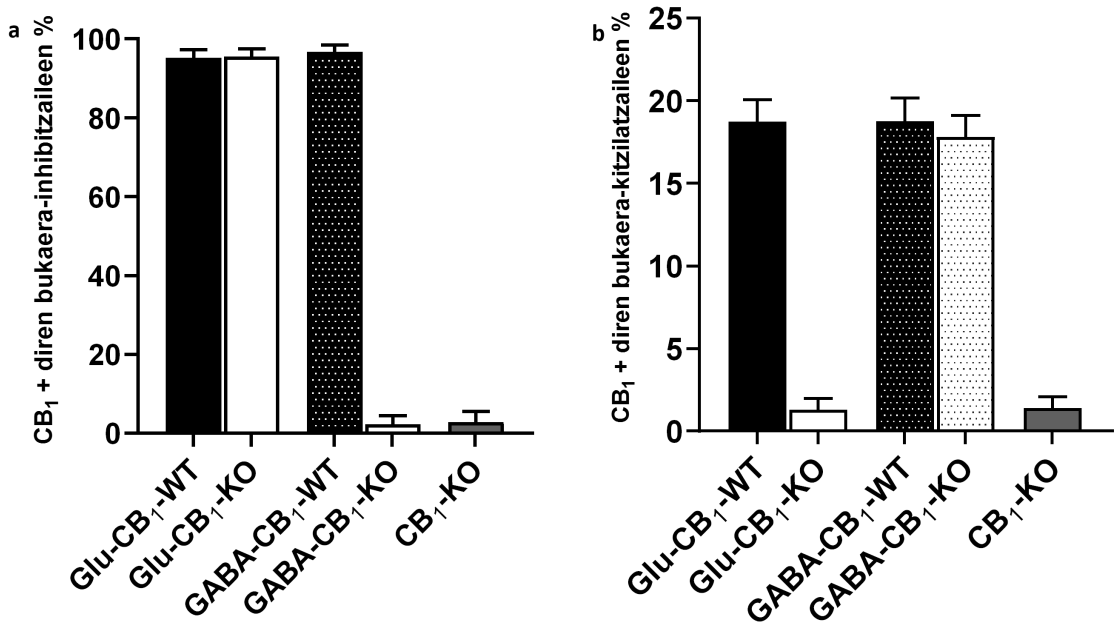

6. irudia. CB_1 hartzailearekiko positibo diren bukaera-inhibitzaile (a) eta kitzikatzaileen (b) ehunekoa. Kruskal-Wallis proba. Datu guztiak batezbestekoa ± SEM gisa adierazten dira.

5.3. ASTROZITOEN ETA NEURONEN MITOKONDRIETAKO CB_1 HARTZAILEEN DENTSITATEA

Mikroskopia elektronikorako immunourre metodoak erakutsi zuenmitokondriei lotutako CB_1 hartzaileak zeudela neuronetan (Bernard et al., 2012; Hebert-Chatelain et al., 2014, 2016; Koch et al., 2015). Are gehiago, gure laborategian ikusi zen hipokanpoko astrozitoen mitkondrien mintzetan ere adierazten zirela CB_1 hartzaileak (Gutiérrez-Rodríguez et al., 2018; Jimenez-Blasco et al., 2020). Hala, mikroskopia elektronikorako GLAST-CB_1 immunomarkaketa erabili nuen neurona eta astrozitoen mitokondrietako CB_1 hartzailearen dentsitatea aztertzeko garuneko zenbait eskualdetan: hipokanpoko CA1 eremua, kortex prefrontala, kortex piriformea eta accumbens nukleoa (7. irudia). Astrozitoetan dauden mitokondrietako CB_1 hartzailearen zenbaki absolutuak neuronetan daudenak baino baxuagoak diren arren, astrozitoen mtCB_1 hartzailearen dentsitatea neuronetan baino handiagoa da analizatutako lau garun-eskualdeetan (8. irudia). Hau da, CB_1 hartzaileak gehiago adierazten dira astrozitoen mitokondrietan, neuronen mitokondrietan baino (Jimenez-Blasco et al., 2020).

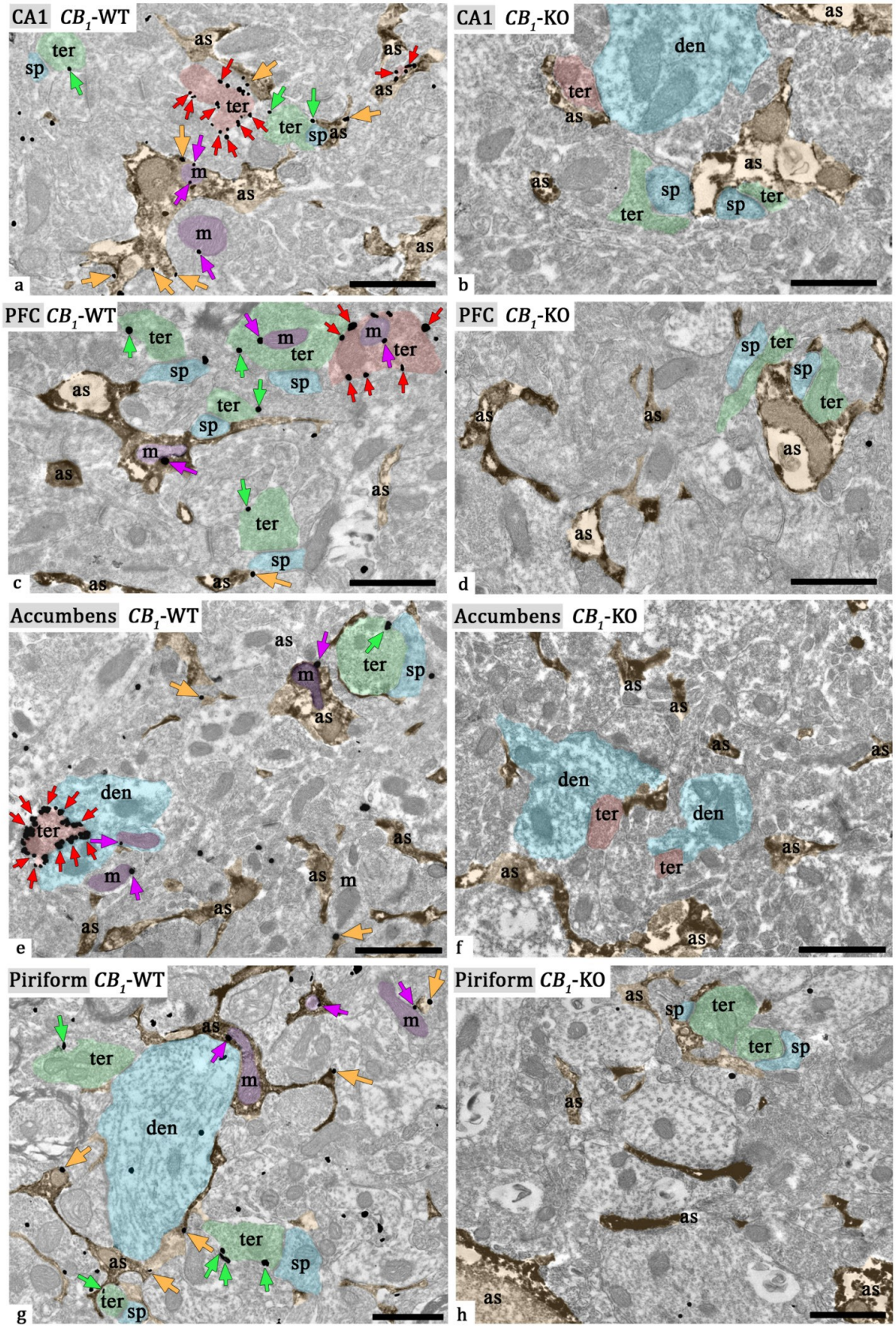

7.irudia. WT eta CB_1-KO saguen hipokanpoko CA1 eremuko, kortex prefrontaleko, accumbens nukleoko eta kortex piriformeko CB_1 hartzailearen banaketa astrozito, neurona eta mitokondrietan. Erretxinan murgildu aurreko immunourre ta immunoperoxidasa metodo bikoitza mikroskopia elektronikorako. Irudi adierazgarriak, immunourre bidez CB_1 hartzailearen detekzioa astrozito (GLAST markaketa bidez identifikatuak) eta neuronen mitokondria-

mintzean, WT eta CB_1-KO saguen hipokanpoan (a, b), kortex prefrontalean (c, d), accumbens nukleoan (e, f) eta kortex piriformean (g, h). CB_1 hartzailearen markaketa (geziak), GABA-bukaera presinaptikoak (ter, gorria), glutamato-bukaera presinaptikoak (ter, berdea), dendrita (den, urdina), arantza (sp, urdina), mitokondria (m, morea), eta astrozitoak (as, laranja). Eskala-barra: 1 μm.

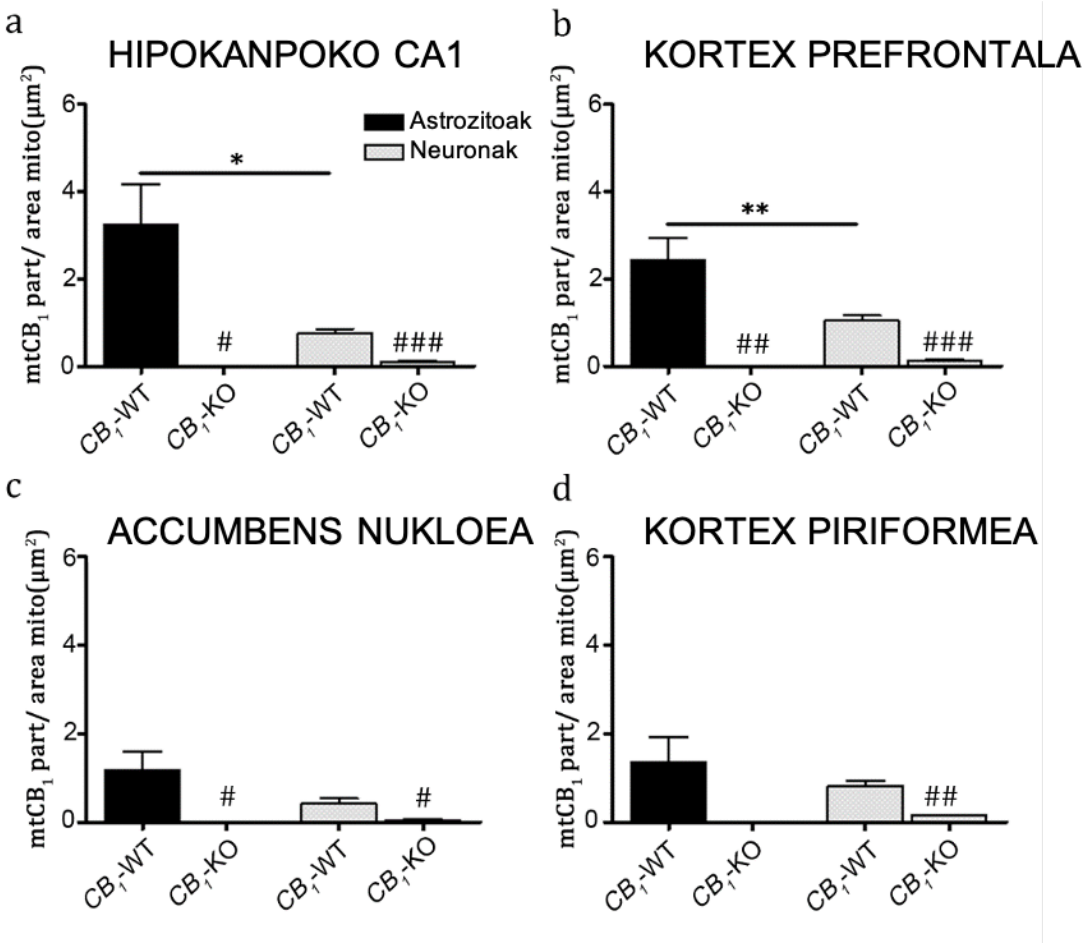

8. irudia. CB_1 hartzailearen dentsitatea astrozitoen eta neuronen mitokondrietan. CB_1 hartzailearen dentsitatea astrozitoen mitokondrietan, CA1 eremuan (3,24 ± 0,94 part/μm²), kortex prefrontalean (2,45 ± 0,49 part/μm²), accumbens nukleoan (1,16 ± 0,44 part/μm²) eta kortex piriformean (1,35 ± 0,57 part/μm²), neuronen mitokondrietako dentsitatea baino handiagoa da, CA1 eremua (0,76 ± 0,09 part/μm²), kortex prefrontala (1,04 ± 0,13 part/μm²), accumbens nukleoa (0,42 ± 0,12 part/μm²) eta kortex piriformea (0,82 ± 0,12 part/μm²). CB_1-KO saguetan oso partikula gutxi ikusi ziren neuronen mitokondriatan, CA1 eremuan (0,09 ± 0,04 part/μm²), kortex prefrontala (0,13 ± 0,02 part/μm²), accumbens nukleoa (0,03 ± 0,03 part/μm²) eta kortex piriformea (0,14 ± 0,02 part/μm²). Datuak batezbestekoa SEM gisa adierazten dira. Datuak proba ez-parametriko edo parametrikoekin analisatu ziren (Mann-Whitney proba edo t proba ez-parekatua. *p < 0,05; **p < 0,01 (WT astrozitoak vs WT neuronak); #p < 0,05; ##p < 0,01; ###p < 0,001 (WT vs CB_1-KO).

5.4. GFAP-CB_1-WT/KO SAGUEN KORTEX PREFRONTALEKO (PRELINBIKOA) II/III GERUZEN AZTERKETA ULTRAESTRUKTURALA ETA FUNTZIONALA

Ondoren, astrozitoetan CB_1 hartzailerik ez zuten 14 asteko saguak (GFAP-CB_1-KO) eta kumaldi bereko mutaziorik gabeko kideak (GFAP-CB_1-WT) erabili ziren (9. irudia). PFC prelinbikoaren II/III geruzetako neurona eta astrozitoen konpartimentu nagusietako CB_1 hartzaileen banaketa aztertu zen, bai eta CB_1 hartzailearentzat positibo diren bukaera-inhibitzaile eta kitzikatzaileen proportzioa ere. Datu guztiak aurreko esperimentuetan erabilitako CB_1-KO saguekin alderatu ziren. Gainera, grabaketa elektrofisiologikoak egin ziren bihurgune horzduneko MPP sinapsietan eta PFCaren eremu prelimbikoan eKB-menpeko sinapsi-plastikotasunen bat ematen den ikertzeko.

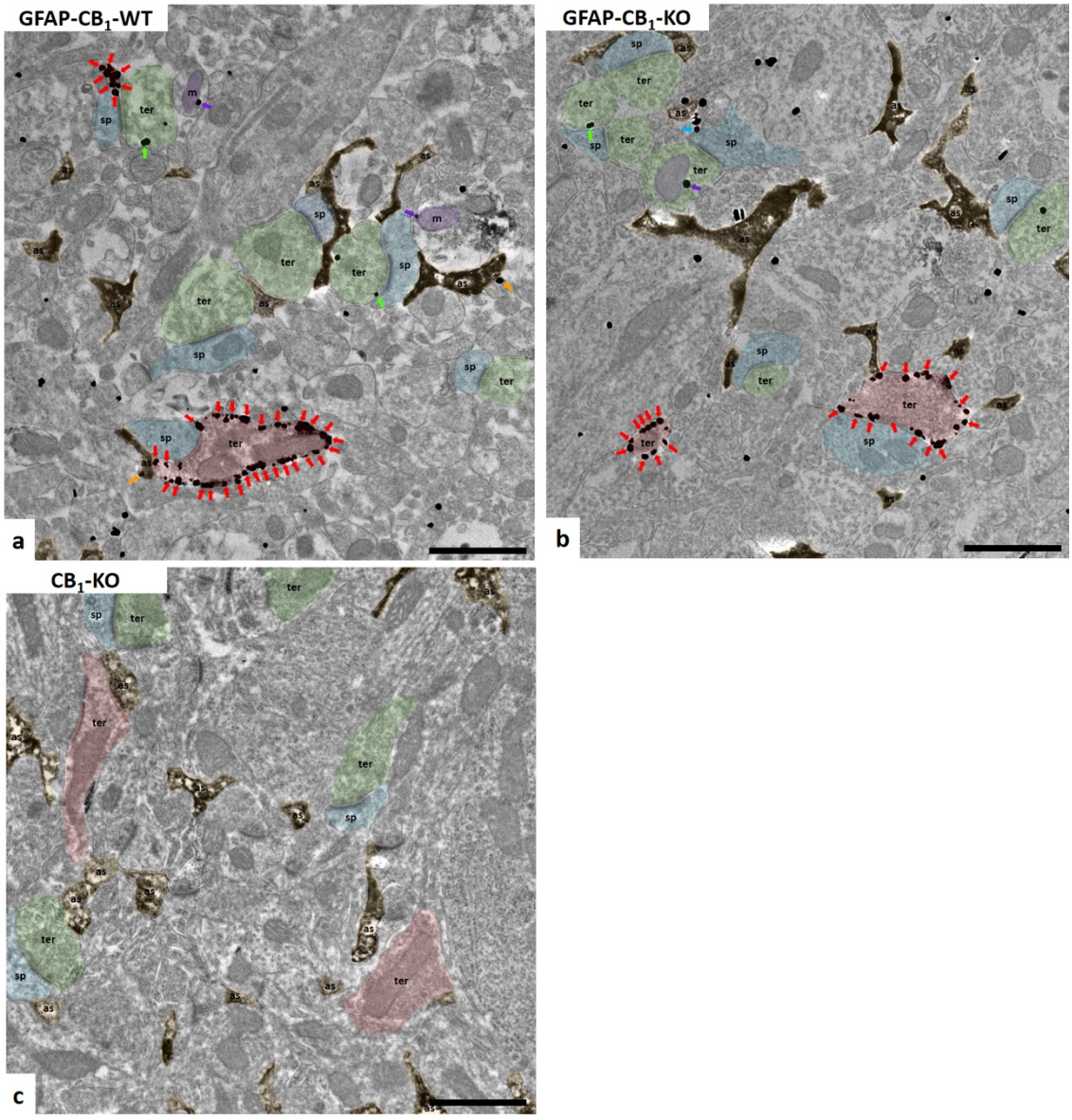

9. irudia. GFAP-CB_1-WT/KO eta CB_1-KO saguen kortex prefrontalare eremu prelinbikoaren II/III geruzetako CB_1 hartzailearen banaketa. CB_1 hartzailearen markaketa (geziak), GABA-bukaera presinaptikoak (ter, gorria), glutamato-bukaera presinaptikoak (ter, berdea), dendrita (den, urdina), arantza (sp, urdina), mitokondria (m, morea), eta astrozitoak (as, laranja). Eskala-barra: 1 μm.

5.4.1. GFAP-CB_1-WT/KO saguen PFC-aren eremu prelinbikoaren II/III geruzetako CB_1 hartzailearen banaketa

Bukaera-inhibitzaileetako CB_1 hartzailearen markaketari dagokionez, lehenago deskribatu bezalako patroi bat ikusi nuen (GFAP-CB_1-WT: 49,78 ± 7,010 CB_1 partikula/100 μm^2; GFAP-CB_1-KO: 46,95 ± 6,888; CB_1-KO: 0,1247 ± 0,1247; 10a irudia). Ezberdintasun esanguratsuak aurkitu ziren CB_1-KO saguekin alderatuz: GFAP-CB_1-WT vs CB_1-KO, ***p = 0,0006; GFAP-CB_1-KO vs CB_1-KO, **p = 0,0010.

GFAP-CB_1-WT eta GFAP-CB_1-KO saguen bukaera-kitzikatzaileek ere markaketa arrunta erakutsi zuten beraien mintzetan (GFAP-CB_1-WT: 4037 ± 0,2994 CB_1 partikula/100 μm^2; GFAP-CB_1-KO: 3,987 ± 0,4053; CB_1-KO: 0,3738 ± 0,08728; 10b irudia). Analisi estatistikoa burutu zen: GFAP-CB_1-WT vs CB_1-KO, ****p < 0,0001; GFAP-CB_1-KO vs CB_1-KO, ****p < 0,0001.

Espero bezala, CB_1 hartzaile astroglialak ez ziren aurkitu GFAP-CB_1-KO saguetan, sagu hauen astrozitoei CB_1 hartzailea falta zaielako, CB_1-KO saguei bezala (GFAP-CB_1-WT, 3,934 ± 0,5558 CB_1 partikula/100 μm^2; GFAP-CB_1-KO: 0,4078 ± 0,1287; CB_1-KO: 1,124 ± 0,1886; 10. irudia c). Ezberdintasun estatistikoak aurkitu ziren: GFAP-CB_1-WT vs GFAP-CB_1-KO, ****p < 0,0001; GFAP-CB_1-WT vs CB_1-KO, ****p < 0,0001.

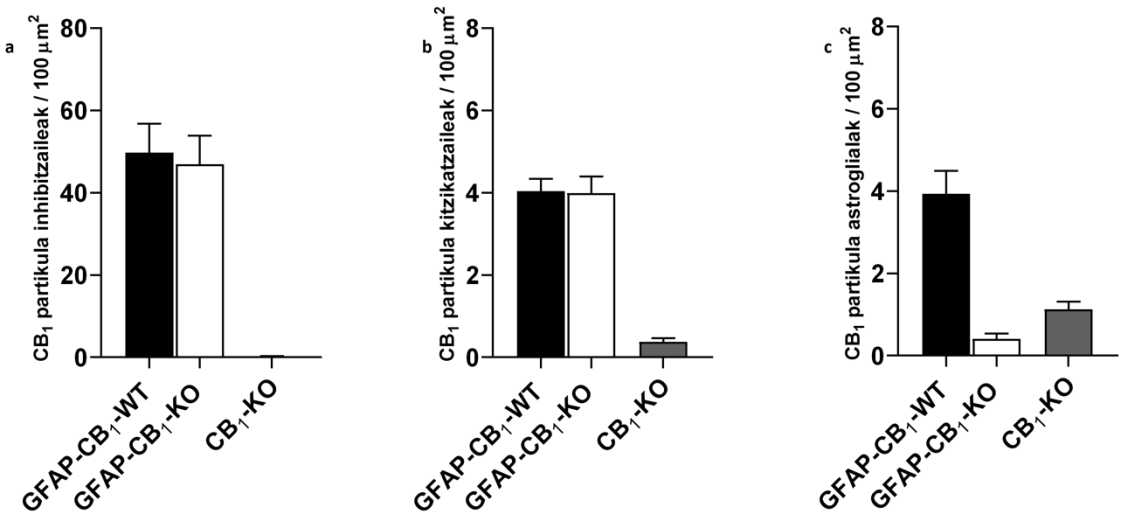

10. irudia. GFAP-CB_1-WT/KO eta CB_1-KO saguen kortex prefrontalaren eremu prelinbikoaren II/III geruzetako konpartimentu nagusietako CB_1 hartzailearen banaketaren analisi estatistikoa. a) CB_1 hartzaileen banaketa bukaera-inhibitzaileetan, b) bukaera-kitzikatzaileetan eta c) astrozitoetan. Kruskal-Wallis edo bide-bakarreko ANOVA proba arrunta. Datu guztiak batezbestekoa ± SEM gisa adierazten dira.

5.4.2. GFAP-CB_1-WT/KO saguen PFC-aren eremu prelinbikoaren II/III geruzetan CB_1 hartzailearekiko immunopositibo diren bukaera-inhibitzaile eta kitzikatzaileen proportzioak

Glu-CB_1-WT/KO eta GABA-CB_1-WT/KO saguetan bezala, GFAP-CB_1-WT/KO saguen bukaera-inhibitzaile gehienek CB_1 hartzailea zuten (GFAP-CB_1-WT: % 93,21 ± 2,523; GFAP-CB_1-KO: % 93,06 ± 2,560; CB_1-KO: % 2,778 ± 2,778; 11a irudia). Desberdintasun esanguratsuak aurkitu ziren CB_1-KO saguarekin alderatuz: GFAP-CB_1-WT vs CB_1-KO, ***p = 0.0006; GFAP-CB_1-KO vs CB_1-KO, ***p = 0.0007.

CB_1 hartzaile immunopositibo diren bukaera-kitzikatzaileen proportzioa ere goian lehenago deskribatu bezalakoa izan zen (GFAP-CB_1-WT: % 18,85 ± 1,197; GFAP-CB_1-KO: % 17,67 ± 1,135; CB_1-KO: % 1,394 ± 0,6984; 11b irudia). Ezberdintasun esanguratsuak aurkitu ziren: GFAP-CB_1-WT vs CB_1-KO, ***p = 0,0003; GFAP-CB_1-KO vs CB_1-KO, **p = 0,0023.

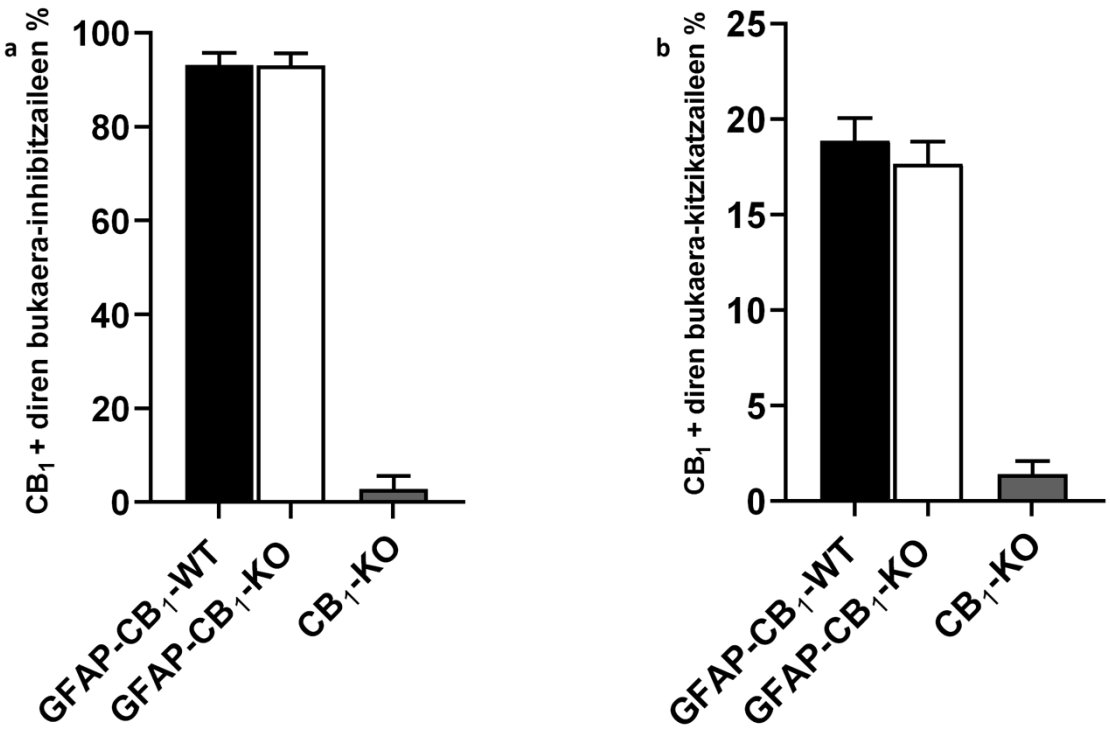

11. irudia. GFAP-CB_1-WT/KO eta CB_1-KO saguetan CB_1 hartzailearekiko immunopositibo diren bukaera-inhibitzaile (a) eta -kitzikatzaileen (b) ehunekoa kortex prefrontalaren eremu prelinbikoaren II/III geruzetan. Kruskal-Wallis proba. Datu guztiak batezbestekoa ± SEM gisa adierazten dira.

5.4.3. GFAP-CB_1-WT/KO saguen bihurgune horzduneko MPP-ko sinapsi kitzikatzaileen sinapsi-plastikotasuna

LFS ondoren bihurgune horzduneko MPPko sinapsietan ematen den sinapsi-plastikotasuna ikertu nahi izan nuen 14 asteko saguetan. Gure laborategiak lehenago deskribatutako eKB-ek gidaturiko LTDan ez bezala, LTP esanguratsu bat aurkitu zen GFAP-CB_1-WT saguetan (% 123 ± 6,688; ***p* = 0,0038) baina ez GFAP-CB_1-KO saguetan (% 108,8 ± 4,742; ns *p*= 0,1041; 12. irudia). Hala ere, ez zen ikusi ezberdintasun esanguratsurik beraien artean, astrozitoen CB_1 hartzaileak GFAP-CB_1-WT saguen sinapsi-plastikotasun horretan ez duela partehartzerik iradokiz (ns *p* = 0,1478; 12b irudia).

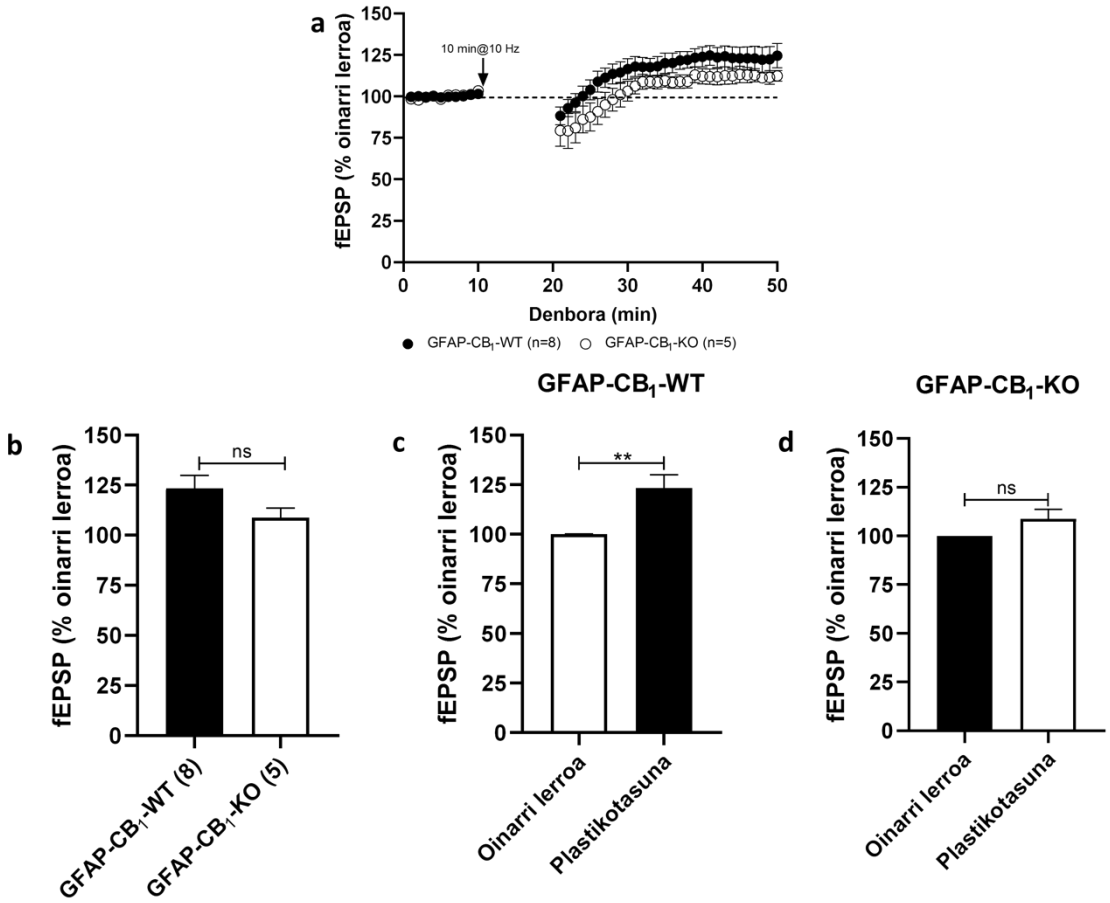

12. irudia. Kitzikapenaren epe-luzeko indartzea (eLTP) 14 aste zituzten GFAP-CB_1-WT saguen MPP-sinapsietan (MPP-LTP). Irudikatzeko, esperimentu bakoitza bere oinarrizko lerrora normalizatu zen. fEPSP-en batezbesteko eremua adierazten da. Gezi beltzak maiztasun baxuko estimulazio-protokoloaren aplikazioa (LFS) adierazten du. a) LFS-ak (10 min, 10 Hz) LTP bat eragiten du GFAP-CB_1-WT saguen MPP-sinapsietan (zirkulu beltzak), baina bakarrik indartze ez-esanguratsu bat adin bereko GFAP-CB_1-KO saguetan (zirkulu zuriak). b) fEPSP-en azken 10 minutuen histograma adierazgarria, LFS ondoren, GFAP-CB_1-WT eta GFAP-CB_1-KO saguen MPP-sinapsietan. t proba ez-parekatua. ns, p=0,1478. c) fEPSP-en azken 10 minutuen histograma adierazgarria, LFS ondoren, GFAP-CB_1-WT saguen MPP-sinapsietan. t proba ez-parekatua. ***p* = 0,0038. d) fEPSP-en azken 10 minutuen histograma adierazgarria, LFS ondoren, GFAP-CB_1-KO saguen MPP-sinapsietan. t proba ez-parekatua. ns *p* = 0,1041. Datu guztiak batezbestekoa ± SEM gisa adierazten dira.

CB_1 hartzaileek GFAP-CB_1-WT MPP-LTP horretan parte hartzen zuten argitzeko, CB_1 hartzailearen AM251 alderantzizko agonista aplikatu zen. Ondorio ezberdinak ikusi ziren: GFAP-CB_1-WT saguen MPP-LTP-a blokeatu zen AM251-rekin ([4 μM]; % 92,64 ± 12,35; **p* = 0,0356). Hala ere, GFAP-CB_1-KO saguen fEPSP-en indartzea ez-esanguratsua ez zen aldatu botikarekin ([4 μM]; % 122,5 ± 5,455; ns, *p* = 0,0931; 13. irudia). Oro har,

emaitza hauek CB_1 hartzailea GFAP-CB_1-WT saguen MPP-LTP-an parte hartzen zegoela frogatu zen.

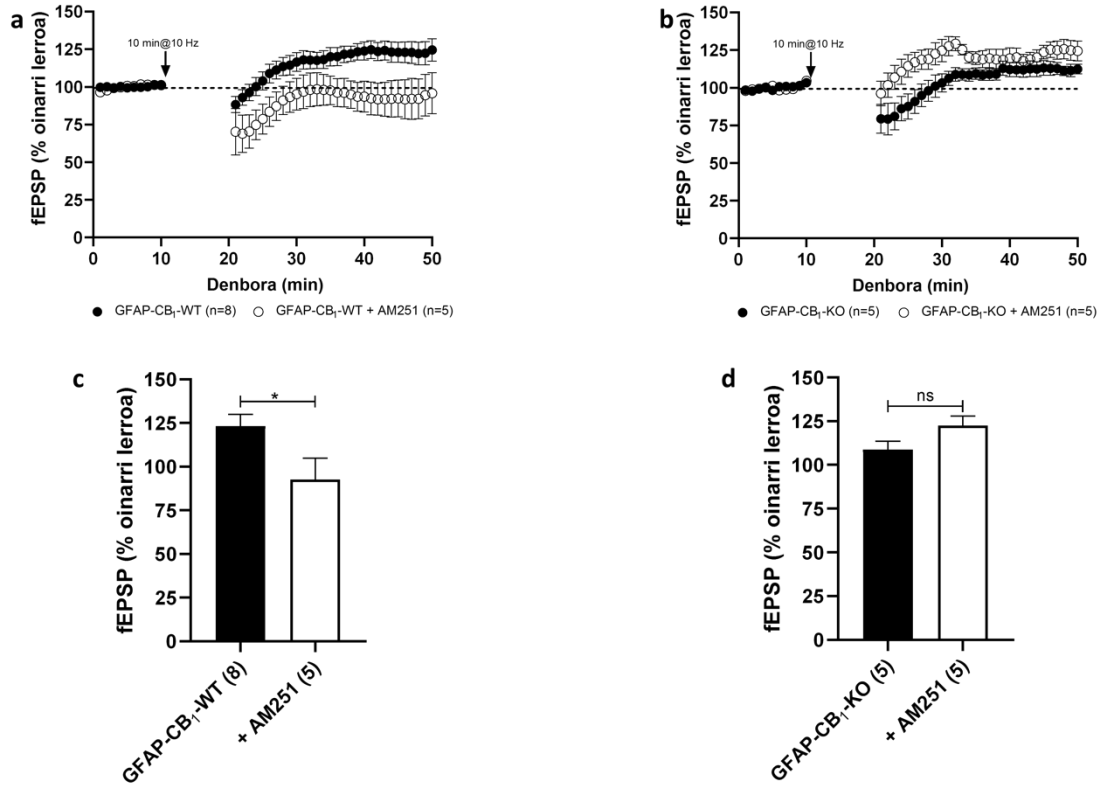

13. irudia. GFAP-CB_1-WT saguen MPP-sinapsietako LTP-a CB_1 hartzailearen menpekoa da. Irudikatzeko, esperimentu bakoitza bere oinarrizko lerrora normalizatu zen. fEPSP-en batezbesteko eremua adierazten da. Gezi beltzak maiztasun baxuko estimulazio-protokoloaren aplikazioa (LFS) adierazten du. a) AM251 [4 μM] botikak ondorio esanguratsua du GFAP-CB_1-WT saguetan LFS ostean ematen den MPP-LTPan (zirkulu zuriak). b) AM251 [4 μM] botikak ez du eragin esanguratsurik GFAP-CB_1-KO saguetan (zirkulu zuriak). c) fEPSP-en azken 10 minutuen histograma adierazgarria, LFS ondoren, GFAP-CB_1-WT saguetan AM251-aren presentzian. t proba ez-parekatua. *p = 0,0356. d) fEPSP-en azken 10 minutuen histograma adierazgarria, LFS ondoren, GFAP-CB_1-KO saguetan AM251-aren presentzian. ns, p = 0,0931. Datu guztiak batezbestekoa ± SEM gisa adierazten dira.

5.4.4. GFAP-CB_1-WT/KO saguen PFC-aren eremu prelinbikoko sinapsi-plastikotasuna

MPP-ko sinapsi-plastikotasuna aztertzeko erabilitako sagu berak erabili ziren GFAP-CB_1-WT/KO saguen PFC-aren eremu prelinbikoko II/III geruzetan LFS osteko fEPSP aldaketak grabatzeko. MPP-an bezala, fEPSP-en indartze esanguratsu ikusi zen 14 asteko GFAP-CB_1-WT saguetan (% 123,6 ± 4,480; ***p = 0,0007), GFAP-CB_1-KO saguetan eraginik ikusi ez zen bitartean (% 99,01 ± 17,29; ns, p > 0,9999; 4. irudia).

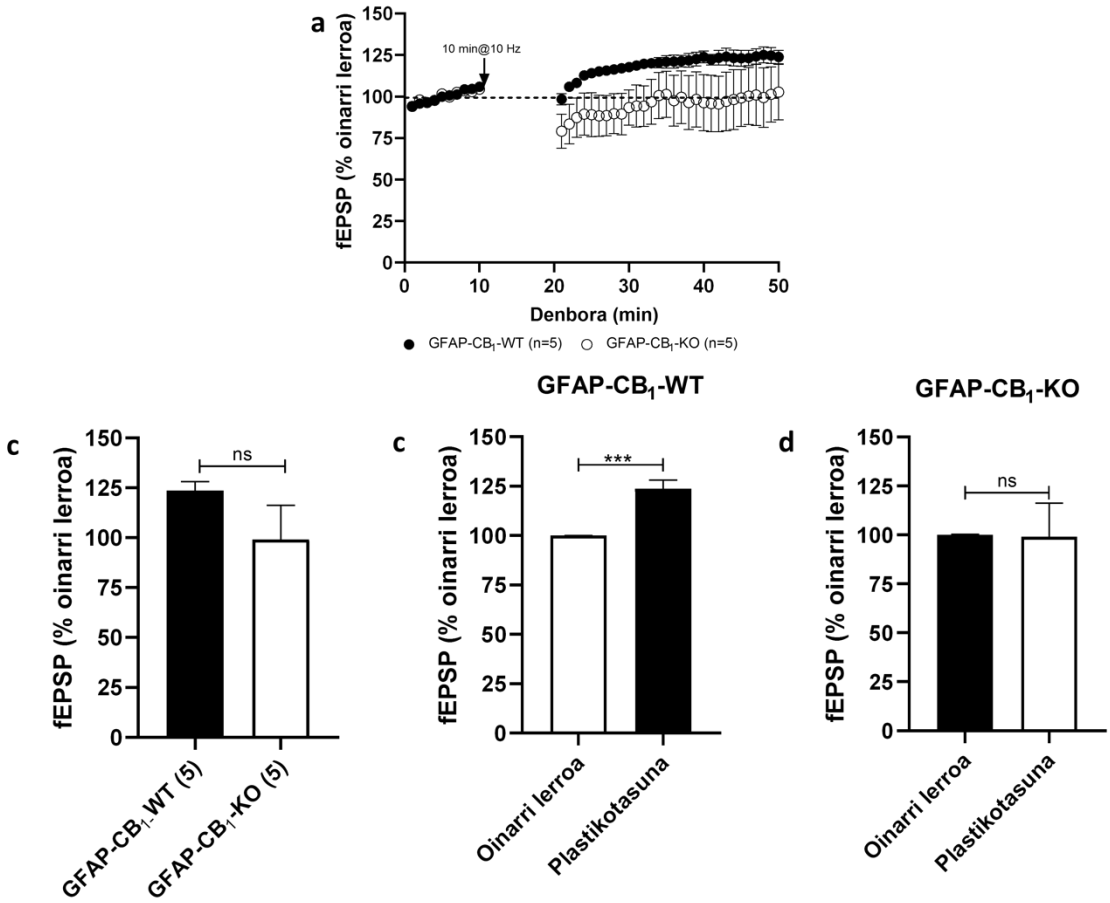

14. irudia. Kitzikapenaren epe-luzeko indartzea (eLTP) 14 aste zituzten GFAP-CB_1-WT saguen PFC prelinbikoko II/III geruzako sinapsietan, baina ez GFAP-CB_1-KO saguetan. Irudikatzeko, esperimentu bakoitza bere oinarrizko lerrora normalizatu zen. fEPSP-en batezbesteko eremua adierazten da. Gezi beltzak maiztasun baxuko estimulazio-protokoloaren aplikazioa (LFS) adierazten du. a) LFSak (10 min, 10 Hz) LTP bat eragiten du GFAP-CB_1-WT saguen PFC prelimbikoko II/III geruzetako sinapsietan (zirkulu beltzak), baina ez du ondoriorik bat bereko GFAP-CB_1-KO saguetan (zirkulu zuriak). b) fEPSP-en azken 10 minutuen histograma adierazgarria, LFS ondoren, GFAP-CB_1-WT eta GFAP-CB_1-KO saguen PFC-sinapsietan. t proba ez-parekatua. ns, p = 0,1679. c) fEPSP-en azken 10 minutuen histograma adierazgarria, LFS ondoren, GFAP-CB_1-WT saguen PFC-sinapsietan. t proba ez-parekatua. ***p = 0,0007. d) fEPSP-en azken 10 minutuen histograma adierazgarria, LFS ondoren, GFAP-CB_1-KO saguen PFC-sinapsietan. Mann-Whitney proba. ns, p > 0.9999. Datu guztiak batezbestekoa ± SEM gisa adierazten dira.

5.4.6. KAk eragindako epilepsiaren ondorioa GFAP-CB_1-WT/KO saguen sinapsi-plastikotasunean

Egoera patologikoetan CB_1 hartzaileen eta astrozitoen garrantzia kontuan izanik, kainatoak eragindako epilepsiak GFAP-CB_1-WT/KO saguen eKB-bidezko sinapsi-plastikotasunean izan zitekeen ondorioak ikertu nahi izan nituen. Kainatoak ez zuen eragin esanguratsurik izan GFAP-CB_1-WT saguen MPP-LTP-an (%102,8 ± 7,928; ns, p =

0,0699) ezta GFAP-CB_1-KO saguetan ikusitako potentziazio txikian (% 100,9 ± 7.,51; ns, p = 0,4440)(15. irudia).

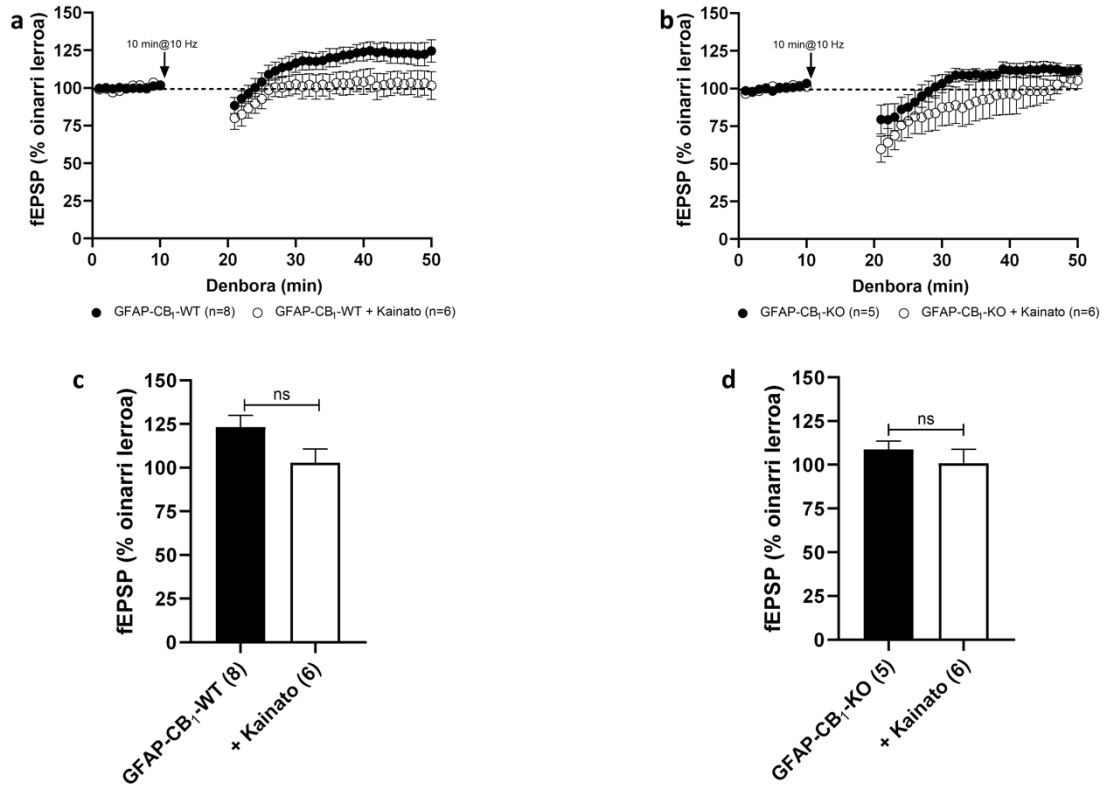

15. irudia. KAk ez du eraginik GFAP-CB_1-WT saguen MPP sinapsietako LTPan. Irudikatzeko, esperimentu bakoitza bere oinarrizko lerrora normalizatu zen. fEPSP-en batezbesteko eremua adierazten da. Gezi beltzak maiztasun baxuko estimulazio-protokoloaren aplikazioa (LFS) adierazten du. Datu guztiak batezbestekoa ± SEM gisa adierazten dira. a) GFAP-CB_1-WT saguen LFS osteko LTPa ez da esanguratsuki blokeatzen KA-eragindako sagu epileptikoetan (zirkulu zuriak). b) Era berean, GFAP-CB_1-KO saguetan ikusitako indartze txikia ere ez da aldatzen KArekin. c) fEPSP-en azken 10 minutuen histograma adierazgarria, LFS ondoren, KArekin tratatu diren GFAP-CB_1-WTsaguetan. t proba ez-parekatua. ns, p = 0,0699. d) fEPSP-en azken 10 minutuen histograma adierazgarria, LFS ondoren, KA txertatu zaien GFAP-CB_1-KO saguen MPPan. t proba ez-parekatua. ns, p = 0,4440. Datu guztiak batezbestekoa ± SEM gisa adierazten dira.

Antzera, kainatoak ez zuen eraginik izan GFAP-CB_1-WT saguen(%118,6 ± 6,613; ns, p = 0,5586) eta GFAP-CB_1-KO saguen (%103,5 ± 4,638, ns, p > 0,9999) PFC prelimbikoko II/II geruzetako sinapsien fEPSP-etan (16. irudia).

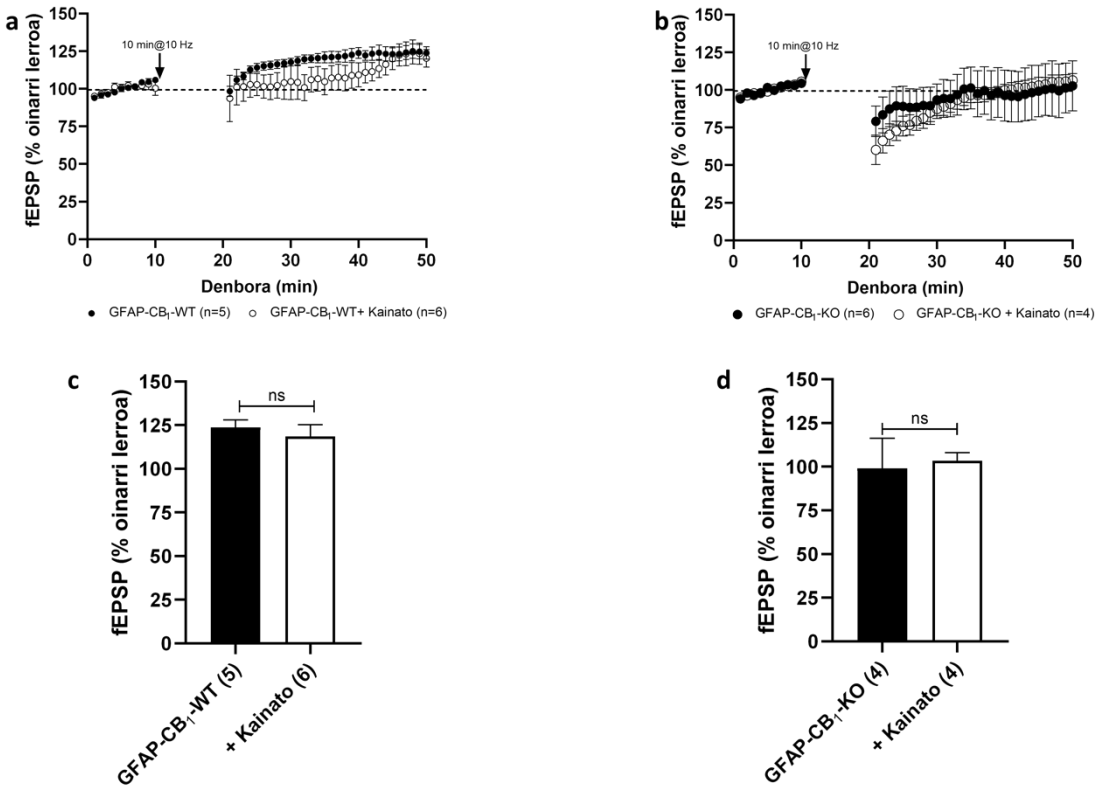

16. irudia. KA tratamenduak ez du eraginik GFAP-CB_1-WT saguen kortex prefrontal prelinbikoko II/III geruzetako LTPan. Irudikatzeko, esperimentu bakoitza bere oinarrizko lerrora normalizatu zen. fEPSP-en batezbesteko eremua adierazten da. Gezi beltzak maiztasun baxuko estimulazio-protokoloaren aplikazioa (LFS) adierazten du. a) GFAP-CB_1-WT saguetan LFS ondoren ematen den PFC-LTPa ez da aldatzen KA tratamenduarekin (zirkulu zuriak). b) Ez zen Karen eraginik ikusi GFAP-CB_1-KO saguetan (zirkulu zuriak). c) fEPSP-en azken 10 minutuen histograma adierazgarria, LFS ondoren, KArekin tratatu diren GFAP-CB_1-WTsaguetan. t proba ez-parekatua. ns, p = 0,5586. d) fEPSP-en azken 10 minutuen histograma adierazgarria, LFS ondoren, KA txertatu zaien GFAP-CB_1-KO saguen PFCan. t proba ez-parekatua. ns, p > 0,9999. Datu guztiak batezbestekoa ± SEM gisa adierazten dira.

5.4. 14 ASTETAKO SAGUEN BIHURGUNE HORZDUNEKO MPP ETA PFC-EKO SINAPSIETAKO SINAPSI-PLASTIKOTASUNA

5.4.1. 14 asteko saguen MPPko sinapsi-plastikotasuna

8 aste zituzten saguetan, LFS-ak (10 min, 10 Hz) ez zuen eraginik izan fEPSP-etan. LFS berdinak 14 asteko saguetan, ordea, LTPa eragin zuen (% 114,1 ± 5,256; **p* = 0,0147; 17a, c. irudiak). MPP-LTP hau AM251rekin, CB_1 hartzailearen agonista, era esanguratsuan deuseztatzen zen ([4 μM]; % 92,78 ± 6.911; **p* = 0,0204; 18a, d. irudiak). Emaitza hauek aditzera ematen dute CB_1 hartzaileak 14 asteko saguen MPP-LTP horretan parte hartzen duela.

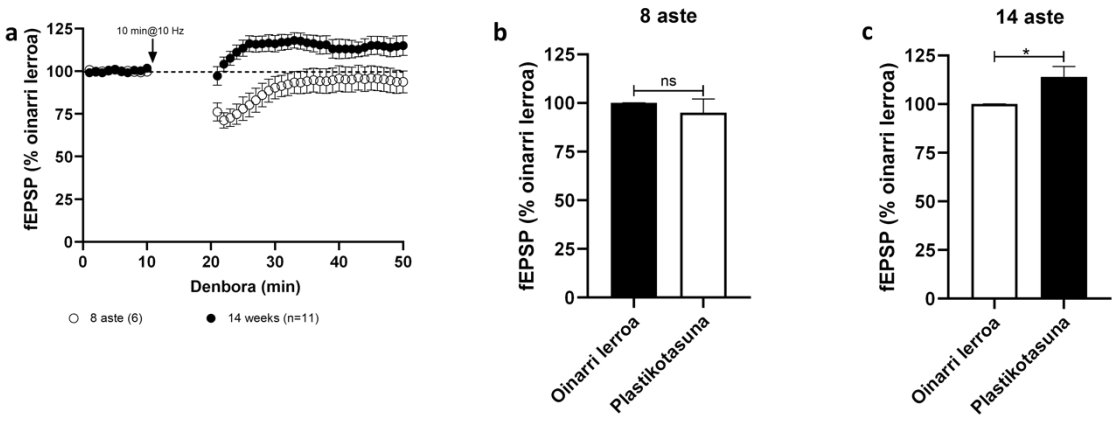

17. irudia. Kitzikapenaren epe-luzeko indartzea (eLTP) 14 aste zituzten WT saguen MPP-sinapsietan. Irudikatzeko, esperimentu bakoitza bere oinarrizko lerrora normalizatu zen. fEPSP-en batezbesteko eremua adierazten da. Gezi beltzak maiztasun baxuko estimulazio-protokoloaren aplikazioa (LFS) adierazten du. a) LFS-ak (10 min, 10 Hz) MPP-LTP bat eragiten du 14 astetako saguetan (zirkulu beltzak), baina ez du eragin esanguratsurik 8 astetako saguetan (zirkulu zuriak). b) fEPSP-en azken 10 minutuen histograma adierazgarria, LFS ondoren, 8 astetako saguen MPP-sinapsietan. t proba ez-parekatua. ns, *p* = 0,4956. c) fEPSP-en azken 10 minutuen histograma adierazgarria, LFS ondoren, 14 astetako saguen MPP-sinapsietan. t proba ez-parekatua. **p* = 0,0147. Datu guztiak batezbestekoa ± SEM gisa adierazten dira.

Bestalde, DL-APV NMDA hartzaileen antagonistak ([50 μM]; % 98,74 ± 7,041; ns, *p* = 0,0693; 18c, f irudiak) eta AMG9810 TRPV1 hartzaileen antagonistak AMG9810 ([3 μM]; % 99,06 ± 6,302; ns, *p* = 0,0815) ez zuten eragin nabarmenik fEPSP-etan (18b, e irudiak).

Aktina filamentuen parte hartzea ere ikertu genuen, izan ere, beraien fosforilazioa LPP-ko sinapsietako CB_1 hartzaileek bideratutako LTP baterako beharrezkoa zela ikusi zen (Wang et al., 2018). Aktina filamentuen fosforilazioaren inhibitzaileak, latrunculina-A-k

(LAT-A), ez zuen izan efekturik 14 aste zituzten saguen MPP-LTP-an ([0,5 mM]; % 111,0 ± 7,163; ns, $p > 0,9999$; 18g, h irudiak)

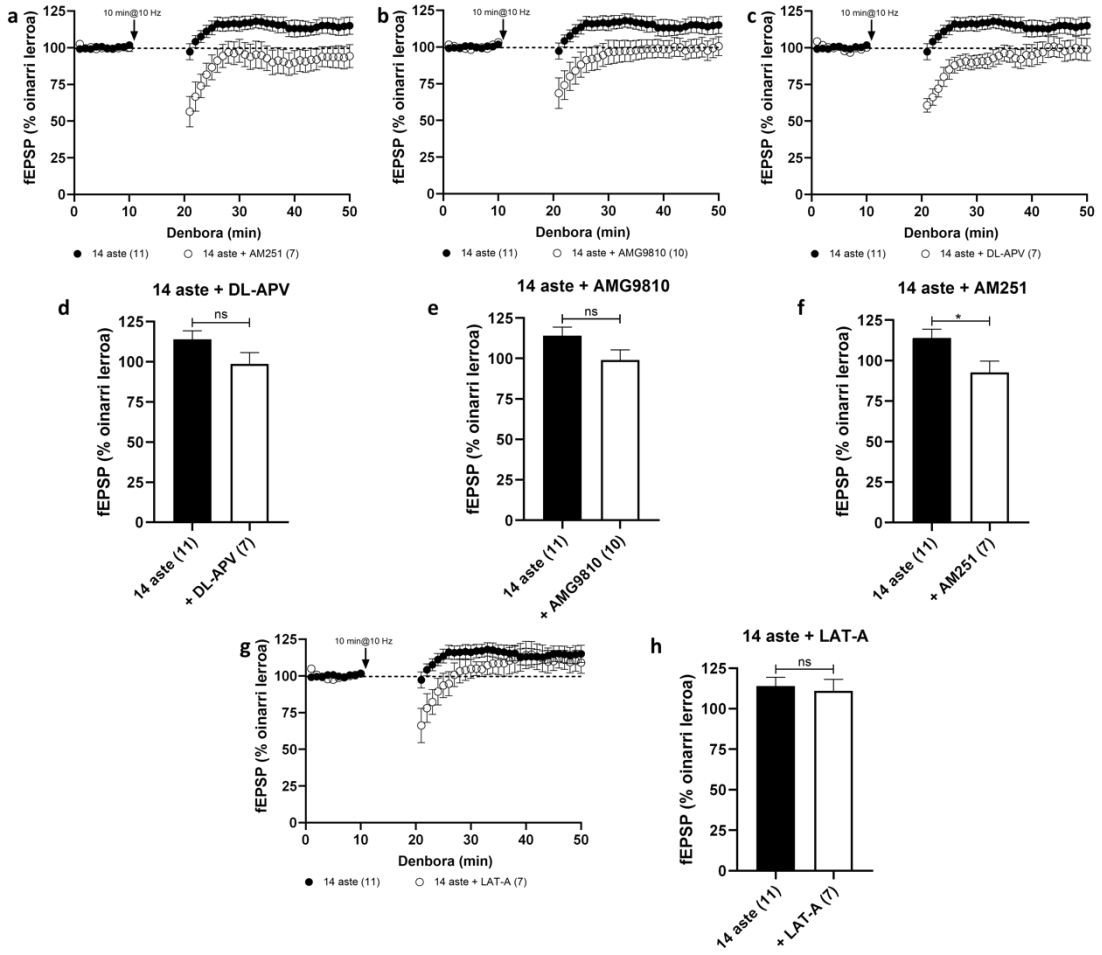

18. irudia. 14 astetako saguen MPP-sinapsietako LTP-a CB_1 hartzailearen menpekoa da, baina badirudi NMDA eta TRPV1 hartzaileek eta aktina filamentuen fosforilazioak ez dutela parte hartzen. Irudikatzeko, esperimentu bakoitza bere oinarrizko lerrora normalizatu zen. fEPSP-en batezbesteko eremua adierazten da. Gezi beltzak maiztasun baxuko estimulazio-protokoloaren aplikazioa (LFS) adierazten du. a) AM251 [4 μM] botikak ondorio esanguratsua du 14 astetako saguetan LFS ostean ematen den MPP-LTPan (zirkulu zuriak). b) AMG9810 [3 μM] (zirkulu zuriak), c) DL-APV [50 μM] botikek ez zuten eragin esanguratsurik fEPSP-etan. d) fEPSP-en azken 10 minutuen histograma adierazgarria, LFS ondoren, 14 astetako saguetan AM251aren presentzian. Mann-Whitney proba. *p = 0,0204. e) fEPSP-en azken 10 minutuen histograma adierazgarria, LFS ondoren, 14 astetako saguetan AMG9810-aren presentzian. t proba ez-parekatua. ns, p = 0,0815. f) fEPSP-en azken 10 minutuen histograma adierazgarria, LFS ondoren, 14 astetako saguetan DL-APV-aren presentzian. Mann-Whitney proba. ns, p = 0,0693. g) LAT-A botikak ez du eraginik 14 astetako saguetan LFS ostean ematen den LTPan (zirkulu zuriak). h) fEPSP-en azken 10 minutuen histograma adierazgarria, LFS ondoren, 14 astetako saguetan LAT-A-aren presentzian. Mann-Whitney proba. ns, $p > 0,9999$. Datu guztiak batezbestekoa ± SEM gisa adierazten dira.

Azkenik, 2-AG edo/eta AEAren parte hartzea aztertu nuen aCSF-an eKB bien sintesi eta degradazioan eragiten duten botika ezberdinak aplikatuz eta aurre inkubatuz. JZL 184 MAGL inhibitzaileak ([50 μM]; % 101,9 ± 3,803; ns, p = 0,0997; 19a, d irudiak), THL DAGα inhibitzaileak ([10 μM]; % 108,3 ± 3,892; ns, p = 0,4623; 19b, e irudiak), eta URB597 FAAH inhibitzaileak ([2 μM]; % 112,5 ± 4,866; ns, p = 0,8257; 19c, f irudiak) ez zuten izan efekturik 14 astetako saguen MPP-LTPan.

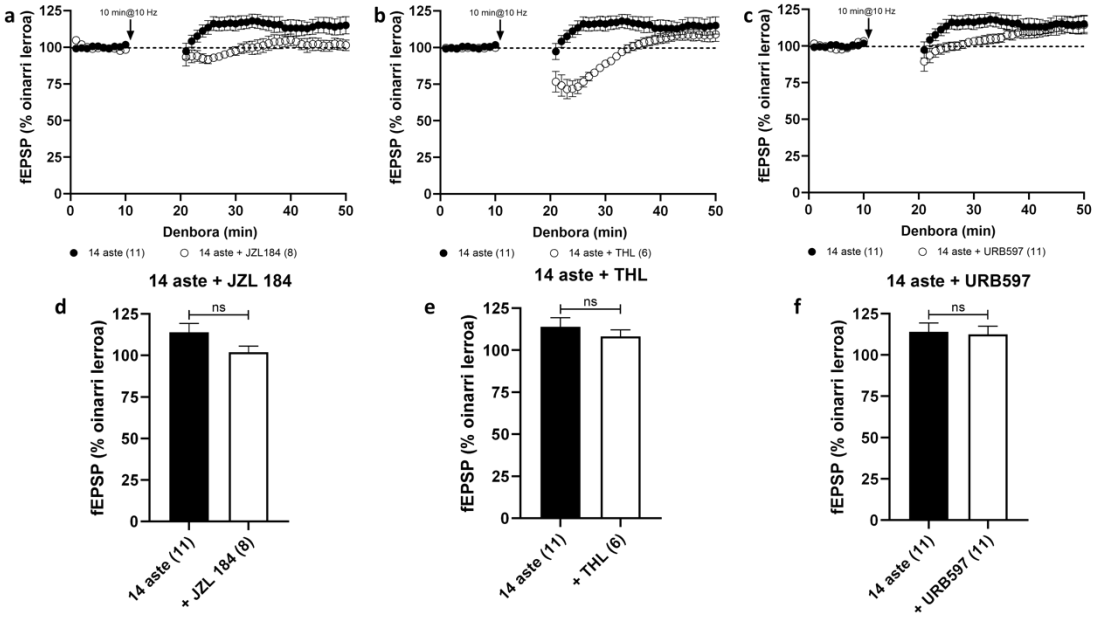

19. irudia. 2-AG eta AEA mailaren aldaketek ez dute eraginik 14 astetako saguen MPP-LTP-an. Irudikatzeko, esperimentu bakoitza bere oinarrizko lerrora normalizatu zen. fEPSP-en batezbesteko eremua adierazten da. Gezi beltzak maiztasun baxuko estimulazio-protokoloaren aplikazioa (LFS) adierazten du. a) JZL 184 [50 μM] botikak ez du ondorio esanguratsurik 14 astetako saguen MPP-LTPan (zirkulu zuriak), ez eta b) THL [10 μM] (zirkulu zuriak) eta c) URB597 [2 μM] (zirkulu zuriak) botikek. d) fEPSP-en azken 10 minutuen histograma adierazgarria, LFS ondoren, 14 astetako saguetan JZL 184aren presentzian. t proba ez-parekatua. ns, p = 0,0997. e) fEPSP-en azken 10 minutuen histograma adierazgarria, LFS ondoren, 14 astetako saguetan THLaren presentzian. Mann-Whitney proba. ns, p = 0,4623. f) fEPSP-en azken 10 minutuen histograma adierazgarria, LFS ondoren, 14 astetako saguetan URB597-aren presentzian. Mann-Whitney proba. ns, p = 0,8257. Datu guztiak batezbestekoa ± SEM gisa adierazten dira.

5.4.2. 14 astetako saguen PFC prelinbikoaren sinapsi-plastikotasuna

Sagu berak erabili ziren PFC-aren eremu prelinbikoko II/III geruzen sinapsi-plastikotasuna aztertzeko. Lehenago, 8 astetako saguetan CB_1 hartzaileak bideratutako LTD bat deskribatu genuen V/VI geruzetan, II/III geruzetan aplikaturiko LFS baten ostean

(Lafourcade et al., 2007). Bitxia bada ere, estimulazio paradigma berak, 14 astetako saguetan LTP kitzikatzaile bat eragiten du II/III geruzetako sinapsi prelimbiko kortikaletan (% 115,5 ± 4,836; ***p = 0,0008; 20a, b irudiak). Gainera, LTP hau ez zen CB_1 hartzailearen AM251 alderantzizko agonistarekin era esanguratsuan blokeatzen ([50 μM]; % 104,3 ± 6,578; ns, p = 0,2350; 20a, c irudiak).

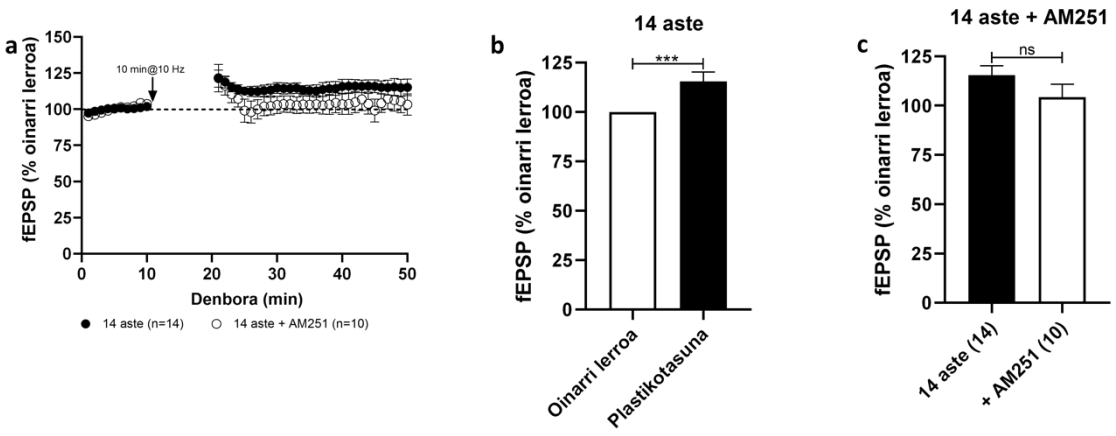

20. irudia. 14 astetako saguen kortex prefrontalaren eremu prelinbikoaren II/III geruzetako sinapsi-kitzikatzaileen LTP-a ez da oztopatzen era esanguratsuan AM251 botikarekin. Irudikatzeko, esperimentu bakoitza bere oinarrizko lerrora normalizatu zen. fEPSP-en batezbesteko eremua adierazten da. Gezi beltzak maiztasun baxuko estimulazio-protokoloaren aplikazioa (LFS) adierazten du. a) LFSak (10 min, 10 Hz) LTP bat eragiten du (zirkulu beltzak), zeina ez den blokeatzen AM251rekin [4 μM] (zirkulu zuriak). b) fEPSP-en azken 10 minutuen histograma adierazgarria, LFS ondoren, 14 astetako saguen PFC-an. Mann-Whitney proba. ***p = 0,0008. c) fEPSP-en azken 10 minutuen histograma adierazgarria, LFS ondoren, 14 astetako saguetan AM251ren presentzian. Mann-Whitney proba. ns, p = 0,2350. Datu guztiak batezbestekoa ± SEM gisa adierazten dira.

DL-APV ([50 μM]; % 106,5 ± 5,346; ns, p = 0,7267; 21a, c irudiak) eta AMG9810 botikek ([3 μM]; % 117,6 ± 4,786; ns, p = 0,5466; 21b, d irudiak) ez zuten aldatu PFC-LTP-a.

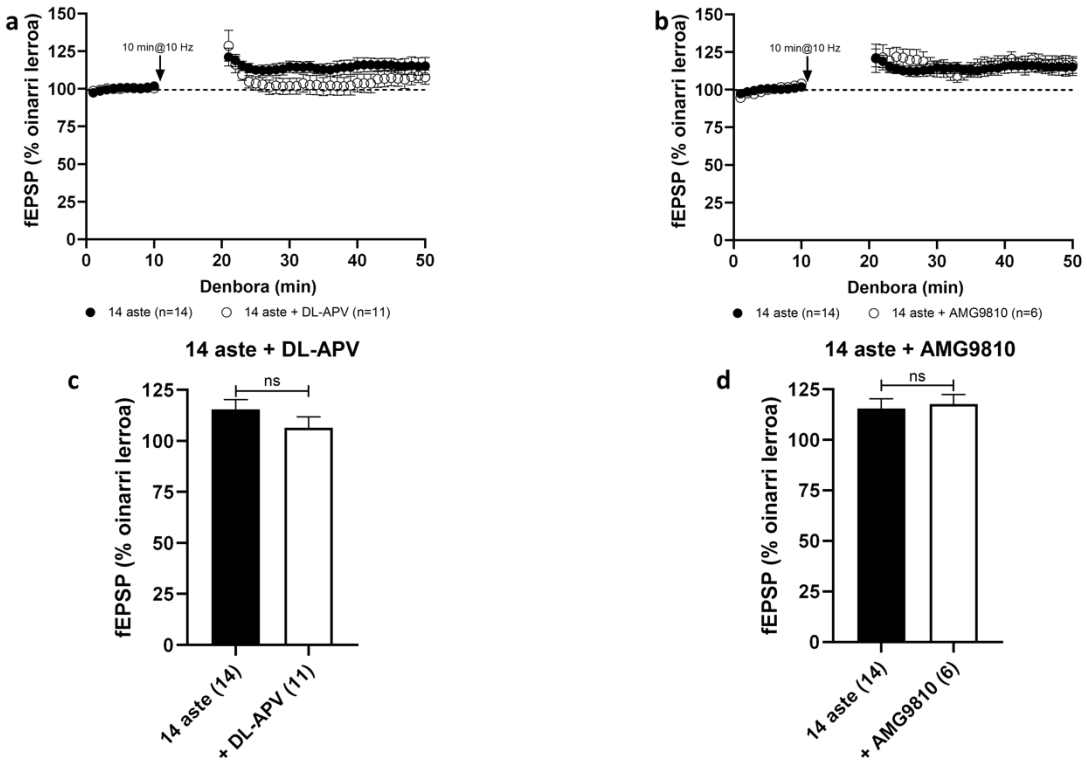

21. irudia. NMDA eta TRPV1 hartzaileek ez dute 14 astetako saguen II/III geruzetako PFC-LTP horretan parte hartzen. Irudikatzeko, esperimentu bakoitza bere oinarrizko lerrora normalizatu zen. fEPSP-en batezbesteko eremua adierazten da. Gezi beltzak maiztasun baxuko estimulazio-protokoloaren aplikazioa (LFS) adierazten du. a) DL-APV [50 μM](zirkulu zuriak) eta b) AMG9810 [3 μM] (zirkulu zuriak) ez dute eragin esanguratsurik LTP-an. c) fEPSP-en azken 10 minutuen histograma adierazgarria, LFS ondoren, 14 astetako saguetan DL-APVaren presentzian. t proba ez-parekatua. ns, p = 0,7267. d) fEPSP-en azken 10 minutuen histograma adierazgarria, LFS ondoren, 14 astetako saguetan AMG9810aren presentzian. Mann-Whitney proba. ns, p = 0,5466. Datu guztiak batezbestekoa ± SEM gisa adierazten dira.

Azkenik, JZL 184 ([50 μM]; % 118,7 ± 7,692; ns, p = 0,9203; 22a, d irudiak), THL ([10 μM]; % 117,5 ± 2,260; ns, p = 0,2667; 22b, e irudiak) eta URB597 ([2 μM]; % 107,9 ± 1,2; ns, p = 0,0913; 22c, f irudiak) botikek ere ez zuten eragin esanguratsurik.

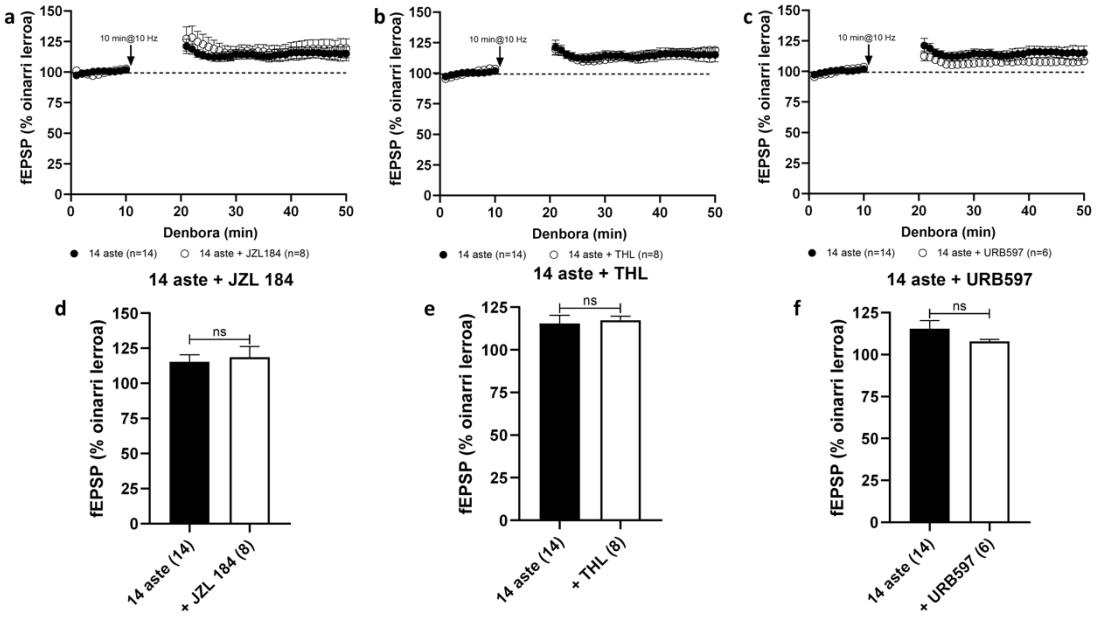

22. irudia. 2-AG eta anandamidaren mailak ez du eraginik 14 astetako saguen PFC-LTPan. Irudikatzeko, esperimentu bakoitza bere oinarrizko lerrora normalizatu zen. fEPSP-en batezbesteko eremua adierazten da. Gezi beltzak maiztasun baxuko estimulazio-protokoloaren aplikazioa (LFS) adierazten du. a) JZL 184 184 [50 μM] (zirkulu zuriak), b) THL [10 μM] (zirkulu zuriak), eta c) URB597 [2 μM] (zirkulu zuriak) botikek ez zuten inhibitzen PFC-LTP-a era esanguratsu batean. d) fEPSP-en azken 10 minutuen histograma adierazgarria, LFS ondoren, 14 astetako saguetan JZL 184aren presentzian. t proba ez-parekatua. ns, p = 0,9203. e) fEPSP-en azken 10 minutuen histograma adierazgarria, LFS ondoren, 14 astetako saguetan THLaren presentzian. Mann-Whitney proba. ns, p = 0,2667. f) fEPSP-en azken 10 minutuen histograma adierazgarria, LFS ondoren, 14 astetako saguetan URB597aren presentzian. Mann-Whitney proba. ns, p = 0,7267. Datu guztiak batezbestekoa ± SEM gisa adierazten dira.

EZTABAIDA

6.1. GFAP ETA GLAST-EN ARTEKO KONPARAZIOA BEREIZMEN HANDIKO MIKROSKOPIA ELEKTRONIKORAKO ASTROZITOEN MARKATZAILE GISA

Azken urteetan frogatu da CB_1 hartzaileen presentzia astrozitoetan (Navarrete eta Araque, 2008, 2010; Stella, 2010; Han et al., 2012; Bosier et al., 2013; Metna-Laurent eta Marsicano, 2015; Viader et al., 2015; Oliveira Da Cruz et al., 2016; Jimenez-Blasco et al., 2020; Bonilla-Del Río et al., 2019, 2021; Egaña-Huguet et al., 2021). CB_1 hartzaileak bideratutako astrozitoen funtzioak, CB_1 hartzaileak sinapsietatik hurbil dauden astrozitoetan duen banaketaren oso mende daude, bai baldintza normal zein patologikoetan (Bonilla-Del Río et al., 2019, 2021). Hala ere, CB_1 hartzaileak konpartimentu astroglialetan duen banaketa subzelularraren irudi osoa osatu gabe dago, astrozitoetan CB_1 hartzaileak duen adierazpena baxua baita (Rodríguez et al., 2001; Bosier et al., 2013; Han et al., 2012; Kovács et al., 2017). Alde horretatik, gure laborategiak kalkulatu zuen hipokanpoko CA1 *stratum radiatum*-ean CB_1 hartzaile guztien % 5-6 inguru astrozitoetan daudela (Gutiérrez-Rodríguez et al., 2018; Bonilla-Del Río et al., 2019, 2021). Antzeko balioak lortu ziren amigdalaren oinalde-alboko nukleoan eta atzeko asoziazio pareta-kortexaren II/III geruzetan (Bonilla-Del Río et al., 2021). Ehuneko horiek mikroskopia elektronikorako immunohistokimika bikoitzarekin lortu ziren, astrozitoak markatzeko anti-GFAP antigorputza erabiliz. Hala ere, GFAP tarteko filamentuetako proteina zitoeskeletikoa da (Hol eta Pekny, 2015), eta batez ere astrozitoen zelula-gorputzera eta haien adar nagusietara mugatzen da (Sullivan et al., 2007). Bestalde, aldez aurretik frogatu dugu CB_1 hartzaileen ~ % 12a astrozitoetan kokatzen dela, gizakiaren GFAP promotorearen kontrolpean gizatiartutako proteina fluoreszente berdea (*humanized renilla green fluorescent protein,* hrGFP) adierazten duen adeno-asoziaturiko birusa intra-hipokanpalki injektatutako saguetan (GFAPhrGFP-CB_1-WT saguak) (Gutiérrez-Rodríguez et al., 2018). Gainera, sagu hauek genetikoki erreskatatutako CB_1 hartzaileak bakarrik astrozitoetan biradierazten zituzten saguak (GFAP-CB_1-RS) baino CB_1 hartzailearekiko immunopositibo ziren astrozito-prozesuen proportzioa ~ %34 gehiago zuten eta %64 partikula dentsitate gehiago zuten (Gutiérrez-Rodríguez et al., 2018). hrGFP normalean GFAP iristen ez den astrozito-prozesu txikienetara heda daitekeen proteina denez (Nolte et al., 2001), emaitza hauek adierazten dute astrozitoetako CB_1 hartzaileen adierazpena handiagoa dela aurretiaz

GFAP-positibo ziren prozesuetan erakutsitakoa baino (Bosier et al., 2013; Han et al., 2012).

Arrazoibide horri jarraituz, bereizmen handiko mikroskopia immunoelektronikoa erabiliz nire tesian egiaztatu dut , GFAP astrozitoen zelula-gorputz eta adarkadura nagusietara mugatzen dela, eta astrozito-prozesu txikienak eta finenak, berriz, GFAP-DAB immunosedimentuetatik libre daudela.

GLAST (EEAT1) hainbat arrazoirengatik ere erabiltzen da astrozitoen markatzaile gisa: 1) arantza dendritiko gehienak astrozitoekin kontaktuan daude, nahiz eta CA1eko *stratum radiatum*-ean hauen zati bat bakarrik dagoen gliaz estalita; 2) arratoi helduen hipokanpoko CA1-eko *stratum radiatum*-ean μm^3-ko 3.200 garraiatzaile daudela kalkulatzen da (Lehre eta Danbolt, 1998); 3) astrozitoen azalera totala 1,4 m^2/cm^3 dela uste denez, GLAST molekulen batezbesteko dentsitatea astrozitoen mintzean ~ 2,300 μm^2-koa da (Lehre eta Danbolt, 1998); 4) GLAST markaketa astrozitoen plasma-mintzean kokatzen da, azalera osoan zehar (Chaudhry et al., 1995; baita tesi honetan ere). Beraz, nire ikerketan, GLAST-immunoperoxidasa markaketak GFAP erabiliz baino ~ hiru aldiz astrozito-azalera eta lau aldiz astrozito-mintza gehiago detektatzen ditu. Ondoren, GLAST-immunoperoxidasa markaketa mikroskopio elektronikorako CB_1 hartzailearen immunourre markaketarekin konbinatu nuen astrozitoetako CB_1 hartzailearen ehunekoa aztertzeko. Baldintza hauetan antzemandako CB_1 hartzaileak (~ 12%) GFAP markaketarekin hipokanpoko CA1ean antzemandakoaren bikoitza dira (Gutiérrez-Rodríguez et al., 2018; Bonilla-Del Río et al., 2019, 2021). Gainera, GLAST bidez baina ez GFAP bidez markatutako astrozitoen prozesu meheak sinapsiekin estuki loturikoak dira (Cholet et al., 2002), non hartzaile gehienak biltzen diren. Are gehiago, arantza dendritikoen eta astrozitoen morfologian ematen diren aldaketa dinamiko orokorrak (Wenzel et al., 1991; Fischer et al., 1998) glutamato-hartzaile eta -garraiatzaileen dentsitatean eragiten dute (Gegelashvilli et al., 1997; Rao eta Craig, 1997). Hala ere, etanolaren kontsumoa bezalako baldintza anormalek ere hartzaileen adierazpena eraldatzen dute. Zentsu horretan, duela gutxi egindako ikerketa batean ikusi dugu 4 astetan zehar botiloia jasan duten sagu ar nerabeek, helduaroan ~ % 40ko murrizten zaizkie CB_1-positibo diren astrozitoen prozesuak, eta % 30eko murrizketa dute CA1eko *stratum radiatum*-eko astrozitoetako CB_1 hartzailearen dentsitatean (Bonilla-

Del Río et al., 2019). Gainera, astrozitoetako CB_1 hartzaileen kopuruaren ehunekoa askoz baxuagoa zen etanola hartu ondoren (Bonilla-Del Río et al., 2019). CB_1 hartzailearen adierazpenean ikusten ziren aldaketa horiek GFAPren haustura zekarren hantura astroglial batekin lotu ziren (Renau-Piqueras et al., 1989; Adermark eta Bowers, 2016). Interesgarria da etanola hartu ondoren GLAST gainadierazten dela (Rimondini et al., 2002), zeinak teorikoki glutamatoaren garbiketan laguntzen duen. Hala eta guztiz ere, GLAST ez duten baina CB_1 hartzaile normalak bai dituzten saguek etanol gutxiago kontsumitzen dute, motibazio eta sari gutxiago erakutsiz (Karlsson et al., 2012).

Guzti honek batera aditzera ematen duena da, GLAST GFAP baino markatzaile hobea dela astrozitoak ikustarazteko mikroskopio elektronikoan. Are gehiago, astrozitoen azalera eta mintza gehiago markatzen direnez, astrozito-prozesuetan kokatzen diren CB_1 hartzaile gehiago ere antzeman daitezke.

6.2. CB_1 HARTZAILEAK ASTROZITOEN ETA NEURONEN MITOKONDRIATAN

Berriki egindako ikerketek frogatu dute garuneko CB_1 hartzaileen proportzio txiki baina esanguratsu bat funtzionalki mitokondrien mintzera lotuta daudela, non kannabinoideen ondorioak bideratzen dituzten, zelulen mitokondrien aktibitatean, jokabidean elikagaiak irenstean eta memoriaren finkatzean (Koch et al., 2015, Hebert-Chatelain et al., 2016). Lehenago erakutsi dugu CB_1 hartzaileak hipokanpoko neuronen zein astrozitoen mitokondria-mintzetan adierazten direla (Bénard et al., 2012; Hebert-Chatelain et al., 2014, 2016; Melser et al., 2017; Gutiérrez-Rodríguez et al., 2018; Bonilla-del Río et al., 2019, 2021; Egaña-Huguet et al., 2021).Era berean, CB_1 hartzaileak muskuluko mitokondriatan ere adierazten dira (Mendizabal-Zubiaga et al., 2016). Hala ere, zalantzak agertu ziren garuneko beste eskualdeetako mitokondriek ere CB_1 hartzaileak adierazten ote zituzten, ez bait dago ikerketarik hori jakiteko. Hala, nire doktorego-tesian hori ikertzeko xedea izan nuen kortex prefrontalean, accumbens nukleoan eta kortex piriformean, eta garuneko eskualde horietan CB_1 hartzaileak duen banaketa hipokanpoko CA1 eremuko banaketarekin alderatzeko. Astrozitoen markatzaile ona dela erakutsi denez (ikusi aurreko atala) GLAST markaketa erabili nuen mikroskopio elektronikoan CB_1 hartzailearen immunolokalizazioarekin konbinatuz. Emaitzek erakutsi zutenez, mitokondrietako CB_1 hartzaileak, gure laborategiak arinago deskribatu zuen bezala hipokanpoko neuronetan, hor egoteaz gain (Bénard et al., 2012; Hebert-Chatelain et al., 2014, 2016; Melser et al., 2017; Gutiérrez-Rodríguez et al., 2018, 2019; Bonilla-del Río et al., 2019, 2021; Egaña-Huguet et al., 2021), kortex prefrontaleko, accumbens nukleoko eta kortex piriformeko astrozitoen mitokondrietan ere daude (Jimenez-Blasco et al., 2020).

Baldintza normaletan, CB_1 hartzaileen adierazpena oso handia da bukaera inhibitzaileetan (Katona eta Freund, 2012; Lu eta Mackie, 2016; Gutiérrez-Rodríguez et al., 2017), baxua bukaera kitzikatzaileetan (Katona et al., 2006; Monory et al., 2006; Gutiérrez-Rodríguez et al., 2017) eta are baxuagoa astrozitoetan (Gutiérrez-Rodríguez et al., 2018). Aurretik egindako ikerketetan neurtu genuen CB_1 hartzailearen markaketaren % 56 GABA-bukaeratan dagoela, % 12 glutamato-bukaeratan, % 6 astrozitoetan eta % 15 mitokondriatan (Gutiérrez-Rodríguez et al., 2018; Bonilla-Del Río et al., 2019). Nabarmentzekoa da partikulen % 11 beste leku batzuetan aurkitu zela

(Gutiérrez-Rodríguez et al., 2018; Bonilla-Del Río et al., 2019), lisosoma/endosometan (Rozenfeld eta Devi, 2008) edo beste konpartimentu batzuetakoak izan daitezkeenak. Bitxia bada ere, nahiz eta CB_1 hartzailearen maila absolutuak astrozitoetan neuronetan baino txikiagoak izan (Metna-Laurent eta Marsicano, 2015), nire tesian aurkitu nuen mitokondriatako CB_1 hartzaileen dentsitate handiagoa astrozitoen mitokondriatan neuronenetan baino, kortex prefrontalean, accumbens nukleoan, kortex piriformean eta hipokanpoko CA1 eremuan.

Mitokondriatako CB_1 hartzailea aktibatzeak neuronetako energia-ekoizpena aldatzen du (Bénard et al., 2012; Hebert-Chatelain et al., 2014; Koch et al., 2015) eta memoria kaltetu dezake (Hebert-Chatelain et al., 2016). Are gehiago, astrozitoen mitokondriatako CB_1 hartzailearen aktibazioak eragina du glukosaren metabolismoan eta laktato-ekoizpenean, neurona-funtzioak eta jokabide soziala aldatuz (Jimenez-Blasco et al., 2020). Aztertutako garuneko lau eskualdeetako astrozitoen mitokondriak neuronenak baino CB_1 hartzaile gehiago edukitzeak eta kannabinoideek oxigeno-kontsumoan eragindako murrizketa (Bérnard et al., 2012) ez emateak GFAP-CB_1-KO saguen aurre-garunetik isolatutako mitokondrietan (Jimenez-Blasco et al., 2020), astrozitoetako mitokondriatako CB_1 hartzaileek kannabinoideek arnasketa mitokondrialean duten eragin orokorrean ezinbesteko eginkizuna dutela iradokitzen dute. Neuronek astrozitoek baino CB_1 hartzailearen maila absolutuak askoz handiagoak adierazten dituztela kontuan hartuta (Busquets-García et al., 2018), neuronen mitokondriatako CB_1 hartzaileek kannabinoideek mitokondriatan dituzten beste ondorio espezifiko batzuk bideratu ditzakete (Hebert-Chatelain et al., 2016). Alde horretatik, gure laborategiak frogatu du CB_1 hartzaileak murriztu egiten direla hipokanpoko CA1 eremuko mitokondriatan THC tratamendu akutuaren ondorioz (CB_1-positibo ziren miitokondriak % 42 jaitsi ziren neuronetan eta % 50 astrozitoetan; Bonilla del Río et al., 2021). Hipokanpoan mitokondriatako CB_1 hartzaileen aktibazioak mitokondria-aktibitatea eta zelula-arnasketa gutxitzen ditu, adenilil ziklasa disolbagarria inhibitzen du eta cAMP maila eta mitokondriako elektroi-garraio sistemako azpiunitate espezifikoen A-proteina kinasa (PKA)-menpeko fosforilazioa jaisten du (Hebert-Chatelain et al., 2016). Ondorioz, mitokondrien mugikortasuna murriztu egiten da axoietan, eta, beraz, baliteke ez lortzea mitokondrien bilera energia-eskaera handiko neuronen gunetan. THC tratamendu

akutuaren ostean dendrita eta sinapsi-bukaeratan mitokondria ugariago baina txikiagoak erakusten dituzten gure aurreko aurkikuntzek (Bonilla-Del Río et al., 2021) iradokitzen dute THCak beraien dinamikak eraldatzen dituztela, zeinak ezinbestekoak diren mitokondria-funtzioetarako. Izan ere, cAMP menpeko PKAk modulatzen du dinaminarekin-erlazionatutako 1 proteinaren (*dynamin-related protein 1*, dRP1) jarduera, zeina mitokondria-fisioaren entzima da, mitokondrien zatitzean eta arantza dendritiko eta sinapsien mantentzerako beharrezkoa den mitokondrien biltzean ezinbestekoa dena (Li et al., 2004; Cribbs eta Strack, 2007). Drp1-aren fosforilazioak mitokondria-fisioa inhibitzen eta apoptosia murrizten duenez (Cribbs eta Strack, 2007), baliteke THC tratamendu akutuaren ostean aurkitutako mitokondria ugari eta txikiak, neuronetako CB_1 hartzaileen aktibazioak eragindako mitokondria-funtzioen galera eta arnasketa zelularraren murrizketaren isla izatea. Mitokondria-morfologian THCak dituen ondorioak oraindik ez dira argitu. Hala ere, mitokondria-mugikortasuna murrizten da astrozitoetan neuronen aktibitatearen eta astrozitoetako glutamatoaren hartzearen eraginez, eta areagotzen da tetrodoxinaren eraginez (Jackson et al., 2014). Hala, THC akutuaren ondoren CA1 eremuko bukaera inhibitzaileetan ikusten den CB_1 hartzailearen beherapen gogorrak (Bonilla-Del Río et al., 2021) sarearen inhibizioa erraztuko luke eta, seguruenik, astrozitoetako mitokondria-mugikortasunean aldaketak sustatuko lituzke. Azkenik, astrozitoen mitokondriatako CB_1 hartzailearen aktibazioak eta aldi bereko cAMP-mendeko PKA murrizketak (Jimenez-Blasco et al., 2020), baliteke astrozito eta neuronen mitokondrien dinamika mekanismo komun batzuk erakustea. Halaber, baliteke kannabinoideek neuronen mitokondrien arnasketan dituzten ondorioak garuneko eremu espezifiko batzuetara, domeinu subzelular bati edo/eta neurona mota bati mugatuta egotea. Esperimentuek iradokitzen dutenez, CB_1 hartzailearen menpeko ondorioetan parte hartzen duen zelula-mota, funtzioaren eta jokabidearen zereginaren araberakoa dela eta baita sujetuaren egoeraren araberakoa (Busquets-García et al., 2015).

6.3. CB_1 HARTZAILEAREKIKO SAGU MUTANTEEN GARRANTZIA CB_1 HARTZAILEAREN KOKAPENAREN AZTERKETAN

CB_1 hartzilea garuneko zenbait zelula-motatan adierazten da (Marsicano eta Lutz, 1999; Tsou et al., 1999; Nyíri et al., 2005b; Monory et al., 2006; Häring et al., 2007; Scavone et al., 2010; Han et al., 2012; Metna-Laurent eta Marsicano, 2015). Gainera, bere aktibazioak zelula barneko hainbat ondorio ditu (Bosier et al., 2010; Pertwee, 2015). Atzerazko neurotransmisore-askapenaren inhibizioa da gehien ezagutzen denetarikoa eta zelula barneko gertaeren eragin garrantzitsua (Kano et al., 2009). Horren ondorioz, CB_1 hartzailearen aktibazioak hainbat neurotransmisoreren askapena modulatzen du (Kano et al., 2009).

Anatomikoki ere, CB_1 hartzailea oso zabaldua dago garunean, batez ere zeregin motor, linbiko, sari eta kortikala duten eskualdeetan (Matsuda et al., 1993; Tsou et al., 1998). Garuneko zenbait eremutan duen kontzentrazio handia abantaila bat da hartzailearen funtzioa aztertzeko eskualde horietan (Katona et al., 1999; Kawamura et al., 2006; Ludányi et al., 2008; Marsicano eta Kuner, 2008; Katona eta Freund, 2012; De-May eta Ali, 2013; Steindel et al., 2013; Hu eta Mackie, 2015). Hala ere, CB_1 hartzailearen dentsitatea ez da uniformea adierazten den eskualdeetan, eta horrek oso zaila egiten du CB_1 hartzailea identifikatzea maila baxuak dituzten sagu basatien zelula-mota eta konpartimentu subzelularretan (Busquets-Garcia et al., 2015).

CB_1 hartzailearen gabezia zelula-populazio jakin batean duten sagu mutante espezifikoen garapen eta erabilerak, CB_1 hartzailearen maila baxuen adierazpena zelula-mota edota konpartimentu subzelular eta intrazelular ezberdinetan identifikatzeko eta hartzailearen funtzio fisiologikoak ulertzeko balio zuen (Marsicano et al., 2003; Monory et al., 2006, 2007; Bellocchio et al., 2010; Bénard et al., 2012; Han et al., 2012; Ruehle et al., 2013; Steindel et al., 2013; Soria-Gómez et al., 2014; Busquets-Garcia et al., 2015; Martín-García et al., 2015; Oliveira da Cruz et al., 2016). Adibidez, GABA-CB_1-KO saguen hipokanpoan CB_1 hartzailearen galera handia ikusi zen, baina DMLko barneko herenean banda immunoerreaktibo nabarmen bat mantentzen zen (Martín-García et al., 2015). Bestalde, Glu-CB_1-KO saguen hipokanpoan CB_1 hartzaileen immunomarkaketaren murrizketa txikia baino ez zen hauteman (Martín-García et al., 2015; Gutiérrez-Rodríguez et al., 2017). Hala ere, sagu bi hauetan CB_1 hartzailearen markaketa ez zen

CB_1-KO saguetan bezala erabat ezabatu. Izan ere, CB_1 hartzailearen kokapena, batez ere, neuronen mintzetara mugatzen da, baina ez bakarrik; hala, CB_1 hartzaileak astrozitoen prozesuetan (Bosier et al., 2013) eta hipokanpoko zelula-mota ezberdinen mitokondria-mintzetan ere daude (Bénard et al., 2012; Hebert- Chatelain et al., 2014a; b), lehen esan bezala. Hala ere, baldintzapeko sagu mutante horiek mugak dituzte, CB_1 hartzailearen deleziotik eratorritako konpentsazio biologikoak gerta baitaitezke. Gainera, nerbio-zelula batzuetan CB_1 hartzaileak duen kokapenaren eta eginkizun fisiologiko batzuen arteko lotura ezartzea ez da posible (Ruehle et al., 2013).

GFAP-CB_1-KO saguen erabilerak erakutsi du, CA1 eremuko astrozitoetan CB_1 hartzaileen aktibazioak kannabinoideen dosi akutu baten ostean lan-memorian ematen den kaltea bideratzen duela, hipokanpoko LTDa modulatuz (Han et al., 2012). Nire tesian hipokanpoko CA1 eremuan CB_1-positibo diren astrozitoen ehunekoa, gure aurreko lanean deskribatutako balioaren antzekoa da (Han et al., 2012). Gainera, GFAP-CB_1-KO saguen sinapsi-bukaeratan neurtutako CB_1 hartzailearen immunopartikulak CB_1-WT saguen balioekin alderatu daitezke, GFAP-CB_1-KO saguak astrozitoetan CB_1 hartzaileen funtzioen galeran oinarritzen diren ikerketak burutzeko tresna erabilgarria direla iradokiz (Han et al., 2012).

6.4. SAGU TRANSGENIKO EZBERDINEN KORTEX PREFRONTAL PRELINBIKOKO II/III GERUZETAKO CB_1 HARTZAILEAREN BANAKETA

Jakina da CB_1 hartzailea PFCean dagoela, non batez ere II/III eta V/VI geruzetan banatzen da (Lafourcade et al., 2007). Hala ere, ez da inoiz CB_1 hartzailearen banaketaren azterketarik egin sinapsi-bukaera edo zelula-mota ezberdinetan. Nire tesian Glu-CB_1-WT, Glu-CB_1-KO, GABA-CB_1-WT, GABA-CB_1-KO eta CB_1-KO saguak erabili ditut PFC prelinbikoko II/III geruzetan CB_1 hartzailearen banaketa aztertzeko. Horrela, lortutako markaketa patroia, sagu hauetan ikusi den beste garuneko eskualde batzuetan aurkitutakoaren antzekoa da (Martín-García et al., 2016; Gutiérrez-Rodríguez et al., 2017). Hortaz, CB_1 hartzailearen immunomarkaketa oso txikia izan zen GABA-CB_1-KO saguetan beraien kumaldi bereko anai basatiekin alderatuz, PFCean CB_1 hartzaile gehienak GABA-neuronetan baitzeuden. Glu-CB_1-KO saguetan, ordea, CB_1 hartzailearen markaketa totala sagu basatien antzekoa zen, baina, kasu honetan, ez zen CB_1 hartzailerik aurkitu bukaera kitzikatzaileetan. Azkenik, bukaera inhibitzaileen % 90 baino gehiago eta bukaera kitzikatzaileen ia % 20 CB_1 hartzailearekiko immunopositiboak ziren, hipokanpoko CA1 eremuan bezala (Bonilla-Del Río et al., 2019).

Astrozitoetako CB_1 hartzaileen partikulen dentsitatea bukaera kitzikagarrietakoaren antzekoa edo zertxobait handiagoa zen. Azpimarratu behar da CB_1 hartzaileen partikulak ez zirela aurkitu GFAP-CB_1-KO saguen GLAST-positibo ziren astrozitoen prozesuetan. Gure aurreko ikerketetan astrozitoen markatzaile gisa GFAP erabiliz hipokanpoan deskribatutako emaitzak ezberdinak dira orain PFC prelinbikoaren II/III geruzetan lortutako emaitzekin alderatuz. Horrek adieraz dezake, lehenik eta behin, astrozitoetako CB_1 hartzaileen kopurua aldatu egiten dela garun eskualdearen arabera; bigarrenik, CB_1 hartzaile gehiago hautematen dela GLAST erabiliz GFAPren ordez; hirugarrenez, erabilitako kuantifikazio-metodoek (partikula/100 μm^2 *versus* partikulak/µm mintza) dentsitate-balio ezberdinak emango lituzkela. Astrozitoetako CB_1 hartzaileek ezinbesteko eginkizuna dute neurona eta astrozitoen arteko bi-noranzko komunikazioan, astrozitoetan sinapsi-transmisioa eta –plastikotasuna modulatzen duen kaltzio gorakada sortuz (Navarrete eta Araque, 2008, 2010; Navarrete et al., 2013; Navarrete et al., 2014; Gómez-Gonzalo et al., 2015; Araque et al., 2017; Martin-Fernandez et al., 2017). Astrozitoetako CB_1 hartzaileen aktibazioak bertako D-

aspartatoaren bilkura erregulatzen du (Shivachar, 2007) eta, honek, garuneko energia-hornidurari lagundu dezake astrozitoetako leptina hartzaileen adierazpena kontrolatuz (Bosier et al., 2013). Gainera, duela gutxi ikusi da CB_1 hartzaileak nabarmen jaisten direla sagu helduen CA1eko astrozitoetan, nerabezaroko etanolaren gaueko edate patroi baten ostean (Bonilla-Del Río et al., 2019).

EKSk funtsezko zeregina du NSZeko dopamina-mailen modulazioan (Hermann, et al., 2002). Adibidez, CB_1 hartzailearen aktibazioak dopamina handitzen eta GABA murrizten du PFCean (Pistis et al., 2002). CB_1 hartzailearen adierazpen handia aurkitu zen kolezistokinina (*cholecystokinin*, CKK) asko zuten saski-interneuronetan (Marsicano eta Lutz, 1999), eta, parbalbumina eta somatostatina zuten interneuronek, aldiz, ez zuten hartzailerik (Tsou et al., 1999; Bodor et al., 2005). CB_1 hartzailearen ARNm maila baxu baina detektagarriak deskribatu ziren eskualde kortikal askotako glutamato-neuronetan (Monory et al., 2006; Hill et al., 2007). Berriki ikusi dugu CB_1 hartzailearen markaketa nabarmena dela hartzailearen genea bakarrik glutamato-neurona telenzefalikoetan berreskuratzen duten saguen (Glu-CB_1-RS) gorputz ildaskatuan, kortexean, PFCan eta amigdalan. (Gutiérrez-Rodríguez et al., 2017). Are gehiago, CB_1 hartzailearen kokapena batez ere PFC prelinbikoko II/III eta V/VI geruzetara mugatzen da (Egertova eta Elphick 2000). Gainera, sabelaldeko eremu tegmentaleko (*ventral tegmental area*, VTA) PFCeko proiekzio kitzikatzaile gehienak neurona prelinbiko eta zingulatuenak dira, zeinek sinapsi kitzikatzaileak sortzen dituzten GABA-neurona eta dopamina-neuronekin (Carr eta Sesack, 2000; Geisler et al., 2007). Kannabisaren deribatuek kalte egiten die gune prefrontaleko funtzioei eta frogek adierazten dute kannabisak eskizofrenia garatu edo garatzeko arriskua handitu dezakeela, izan ere, PFCan EKSren asaldurak ere buruko gaixotasun hori garatzen lagun baitezake (Andreasson et al., 1988; Mathers eta Ghodse, 1992). Guzti hau dela eta, tesi honetan deskribatutako CB_1 hartzailearen kokapen azpizelularraren ezagutzak, bide berriak irekitzen ditu kannabisak PFCaren funtzioak nola aldatzen dituen ikertzeko.

6.5. CB_1 HARTZAILEAREN MENDEKO MPP-LTP 14 ASTEKO SAGUETAN

EKSk doitutako garun-funtzioak eskualde ezberdinetan sistemak duen banaketaren mende dago (Busquets-Garcia et al., 2018; Castillo et al., 2012; Hu eta Mackie, 2015; Katona eta Freund, 2012). Hipokanpoa beharrezkoa da adierazpen/aldikazko oroimenean eta espazioaren eta testuinguruaren araberako ikaskuntzan parte hartzen du (Eichenbaum et al., 2012). Kortex postrinaletik datozen sarrerak espazio-informazioa dakarte atze-alboko erdiko kortex entorrinalera, zeinek hipokanpo dortsalera proiektatzen duten MPPan zehar (Fyhn et al., 2004; Hargreaves et al., 2005). Bestalde, kortex perirrinalak alboko kortex entorrinalera proiektatzen du, zeinak LPParekin lotzen duen (Burwell, 2000).

LPP bideak informazio ez-espaziala transmititzen du, eta, MPPak DGri transmititutako ideia espazialekin batera, objetu-toki edo gertaera-toki bezalako ideiak garatzen direla uste da (Suzuki et al., 1997; Gaffan, 1998; Hargreaves et al., 2005). Aldi berean, zelula pikorrengatik barneratutako ingurumenarekin edo testuinguruarekin zerikusia duten seinaleak goroldio-zelulen kontrolpean daude, zeinak funtsezkoak dira informazio-sekuentzien ikaskuntzan (Lisman et al., 2005). Goroldio-zelulek glutamato-zuntz pikor kolateralak jasotzen dituzte, eta era berean, zuntz komisural/asoziatiboak bidaltzen dituzte; zuntz horiek distantzia luzeak egiten dituzte zenbait DG-zelula inerbatuz, goroldio- eta pikor-zelulen arteko sinapsiak sortuz (Amaral eta Witter, 1989; Scharfman eta Myers, 2013). Horzdun zelula-pikorrei zuzendutako hiru bide kitzikagarrien glutamato-sinapsiek CB_1 hartzaileak dituzte (Marsicano eta Lutz, 1999; Katona et al., 2006; Kawamura et al., 2006; Monory et al., 2006; Uchigashima et al., 2011; Katona eta Freund, 2012; Wang et al., 2016; Gutiérrez-Rodríguez et al., 2017) eta eKB-menpeko hainbat sinapsi-plastikotasun mota erakusten dituzte Chiu eta Castillo, 2008; Chávez et al., 2010; Wang et al., 2016, 2018), zeinak bat datoz bidezidor bakoitzak barneratutako informazio ezberdinekin.

14 asteko GFAP-CB_1-WT saguetan behatutako LTPa CB_1 hartzaileen mende dagoenez, sinapsi-plastikotasun honetan parte hartzen zeuden beste elementuak ezagutzea izan zen gure helburua. GFAP-CB_1-WT saguen MPP-LTPan bezala, 14 astetako sagu basatietan ikusitako fEPSP-en indartzea CB_1 hartzaileen AM251 alderantzizko agonistarekin blokeatzen zen, CB_1 hartzaileen partaidetza berretsiz. Hala ere, ez zen

aldaketarik behatu DL-APV aplikatzean, CB_1 hartzaileak bideratutako LTP hau NMDA hartzaileekiko independentea zela iradokiz. Hala eta guztiz ere, nahiz eta esanahi esanguratsurik ez izan, badirudi NMDA hartzaileen antagonistak zenbaki absolutuetan indartzea oztopatzen duela, eta, beraz, esperimentu gehiago beharrezkoak izango dira baieztatzeko. Veste ikerketa batzuetan arinago ikusi dugu MPP-GC sinapsietan LFS ostean ematen den eKB-LTDren tamaina ere ez zela aldatzen DL-APVrekin (Peñasco et al., 2019); honek NMDA hartzaileak eKB-LTD horretan parte hartzen ez dutela iradokitzen du, nahiz eta beste eKB-LTD batzuetan beharrezkoak izan (Sjöström et al., 2003; Bender et al., 2006; Lutzu eta Castillo 2020).

Frogatua dago TRPV1 hartzaileek sinapsi-plastikotasunean parte hartzen dutela (Marsch et al., 2007; Gibson et al., 2008; Kauer eta Gibson, 2009; Maione et al., 2009; Chávez et al., 2010, 2014; Grueter et al., 2010; Puente et al., 2011), eta baita ikaskuntzan eta memorian (Marsch et al., 2007; Li et al., 2008), beldur eta antsietatean (Marsch et al., 2007; Micale et al., 2009). Gainera, gizakietan kitzikagarritasun kortikala modulatzen dute (Mori et al., 2012). TRPV1 hartzaileak eta AEA bere agonista endogenoak hainbat garun eskualdetako sinapsi-LTDan parte hartzen dute (Di Marzo et al., 2001; 2002; 2008; Ross, 2003; Gibson et al., 2008; Kauer eta Gibson, 2009; Maione et al., 2009; Grueter et al., 2010; Chávez et al., 2011). Gainera, frogatu da TRPV1 hartzaileak NMDA hartzailearen mendeko LTP batean parte hartzen duela hipokanpoan, TRPV1 aktibatzean emendatzen dena (Marsch et al. 2007; Li et al. 2008). AMG9810 TRPV1 hartzailearen antagonista aplikatu zen 14 asteko saguetan behatutako MPP-LTPan parte hartzen duten aztertzeko. Estatistikoki esanguratsua izan ez arren, AMG9810 botikak fEPSP-etan ikusitako indartzea ekidin zuen.

LPPko sinapsi-bukaeratako CB_1 hartzailearen aktibazioak latrunkulinari sentikorrak diren aktina-harizpien muntaketa eragiten zuela ikusi zen, glutamato-askapena eta LTP bat eraginez (Wang et al., 2018). Integrinari loturiko kinasaren (FAK) eta hurrengo erantzue den ROCKen bidezko zen aktina-zitoeskeleto birantolaketa hori. Hala, mekanismo honek 14 asteko saguetan ematen den CB_1 hartzailearen mendeko MPP-LTPan parte hartzen zuen ala ez ikertu genuen. Hala ere, LAT-A aktinaren polimerizazioaren inhibitzaileak ez zuen indartzea aldatu. Duela gutxi, gure laborategiak jakinarazi du TRPV1aren gabezia duten saguetan MPP-LTP bat existitzen dela, LAT-A-rekin nabarmen gutxitzen dena

(Egaña-Huguet et al., 2021); horrek, HFSak (100 Hz) eragindako LPP-LTPan ematen den mekanismoaren antzekoa iradokitzen du (Wang et al., 2016, 2018). Gainera, NO emaile den SNAPek TRPV1$^{-/-}$ saguen MPP-LTPa blokeatu zuen (Egaña-Huguet et al., 2021). TRPV1 kaltzioarekiko oso iragazkorra denez (Caterina et al., 1997; Caterina eta Julius, 2001), baliteke MPP-GC dendrita-arantza sinapsietan TRPV1 gabeziak eragindako kaltzio intrazelularraren murrizketak NO sintetasa postsinaptikoa geldiaraztea, eta, horrenbestez, NO ekoizpena jaistea, hipokanpoko LTD presinaptikoa emateko beharrezkoa dena (Reyes-Harde et al., 1999). Baldintza normaletan, NOk cGMP-ren mendeko proteina kinasa postsinaptikoa (PKG) aktibatzen du (Sawada et al., 2001). Jakina da kinasa hau RhoA GTPasa txikia fosforilatzeko eta inaktibatzeko gai dela (Sawada et al., 2001), eta baita aktina-zitoeskeletoa erregulatzeko (Francis et al., 2010). Hala, TRPV1aren gabezian ematen den NO faltak, seinaleztapen bidezidor molekular presinaptikoak ekarri ditzake, azkenik glutamato-askapena emendatuz eta MPP-LTP emanez (Egaña-Huguet et al., 2021).

Kontuan hartu behar dira CB_1 hartzaileek astrozitoak bezalako beste zelula batzuetan izan ditzaketen zeharkako ondorioak, izan ere, astrozitoen CB_1 hartzaileek LTD kitzikagarria sustatzen dute, lekuko glutamatoaren erabilgarritasuna lagunduz (Han et al., 2012) eta urruneko sinapsietan LTP sustatuz (Araque et al., 2017). Ildo horretatik, 14 asteko CB_1 hartzaileen gabezia zuten saguak (GFAP-CB_1-KO) eta beraien kumaldi bereko anai basatiak (GFAP-CB_1-WT) ere erabili nituen. GFAP-CB_1-WT saguetan LTP bat behatu nuen LFS ostean, baina GFAP-CB_1-KO saguetan, aldiz, ez nuen ikusi ezberdintasun esanguratsurik, 14 asteko MPP-LTP honetan astrozitoen CB_1 hartzaileek funtzesko parte hartzea ez zutela aditzera emanez. Hala ere, AM251k indartzea oztopatu zuen, zelula ez-astroglialetan kokatutako CB_1 hartzaileen parte-hartzea adieraziz.

Oro har, beste esperimentu batzuk egin beharko dira TRPV1 hartzaileak 14 asteko saguen MPP-LTP honetan murgilduta dauden argitzeko. Era berean, goian azaldutako sinaleztapen bideak ikertu behar dira.

eKBen sintesian eta degradazioan eragiten duten botika ezberdinak ere erabili ziren 2-AG eta AEA plastikotasun honetan sartuta zeuden ala ez argitzeko. Farmako batek ere ez zuen eragin nabarmenik izan 14 asteko saguetan ikusitako fEPSPen indartzean. Hala ere, indartzea oztopatu egin zen MAGLren JZL 184 inhibitzailearekin baina era ez-

esanguratsuan. Horrela, grabaketa aurretik JZL 184aren inkubazio-denbora ondoren lortutako 2-AG kontzentrazio handiek eragindako CB_1 hartzailearen desentsibilizazioa hartzailearen blokeoaren erantzulea izan daiteke, sagu gazteagoetan MPP-GC sinapsietan deskribatutako eKB-LTDan bezala (Peñasco et al., 2019). Gainera, hau bat dator lehenago egindako ikerketekin non epe-luzeko 2-AGaren igoerak CB_1 hartzailearen desentsibilizazioa eragiten duela erakusten duten (Chanda et al., 2010; Schlosburg et al., 2010).

Ondorio gisa, CB_1 hartzailearen mendeko MPP-LTDa, 14 asteko saguetan MPP-LTP bihurtzeak baliteke memorian eragina izatea, izan ere, hipokanpoa, oro har (Eichenbaum et al., 2012), eta MPP-sinapsiak, bereziki, memoria espazialaren prozesamenduan sartuta daude (Fyhn et al., 2004; Hargreaves et al., 2005).

6.6. CB_1 HARTZAILEAREN MENPEKO LTP 14 ASTEKO SAGUEN PFC SINAPSIETAN

PFCak lan-oroimenean eta norberaren erregulazio eta helburuetara bideratutako jokabidetan parte hartzen du, eta, gainera, bizitzan zehar egitura- eta funtzio-plastikotasun nabarmena du. Neurona-sare, molekula-profila eta neurokimika esperientziarekin alda daiteke, portaeran eraginez, eta baita funtzio neuroendokrino eta autonomikoetan. LFSak LTP bat eragiten zuen 14 astetako saguen PFC prelimbikoko II/III geruzetako sinapsi kitzikatzaileetan, AM251rekin blokeatzen zena. Nabarmentzekoa da, GFAP-CB_1-WT saguetan ikusten den indartze esanguratsua ez zela ikusten GFAP-CB_1-KO saguetan. Hala ere, egindako esperimentu kopurua ez zen izan nahikoa GFAP-CB_1-KO saguetan. Beraz, sagu mutante gehiago behar dira astrozitoen CB_1 hartzaileen partaidetza probatzeko PFC-LTPan.

NMDA eta TRPV1 hartzaileen antagonistek ez zuten eraginik izan indartzean, hartzaile hauek PFC-LTP honetan parte hartzen ez zutela adieraziz. MPP-LTP-an bezala, JZL 184 eta THL botikek ez zuten eraginik izan 14 asteko sagu basatien PFCean ikusitako fEPSPen indartzean. Hala ere, FAAH inhibitzen duen URB597k hein batean aldatzen du LTP hori, baina ez modu esanguratsuan. Beraz, esperimentu gehiago beharko dira PFC-LTP honetan AEAren parte-hartze posiblea baieztatzeko.

Biak, PFCa eta EKSa, partaide garrantzitsuak dira oroimen higuingarrien desagertzean (Marsicano et al., 2002; Myers eta Davis, 2002) eta ikaskuntza emozionalen plastikotasunean (Laviolette eta Grace, 2006). CB_1 hartzaileak asko adierazten dira PFCean (Mackie 2005; Eggan eta Lewis 2007; Hu eta Mackie, 2015), non beldurrak eragindako memoriaren suntsipena bideratzen duen eta dopamina-transmisioa emendatzen duen (Diana et al., 1998; Lin et al., 2009). DAGLα ere zuten dendritetan zeuden 5-motako glutamato-hartzaile metobotropiko (*metabotropic glutamate receptor type-5*, mGluR5) postsinaptikoen aurrean kokatzen ziren CB_1 hartzaile presinaptikoak ikusi ziren (Lafourcade et al., 2007). Kokapen molekular hau zen V/VI geruzetako sarrera kitzikatzaileen luzaroko sinapsi estimulazioaren ondorioz ematen den eKB bidezko epe luzeko depresioaren erantzulea (Lafourcade et al., 2007). Oro har, 14 asteko saguen PFC prelimbikoko sinapsi kitzikatzaileetan CB_1 hartzaileak bideratutako LTP bat ikusi nuen, LFS berak 8-10 asteko saguetan eragindako LTDaren kontrara (Lafourcade et al., 2007; Peñasco et al., 2019). Oraindik EKSren elementuak

mikroskopio immunoelektronikoan aztertu behar dira 14 asteko PFC-LTP honen azpian dauden molekula-gertaerak azaltzeko.

ONDORIOAK

1. GFAP metal-partikulak astrozitoen somako eta adarkadura nagusien zitoplasman kokatzen ziren bitartean, GLAST-markaketa astrozitoen mintzean zehar aurkitzen zen, zelula-gorputzean eta neurona, kapilar eta beste glia-zelula batzuekin kontaktuan zeuden astrozitoen prozesu txikienetan ere adierazten zelarik. Oro har, GFAPk baino askoz eremu markatu gehiago estaltzen zuen GLAST-markaketak.
2. Ia hiru aldiz astrozitoen azalera gehiago eta lau aldiz astrozitoen mintz gehiago ikusarazten da GLASTekin GFAPrekin baino.
3. CB_1 hartzailearen partikulen % 12 GLAST-positibo ziren astrozitoetan kokatzen zirela ikusi zen, eta, GFAP antigorputzarekin, ordea, bakarrik % 5 zegoen astrozitoetan.
4. GLAST CB_1 hartzaileak astrozitoen mitokondriatan zehazki detektatzeko markatzaile bikaina da, tesi honetan hainbat garun-eskualdetan frogatu bezala: hipokanpoa, kortex prefrontala, accumbens nukleoa eta kortex piriformea.
5. Mitokondriatako CB_1 hartzaileen dentsitatea handiagoa astrozitoetan neuronetan baino.
6. CB_1 hartzaile-positibo diren konpartimentuen proportzioa eta hartzailearen partikulen banaketa GFAP-CB_1-WT eta GFAP-CB_1-KO saguen kortex prefrontal prelinbikoko II/III geruzetan, lehenago hipokanpoan deskribatutakoaren antzekoa da.
7. 14 asteko saguen MPP eta kortex prefrontal prelinbikoko II/III geruzetan LTP esanguratsu bat ikusi zen. Gainera, LTP hau CB_1 hartzailearen mende dago. Badirudi NMDA etaTRPV1 hartzaileek ez dutela parte-hartzen.
8. Astrozitoetako CB_1 hartzaileak ez dute LTPan parte-hartzen, GFAP-CB_1-KO saguetan ez baita aldatzen.

BIBLIOGRAFIA

Acin-Perez, R., Salazar, E., Kamenetsky, M., Buck, J., Levin, L. R., & Manfredi, G. (2009). Cyclic AMP produced inside mitochondria regulates oxidative phosphorylation. *Cell metabolism*, 9(3), 265–276.

Acin-Perez, R., Russwurm, M., Günnewig, K., Gertz, M., Zoidl, G., Ramos, L., Buck, J., Levin, L. R., Rassow, J., Manfredi, G., & Steegborn, C. (2011). A phosphodiesterase 2A isoform localized to mitochondria regulates respiration. *Journal of Biological Chemistry*, *286*(35), 30423–30432.

Adermark, L., & Bowers, M. S. (2016). Disentangling the Role of Astrocytes in Alcohol Use Disorder. *Alcoholism, clinical and experimental research*, 40(9), 1802–1816.

Aggleton, J. P., & Brown, M. W. (1999). Episodic memory, amnesia, and the hippocampal-anterior thalamic axis. *The Behavioral and brain sciences*, 22(3), 425–489.

Aguado, T., Palazuelos, J., Monory, K., Stella, N., Cravatt, B., Lutz, B., Marsicano, G., Kokaia, Z., Guzmán, M., & Galve-Roperh, I. (2006). The endocannabinoid system promotes astroglial differentiation by acting on neural progenitor cells. *Journal of Neuroscience*, *26*(5), 1551–1561.

Aguado, T., Romero, E., Monory, K., Palazuelos, J., Sendtner, M., Marsicano, G., Lutz, B., Guzmán, M., & Galve-Roperh, I. (2007). The CB_1 cannabinoid receptor mediates excitotoxicity-induced neural progenitor proliferation and neurogenesis. *Journal of Biological Chemistry*, *282*(33), 23892–23898.

Alger B. E. (2002). Retrograde signaling in the regulation of synaptic transmission: focus on endocannabinoids. *Progress in neurobiology*, 68(4), 247–286.

Alger, B. E. (2006). Not too excited? Thank your endocannabinoids. *Neuron*, 51(4), 393–395.

Alhouayek, M., Masquelier, J., & Muccioli, G. G. (2014). Controlling 2-arachidonoylglycerol metabolism as an anti-inflammatory strategy. *Drug Discovery Today*, *19*(3), 295–304.

Allen, N. J., & Barres, B. A. (2009). How do glia differ from neurons? *Nature Q&A*, *457*(February), 675–677.

Amaral, D. G., & Witter, M. P. (1989). The three-dimensional organization of the hippocampal formation: a review of anatomical data. *Neuroscience*, *31*(3), 571–591.

Ameri A. (1999). The effects of cannabinoids on the brain. *Progress in neurobiology*, 58(4), 315–348.

Andre, C. M., Hausman, J. F., & Guerriero, G. (2016). Cannabis sativa: The plant of the thousand and one molecules. *Frontiers in Plant Science*, *7*(FEB2016), 1–17.

Andréasson, S., Allebeck, P., Engström, A., & Rydberg, U. (1988). *Cannabis and schizophrenia. Lancet (London, England), 1(8592),* 1000–1001.

Andreeva, A. V., Kutuzov, M. A., & Voyno-Yasenetskaya, T. A. (2008). Gα12 is targeted to the mitochondria and affects mitochondrial morphology and motility. *The FASEB Journal*, *22*(8), 2821–2831.

Angulo, M. C., Kozlov, A. S., Charpak, S., & Audinat, E. (2004). Glutamate released from glial cells synchronizes neuronal activity in the hippocampus. *Journal of Neuroscience*, *24*(31), 6920–6927.

Antzoulatos, E. G., & Miller, E. K. (2011). Differences between neural activity in prefrontal cortex and striatum during learning of novel abstract categories. *Neuron*, *71*(2), 243–249.

Aquila, S., Guido, C., Santoro, A., Perrotta, I., Laezza, C., Bifulco, M., & Sebastiano, A. (2010). Human sperm anatomy: Ultrastructural localization of the cannabinoid1 receptor and a potential role of anandamide in sperm survival and acrosome reaction. *Anatomical Record*, *293*(2), 298–309.

Araque, A., Parpura, V., Sanzgiri, R. P., & Haydon, P. G. (1999). Tripartite synapses: glia, the unacknowledged partner. *Trends in neurosciences*, 22(5), 208–215.

Araque, A., Carmignoto, G., & Haydon, P. G. (2001). Dynamic signaling between astrocytes and neurons. *Annual review of physiology*, 63, 795–813.

Araque, A., & Navarrete, M. (2010). Glial cells in neuronal network function. *Philosophical Transactions of the Royal Society B: Biological Sciences*, *365*(1551), 2375–2381.

Araque, A., Castillo, P. E., Manzoni, O. J., & Tonini, R. (2017). Synaptic functions of endocannabinoid signaling in health and disease. *Neuropharmacology*, *124*, 13–24.

Arriza, J. L., Fairman, W. A., Amara, S. G., Kavanaugh, P., Wadiche, I., & Murdoch, H. (1994). Functional Comparisons of Three Glutamate Cloned from Human Motor Cortex Transporter. *The Journal of Neuroscience : The Official Journal of the Society for Neuroscience*, *14*(9), 5559–5569.

Ashton, J. C., Friberg, D., Darlington, C. L., & Smith, P. F. (2006). Expression of the cannabinoid CB_2 receptor in the rat cerebellum: An immunohistochemical study. *Neuroscience Letters*, *396*(2), 113–116.

Attwell, D., & Laughlin, S. B. (2001). An energy budget for signaling in the grey matter of the brain. *Journal of Cerebral Blood Flow and Metabolism*, *21*(10), 1133–1145.

Atwood, B. K., & MacKie, K. (2010). CB_2: A cannabinoid receptor with an identity crisis. *British Journal of Pharmacology*, *160*(3), 467–479.

Azad, S. C., Kurz, J., Marsicano, G., Lutz, B., Zieglgänsberger, W., & Rammes, G. (2008). Activation of CB_1 specifically located on GABAergic interneurons inhibits LTD in the lateral amygdala. *Learning and Memory*, *15*(3), 143–152.

Barros, L. F., & Weber, B. (2018). CrossTalk proposal: an important astrocyte-to-neuron lactate shuttle couples neuronal activity to glucose utilisation in the brain. *Journal of Physiology*, *596*(3), 347–350.

Bartholomä, A., & Nave, K. A. (1994). NEX-1: a novel brain-specific helix-loop-helix protein with autoregulation and sustained expression in mature cortical neurons. *Mechanisms of development*, 48(3), 217–228.

Bélanger, M., & Magistretti, P. J. (2009). The role of astroglia in neuroprotection. *Dialogues in Clinical Neuroscience*, *11*(3), 281–296.

Bélanger, M., Allaman, I., & Magistretti, P. J. (2011). Brain energy metabolism: Focus on Astrocyte-neuron metabolic cooperation. *Cell Metabolism*, *14*(6), 724–738.

Bellocchio, L., Lafentre, P., Cannich, A., Cota, D., Puente, N., Grandes, P., Chaouloff, F., Piazza, P. V., & Marsicano, G. (2010). Bimodal control of stimulated food intake by the endocannabinoid system. *Nature Neuroscience*, *13*(3), 281–283.

Bénard, G., Massa, F., Puente, N., Lourenço, J., Bellocchio, L., Soria-Gómez, E., Matias, I., Delamarre, A., Metna-Laurent, M., Cannich, A., Hebert-Chatelain, E., Mulle, C., Ortega-Gutiérrez, S., Martín-Fontecha, M., Klugmann, M., Guggenhuber, S., Lutz, B., Gertsch, J., Chaouloff, F., López-Rodríguez, M. L., … Marsicano, G. (2012). Mitochondrial CB_1 receptors regulate neuronal energy metabolism. *Nature neuroscience*, 15(4), 558–564.

Bender, V. A., Bender, K. J., Brasier, D. J., & Feldman, D. E. (2006). Two coincidence detectors for spike timing-dependent plasticity in somatosensory cortex. *Journal of Neuroscience*, *26*(16), 4166–4177.

Bilkei-Gorzo, A., Racz, I., Valverde, O., Otto, M., Michel, K., Sastre, M., & Zimmer, A. (2005). Early age-related cognitive impairment in mice lacking cannabinoid CB_1 receptors. *Proceedings of the National Academy of Sciences of the United States of America*, 102(43), 15670–15675.

Bisogno, T., Berrendero, F., Ambrosino, G., Cebeira, M., Ramos, J. A., Fernandez-Ruiz, J. J., & Di Marzo, V. (1999). Brain regional distribution of endocannabinoids: Implications for their biosynthesis and biological function. *Biochemical and Biophysical Research Communications*, *256*(2), 377–380.

Blair, R. E., Deshpande, L. S., & Delorenzo, R. J. (2015). Cannabinoids: Is there a potential treatment role in epilepsy? *Expert Opinion on Pharmacotherapy*, *16*(13), 1911–1914.

Bodor, A. L., Katona, I., Nyíri, G., Mackie, K., Ledent, C., Hájos, N., & Freund, T. F. (2005). Endocannabinoid signaling in rat somatosensory cortex: laminar differences and involvement of specific interneuron types. *The Journal of neuroscience : the official journal of the Society for Neuroscience*, 25(29), 6845–6856.

Bolaños, J. P. (2016). Bioenergetics and redox adaptations of astrocytes to neuronal activity. *Journal of Neurochemistry*, *139*, 115–125.

Bonilla-Del Río, I., Puente, N., Peñasco, S., Rico, I., Gutiérrez-Rodríguez, A., Elezgarai, I., Ramos, A., Reguero, L., Gerrikagoitia, I., Christie, B. R., Nahirney, P., & Grandes, P. (2019). Adolescent ethanol intake alters cannabinoid type-1 receptor localization in astrocytes of the adult mouse hippocampus. *Addiction Biology*, *24*(2), 182–192.

Bonilla-Del Río, I., Puente, N., Mimenza, A., Ramos, A., Serrano, M., Lekunberri, L., Gerrikagoitia, I., Christie, B. R., Nahirney, P. C., & Grandes, P. (2021). Acute Δ9-tetrahydrocannabinol prompts rapid changes in cannabinoid CB_1 receptor immunolabeling and subcellular structure in CA1 hippocampus of young adult male mice. *Journal of Comparative Neurology*, *529*(9), 2332–2346.

Bonini, S. A., Premoli, M., Tambaro, S., Kumar, A., Maccarinelli, G., Memo, M., & Mastinu, A. (2018). Cannabis sativa: A comprehensive ethnopharmacological review of a medicinal plant with a long history. *Journal of Ethnopharmacology*, *227*(September), 300–315.

Bosier, B., Bellocchio, L., Metna-Laurent, M., Soria-Gomez, E., Matias, I., Hebert-Chatelain, E., Cannich, A., Maitre, M., Leste-Lasserre, T., Cardinal, P., Mendizabal-Zubiaga, J., Canduela, M. J., Reguero, L., Hermans, E., Grandes, P., Cota, D., & Marsicano, G. (2013). Astroglial CB_1 cannabinoid receptors regulate leptin signaling in mouse brain astrocytes. *Molecular Metabolism*, *2*(4), 393–404.

Bouaboula, M., Bourrié, B., Rinaldi-Carmona, M., Shire, D., Le Fur, G., & Casellas, P. (1995). Stimulation of cannabinoid receptor CB_1 induces krox-24 expression in human astrocytoma cells. *Journal of Biological Chemistry*, *270*(23), 13973–13980.

Burwell R. D. (2000). The parahippocampal region: corticocortical connectivity. *Annals of the New York Academy of Sciences*, 911, 25–42.

Busquets-Garcia, A., Desprez, T., Metna-Laurent, M., Bellocchio, L., Marsicano, G., & Soria-Gomez, E. (2015). Dissecting the cannabinergic control of behavior: The where matters. *BioEssays : news and reviews in molecular, cellular and developmental biology*, 37(11), 1215–1225.

Busquets-Garcia, A., Bains, J., & Marsicano, G. (2018). CB_1 Receptor Signaling in the Brain: Extracting Specificity from Ubiquity. *Neuropsychopharmacology*, *43*(1), 4–20.

Cabral, G. A., Rogers, T. J., & Lichtman, A. H. (2015). Turning Over a New Leaf: Cannabinoid and Endocannabinoid Modulation of Immune Function. *Journal of neuroimmune pharmacology: the official journal of the Society on NeuroImmune Pharmacology*, 10(2), 193–203.

Carr, D. B., & Sesack, S. R. (2000). Dopamine terminals synapse on callosal projection neurons in the rat prefrontal cortex. *The Journal of comparative neurology*, 425(2), 275–283.

Castillo, P. E., Younts, T. J., Chávez, A. E., & Hashimotodani, Y. (2012). Endocannabinoid signaling and synaptic function. *Neuron*, 76(1), 70–81.

Caterina, M. J., Schumacher, M. A., Tominaga, M., Rosen, T. A., Levine, J. D., & Julius, D. (1997). The capsaicin receptor: a heat-activated ion channel in the pain pathway. *Nature*, 389(6653), 816–824.

Caterina, M. J., & Julius, D. (2001). The vanilloid receptor: a molecular gateway to the pain pathway. *Annual review of neuroscience*, 24, 487–517.

Chanda, P. K., Gao, Y., Mark, L., Btesh, J., Strassle, B. W., Lu, P., Piesla, M. J., Zhang, M. Y., Bingham, B., Uveges, A., Kowal, D., Garbe, D., Kouranova, E. V., Ring, R. H., Bates, B., Pangalos, M. N., Kennedy, J. D., Whiteside, G. T., & Samad, T. A. (2010). Monoacylglycerol lipase activity is a critical modulator of the tone and integrity of the endocannabinoid system. *Molecular pharmacology*, 78(6), 996–1003.

Chaudhry, F. A., Lehre, K. P., van Lookeren Campagne, M., Ottersen, O. P., Danbolt, N. C., & Storm-Mathisen, J. (1995). Glutamate transporters in glial plasma membranes: highly differentiated localizations revealed by quantitative ultrastructural immunocytochemistry. *Neuron*, 15(3), 711–720.

Chávez, A. E., Chiu, C. Q., & Castillo, P. E. (2010). TRPV1 activation by endogenous anandamide triggers postsynaptic long-term depression in dentate gyrus. *Nature Neuroscience*, *13*(12), 1511–1519.

Chen, C., Ko, Y., Delannoy, M., Ludtke, S. J., Chiu, W., & Pedersen, P. L. (2004). Mitochondrial ATP synthasome. Three-dimensional structure by electron microscopy of the ATP synthase in complex formation with carriers for P i and ADP/ATP. *Journal of Biological Chemistry*, *279*(30), 31761–31768.

Chiu, C. Q., & Castillo, P. E. (2008). Input-specific plasticity at excitatory synapses mediated by endocannabinoids in the dentate gyrus. *Neuropharmacology*, 54(1), 68–78.

Cholet, N., Pellerin, L., Magistretti, P. J., & Hamel, E. (2002). Similar perisynaptic glial localization for the Na+,K+-ATPase α2 subunit and the glutamate transporters GLAST and GLT-1 in the rat somatosensory cortex. *Cerebral Cortex*, *12*(5), 515–525.

Christie, B. R., & Abraham, W. C. (1994). L-type voltage-sensitive calcium channel antagonists block heterosynaptic long-term depression in the dentate gyrus of anaesthetized rats. *Neuroscience letters*, 167(1-2), 41–45.

Chudasama, Y., Baunez, C., & Robbins, T. W. (2003). Functional disconnection of the medial prefrontal cortex and subthalamic nucleus in attentional performance: Evidence for corticosubthalamic interaction. *Journal of Neuroscience*, *23*(13), 5477–5485.

Clarke, H. F., Dalley, J. W., Crofts, H. S., Robbins, T. W., & Roberts, A. C. (2004). Cognitive inflexibility after prefrontal serotonin depletion. *Science*, 304(5672), 878–880.

Clement, A. B., Hawkins, E. G., Lichtman, A. H., & Cravatt, B. F. (2003). Increased seizure susceptibility and proconvulsant activity of anandamide in mice lacking fatty acid amide hydrolase. *Journal of Neuroscience*, *23*(9), 3916–3923.

Cravatt, B. F., Giang, D. K., Mayfield, S. P., Boger, D. L., Lerner, R. A., & Gilula, N. B. (1996). Molecular characterization of an enzyme that degrades neuromodulatory fatty-acid amides. *Nature*, 384(6604), 83–87.

Cribbs, J. T., & Strack, S. (2007). Reversible phosphorylation of Drp1 by cyclic AMP-dependent protein kinase and calcineurin regulates mitochondrial fission and cell death. *EMBO reports*, 8(10), 939–944.

Cristino, L., Starowicz, K., De Petrocellis, L., Morishita, J., Ueda, N., Guglielmotti, V., & Di Marzo, V. (2008). Immunohistochemical localization of anabolic and catabolic enzymes for anandamide and other putative endovanilloids in the hippocampus and cerebellar cortex of the mouse brain. *Neuroscience*, *151*(4), 955–968.

Dalley, J. W., Everitt, B. J., & Robbins, T. W. (2011). Impulsivity, Compulsivity, and Top-Down Cognitive Control. *Neuron*, *69*(4), 680–694.

Danbolt, N. C. (1994). The high affinity uptake system for excitatory amino acids in the brain. *Progress in neurobiology*, 44(4), 377–396.

Danbolt, N. C. (2001). Glutamate uptake. *Progress in neurobiology*, 65(1), 1–105.

Danbolt, N. C., Furness, D. N., & Zhou, Y. (2016). Neuronal vs glial glutamate uptake: Resolving the conundrum. *Neurochemistry International*, *98*, 29–45.

De Petrocellis, L., Vellani, V., Schiano-Moriello, A., Marini, P., Magherini, P. C., Orlando, P., Di Marzo, V. (2008). Plant-derived cannabinoids modulate the activity of transient receptor potential channels of ankyrin type-1 and melastatin type-8. *The Journal of pharmacology and experimental therapeutics*, 325(3), 1007-1015.

De Petrocellis, L., & Di Marzo, V. (2009). Role of endocannabinoids and endovanilloids in Ca^{2+} signalling. *Cell Calcium*, *45*(6), 611–624.

De-May, C. L., & Ali, A. B. (2013). Cell type-specific regulation of inhibition via cannabinoid type 1 receptors in rat neocortex. *Journal of Neurophysiology*, *109*(1), 216–224.

Devane, W. A., Hanus, L., Breuer, A., Pertwee, R. G., Stevenson, L. A., Griffin, G., Gibson, D., Mandelbaum, A., Etinger, A., Mechoulam, R. (1992). Isolation and structure of a brain constituent that binds to the cannabinoid receptor. *Science*, 18, 258(5090), 1946-9.

Di Marzo, V., Melck, D., Bisogno, T., & De Petrocellis, L. (1998). Endocannabinoids: endogenous cannabinoid receptor ligands with neuromodulatory action. *Trends in neurosciences*, 21(12), 521–528.

Di Marzo, V., Bisogno, T., De Petrocellis, L., Brandi, I., Jefferson, R. G., Winckler, R. L., Davis, J. B., Dasse, O., Mahadevan, A., Razdan, R. K., & Martin, B. R. (2001). Highly selective CB(1) cannabinoid receptor ligands and novel CB(1)/VR(1) vanilloid receptor "hybrid" ligands. *Biochemical and biophysical research communications*, 281(2), 444–451.

Di Marzo, V., De Petrocellis, L., Fezza, F., Ligresti, A., & Bisogno, T. (2002). Anandamide receptors. *Prostaglandins, leukotrienes, and essential fatty acids*, 66(2-3), 377–391.

Di Marzo, V., Gobbi, G., & Szallasi, A. (2008). Brain TRPV1: a depressing TR(i)P down memory lane?. *Trends in pharmacological sciences*, 29(12), 594–600.

Di Marzo, V., Stella, N., & Zimmer, A. (2015). Endocannabinoid signalling and the deteriorating brain. Nature reviews. *Neuroscience*, 16(1), 30–42.

Diana, M., Melis, M., Muntoni, A. L., & Gessa, G. L. (1998). Mesolimbic dopaminergic decline after cannabinoid withdrawal. *Proceedings of the National Academy of Sciences of the United States of America*, 95(17), 10269–10273.

Domenici, M. R., Azad, S. C., Marsicano, G., Schierloh, A., Wotjak, C. T., Dodt, H. U., Zieglgänsberger, W., Lutz, B., & Rammes, G. (2006). Cannabinoid receptor type 1 located on presynaptic terminals of principal neurons in the forebrain controls glutamatergic synaptic transmission. *Journal of Neuroscience*, *26*(21), 5794–5799.

Durkee, C. A., & Araque, A. (2019). Diversity and Specificity of Astrocyte-neuron Communication. *Neuroscience*, 396, 73–78.

Egaña-Huguet, J., Bonilla-Del Río, I., Gómez-Urquijo, S. M., Mimenza, A., Saumell-Esnaola, M., Borrega-Roman, L., García del Caño, G., Sallés, J., Puente, N., Gerrikagoitia, I., Elezgarai, I., & Grandes, P. (2021). The Absence of the Transient Receptor Potential Vanilloid 1 Directly Impacts on the Expression and Localization of the Endocannabinoid System in the Mouse Hippocampus. *Frontiers in Neuroanatomy*, *15*(February), 1–17.

Egertova, M., Giang, D. K., Cravatt, B. F., & Elphick, M. R. (1998). A new perspective on cannabinoid signalling: Complementary localization of fatty acid amide hydrolase and the CB_1 receptor in rat brain. *Proceedings of the Royal Society B: Biological Sciences*, *265*(1410), 2081–2085.

Egertová, M., & Elphick, M. R. (2000). Localisation of cannabinoid receptors in the rat brain using antibodies to the intracellular C-terminal tail of CB_1. *Journal of Comparative Neurology*, *422*(2), 159–171.

Eggan, S. M., & Lewis, D. A. (2007). Immunocytochemical distribution of the cannabinoid CB_1 receptor in the primate neocortex: a regional and laminar analysis. *Cerebral cortex (New York, N.Y. : 1991)*, 17(1), 175–191.

Eichenbaum, H. (2000). Hippocampus: Mapping or memory? *Current Biology*, *10*(21), 785–787.

Eichenbaum, H., Sauvage, M., Fortin, N., Komorowski, R., & Lipton, P. (2012). Towards a functional organization of episodic memory in the medial temporal lobe. *Neuroscience and biobehavioral reviews*, 36(7), 1597–1608.

Elphick, M. R., & Egertová, M. (2005). The phylogenetic distribution and evolutionary origins of endocannabinoid signalling. *Handbook of experimental pharmacology*, (168), 283–297.

Eng L. F. (1985). Glial fibrillary acidic protein (GFAP): the major protein of glial intermediate filaments in differentiated astrocytes. *Journal of neuroimmunology*, 8(4-6), 203–214.

Eng, L. F., Ghirnikar, R. S., & Lee, Y. L. (2000). Glial fibrillary acidic protein: GFAP-thirty-one years (1969-2000). *Neurochemical research*, 25(9-10), 1439–1451.

Felder, C. C., & Glass, M. (1998). Cannabinoid receptors and their endogenous agonists. *Annual review of pharmacology and toxicology*, 38, 179–200.

Fellin, T. (2009). Communication between neurons and astrocytes: Relevance to the modulation of synaptic and network activity. *Journal of Neurochemistry*, *108*(3), 533–544.

Fezza, F., Bari, M., Florio, R., Talamonti, E., Feole, M., & Maccarrone, M. (2014). Endocannabinoids, related compounds and their metabolic routes. *Molecules*, *19*(11), 17078–17106.

Fischer, M., Kaech, S., Knutti, D., & Matus, A. (1998). Rapid actin-based plasticity in dendritic spines. *Neuron*, 20(5), 847–854.

Flores, Á., Maldonado, R., & Berrendero, F. (2013). Cannabinoid-hypocretin cross-talk in the central nervous system: What we know so far. *Frontiers in Neuroscience*, *7*(7 DEC), 1–17.

Fontaine, C. J., Gräfe, E. L., Pinar, C., Bonilla-Del Río, I., Grandes, P., & Christie, B. R. (2020). Endocannabinoid receptors contribute significantly to multiple forms of long-term depression in the rat dentate gyrus. *Learning & memory*, 27(9), 380–389.

Francis, S. H., Busch, J. L., Corbin, J. D., & Sibley, D. (2010). cGMP-dependent protein kinases and cGMP phosphodiesterases in nitric oxide and cGMP action. *Pharmacological reviews*, 62(3), 525–563.

Freedman, D. J., Riesenhuber, M., Poggio, T., & Miller, E. K. (2001). Categorical representation of visual stimuli in the primate prefrontal cortex. *Science*, 291(5502), 312–316.

Friedman, D., & Devinsky, O. (2015). Cannabinoids in the Treatment of Epilepsy. *The New England journal of medicine*, 373(11), 1048–1058.

Fyhn, M., Molden, S., Witter, M. P., Moser, E. I., & Moser, M. B. (2004). Spatial representation in the entorhinal cortex. *Science (New York, N.Y.)*, 305(5688), 1258–1264.

Gaffan D. (1998). Idiothetic input into object-place configuration as the contribution to memory of the monkey and human hippocampus: a review. *Experimental brain research*, 123(1-2), 201–209.

Galiègue, S., Mary, S., Marchand, J., Dussossoy, D., Carrière, D., Carayon, P., Bouaboula, M., Shire, D., LE Fur, G., & Casellas, P. (1995). Expression of Central and Peripheral Cannabinoid Receptors in Human Immune Tissues and Leukocyte Subpopulations. *European Journal of Biochemistry*, *232*(1), 54–61.

Galve-Roperh, I., Palazuelos, J., Aguado, T., & Guzmán, M. (2009). The endocannabinoid system and the regulation of neural development: Potential implications in psychiatric disorders. *European Archives of Psychiatry and Clinical Neuroscience*, *259*(7), 371–382.

Gegelashvili, G., Danbolt, N. C., & Schousboe, A. (1997). Neuronal soluble factors differentially regulate the expression of the GLT1 and GLAST glutamate transporters in cultured astroglia. *Journal of neurochemistry*, 69(6), 2612–2615.

Geisler, S., Derst, C., Veh, R. W., & Zahm, D. S. (2007). Glutamatergic afferents of the ventral tegmental area in the rat. *The Journal of neuroscience: the official journal of the Society for Neuroscience*, 27(21), 5730–5743.

Gerdeman, G. L., & Lovinger, D. M. (2003). Emerging roles for endocannabinoids in long-term synaptic plasticity. *British journal of pharmacology*, 140(5), 781–789.

Gibson, H. E., Edwards, J. G., Page, R. S., Van Hook, M. J., & Kauer, J. A. (2008). TRPV1 channels mediate long-term depression at synapses on hippocampal interneurons. *Neuron*, 57(5), 746–759.

Golech, S. A., McCarron, R. M., Chen, Y., Bembry, J., Lenz, F., Mechoulam, R., Shohami, E., & Spatz, M. (2004). Human brain endothelium: Coexpression and function of vanilloid and endocannabinoid receptors. *Molecular Brain Research*, *132*(1), 87–92.

Gómez-Gonzalo, M., Navarrete, M., Perea, G., Covelo, A., Martín-Fernández, M., Shigemoto, R., Luján, R., & Araque, A. (2015). Endocannabinoids induce lateral long-term potentiation of transmitter release by stimulation of gliotransmission. *Cerebral Cortex*, *25*(10), 3699–3712.

Gómez-Gonzalo, M., Martin-fernandez, M., Martínez-murillo, R., Hernández-vivanco, A., Jamison, S., Fernandez, A. P., Calero, P., Futch, H. S., Corpas, R., Sanfeliu, C., & Araque, A. (2018). Neuron.-astrocye signaling is preserved in the ageing brain. *Glia*, *65*(4), 612–624.

Gonsiorek, W., Lunn, C., Fan, X., Narula, S., Lundell, D., & Hipkin, R. W. (2000). Endocannabinoid 2-arachidonyl glycerol is a full agonist through human type 2 cannabinoid receptor: Antagonism by anandamide. *Molecular Pharmacology*, *57*(5), 1045–1050.

Grandes, P., & Streit, P. (1991). Effect of perforant path lesion on pattern of glutamate-like immunoreactivity in rat dentate gyrus. *Neuroscience*, 41(2-3), 391–400.

Gruber, A. J., Calhoon, G. G., Shusterman, I., Schoenbaum, G., Roesch, M. R., & O'Donnell, P. (2010). More is less: A disinhibited prefrontal cortex impairs cognitive flexibility. *Journal of Neuroscience*, *30*(50), 17102–17110.

Grueter, B. A., Brasnjo, G., & Malenka, R. C. (2010). Postsynaptic TRPV1 triggers cell type-specific long-term depression in the nucleus accumbens. *Nature neuroscience*, 13(12), 1519–1525.

Guggenhuber, S., Monory, K., Lutz, B., & Klugmann, M. (2010). AAV vector-mediated overexpression of CB_1 cannabinoid receptor in pyramidal neurons of the hippocampus protects against seizure-induced excitoxicity. *PloS one*, 5(12), e15707.

Gutiérrez-Rodríguez, A., Puente, N., Elezgarai, I., Ruehle, S., Lutz, B., Reguero, L., Gerrikagoitia, I., Marsicano, G., & Grandes, P. (2017). Anatomical characterization of the cannabinoid CB_1 receptor in cell-type–specific mutant mouse rescue models. *Journal of Comparative Neurology*, *525*(2), 302–318.

Gutiérrez-Rodríguez, A., Bonilla-Del Río, I., Puente, N., Gómez-Urquijo, S. M., Fontaine, C. J., Egaña-Huguet, J., Elezgarai, I., Ruehle, S., Lutz, B., Robin, L. M., Soria-Gómez, E., Bellocchio, L., Padwal, J. D., van der Stelt, M., Mendizabal-Zubiaga, J., Reguero, L., Ramos, A., Gerrikagoitia, I., Marsicano, G., & Grandes, P. (2018). Localization of the cannabinoid type-1 receptor in subcellular astrocyte compartments of mutant mouse hippocampus. *Glia*, *66*(7), 1417–1431.

Guzmán, M., Galve-Roperh, I., & Sánchez, C. (2001). Ceramide: a new second messenger of cannabinoid action. *Trends in pharmacological sciences*, 22(1), 19–22.

Hájos, N., Ledent, C., & Freund, T. F. (2001). Novel cannabinoid-sensitive receptor mediates inhibition of glutamatergic synaptic transmission in the hippocampus. *Neuroscience*, *106*(1), 1–4.

Halassa, M. M., Fellin, T., Takano, H., Dong, J. H., & Haydon, P. G. (2007). Synaptic islands defined by the territory of a single astrocyte. *Journal of Neuroscience*, *27*(24), 6473–6477.

Han, J., Kesner, P., Metna-Laurent, M., Duan, T., Xu, L., Georges, F., Koehl, M., Abrous, D. N., Mendizabal-Zubiaga, J., Grandes, P., Liu, Q., Bai, G., Wang, W., Xiong, L., Ren, W., Marsicano, G., & Zhang, X. (2012). Acute cannabinoids impair working memory through astroglial CB_1 receptor modulation of hippocampal LTD. *Cell*, *148*(5), 1039–1050.

Hargreaves, E. L., Rao, G., Lee, I., & Knierim, J. J. (2005). Major dissociation between medial and lateral entorhinal input to dorsal hippocampus. *Science (New York, N.Y.)*, 308(5729), 1792–1794.

Häring, M., Marsicano, G., Lutz, B., & Monory, K. (2007). Identification of the cannabinoid receptor type 1 in serotonergic cells of raphe nuclei in mice. *Neuroscience*, *146*(3), 1212–1219.

Haydon, P. G., & Carmignoto, G. (2006). Astrocyte control of synaptic transmission and neurovascular coupling. *Physiological Reviews*, *86*(3), 1009–1031.

Haydon P. G. (2017). Astrocytes and the modulation of sleep. *Current opinion in neurobiology*, 44, 28–33.

Hirrlinger, P. G., Scheller, A., Braun, C., Hirrlinger, J., & Kirchhoff, F. (2006). Temporal control of gene recombination in astrocytes by transgenic expression of the tamoxifen-inducible DNA recombinase variant CreERT2. *Glia*, 54(1), 11–20.

Hebert-Chatelain, E., Reguero, L., Puente, N., Lutz, B., Chaouloff, F., Rossignol, R., Piazza, P. V., Benard, G., Grandes, P., & Marsicano, G. (2014). Studying mitochondrial CB_1 receptors: Yes we can. *Molecular Metabolism*, *3*(4), 339.

Hebert-Chatelain, E., Reguero, L., Puente, N., Lutz, B., Chaouloff, F., Rossignol, R., Piazza, P. V., Benard, G., Grandes, P., & Marsicano, G. (2014). Cannabinoid control of brain bioenergetics: Exploring the subcellular localization of the CB_1 receptor. *Molecular Metabolism*, *3*(4), 495–504.

Hebert-Chatelain, E., Desprez, T., Serrat, R., Bellocchio, L., Soria-Gomez, E., Busquets-Garcia, A., Pagano Zottola, A. C., Delamarre, A., Cannich, A., Vincent, P., Varilh, M., Robin, L. M., Terral, G., García-Fernández, M. D., Colavita, M., Mazier, W., Drago, F., Puente, N., Reguero, L., … Marsicano, G. (2016). A cannabinoid link between mitochondria and memory. *Nature*, *539*(7630), 555–559.

Heifets, B. D., & Castillo, P. E. (2009). Endocannabinoid signaling and long-term synaptic plasticity. *Annual review of physiology*, 71, 283–306.

Helling, S., Vogt, S., Rhiel, A., Ramzan, R., Wen, L., Marcus, K., & Kadenbach, B. (2008). Phosphorylation and kinetics of mammalian cytochrome c oxidase. *Molecular and Cellular Proteomics*, *7*(9), 1714–1724.

Henneberger, C. (2017). Does rapid and physiological astrocyte–neuron signalling amplify epileptic activity? *Journal of Physiology*, *595*(6), 1917–1927.

Herkenham, M., Lynn, A. B., Little, M. D., Johnson, M. R., Melvin, L. S., de Costa, B. R., & Rice, K. C. (1990). Cannabinoid receptor localization in brain. *Proceedings of the National Academy of Sciences of the United States of America*, 87(5), 1932–1936.

Hermann, H., Marsicano, G., & Lutz, B. (2002). Coexpression of the cannabinoid receptor type 1 with dopamine and serotonin receptors in distinct neuronal subpopulations of the adult mouse forebrain. *Neuroscience*, *109*(3), 451–460.

Hill, E. L., Gallopin, T., Férézou, I., Cauli, B., Rossier, J., Schweitzer, P., & Lambolez, B. (2007). Functional CB_1 receptors are broadly expressed in neocortical GABAergic and glutamatergic neurons. *Journal of neurophysiology*, 97(4), 2580–2589.

Hillard, C. J. (2014). Stress regulates endocannabinoid-CB_1 receptor signaling. *Seminars in Immunology*, *26*(5), 380–388.

Hol, E. M., & Pekny, M. (2015). Glial fibrillary acidic protein (GFAP) and the astrocyte intermediate filament system in diseases of the central nervous system. *Current opinion in cell biology*, 32, 121–130.

Howlett, A. C., Barth, F., Bonner, T. I., Cabral, G., Casellas, P., Devane, W. A., Felder, C. C., Herkenham, M., Mackie, K., Martin, B. R., Mechoulam, R., & Pertwee, R. G. (2002). International Union of Pharmacology. XXVII. Classification of cannabinoid receptors. *Pharmacological Reviews*, *54*(2), 161–202.

Hu, S. S., & Mackie, K. (2015). Distribution of the Endocannabinoid System in the Central Nervous System. *Handbook of experimental pharmacology*, 231, 59–93.

Ishac, E. J. N., Jiang, L., Lake, K. D., Varga, K., Abood, M. E., & Kunos, G. (1996). Inhibition of exocytotic noradrenaline release by presynaptic cannabinoid CB_1 receptors on peripheral sympathetic nerves. *British Journal of Pharmacology*, *118*(8), 2023–2028.

Jackson, J. G., O'Donnell, J. C., Takano, H., Coulter, D. A., & Robinson, M. B. (2014). Neuronal activity and glutamate uptake decrease mitochondrial mobility in astrocytes and position mitochondria near glutamate transporters. *The Journal of neuroscience: the official journal of the Society for Neuroscience*, 34(5), 1613–1624.

Jimenez-Blasco, D., Busquets-Garcia, A., Hebert-Chatelain, E., Serrat, R., Vicente-Gutierrez, C., Ioannidou, C., Gómez-Sotres, P., Lopez-Fabuel, I., Resch-Beusher, M., Resel, E., Arnouil, D., Saraswat, D., Varilh, M., Cannich, A., Julio-Kalajzic, F., Bonilla-Del Río, I., Almeida, A., Puente, N., Achicallende, S., Lopez-Rodriguez, M. L., … Marsicano, G. (2020). Glucose metabolism links astroglial mitochondria to cannabinoid effects. *Nature*, 583(7817), 603–608.

Kamprath, K., Plendl, W., Marsicano, G., Deussing, J. M., Wurst, W., Lutz, B., & Wotjak, C. T. (2009). Endocannabinoids mediate acute fear adaptation via glutamatergic neurons independently of corticotropin-releasing hormone signaling. *Genes, Brain and Behavior*, *8*(2), 203–211.

Kano, M., Ohno-Shosaku, T., Hashimotodani, Y., Uchigashima, M., & Watanabe, M. (2009). Endocannabinoid-mediated control of synaptic transmission. *Physiological Reviews*, *89*(1), 309–380.

Karlsson, R. M., Adermark, L., Molander, A., Perreau-Lenz, S., Singley, E., Solomon, M., Holmes, A., Tanaka, K., Lovinger, D. M., Spanagel, R., & Heilig, M. (2012). Reduced alcohol intake and reward associated with impaired endocannabinoid signaling in mice with a deletion of the glutamate transporter GLAST. *Neuropharmacology*, 63(2), 181–189.

Katona, I., Sperlágh, B., Sík, A., Käfalvi, A., Vizi, E. S., Mackie, K., & Freund, T. F. (1999). Presynaptically located CB_1 cannabinoid receptors regulate GABA release from axon terminals of specific hippocampal interneurons. *Journal of Neuroscience*, *19*(11), 4544–4558.

Katona, I., Sperlágh, B., Maglóczky, Z., Sántha, E., Köfalvi, A., Czirják, S., Mackie, K., Vizi, E. S., & Freund, T. F. (2000). GABAergic interneurons are the targets of cannabinoid actions in the human hippocampus. *Neuroscience*, *100*(4), 797–804.

Katona, I., Urbán, G. M., Wallace, M., Ledent, C., Jung, K. M., Piomelli, D., Mackie, K., & Freund, T. F. (2006). Molecular composition of the endocannabinoid system at glutamatergic synapses. *Journal of Neuroscience*, *26*(21), 5628–5637.

Katona, I., & Freund, T. F. (2012). Multiple functions of endocannabinoid signaling in the brain. *Annual review of neuroscience*, 35, 529–558.

Katona I. (2015). Cannabis and Endocannabinoid Signaling in Epilepsy. *Handbook of experimental pharmacology*, 231, 285–316.

Kauer, J. A., & Gibson, H. E. (2009). Hot flash: TRPV channels in the brain. *Trends in neurosciences*, 32(4), 215–224.

Kawamura, Y., Fukaya, M., Maejima, T., Yoshida, T., Miura, E., Watanabe, M., Ohno-Shosaku, T., & Kano, M. (2006). The CB_1 cannabinoid receptor is the major cannabinoid receptor at excitatory presynaptic sites in the hippocampus and cerebellum. *Journal of Neuroscience*, *26*(11), 2991–3001.

Kleppisch, T., Wolfsgruber, W., Feil, S., Allmann, R., Wotjak, C. T., Goebbels, S., Nave, K. A., Hofmann, F., & Feil, R. (2003). Hippocampal cGMP-dependent protein kinase I supports an age- and protein

synthesis-dependent component of long-term potentiation but is not essential for spatial reference and contextual memory. *Journal of Neuroscience*, *23*(14), 6005–6012.

Koch, M., Varela, L., Kim, J. G., Kim, J. D., Hernández-Nuño, F., Simonds, S. E., Castorena, C. M., Vianna, C. R., Elmquist, J. K., Morozov, Y. M., Rakic, P., Bechmann, I., Cowley, M. A., Szigeti-Buck, K., Dietrich, M. O., Gao, X. B., Diano, S., & Horvath, T. L. (2015). Hypothalamic POMC neurons promote cannabinoid-induced feeding. *Nature*, 519(7541), 45–50.

Kofuji, P., & Araque, A. (2021). G-Protein-Coupled Receptors in Astrocyte–Neuron Communication. *Neuroscience*, *456*, 71–84.

Kovács, A., Bordás, C., Bíró, T., Hegyi, Z., Antal, M., Szücs, P., & Pál, B. (2017). Direct presynaptic and indirect astrocyte-mediated mechanisms both contribute to endocannabinoid signaling in the pedunculopontine nucleus of mice. *Brain structure & function*, 222(1), 247–266.

Lafourcade, M., Elezgarai, I., Mato, S., Bakiri, Y., Grandes, P., & Manzoni, O. J. (2007). Molecular Components and Functions of the Endocannabinoid System in Mouse Prefrontal Cortex. *PLoS ONE*, *2*(8), 1–11.

Laughlin, S. B., de Ruyter van Steveninck, R. R., & Anderson, J. C. (1998). The metabolic cost of neural information. *Nature neuroscience*, 1(1), 36–41.

Laviolette, S. R., & Grace, A. A. (2006). Cannabinoids Potentiate Emotional Learning Plasticity in Neurons of the Medial Prefrontal Cortex through Basolateral Amygdala Inputs. *The Journal of neuroscience : the official journal of the Society for Neuroscience*, 26(24), 6458–6468.

Lehre, K. P., & Danbolt, N. C. (1998). The number of glutamate transporter subtype molecules at glutamatergic synapses: chemical and stereological quantification in young adult rat brain. The Journal of neuroscience: the official journal of the *Society for Neuroscience*, 18(21), 8751–8757.

Leo, A., Russo, E., & Elia, M. (2016). Cannabidiol and epilepsy: Rationale and therapeutic potential. *Pharmacological Research*, *107*, 85–92.

Lévesque, M., & Avoli, M. (2013). The kainic acid model of temporal lobe epilepsy. *Neuroscience and biobehavioral reviews*, 37(10 Pt 2), 2887–2899.

Li, Z., Okamoto, K., Hayashi, Y., & Sheng, M. (2004). The importance of dendritic mitochondria in the morphogenesis and plasticity of spines and synapses. *Cell*, 119(6), 873–887.

Li, H. B., Mao, R. R., Zhang, J. C., Yang, Y., Cao, J., & Xu, L. (2008). Antistress effect of TRPV1 channel on synaptic plasticity and spatial memory. *Biological psychiatry*, 64(4), 286–292.

Lin, H. C., Mao, S. C., Su, C. L., & Gean, P. W. (2009). The role of prefrontal cortex CB_1 receptors in the modulation of fear memory. *Cerebral cortex (New York, N.Y. : 1991)*, 19(1), 165–175.

Lisman, J. E., Talamini, L. M., & Raffone, A. (2005). Recall of memory sequences by interaction of the dentate and CA3: a revised model of the phase precession. *Neural networks : the official journal of the International Neural Network Society*, 18(9), 1191–1201.

López, A., Aparicio, N., Pazos, M. R., Grande, M. T., Barreda-Manso, M. A., Benito-Cuesta, I., Vázquez, C., Amores, M., Ruiz-Pérez, G., García-García, E., Beatka, M., Tolón, R. M., Dittel, B. N., Hillard, C. J., & Romero, J. (2018). Cannabinoid CB_2 receptors in the mouse brain: Relevance for Alzheimer's disease. *Journal of Neuroinflammation*, *15*(1), 1–11.

Lu, H. C., & Mackie, K. (2016). An Introduction to the Endogenous Cannabinoid System. *Biological psychiatry,* 79(7), 516–525.

Ludányi, A., Eross, L., Czirják, S., Vajda, J., Halász, P., Watanabe, M., Palkovits, M., Maglóczky, Z., Freund, T. F., & Katona, I. (2008). Downregulation of the CB_1 cannabinoid receptor and related molecular elements of the endocannabinoid system in epileptic human hippocampus. *Journal of Neuroscience*, *28*(12), 2976–2990.

Luk, T., Jin, W., Zvonok, A., Lu, D., Lin, X. Z., Chavkin, C., Makriyannis, A., & Mackie, K. (2004). Identification of a potent and highly efficacious, yet slowly desensitizing CB_1 cannabinoid receptor agonist. *British Journal of Pharmacology*, *142*(3), 495–500.

Lüttjohann, A., Fabene, P. F., & van Luijtelaar, G. (2009). A revised Racine's scale for PTZ-induced seizures in rats. *Physiology and Behavior*, *98*(5), 579–586.

Lutz, B., Marsicano, G., Maldonado, R., & Hillard, C. J. (2015). The endocannabinoid system in guarding against fear, anxiety and stress. *Nature reviews. Neuroscience*, 16(12), 705–718.

Lutzu, S., & Castillo, P. E. (2021). Modulation of NMDA Receptors by G-protein-coupled receptors: Role in Synaptic Transmission, Plasticity and Beyond. *Neuroscience*, 456, 27–42.

Lyssand, J. S., & Bajjalieh, S. M. (2007). The heterotrimeric [corrected] G protein subunit G alpha i is present on mitochondria. *FEBS letters*, 581(30), 5765–5768.

MacAskill, A. F., & Kittler, J. T. (2010). Control of mitochondrial transport and localization in neurons. *Trends in cell biology*, 20(2), 102–112.

Maccarrone, M., Rossi, S., Bari, M., De Chiara, V., Fezza, F., Musella, A., Gasperi, V., Prosperetti, C., Bernardi, G., Finazzi-Agrò, A., Cravatt, B. F., Centonze, D. (2008). Anandamide inhibits metabolism and physiological actions of 2-arachidonoylglycerol in the striatum. *Nature Neuroscience,* 11, 152–159.

Maccarone, R., Rapino, C., Zerti, D., Di Tommaso, M., Battista, N., Di Marco, S., Bisti, S., & Maccarrone, M. (2016). Modulation of Type-1 and Type-2 cannabinoid receptors by saffron in a rat model of retinal neurodegeneration. *PLoS ONE*, *11*(11), 1–20.

Mackie K. (2005). Distribution of cannabinoid receptors in the central and peripheral nervous system. *Handbook of experimental pharmacology*, (168), 299–325.

Mackie, K., & Stella, N. (2006). Cannabinoid receptors and endocannabinoids: Evidence for new players. *The AAPS Journal*, *8*(2), E298–E306.

Magistretti, P. J., & Pellerin, L. (1999). Astrocytes couple synaptic activity to glucose utilization in the brain. *News in Physiological Sciences*, *14*(5), 177–182.

Magistretti, P. J., & Allaman, I. (2018). Lactate in the brain: from metabolic end-product to signalling molecule. *Nature reviews. Neuroscience*, 19(4), 235–249.

Mailleux, P., & Vanderhaeghen, J. J. (1992). Age-related loss of cannabinoid receptor binding sites and mRNA in the rat striatum. *Neuroscience letters*, 147(2), 179–181.

Maione, S., Cristino, L., Migliozzi, A. L., Georgiou, A. L., Starowicz, K., Salt, T. E., & Di Marzo, V. (2009). TRPV1 channels control synaptic plasticity in the developing superior colliculus. *The Journal of physiology*, 587(Pt 11), 2521–2535.

Marsch, R., Foeller, E., Rammes, G., Bunck, M., Kössl, M., Holsboer, F., Zieglgänsberger, W., Landgraf, R., Lutz, B., & Wotjak, C. T. (2007). Reduced anxiety, conditioned fear, and hippocampal long-term potentiation in transient receptor potential vanilloid type 1 receptor-deficient mice. *The Journal of neuroscience : the official journal of the Society for Neuroscience*, 27(4), 832–839.

Marsicano, G., & Lutz, B. (1999). Expression of the cannabinoid receptor CB_1 in distinct neuronal subpopulations in the adult mouse forebrain. *European Journal of Neuroscience*, *11*(12), 4213–4225.

Marsicano, G., Wotjak, C. T., Azad, S. C., Bisogno, T., Rammes, G., Cascioll, M. G., Hermann, H., Tang, J., Hofmann, C., Zieglgänsberger, W., Di Marzo, V., & Lutz, B. (2002). The endogenous cannabinoid system controls extinction of aversive memories. *Nature*, *418*(6897), 530–534.

Marsicano, G., Goodenough, S., Monory, K., Hermann, H., Eder, M., Cannich, A., Azad, S. C., Cascio, M. G., Gutiérrez, S. O., van der Stelt, M., López-Rodriguez, M. L., Casanova, E., Schütz, G., Zieglgänsberger, W., Di Marzo, V., Behl, C., & Lutz, B. (2003). CB_1 cannabinoid receptors and on-demand defense against excitotoxicity. *Science*, 302(5642), 84–88.

Marsicano, G. & Lutz, B. (2006). Neuromodulatory functions of the endocannabinoid system. *Journal of endocrinological investigation*, 29(3), 27.

Marsicano, G. & Kuner, R. (2008). Anatomical distribution of receptors, ligands and enzymes in the brain and in the spinal cord: circuitries and neurochemistry. In *Cannabinoids and the Brain, Springer, Boston, MA.*, 161-201.

Martin-Fernandez, M., Jamison, S., Robin, L. M., Zhao, Z., Martin, E. D., Aguilar, J., Benneyworth, M. A., Marsicano, G., & Araque, A. (2017). Synapse-specific astrocyte gating of amygdala-related behavior. *Nature neuroscience*, 20(11), 1540–1548.

Martín-García, E., Fernández-Castillo, N., Burokas, A., Gutiérrez-Cuesta, J., Sánchez-Mora, C., Casas, M., Ribasés, M., Cormand, B., & Maldonado, R. (2015). Frustrated expected reward induces differential transcriptional changes in the mouse brain. *Addiction Biology*, *20*(1), 22–27.

Mathers, D. C., & Ghodse, A. H. (1992). Cannabis and psychotic illness. *The British journal of psychiatry : the journal of mental science, 161*, 648–653.

Matsuda, L. A., Lolait, S. J., Brownstein, M. J., Young, A. C., & Bonner, T. I. (1990). Structure of a cannabinoid receptor and functional expression of the cloned cDNA. *Nature*, *346*(6284), 561–564.

Matsuda, L. A., Bonner, T. I. & Lolait, S. J. (1993). Localization of cannabinoid receptor mRNA in rat brain. *Journal of Comparative Neurology*, 327(4), 535-550.

Mattson, M. P., Gleichmann, M., & Cheng, A. (2008). Mitochondria in neuroplasticity and neurological disorders. *Neuron*, 60(5), 748–766.

Mechoulam, R., Ben-Shabat, S., Hanus, L., Ligumsky, M., Kaminski, N. E., Schatz, A. R., Gopher, A., Almog, S., Martin, B. R., Compton, D. R., Pertwee, R. G., Griffin, G., Bayewitch, M., Barg, J., & Vogel, Z. (1995). Identification of an endogenous 2-monoglyceride, present in canine gut, that binds to cannabinoid receptors. *Biochemical Pharmacology*, *50*(1), 83–90.

Melser, S., Pagano Zottola, A. C., Serrat, R., Puente, N., Grandes, P., Marsicano, G., & Hebert-Chatelain, E. (2017). Functional Analysis of Mitochondrial CB_1 Cannabinoid Receptors ($mtCB_1$) in the Brain. *Methods in enzymology*, 593, 143–174.

Mendizabal-Zubiaga, J., Melser, S., Bénard, G., Ramos, A., Reguero, L., Arrabal, S., Elezgarai, I., Gerrikagoitia, I., Suarez, J., De Fonseca, F. R., Puente, N., Marsicano, G., & Grandes, P. (2016). Cannabinoid CB_1 receptors are localized in striated muscle mitochondria and regulate mitochondrial respiration. *Frontiers in Physiology*, *7*(OCT), 1–10.

Metna-Laurent, M., & Marsicano, G. (2015). Rising stars: Modulation of brain functions by astroglial type-1 cannabinoid receptors. *Glia*, *63*(3), 353–364.

Micale, V., Cristino, L., Tamburella, A., Petrosino, S., Leggio, G. M., Drago, F., & Di Marzo, V. (2009). Anxiolytic effects in mice of a dual blocker of fatty acid amide hydrolase and transient receptor potential vanilloid type-1 channels. *Neuropsychopharmacology : official publication of the American College of Neuropsychopharmacology*, 34(3), 593–606.

Moldrich, G., & Wenger, T. (2000). Localization of the CB_1 cannabinoid receptor in the rat brain. An immunohistochemical study. *Peptides*, *21*(11), 1735–1742.

Molina-Holgado, F., Molina-Holgado, E., Guaza, C., & Rothwell, N. J. (2002). Role of CB_1 and CB_2 receptors in the inhibitory effects of cannabinoids on lipopolysaccharide-induced nitric oxide release in astrocyte cultures. *Journal of Neuroscience Research*, *67*(6), 829–836.

Monory, K., Massa, F., Egertová, M., Eder, M., Blaudzun, H., Westenbroek, R., Kelsch, W., Jacob, W., Marsch, R., Ekker, M., Long, J., Rubenstein, J. L., Goebbels, S., Nave, K. A., During, M., Klugmann, M., Wölfel, B., Dodt, H. U., Zieglgänsberger, W., Wotjak, C. T., … Lutz, B. (2006). The endocannabinoid system controls key epileptogenic circuits in the hippocampus. *Neuron*, 51(4), 455–466.

Monory, K., Blaudzun, H., Massa, F., Kaiser, N., Lemberger, T., Schütz, G., Wotjak, C. T., Lutz, B., & Marsicano, G. (2007). Genetic dissection of behavioural and autonomic effects of Delta(9)-tetrahydrocannabinol in mice. *PLoS biology*, 5(10), e269.

Mori, F., Ribolsi, M., Kusayanagi, H., Monteleone, F., Mantovani, V., Buttari, F., Marasco, E., Bernardi, G., Maccarrone, M., & Centonze, D. (2012). TRPV1 channels regulate cortical excitability in humans. *The Journal of neuroscience : the official journal of the Society for Neuroscience*, 32(3), 873–879.

Morozov, Y. M., Torii, M., & Rakic, P. (2009). Origin, early commitment, migratory routes, and destination of cannabinoid type 1 receptor-containing interneurons. *Cerebral Cortex*, *19*(SUPPL. 1).

Munro, S., Thomas, K. L., & Abu-Shaar, M. (1993). Molecular characterization of a peripheral receptor for cannabinoids. *Nature*, *365*(6441), 61–65.

Myers, K. M., & Davis, M. (2002). Systems-level reconsolidation: reengagement of the hippocampus with memory reactivation. *Neuron*, 36(3), 340–343.

Navarrete, M., & Araque, A. (2008). Endocannabinoids Mediate Neuron-Astrocyte Communication. *Neuron*, *57*(6), 883–893.

Navarrete, M., & Araque, A. (2010). Endocannabinoids potentiate synaptic transmission through stimulation of astrocytes. *Neuron*, *68*(1), 113–126.

Navarrete, M., Perea, G., Maglio, L., Pastor, J., García De Sola, R., & Araque, A. (2013). Astrocyte calcium signal and gliotransmission in human brain tissue. *Cerebral Cortex*, *23*(5), 1240–1246.

Navarrete, M., Díez, A., & Araque, A. (2014). Astrocytes in endocannabinoid signalling. *Philosophical Transactions of the Royal Society B: Biological Sciences*, *369*(1654).

Nicholls, D. G., and Ferguson, S. J. (2002). Bioenergetics. *Biochemistry*, 69, 818–819.

Nolte, C., Matyash, M., Pivneva, T., Schipke, C. G., Ohlemeyer, C., Hanisch, U. K., Kirchhoff, F., & Kettenmann, H. (2001). GFAP promoter-controlled EGFP-expressing transgenic mice: a tool to visualize astrocytes and astrogliosis in living brain tissue. *Glia*, 33(1), 72–86.

Nyíri, G., Szabadits, E., Cserép, C., Mackie, K., Shigemoto, R., & Freund, T. F. (2005). GABAB and CB_1 cannabinoid receptor expression identifies two types of septal cholinergic neurons. *The European journal of neuroscience*, 21(11), 3034–3042.

Oliveira, J. F., Sardinha, V. M., Guerra-Gomes, S., Araque, A., & Sousa, N. (2015). Do stars govern our actions? Astrocyte involvement in rodent behavior. *Trends in neurosciences*, 38(9), 535–549.

Oliveira da Cruz, J. F., Robin, L. M., Drago, F., Marsicano, G., & Metna-Laurent, M. (2016). Astroglial type-1 cannabinoid receptor (CB_1): A new player in the tripartite synapse. *Neuroscience*, *323*, 35–42.

Oropeza, V. C., Mackie, K., & Van Bockstaele, E. J. (2007). Cannabinoid receptors are localized to noradrenergic axon terminals in the rat frontal cortex. *Brain research*, 1127(1), 36–44.

Pasupathy, A., & Miller, E. K. (2005). Different time courses of learning-related activity in the prefrontal cortex and striatum. *Nature*, *433*(7028), 873–876.

Pekny, M., & Pekna, M. (2014). Astrocyte reactivity and reactive astrogliosis: Costs and benefits. *Physiological Reviews*, *94*(4), 1077–1098.

Peñasco, S., Rico-Barrio, I., Puente, N., Gómez-Urquijo, S. M., Fontaine, C. J., Egaña-Huguet, J., Achicallende, S., Ramos, A., Reguero, L., Elezgarai, I., Nahirney, P. C., Christie, B. R., & Grandes, P. (2019). Endocannabinoid long-term depression revealed at medial perforant path excitatory synapses in the dentate gyrus. *Neuropharmacology*, 153, 32–40.

Peñasco, S., Rico-Barrio, I., Puente, N., Fontaine, C. J., Ramos, A., Reguero, L., Gerrikagoitia, I., de Fonseca, F. R., Suarez, J., Barrondo, S., Aretxabala, X., García del Caño, G., Sallés, J., Elezgarai, I., Nahirney, P. C., Christie, B. R., & Grandes, P. (2020). Intermittent ethanol exposure during adolescence impairs cannabinoid type 1 receptor-dependent long-term depression and recognition memory in adult mice. *Neuropsychopharmacology*, *45*(2), 309–318.

Perea, G., & Araque, A. (2002). Communication between astrocytes and neurons: A complex language. *Journal of Physiology, Paris*, *96*(3–4), 199–207.

Perea, G., & Araque, A. (2005). Synaptic regulation of the astrocyte calcium signal. *Journal of Neural Transmission*, *112*(1), 127–135.

Perea, G., & Araque, A. (2005). Properties of synaptically evoked astrocyte calcium signal reveal synaptic information processing by astrocytes. *Journal of Neuroscience*, *25*(9), 2192–2203.

Perea, G., Navarrete, M., & Araque, A. (2009). Tripartite synapses: astrocytes process and control synaptic information. *Trends in neurosciences*, 32(8), 421–431.

Perea, G., & Araque, A. (2010). GLIA modulates synaptic transmission. *Brain research reviews*, 63(1-2), 93–102.

Pertwee R. G. (2001). Cannabinoid receptors and pain. *Progress in neurobiology*, 63(5), 569–611.

Pertwee, R. G. (2009). Emerging strategies for exploiting cannabinoid receptor agonists as medicines. *British Journal of Pharmacology*, *156*(3), 397–411.

Pertwee, R. G., Howlett, A. C., Abood, M. E., Alexander, S. P. H., Di Marzo, V., Elphick, M. R., Greasley, P. J., Hansen, H. S., Kunos, G., Mackie, K., Mechoulam, R., & Ross, R. A. (2010). International Union of Basic and Clinical Pharmacology. LXXIX. Cannabinoid receptors and their ligands: Beyond CB_1 and CB_2. *Pharmacological Reviews*, *62*(4), 588–631.

Pertwee R. G. (2015). Endocannabinoids and Their Pharmacological Actions. *Handbook of experimental pharmacology*, 231, 1–37.

Petersen, R. P., Moradpour, F., Eadie, B. D., Shin, J. D., Kannangara, T. S., Delaney, K. R., & Christie, B. R. (2013). Electrophysiological identification of medial and lateral perforant path inputs to the dentate gyrus. *Neuroscience*, *252*, 154–168.

Petit, J. M., & Magistretti, P. J. (2016). Regulation of neuron-astrocyte metabolic coupling across the sleep-wake cycle. *Neuroscience*, *323*, 135–156.

Piazza, P. V., Cota, D., & Marsicano, G. (2017). The CB_1 Receptor as the Cornerstone of Exostasis. *Neuron*, *93*(6), 1252–1274.

Piluzza, G., Delogu, G., Cabras, A., Marceddu, S., & Bullitta, S. (2013). Differentiation between fiber and drug types of hemp (Cannabis sativa L.) from a collection of wild and domesticated accessions. *Genetic Resources and Crop Evolution*, *60*(8), 2331–2342.

Piomelli, D. (2003). The molecular logic of endocannabinoid signalling. *Nature Reviews Neuroscience*, *4*(11), 873–884.

Piomelli D. (2014). More surprises lying ahead. The endocannabinoids keep us guessing. *Neuropharmacology*, 76 Pt B, 228–234.

Pistis, M., Muntoni, A. L., Pillolla, G., & Gessa, G. L. (2002). Cannabinoids inhibit excitatory inputs to neurons in the shell of the nucleus accumbens: an in vivo electrophysiological study. *The European journal of neuroscience*, 15(11), 1795–1802.

Puente, N., Cui, Y., Lassalle, O., Lafourcade, M., Georges, F., Venance, L., Grandes, P., & Manzoni, O. J. (2011). Polymodal activation of the endocannabinoid system in the extended amygdala. *Nature Neuroscience*, *14*(12), 1542–1547.

Puente, N., Bonilla-Del Río, I., Achicallende, S., Nahirney, P., & Grandes, P. (2019). High-resolution Immunoelectron Microscopy Techniques for Revealing Distinct Subcellular Type 1 Cannabinoid Receptor Domains in Brain. *Bio-Protocol*, *9*(2).

Puig, M. V., & Gulledge, A. T. (2011). Serotonin and prefrontal cortex function: neurons, networks, and circuits. *Molecular Neurobiology*, *44*(3), 449–464.

Ortinski, P. I., Dong, J., Mungenast, A., Yue, C., Takano, H., Watson, D. J., Haydon, P. G., & Coulter, D. A. (2010). Selective induction of astrocytic gliosis generates deficits in neuronal inhibition. *Nature neuroscience*, 13(5), 584–591.

Racine R. J. (1972). Modification of seizure activity by electrical stimulation. II. Motor seizure. *Electroencephalography and clinical neurophysiology*, 32(3), 281–294.

Rao, A., & Craig, A. M. (1997). Activity regulates the synaptic localization of the NMDA receptor in hippocampal neurons. *Neuron*, 19(4), 801–812.

Reddy D. S. (2014). Neurosteroids and their role in sex-specific epilepsies. *Neurobiology of disease*, 72 Pt B, 198–209.

Reddy, D. S., & Golub, V. M. (2016). The pharmacological basis of cannabis therapy for epilepsy. *Journal of Pharmacology and Experimental Therapeutics*, *357*(1), 45–55.

Reguero, L., Puente, N., Elezgarai, I., Mendizabal-Zubiaga, J., Canduela, M. J., Buceta, I., Ramos, A., Suárez, J., de Fonseca, F. R., Marsicano, G., & Grandes, P. (2011). GABAergic and cortical and subcortical glutamatergic axon terminals contain CB_1 cannabinoid receptors in the ventromedial nucleus of the hypothalamus. *PLoS ONE*, *6*(10).

Renau-Piqueras, J., Zaragoza, R., De Paz, P., Baguena-Cervellera, R., Megias, L., & Guerri, C. (1989). Effects of prolonged ethanol exposure on the glial fibrillary acidic protein-containing intermediate filaments of astrocytes in primary culture: a quantitative immunofluorescence and immunogold electron microscopic study. *The journal of histochemistry and cytochemistry: official journal of the Histochemistry Society,* 37(2), 229–240.

Reyes-Harde, M., Potter, B. V., Galione, A., & Stanton, P. K. (1999). Induction of hippocampal LTD requires nitric-oxide-stimulated PKG activity and Ca2+ release from cyclic ADP-ribose-sensitive stores. *Journal of neurophysiology*, 82(3), 1569–1576.

Rimondini, R., Arlinde, C., Sommer, W., & Heilig, M. (2002). Long-lasting increase in voluntary ethanol consumption and transcriptional regulation in the rat brain after intermittent exposure to alcohol. *FASEB journal: official publication of the Federation of American Societies for Experimental Biology*, 16(1), 27–35.

Robel, S., Buckingham, S. C., Boni, J. L., Campbell, S. L., Danbolt, N. C., Riedemann, T., Sutor, B., & Sontheimer, H. (2015). Reactive astrogliosis causes the development of spontaneous seizures. *Journal of Neuroscience*, *35*(8), 3330–3345.

Robin, L. M., Oliveira da Cruz, J. F., Langlais, V. C., Martin-Fernandez, M., Metna-Laurent, M., Busquets-Garcia, A., Bellocchio, L., Soria-Gomez, E., Papouin, T., Varilh, M., Sherwood, M. W., Belluomo, I., Balcells, G., Matias, I., Bosier, B., Drago, F., Van Eeckhaut, A., Smolders, I., Georges, F., … Marsicano, G. (2018). Astroglial CB_1 Receptors Determine Synaptic D-Serine Availability to Enable Recognition Memory. *Neuron*, *98*(5), 935-944.e5.

Rodríguez, J. J., Mackie, K., & Pickel, V. M. (2001). Ultrastructural localization of the CB_1 cannabinoid receptor in μ-opioid receptor patches of the rat caudate putamen nucleus. *Journal of Neuroscience*, *21*(3), 823–833.

Rosenberg, E. C., Tsien, R. W., Whalley, B. J., & Devinsky, O. (2015). Cannabinoids and Epilepsy. *Neurotherapeutics*, *12*(4), 747–768.

Ross, R. A. (2003). Anandamide and vanilloid TRPV1 receptors. *British Journal of Pharmacology*, *140*(5), 790–801.

Rossi, S., Motta, C., Musella, A., & Centonze, D. (2015). The interplay between inflammatory cytokines and the endocannabinoid system in the regulation of synaptic transmission. *Neuropharmacology*, *96*(PA), 105–112.

Rozenfeld, R., & Devi, L. A. (2008). Regulation of CB1 cannabinoid receptor trafficking by the adaptor protein AP-3. *FASEB journal: official publication of the Federation of American Societies for Experimental Biology*, 22(7), 2311–2322.

Ruehle, S., Remmers, F., Romo-Parra, H., Massa, F., Wickert, M., Wörtge, S., Häring, M., Kaiser, N., Marsicano, G., Pape, H. C., & Lutz, B. (2013). Cannabinoid CB_1 receptor in dorsal telencephalic glutamatergic neurons: Distinctive sufficiency for hippocampus-dependent and amygdala-dependent synaptic and behavioral functions. *Journal of Neuroscience*, *33*(25), 10264–10277.

Russo, E. B. (2007). History of cannabis and its preparations in saga, science, and sobriquet. *Chemistry and Biodiversity*, *4*(8), 1614–1648.

Ryberg, E., Larsson, N., Sjögren, S., Hjorth, S., Hermansson, N. O., Leonova, J., Elebring, T., Nilsson, K., Drmota, T., & Greasley, P. J. (2007). The orphan receptor GPR55 is a novel cannabinoid receptor. *British Journal of Pharmacology*, *152*(7), 1092–1101.

Rygula, R., Walker, S. C., Clarke, H. F., Robbins, T. W., & Roberts, A. C. (2010). Differential contributions of the primate ventrolateral prefrontal and orbitofrontal cortex to serial reversal learning. *Journal of Neuroscience*, *30*(43), 14552–14559.

Ryu, H., Lee, J., Impey, S., Ratan, R. R., & Ferrante, R. J. (2005). Antioxidants modulate mitochondrial PKA and increase CREB binding to D-loop DNA of the mitochondrial genome in neurons. *Proceedings of the National Academy of Sciences of the United States of America*, *102*(39), 13915–13920.

Sagan, S. (1999). Anandamide and WIN 55212-2 inhibit cyclic AMP formation through G-protein-coupled receptors distinct from CB1 cannabinoid receptors in cultured astrocytes. *European Journal of Neuroscience*, *11*(2), 691–699.

Salio, C., Doly, S., Fischer, J., Franzoni, M. F., & Conrath, M. (2002). Neuronal and astrocytic localization of the cannabinoid receptor-1 in the dorsal horn of the rat spinal cord. *Neuroscience letters*, 329(1), 13–16.

Sánchez, C., Galve-Roperh, I., Canova, C., Brachet, P., & Guzmán, M. (1998). Δ9-Tetrahydrocannabinol induces apoptosis in C6 glioma cells. *FEBS Letters*, *436*(1), 6–10.

Sawada, N., Itoh, H., & Nakao, K. (2001). [Novel actions of HMG-CoA reductase inhibitors(statins)--vascular and cerebral protection through inhibition of small GTPase Rho]. *Nihon rinsho. Japanese journal of clinical medicine*, 59(12), 2470–2475.

Scavone, J. L., Mackie, K., & Van Bockstaele, E. J. (2010). Characterization of cannabinoid-1 receptors in the locus coeruleus: relationship with mu-opioid receptors. *Brain research*, 1312, 18–31.

Scharfman, H. E., & Myers, C. E. (2013). Hilar mossy cells of the dentate gyrus: a historical perspective. *Frontiers in neural circuits*, 6, 106.

Schatz, A. R., Lee, M., Condie, R. B., Pulaski, J. T., & Kaminski, N. E. (1997). Cannabinoid receptors CB1 and CB2: a characterization of expression and adenylate cyclase modulation within the immune system. *Toxicology and applied pharmacology*, 142(2), 278–287.

Schlosburg, J. E., Blankman, J. L., Long, J. Z., Nomura, D. K., Pan, B., Kinsey, S. G., Nguyen, P. T., Ramesh, D., Booker, L., Burston, J. J., Thomas, E. A., Selley, D. E., Sim-Selley, L. J., Liu, Q. S., Lichtman, A. H., & Cravatt, B. F. (2010). Chronic monoacylglycerol lipase blockade causes functional antagonism of the endocannabinoid system. *Nature neuroscience*, 13(9), 1113–1119.

Schwab, M. H., Druffel-Augustin, S., Gass, P., Jung, M., Klugmann, M., Bartholomae, A., Rossner, M. J., & Nave, K. A. (1998). Neuronal basic helix-loop-helix proteins (NEX, neuroD, NDRF): spatiotemporal expression and targeted disruption of the NEX gene in transgenic mice. *The Journal of neuroscience: the official journal of the Society for Neuroscience*, 18(4), 1408–1418.

Sheng, W. S., Hu, S., Min, X., Cabral, G. A., Lokensgard, J. R., & Peterson, P. K. (2005). Synthetic cannabinoid WIN55,212-2 inhibits generation of inflammatory mediators by IL-1β-stimulated human astrocytes. *Glia*, *49*(2), 211–219.

Shivachar A. C. (2007). Cannabinoids inhibit sodium-dependent, high-affinity excitatory amino acid transport in cultured rat cortical astrocytes. *Biochemical pharmacology*, 73(12), 2004–2011.

Showalter, V. M., Compton, D. R., Martin, B. R., & Abood, M. E. (1996). Evaluation of binding in a transfected cell line expressing a peripheral cannabinoid receptor (CB_2): identification of cannabinoid receptor subtype selective ligands. *The Journal of pharmacology and experimental therapeutics*, 278(3), 989–999.

Sillanpää, M., & Schmidt, D. (2012). Is incident drug-resistance of childhood-onset epilepsy reversible? A long-term follow-up study. *Brain*, *135*(7), 2256–2262.

Sjöström, P. J., Turrigiano, G. G., & Nelson, S. B. (2003). Neocortical LTD via coincident activation of presynaptic NMDA and cannabinoid receptors. *Neuron*, *39*(4), 641–654.

Sofroniew, M. V., & Vinters, H. V. (2010). Astrocytes: Biology and pathology. *Acta Neuropathologica*, *119*(1), 7–35.

Soria-Gómez, E., Bellocchio, L., Reguero, L., Lepousez, G., Martín, C., Bendahmane, M., ... & Wiesner, T. (2014). The endocannabinoid system controls food intake via olfactory processes. *Nature neuroscience*, 17(3), 407.

Soria-Gómez, E., Busquets-Garcia, A., Hu, F., Mehidi, A., Cannich, A., Roux, L., Louit, I., Alonso, L., Wiesner, T., Georges, F., Verrier, D., Vincent, P., Ferreira, G., Luo, M., & Marsicano, G. (2015). Habenular CB_1 Receptors Control the Expression of Aversive Memories. *Neuron*, *88*(2), 306–313.

Steindel, F., Lerner, R., Häring, M., Ruehle, S., Marsicano, G., Lutz, B., & Monory, K. (2013). Neuron-type specific cannabinoid-mediated G protein signalling in mouse hippocampus. *Journal of Neurochemistry*, *124*(6), 795–807.

Stella N. (2010). Cannabinoid and cannabinoid-like receptors in microglia, astrocytes, and astrocytomas. *Glia*, 58(9), 1017–1030.

Storck, T., Schulte, S., Hofmann, K., & Stoffel, W. (1992). Structure, expression, and functional analysis of a Na+-dependent glutamate/aspartate transporter from rat brain. *Proceedings of the National Academy of Sciences of the United States of America*, *89*(22), 10955–10959.

Stühmer, T., Puelles, L., Ekker, M., & Rubenstein, J. L. R. (2002). Expression from a Dlx gene enhancer marks adult mouse cortical GABAergic neurons. *Cerebral Cortex*, *12*(1), 75–85.

Suárez, J., Romero-Zerbo, S. Y., Rivera, P., Bermúdez-Silva, F. J., Pérez, J., De Fonseca, F. R., & Fernández-Llebrez, P. (2010). Endocannabinoid system in the adult rat circumventricular areas: An immunohistochemical Study. *Journal of Comparative Neurology*, *518*(15), 3065–3085.

Sugiura, T., Kondo, S., Kishimoto, S., Miyashita, T., Nakane, S., Kodaka, T., Suhara, Y., Takayama, H., & Waku, K. (2000). Evidence that 2-arachidonoylglycerol but not N-palmitoylethanolamine or anandamide is the physiological ligand for the cannabinoid CB_2 receptor. Comparison of the agonistic activities of various cannabinoid receptor ligands in HL-60 cells. *Journal of Biological Chemistry*, *275*(1), 605–612.

Sugiura, T., Kishimoto, S., Oka, S., & Gokoh, M. (2006). Biochemistry, pharmacology and physiology of 2-arachidonoylglycerol, an endogenous cannabinoid receptor ligand. *Progress in Lipid Research*, *45*(5), 405–446.

Sullivan, S. M., Lee, A., Björkman, S. T., Miller, S. M., Sullivan, R. K. P., Poronnik, P., Colditz, P. B., & Pow, D. V. (2007). Cytoskeletal anchoring of GLAST determines susceptibility to brain damage: An identified role for GFAP. *Journal of Biological Chemistry*, *282*(40), 29414–29423.

Sun, Y., Alexander, S. P., Kendall, D. A., & Bennett, A. J. (2006). Cannabinoids and PPARalpha signalling. *Biochemical Society Transactions*, 34, 1095-1097.

Suzuki, F., Makiura, Y., Guilhem, D., Sørensen, J. C., & Onteniente, B. (1997). Correlated axonal sprouting and dendritic spine formation during kainate-induced neuronal morphogenesis in the dentate gyrus of adult mice. *Experimental neurology*, 145(1), 203–213.

Suzuki, A., Stern, S. A., Bozdagi, O., Huntley, G. W., Ruth, H., Magistretti, P. J., & Alberini, C. M. (2012). Memory Formation. *Encyclopedia of Exercise Medicine in Health and Disease*, *144*(5), 557–557.

Takahashi, K. A., & Castillo, P. E. (2006). The CB_1 cannabinoid receptor mediates glutamatergic synaptic suppression in the hippocampus. *Neuroscience*, *139*(3), 795–802.

Taura, F., Sirikantaramas, S., Shoyama, Y., Shoyama, Y., & Morimoto, S. (2007). Phytocannabiniods in Cannabis sativa: Recent studies on biosynthetic enzymes. *Chemistry and Biodiversity*, *4*(8), 1649–1663.

Theodosis, D. T., Poulain, D. A., & Oliet, S. H. R. (2008). Activity-dependent structural and functional plasticity of astrocyte-neuron interactions. *Physiological Reviews*, *88*(3), 983–1008.

Tsou, K., Brown, S., Sañudo-Peña, M. C., Mackie, K., & Walker, J. M. (1998). Immunohistochemical distribution of cannabinoid CB_1 receptors in the rat central nervous system. *Neuroscience*, 83(2), 393–411.

Twitchell, W., Brown, S., & Mackie, K. (1997). Cannabinoids inhibit n- and p/q-type calcium channels in cultured rat hippocampal neurons. *Journal of Neurophysiology*, *78*(1), 43–50.

Uchigashima, M., Yamazaki, M., Yamasaki, M., Tanimura, A., Sakimura, K., Kano, M., & Watanabe, M. (2011). Molecular and morphological configuration for 2-arachidonoylglycerol-mediated retrograde signaling at mossy cell-granule cell synapses in the dentate gyrus. *The Journal of neuroscience : the official journal of the Society for Neuroscience*, 31(21), 7700–7714.

Ujike, H., & Morita, Y. (2004). New perspectives in the studies on endocannabinoid and cannabis: Cannabinoid receptors and schizophrenia. *Journal of Pharmacological Sciences*, *96*(4), 376–381.

Viader, A., Blankman, J. L., Zhong, P., Liu, X., Schlosburg, J. E., Joslyn, C. M., Liu, Q. S., Tomarchio, A. J., Lichtman, A. H., Selley, D. E., Sim-Selley, L. J., & Cravatt, B. F. (2015). Metabolic Interplay between Astrocytes and Neurons Regulates Endocannabinoid Action. *Cell Reports*, *12*(5), 798–808.

Vinogradova, L. V., & Van Rijn, C. M. (2008). Anticonvulsive and antiepileptogenic effects of levetiracetam in the audiogenic kindling model. *Epilepsia*, *49*(7), 1160–1168.

Yi, C. X., Habegger, K. M., Chowen, J. A., Stern, J., & Tschöp, M. H. (2011). A role for astrocytes in the central control of metabolism. *Neuroendocrinology*, 93(3), 143–149.

Walter, L., & Stella, N. (2003). Endothelin-1 increases 2-arachidonoyl glycerol (2-AG) production in astrocytes. *Glia*, *44*(1), 85–90.

Wang, W., Trieu, B. H., Palmer, L. C., Jia, Y., Pham, D. T., Jung, K. M., Karsten, C. A., Merrill, C. B., Mackie, K., Gall, C. M., Piomelli, D., & Lynch, G. (2016). A Primary Cortical Input to Hippocampus Expresses

a Pathway-Specific and Endocannabinoid-Dependent Form of Long-Term Potentiation. *eNeuro*, 3(4), ENEURO.0160-16.2016.

Wang, W., Jia, Y., Pham, D. T., Palmer, L. C., Jung, K. M., Cox, C. D., Rumbaugh, G., Piomelli, D., Gall, C. M., & Lynch, G. (2018). Atypical Endocannabinoid Signaling Initiates a New Form of Memory-Related Plasticity at a Cortical Input to Hippocampus. *Cerebral cortex (New York, N.Y. : 1991)*, 28(7), 2253–2266.

Warden, M. R., & Miller, E. K. (2010). Task-dependent changes in short-term memory in the prefrontal cortex. *Journal of Neuroscience*, *30*(47), 15801–15810.

Wenzel, J., Lammert, G., Meyer, U., & Krug, M. (1991). The influence of long-term potentiation on the spatial relationship between astrocyte processes and potentiated synapses in the dentate gyrus neuropil of rat brain. *Brain research*, 560(1-2), 122–131.

Whiting, P. F., Wolff, R. F., Deshpande, S., Di Nisio, M., Duffy, S., Hernandez, A. V., Keurentjes, J. C., Lang, S., Misso, K., Ryder, S., Schmidlkofer, S., Westwood, M., & Kleijnen, J. (2015). Cannabinoids for Medical Use: A Systematic Review and Meta-analysis. *JAMA*, 313(24), 2456–2473.

Wilcox, K. S., Dixon-Salazar, T., Sills, G. J., Ben-Menachem, E., White, H. S., Porter, R. J., Dichter, M. A., Moshé, S. L., Noebels, J. L., Privitera, M. D., & Rogawski, M. A. (2013). Issues related to development of new antiseizure treatments. *Epilepsia*, *54*(SUPPL.4), 24–34.

Wu, S. X., Goebbels, S., Nakamura, K., Nakamura, K., Kometani, K., Minato, N., Kaneko, T., Nave, K. A., & Tamamaki, N. (2005). Pyramidal neurons of upper cortical layers generated by NEX-positive progenitor cells in the subventricular zone. *Proceedings of the National Academy of Sciences of the United States of America*, *102*(47), 17172–17177.

Zerucha, T., Stühmer, T., Hatch, G., Park, B. K., Long, Q., Yu, G., Gambarotta, A., Schultz, J. R., Rubenstein, J. L. R., & Ekker, M. (2000). A highly conserved enhancer in the Dlx5/Dlx6 intergenic region is the site of cross-regulatory interactions between Dlx genes in the embryonic forebrain. *Journal of Neuroscience*, *20*(2), 709–721.

Zhou, Y., & Danbolt, N. C. (2014). Glutamate as a neurotransmitter in the healthy brain. *Journal of Neural Transmission*, *121*(8), 799–817.

Zippin, J. H., Chen, Y., Nahirney, P., Kamenetsky, M., Wuttke, M. S., Fischman, D. A., Levin, L. R., & Buck, J. (2003). Compartmentalization of bicarbonate-sensitive adenylyl cyclase in distinct signaling microdomains. *The FASEB Journal : Official Publication of the Federation of American Societies for Experimental Biology*, *17*(1), 82–84.

Zou, S., & Kumar, U. (2018). Cannabinoid receptors and the endocannabinoid system: Signaling and function in the central nervous system. *International Journal of Molecular Sciences*, *19*(3).

Zygmunt, P. M., Petersson, J., Andersson, D. A., Chuang, H. H., Sørgård, M., Di Marzo, V., Julius, D., & Högestätt, E. D. (1999). Vanilloid receptors on sensory nerves mediate the vasodilator action of anandamide. *Nature*, *400*(6743), 452–457.